MOLECULAR TARGETING OF REFRIGERANT MIXTURES

By

Brian J. Satola

[BSc (Eng.) / Chemical Engineering; University of Akron – Ohio, U.S.A.]

[MSc (Eng.) / Chemical Engineering; University of KwaZulu-Natal – Durban, ZA]

University of KwaZulu-Natal, School of Engineering, Howard College Campus,

For the degree Doctor of Philosophy in Engineering (Chemical Engineering)

Abstract

Refrigeration units, besides common household refrigerators and air conditioning systems, are necessary components for the successful operation of many industrial processes in the chemical, petrochemical, pharmaceutical etc. industries, where they are often used to maintain process streams and/or unit operations at “lower” temperatures.

Due to their favourable thermodynamic and thermophysical properties[1], as well as price, availability and long-term stability etc., many of these units have historically operated using pure chlorofluorocarbons (CFCs) as their working fluids. Their high volatilities, low boiling points, low reactivity, high compressibility and low odour (just to name a few) made them highly suited as refrigerants. As early as 1974, however, evidence began to appear that suggested that chlorinated hydrocarbons cause catalytic destruction of ozone in the stratosphere (Molina, et al., 1974; Rowland, et al., 1975).

This resulted in a number of international environmental regulations starting in 1987, and has led to the phase-out of all CFC-refrigerants by 2010 (United States Environmental Protection Agency, 2010), including their proposed hydrochloroflurocarbon (HCFC) replacements by 2030 (United States Environmental Protection Agency, 2010). To satisfy the objectives of international protocols, it is necessary to investigate both long-term and short-term alternatives for the CFC and HCFC-refrigerants currently used in practice.

Although many potential refrigerant alternatives have been proposed, such as hydrocarbons (which are used in many large-scale industrial processes), and CO_2 and mixture substitutes, most of these require unique equipment modifications for *each* particular refrigerant replacement due to their special characteristics. Equipment specifications for e.g. new mixtures may be reasonable for new installations, but they are largely prohibitive for existing refrigeration units, i.e. retrofitting cases. This latter case is of fundamental importance to industry, however, since many of these units still have several operating-years left before requiring the mechanical replacement of key components like e.g. the compressor(s).

Unfortunately, there are only a few pure fluids which have properties close to existing halogenated refrigerants (which would require minimum modifications to existing equipment). New environment-friendly alternatives, therefore, are likely to be made from refrigerant *mixtures* instead since they provide the flexibility needed to match the desirable properties of existing refrigerants: systematic performance and material compatibility. This unfortunately makes finding an optimum refrigerant replacement ever more difficult since the performance of the substitute is dependent on its physical properties, which in turn, for mixtures, is dependent on its components and their concentrations (a theoretically infinite number of mixture definitions).

The solution to this type of design problem has been, by and large, based on experience, heuristics, systematic experimental investigations, and at times a bit of luck e.g. the discovery of the

[1] Thermophysical properties can be simply defined as material properties that vary with temperature without altering the material's chemical identity, but it has become customary to limit the scope of the term to properties having a bearing on the transfer and storage of heat (UK National Physical Laboratory, 2012).

original CFC refrigerants by Midgley and crew (Midgley, Jr., 1937; Midgley, Jr., 1938). This “fox-hunt” solution strategy, however, requires the outlay of considerable resources in order to find the optimum solution: the identification of potential chemicals, the carrying out of feasibility tests and candidate reformulations based on experimental results, where the design-cycle then repeats until a sufficiently precise solution is found.

The novelty of this project, therefore, is to combine the component-selection(s) and evaluation steps into a single optimization problem (Duvedi, et al., 1996; Bardow, et al., 2010), by using the PC-SAFT equation of state (Gross, et al., 2000; Gross, et al., 2001) to describe all of the residual thermodynamic properties required for process calculations (versus performing experimental measurements for every potential refrigerant replacement).

In a typical computer-aided-molecular design (CAMD) discrete chemical compounds are constructed from a list of structural groups, whose physical properties are then estimated via reliable group contribution methods (non-continuous molecular approach) while simultaneously optimizing the continuous mixture composition to some process. This mixed continuous – non-continuous optimization, however, requires very specific algorithms that are generally less reliable than a fully continuous optimization. A direct link between process performance and molecular characteristics is thus not achieved.

Since the PC-SAFT equation uses physically based molecular-parameters, i.e. ones that are closely associated with specific molecule attributes, these same model parameters can be bounded and optimized to give the best overall process performance for a given refrigeration cycle, and then these same (realistic) parameters can be used to identify potentially novel refrigerant replacements. Only with the development of models with molecular based parameters like e.g. PC-SAFT (segment number and size, segment interaction etc.) does a *co*ntinuous-*m*olecular-*t*argeting approach then becomes possible. This, however, would require an appropriate mapping procedure to move from the hypothetical pure fluid that is the mixture to individual components that are the mixture, which has been applied e.g. to the design of single-solvent systems (Bardow, et al., 2009; Bardow, et al., 2010).

However, after a quantitative evaluation of the PC-SAFT equation’s ability to represent both pure component and mixture properties, an alternative approach that optimises the component concentrations was used here instead. To accomplish this, a database of pure-component PC-SAFT model parameters was created by regressing thermodynamic properties predicted by REFPROP (which uses the most accurate equations of state and models currently available for select substances). These same model parameters were then used to statistically define different component combinations of the test-mixtures, whose concentrations were then optimised to satisfy specific properties and design-specifications for an existing process originally designed to use R-22 as the working fluid. Both direct substitutes and long-term replacements were identified for the existing process, some of which are known R-22 replacements (at least somewhat validating the proposed approach used).

In this work this approach towards finding novel refrigerant replacements is discussed. Besides the design of new refrigerant mixtures, it is also important to note that the very same procedure may be adapted and used to identify solutions to a large variety of other processes as well as in chemical product design.

Preface

The study presented in this thesis was performed at the University of KwaZulu-Natal, Durban from July 2011 to December 2013. The work was supervised by Prof. D. Ramjugernath, Prof. Dr. J. Rarey and Prof. Dr. J. Vrabec.

As the candidate's supervisor, I, Prof. D. Ramjugernath, have approved this thesis for submission.

_____

Prof. D. Ramjugernath

Declaration

I _____ declare that:

(i.) The research reported in this thesis, except where otherwise indicated, is my original work.

(ii.) This thesis has not been submitted for any degree or examination at any other university.

(iii.) This thesis does not contain other persons' data, pictures, graphs or other information, unless specifically acknowledged as being sourced from other persons.

(iv.) This thesis does not contain other persons' writing, unless specifically acknowledged as being sourced from other researchers. Where other written sources have been quoted, then:

a.) their words have been re-written but the general information attributed to them has been referenced.
b.) where their exact words have been used, their writing has been placed inside quotation marks, and referenced.

(v.) Where I have reproduced a publication of which I am an author, co-author or editor, I have indicated in detail which part of the publication was actually written by myself alone and have fully referenced such publications.

(vi.) This thesis does not contain text, graphics or tables copied and pasted from the internet, unless specifically acknowledged, and the source being detailed in the dissertation/thesis and in the References Chapters.

_____

Acknowledgements

- Firstly, my supervisors, Prof. Dr. J. Rarey, Prof. Dr. D. Ramjugernath and Prof. Dr. J. Vrabec, for their support, ideas, wisdom and motivation during this work. Working with them has been a great learning experience in many, and sometimes surprisingly unexpected, ways.
- My colleagues from the University of Kwazulu-Natal, University of Oldenburg and University of Paderborn for their friendship, advice and support.
- The DST for the PhD bursary under the South African Research Chairs Programme, and the Pelchem and *F*luorochemical *E*xpansion *I*nitiative (FEI) for project funding.
- My parents Chester and Linda Satola (a.k.a "mum!")[2], my sister Krista and my brother-in-law Jakub Budanov, and the friends I left behind for the *years* of support, guidance and the encouragement they gave me to chase my dreams.
- To Marlon Charles, *my brother from another mother*, and the rest of my inner circle, Arisha, Ahista, Dragon! (LOL), Jono, Kumi and Venolan – I did it!

[2] Yes, I'm a momma's boy ;-)

Table of Contents

List of Figures

List of Tables

Nomenclature

Abbreviations

BC	binomial coefficient (“n choose k”)
CAMD	computer-aided-molecular design
CFCs	chlorofluorocarbons
COM	computer object model
COP	coefficient of performance
CPIG (or CPIGDP)	Aspen Plus ideal heat capacity correlation model parameters
DDB	Dortmund Databank
DH	Aspen Plus enthalpy departure calculation
DHL	Aspen Plus liquid phase enthalpy departure calculation
DHS	Aspen Plus solid phase enthalpy departure calculation
DHV	Aspen Plus vapour phase enthalpy departure calculation
DHFORM	Aspen Plus heat of formation calculation (or databank value)
DRS	data regression system in Aspen Plus
EOS	equation-of-state
GHGs	greenhouse gases
GWP	global warming potential
HBFCs	hydrobromofluorocarbons
HCFCs	hydrochlorofluorocarbons
HFCs	hydrofluorocarbons
HIG	Aspen Plus ideal gas enthalpy calculation
LJ	Lennard-Jones
NASA	The National Aeronautics and Space Administration (US)
NOx	mono-nitrogen oxides NO and NO_2
NRTL	Non-Random Two Liquid model
ODP	ozone depletion potential
ODS	ozone-depleting substances
O.F.	objective (or fitness) function
PC-SAFT	Perturbed Chain-Statistical Associating Fluid Theory
PFCs	perfluorocarbons
PR	Peng-Robinson
PVT	pressure-volume-temperature
REFPROP	REFerence fluid PROPerties
RMSD	root-mean-squared-deviation
RK	Redlich-Kwong
PVT	pressure-volume-temperature
SAFT	Statistical Associating Fluid Theory
SRK	Soave-Redlich-Kwong
TRUx	thermodynamic research utilities for Excel
UNIQUAC	UNIversal QUAsiChemical
US (or USA)	United States of America
UV	ultraviolet (UV) light from the sun
vdW	van der Waals
VF	vapour fraction
VBA	Visual Basic for Applications
VLE	vapour-liquid equilibrium

List of Symbols

a	attractive parameter in cubic equations of state [J m^3 mol^{-2}]
a	specific Helmholtz energy [J mol^{-1}, J kg^{-1}]
a_{ij}	cross attractive parameter in cubic equations of state [J m^3 mol^{-2}]
a_{0i}, a_{1i} and a_{2i}	PC-SAFT model constants defined in eq (4-63)
A	Helmholtz energy [J]
A_1	Helmholtz energy of first-order perturbation term in PC-SAFT [J]
A_2	Helmholtz energy of second-order perturbation term in PC-SAFT [J]
b	repulsive parameter in equations of state [m^3 mol^{-1}]
b_{ij}	cross repulsive parameter in equations of state [m^3 mol^{-1}]
b_{0i}, b_{1i} and b_{2i}	PC-SAFT model constants defined in eq (4-64)
B (or $\mathcal{B}_2$)	the second viral coefficient [m^3 mol^{-1}]
C (or $\mathcal{B}_3$)	the third viral coefficient [(m^3)^2 mol^{-2}]
c_p	specific isobaric (constant pressure) heat capacity [J g^{-1} K^{-1}, J kg^{-1} K^{-1}]
c_v	specific isochoric (constant volume) heat capacity [J g^{-1} K^{-1}, J kg^{-1} K^{-1}]
d	hard core diameter [m]
d	temperature-dependent segment diameter (PC-SAFT) [m]
E	energy [J]
f_i	fugacity of component i [Pa]
$f(\dots)$	read as "a function of …"
$f(\dots)$	Mayer f-function defined by eq (4-35)
F	net force between two molecules [N]
$F(r)$	integral distribution function
g	specific Gibbs energy [J mol^{-1}, J kg^{-1}]
g	reduced well width (square-well potential)
g	radial distribution function
G	Gibbs energy [J]
h	specific Enthalpy [J mol^{-1}, J kg^{-1}]
Δh_v (or DHVL)	specific enthalpy of vaporisation [J mol^{-1}, J kg^{-1}]
H	Enthalpy [J]
hv	ultraviolet (UV) light from the sun
$I_1(\eta, m)$, $I_2(\eta, m)$	perturbation theory integrals (PC-SAFT)
k	specific heat capacity ratio, c_p/c_v
k	Boltzmann constant 1.3806488 × 10-23 [J K^{-1}]
k	Planck's constant 6.62607 x 10^{-34} [m^2 kg s^{-1}]
k_{ij}	binary interaction parameter between component i and j
m	number of segments per chain/molecule in SAFT models
$\dot{m}$	mass flow rate [kg s^{-1}]
M_W	molecular weight [g mol^{-1}]
n	number of components
n	number of moles
n	number of data points
N	total number of monomeric units in SAFT models total number of particles, atoms or molecules
N_A	Avogadro's number 6.02214 x 10^{23} mol^{-1}
P	total pressure [Pa]
P	indicates a property (thermodynamic, transport, etc.)
q	specific heat [J mol^{-1}, J kg^{-1}]
q	stream quality (or vapour fraction)
Q	heat [J]

$\dot{Q}$	rate of heat exchange [W]
r (or r_{ij})	radial distance between two molecules (or segments) i and j
R	universal gas constant 8.314472 J/mol K = 1.98721 cal/mol K
R1, R2, R3, …	chemical reactions numbered as 1, 2, 3, …
s	specific entropy [J mol^{-1} K^{-1}, J kg^{-1} K^{-1}]
S	entropy [J K^{-1}]
s_1	constant defining the soft repulsion distance in eq (4-49)
T	absolute temperature [K]
u	specific internal energy [J mol^{-1}, J kg^{-1}]
$u(r)$	potential energy function used in statistical mechanics
$\tilde{u}(x)$	reduced potential energy function
v	molar volume [m^3 mol^{-1}]
V	volume [m^3]
W	technical work [J]
x_i	mole fraction of component i in the liquid phase
X	free radical used in describing atmospheric chemistry reactions
X	fraction of segments that are non-bonded (Wertheim)
y_i	mole fraction of component i in the vapour phase
z_i (or Z)	compressibility factor, v_{real}/v_{ideal}, of component i

Greek & Special Symbols

①, ②, ③, …	indicates process state points on e.g. PH and TS diagrams
$\equiv$	mathematical assignment-operator; read as “equivalent to”
α	function in cubic EOS
$\mathcal{B}_n$	viral coefficients, where $n = 1$ (first), 2 (second)…
$\mathcal{B}_{ij}$	cross second virial coefficient
γ_i	activity coefficient of component i
Δ	difference value
ε	depth of the potential energy well (energy minimum)
ζ_n	abbreviation (n = 0, …, 3) for PC-SAFT defined by eq (4-54) [m^{n-3}]
η	efficiency
η	reduced density in SAFT models
η_s	isentropic efficiency
η_m	mechanical efficiency
Ω_a, Ω_b	constants in RK, SRK and PR cubic EOS
λ	reduced well width
π	Pi = 3.14159…
φ_i	fugacity coefficient of component i
ρ	density [mol m^{-3}, kg m^{-3}]
σ	intermolecular separation when the potential energy is zero (the intermolecular collision-diameter)
$\boldsymbol{\Omega}$	molecular orientation
$\mathbf{r}$	molecular centre, i.e. centres of mass, position
$\mathbf{d}_\alpha$ and $\mathbf{d}_\beta$	represent vectors from the molecular centre to an interaction site
ω	acentric factor
x	reduced radial distance around a sphere, r/σ
∞	infinite value

Superscripts & Accents

A (or Assoc.)	indicates association property
$\alpha, \beta, \gamma, \ldots$	phases, interaction, or association sites
Λ	indicates mixture property
—	indicates partial molar property
—	indicates an averaged value
chain	indicates the contribution due to the formation of bonds between monomeric segments in SAFT models
disp	indicates dispersion contribution in SAFT models
E	indicates excess property
HB	hydrogen-bonding
hc	indicates hard-chain property
hs	indicates hard-sphere property
ig	indicates ideal gas property
ideal	indicates ideal property
L	indicates liquid phase property
s	indicates saturation state property
V	indicates vapour phase property
*	indicates dimensionless property
*	indicates real-process variable
*	indicates calculated reference property, using e.g. PC-SAFT
•	indicates a rate of change with respect to time

Subscripts

0 or Ref.	indicates reference property
b	value at the normal boiling point
c (or C)	indicates critical point property
cold / hot	indicates cold or hot reservoir property
$i, j\ldots$	components, molecules, segments, etc. $i, j\ldots$
ij	cross parameter between component i and component j
in (or input)	indicates input property
m	indicates mechanical or mixture property
l	indicates liquid phase property
out (or output)	indicates output property
r	indicates reduced property, e.g. $P_r = P/P_c$
real	indicates real (actual or true) property
s	indicates isentropic property
sat	indicates saturation (bubble point) property
v	indicates vapour phase property

1 Introduction

1.1 Problem Statement

For decades after being introduced, CFCs were essentially considered a wonder-chemical that could be used in an every-increasing number of applications, without fear that they were in any way harmful. The same qualities that made CFCs ideal refrigerants (stable, nontoxic, non-flammable, etc.) also make them very useful as propellants in applications such as aerosol sprays (e.g. cosmetics, medical inhalers, etc.), as blowing agents for foam or as solvents in the electronics industry. By the mid-1960s less than half of halocarbon production was being applied to refrigeration and, of that, the majority was being used to top-up leaky systems (Pearson, 2004). It is not too surprising, therefore, that detectable amounts of CFCs began showing up in the Earth's atmosphere (Lovelock, et al., 1973).

It was not until the mid-1970s, however, that atmospheric chemistry was understood well enough that the refrigeration industry began to experience significant environmental challenges. Manmade chemicals such as CFC refrigerants, and other similar chemicals containing bromine, have since been linked to the destruction of stratospheric ozone necessary for sustaining life. This has led to a global ban on the production and use of such chemicals. Now with the prospect of manmade global warming, the types of chemicals that can safely be used in refrigeration applications have further diminished to those that also do not significantly absorb infrared re-radiation from the earth's surface, either directly or indirectly from CO_2 generated from energy sources.[3]

The fundamental problem is that, in light of these environmental concerns there exist no "ideal" alternatives that can replace pure component halocarbon refrigerants. The majority of the periodic elements are metals in their elemental form that combine with other elements to form non-volatile compounds that are fundamentally incapable of being used as working fluids in a vapour compression cycle. After discarding chlorine and bromine, this leaves only carbon, nitrogen, oxygen, sulphur, hydrogen and fluorine (in correct proportions with hydrogen) which have the appropriate chemical properties for the purpose. As compounds from these remaining elements are quite definitely not similar enough in their various properties to provide a direct replacement for an existing refrigerant, a mixture of different compounds (conceivably made of these remaining elements) may well be tailored to meet the needs of the refrigeration industry.

Approaches to refrigerant design have traditionally been based on experience, heuristics, and systematic experimental investigations, and at times a bit of luck e.g. the discovery of the original CFC refrigerants (Midgley, Jr., 1937; Midgley, Jr., 1938). Since the properties of refrigerants are intimately linked, in a complex way, to how a working fluid performs in any given cycle, this type of solution strategy often requires the expenditure of considerable resources: the identification of potential chemicals, the carrying out of feasibility tests and candidate reformulation based on experimental results, where the design-cycle repeats itself until a sufficiently precise solution is found. Instead, an intelligent methodology to limit the number of candidate refrigerants requiring further evaluation is desired.

[3] Coal, oil and natural gas provide roughly 87% of the world's energy.

Modern process systems engineering and computer aided process engineering (PSE/CAPE) aims at identifying optimal solutions to such problems by analysing a large number of possible process configurations, preferable in a process simulation environment (Seider, et al., 2008). In case of additional components like solvents and anti-solvents (Mitrofanov, et al., 2012; Karunanithi, et al., 2007), entrainers for special separation operations (Lek-utaiwan, et al., 2009) or working fluids in cooling or heat pump applications (Apostolakou, et al., 2002), computer aided molecular design (Achenie, et al., 2003; Gani, 2007) allows the identification of potential new chemicals (or mixtures) that would simplify a process or increase its efficiency, i.e. the traditional evolutionary process based on experimental results is moved into the computer.

An essential step in PSE/CAPE applications and especially in CAMD is the calculation of the required thermodynamic properties, often involving multiple methods in a single design problem (Achenie, et al., 2003). Model parameters, however, may not be entirely available for every candidate molecule and corresponding properties of interest. In such cases the generated component (or mixtures containing the component) can no longer be considered due to lack of physical information, although their inclusion may result in feasible candidate-solutions to the problem (potentially even the optimum). Different approaches have already been employed in the selection and design of working fluids, mostly pure-components: data bank search (McLinden, et al., 1988), mixed integer nonlinear programming (MINLP) approach (Churi, et al., 1996), combination of different group estimation methods (Achenie, et al., 2003), algorithmic approach (Arcaklioglu, et al., 2005), molecular simulation (Smith, et al., 2010) and most recently the continuous-molecular targeting (CoMT-CAMD) concept (Lampe, et al., 2014; Lampe, et al., 2014) first introduced for integrated solvent design (Bardow, et al., 2009; Bardow, et al., 2010). Only with the development of advanced equations of state like e.g. PC-SAFT, is a consistent picture of all required fluid phase properties obtained using a single equation that can be fitted to a minimal amount of chemical information.

The novelty of this work, therefore, is to combine the component-selection and evaluation steps of refrigerant mixture design for vapour compression cycles into a single CAMD optimisation problem, using the PC-SAFT equation for the calculation of all required thermophysical properties. The problem is decomposed into a traditional number of subproblems: pre-design, design and post design phases involving a case-study of a working cycle originally designed to use pure chlorodifluoromethane (better known as R-22). Feasible binary, ternary and quaternary mixtures are identified for both direct substitutions and long-term replacements for the examined process. Some of the candidates are even well-known, commercially available, R-22 mixture replacements. Besides the design of new refrigerant mixtures, it is also important to note that the very same procedure may be adapted and used to identify solutions to a large variety of other processes as well as in chemical product design.

1.2 Thesis Overview

The work presented in this thesis was performed at the University of KwaZulu-Natal, Durban from July 2011 to December 2013, and is in partial fulfilment of the requirements for the degree Doctor of Philosophy in Engineering (Chemical Engineering). The main goal of this thesis is to discuss the aims of the project, related background information (including literature review), project results and future work pertaining to the title “Molecular Targeting of Refrigerant Mixtures.”

In so doing, a brief history on working fluids used for refrigeration purposes is provided in **Chapter 2**. This includes a background on the environmental concerns that have developed over time, including the international efforts to regulate the types of chemicals used in this industry. In so providing, the chemical properties of ozone depletion potential (ODP) and global warming potential (GWP) are defined and briefly discussed, followed by a list of essential and desirable qualities that refrigerants should aim to satisfy in order to sustain an efficient and reliable refrigeration system.

It then follows in **Chapter 3**, that the vapour-compression cycle process is examined in detail, since it is the underlying thermodynamic process for most refrigeration systems in use today. As such, the Carnot cycle is discussed as an introduction, and serves to establish the connection that such cycles have to thermodynamics. This is then followed by a step-by-step description of the vapour-compression refrigeration cycle, including the fundamentals required to simulate such a process. To conclude the chapter, the thermodynamic properties that would make-up an ideal refrigerant are highlighted.

The modelling of such processes requires sufficiently precise descriptions of the real fluid phase behaviour (see **Appendix D**) and thermodynamic properties of refrigerant candidates. Since this project proposes that this description be obtained using the advanced equation of state known as PC-SAFT, a literature review of selected equations of state is given in **Chapter 4**. This review includes a fundamental overview of the basic thermodynamic relationships used in equilibrium calculations, with emphasis on those required for implementing equations of state. Following this basic review, the virial equation is presented in terms of the ideal gas equation and is related to the actual intermolecular forces occurring between molecules (see **Appendix C**). The equation of van der Waals and the related cubic equations of Redlich-Kwong, Soave-Redlich-Kwong and Peng-Robinson are then discussed. This chapter is then concluded by describing the key concepts of Wertheim's theory and the SAFT equation of state, which are then used in the formulation of the PC-SAFT equation.

To test the feasibility of using the PC-SAFT equation of state for this project, the ability of the equation to represent pure component properties is first evaluated and presented in **Chapter 5**. The pure component model parameters σ, m and ε/k were fitted to thermodynamic property predictions made using REFPROP (at the normal boiling point for each component, T_b). For the case of pure-components, the PC-SAFT equation only has three degrees of freedom (requiring three data points) for fitting purposes. It was shown that even for cases of a "perfect fit", where the saturated vapour pressure, liquid density and heat of vaporisation data used in the fitting procedure were regressed exactly, that it does not necessarily mean that other thermodynamic properties such as e.g. the specific heat capacities of either the liquid and/or vapour phases are correctly represented too. Since all required residual thermodynamic properties can be calculated using the PC-SAFT equation of state, the equation is forced to sacrifice the calculation of other properties not directly used in the fitting procedure in order to successfully matched those that are. An analytical comparison using the PC-SAFT equation can only be meaningful, therefore, if the relative errors are more or less consistent across all of the fluids of interest. For the relatively simple molecules of typical refrigerants, herein studied, this is fortunately shown to be the case.

Chapter 5 then goes on to evaluate the ability of the PC-SAFT equation to represent mixture properties. The pure-component model parameters that were regressed earlier in the chapter are used to examine the calculated behaviours of some common mixture replacements for R-502

(azeotropic mixture) and R-22 (pure-component), while neglecting the optional binary interaction parameter for each mixture. Mixture evaluations, therefore, were carried out without any empirical adjustments ($k_{ij} = 0$). For mixtures with limited temperature glides, i.e. mixtures with behaviours closest to pure-components (azeotropes and near-azeotropes), it was found that the prediction of key-thermodynamic properties is not grossly effected by inaccuracies in the VLE (or PVT) behaviour of the mixture for reduced temperatures of approximately $T_r < 0.95$. This is fortunate, since pure or pure-acting (azeotropic and near-azeotropic mixtures) are often desired over refrigerant mixtures with large temperature glides.

Like other more conventional equations of state, the PC-SAFT equation itself is only capable of describing the behaviour of pure fluids, where suitable mixing and combining rules for the pure component parameters are needed to characterise a "hypothetical" pure fluid that is the mixture. A truly continuous-molecular-targeting approach towards finding novel refrigerant replacements, therefore, requires an appropriate mapping procedure to move from the "hypothetical" pure fluid that is the mixture to the pure components that make up the mixture. For zeotropes, however, it was found that one cannot simply use the mixing and combining rules to map a mixture to the PC-SAFT parameters of existing pure-fluids, i.e. the physical meaning of the equation begins to breakdown without the inclusion of additional adjustable parameters. This, unfortunately, largely prohibits the use of the PC-SAFT equation in a truly a continuous-molecular-targeting approach. Instead of e.g. bounding and optimising model parameters to give the best overall process performance for a given refrigeration cycle, it was alternatively proposed to adjust and optimise the concentrations of mixture components to satisfy specific property and/or design-specifications for some working process (existing or for a new installation). This methodology was verified at the end of **Chapter 5**.

Potential mixture replacements were then identified for an existing refrigeration cycle using R-22 in **Chapter 6**. Accordingly, the chapter begins by describing the development and validation of a process model that reproduces the real operating performance of an existing refrigeration system found in literature. The validated model and the procedure of **Chapter 5** are then used to identify potential blend replacements that give similar operating performance as the R-22 refrigerant that is currently used in the real process (drop-in replacements). The constraints are then relaxed to maximise the COP of the existing process (new installations). Key results are then itemised in **Chapter 7**, followed by recommendations for future work in **Chapter 8**.

2 Environmental Challenges and Requirements of Working Fluids

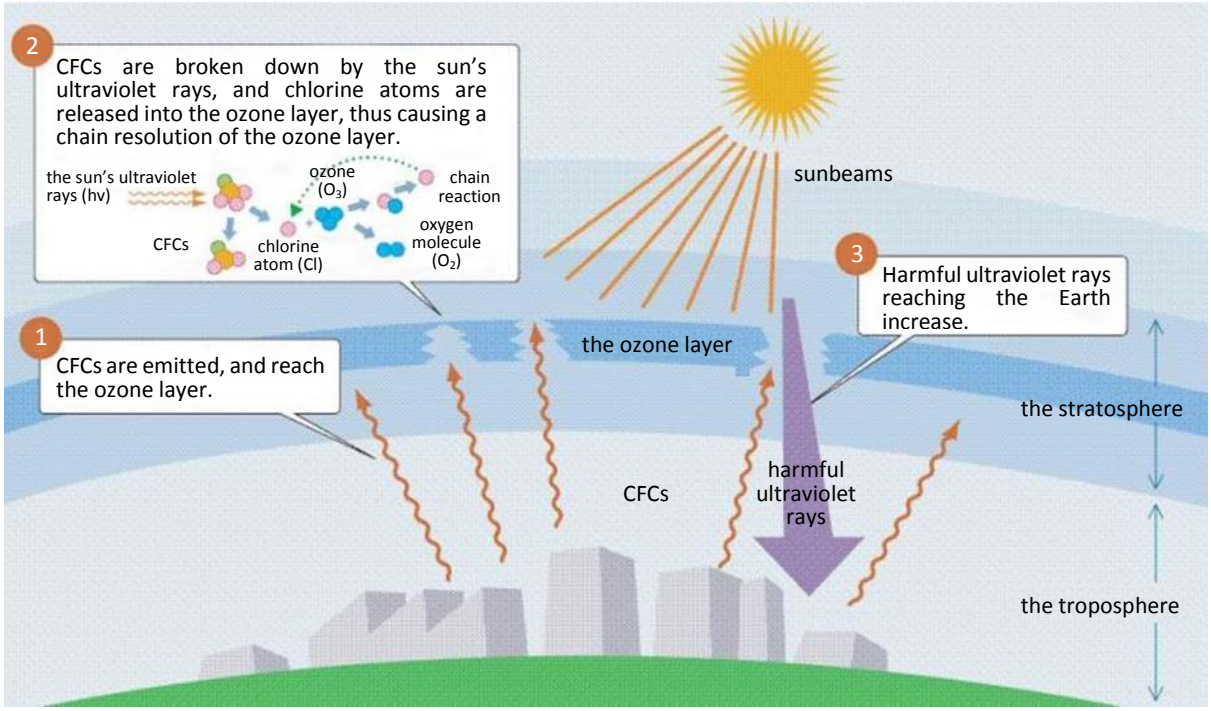

Figure 2-1: Diagram showing the location of the ozone layer in reference to various atmospheric layers (Welch, 2011).

In today's age, it is common knowledge that *naturally occurring* gases such as ozone are essential for life. As depicted in **Figure 2-1** above, for instance, the ozone layer of the upper stratosphere is necessary for shielding the Earth's surface and many living organisms from the harmful effects of solar ultraviolet radiation. In fact, complex life did not move out of the oceans and evolve until the protective ozone shield developed (Samson, 2011). Therefore, it is of great environmental concern that manmade chemicals such as chlorofluorocarbons (CFCs) and other ozone-depleting substances (ODSs) have been linked to its destruction. The reduction of the ozone layer, for instance, could lead to a drastic increase in long-term health effects such as skin cancer and cataracts, and environmental damage to agricultural crops and phytoplankton necessary for sustaining life (Morrisette, 1989). Not only this, but their release into the environment also adds to the greenhouse gases that naturally occur there and may have a negative effect on global warming.

The sun heats the Earth's atmosphere continuously although a large part of this radiated energy is reflected back into outer space. This delicate energy balance, the heat absorbed and reflected back out, largely determines the temperature of the planet. Without greenhouse gases, for instance, the average temperature of the Earth would be below the freezing point of water (Solomon, et al., 2007). Since greenhouse gases (GHGs) are responsible for the absorption and redistribution of this thermal radiation, i.e. the greenhouse effect, it stands to reason that any additional GHGs, beyond those naturally occurring in the environment, will act as additional insulators that may cause the Earth to abnormally warm.

Consequently, the depletion of the protective ozone layer and the prospect of global warming have become great sources of environmental concern during recent decades. These issues, for

instance, have arguably resulted in unparalleled collaboration between global communities, leading to a number of international laws banning, or at least limiting, the production and use of harmful man-made chemicals based on their environmental impact. Because of [this] a number of regulatory "indicators" have since been defined which directly affect the chemicals that can be used as refrigerants. The amount of damage that a refrigerant can cause to the ozone layer is quantified by the *ozone depletion potential* (ODP), while the potential ability to warm the planet abnormally is quantified by the *global warming potential* (GWP). Much of the present research in the field of refrigeration is to find suitable refrigerant replacements that are both energy efficient and have zero ODP, with very little to no GWP.

2.1 Environmental Concerns

The first generation of refrigerants consisted of familiar solvents and other volatile chemicals, mostly "whatever worked" and was on hand (Calm, 2008). A number of these early refrigerants were highly flammable, toxic or both and so commercial refrigeration was typically limited to specialty applications. It was not until the late 1930s, when safe and durable chlorofluorocarbons (CFCs) were identified and synthesized, that the use of refrigeration became commonplace.

For decades after being introduced, CFCs were essentially considered a wonder-chemical that could be used in an ever-increasing number of applications, without fear that they were in any way harmful. The same qualities that made CFCs ideal refrigerants (stable, nontoxic, non-flammable, etc.) also make them very useful as propellants in applications such as aerosol sprays (e.g. cosmetics, medical inhalers, etc.), as blowing agents for foam or as solvents in the electronics industry. By the mid-1960s, less than half of halocarbon production was being applied to refrigeration and of that, the majority was being used to top-up leaky systems (Pearson, 2004). It is not too surprising, therefore, that detectable amounts of CFCs began showing up in the Earth's atmosphere (Lovelock, et al., 1973). This was also during a time in which many people, i.e. the consumers, began to question the wisdom of releasing so many "unnatural" chemicals into the environment. It was not until the 1970s, however, that the chemistry of stratospheric ozone was understood well enough that significant challenges began to assault the halocarbon industry.

2.1.1 Atmospheric Chemistry

Chapman proposed the first photochemical theory on the formation of ozone in 1930, which consisted of only four simple reactions that involved allotropes (different structural modifications) of oxygen—known as the Chapman reactions (Müller, 2009):

R1: $O_2 + h\nu \rightarrow 2O$
R2: $O + O_2 \rightarrow O_3$
R3: $O_3 + h\nu \rightarrow O + O_2$
R4: $O + O_3 \rightarrow 2O_2$

Where the photodissociation of molecular oxygen (reaction no.1, abbreviated here as R1) is balanced by the reaction between atomic oxygen and ozone (R4). This schema was accepted as being sufficiently precise in describing the observed vertical distribution of ozone until around 1960, when new rate constants fell out of agreement with newer atmospheric data obtained from rocket tests (Hunt, 1966):

> *"…the photochemical reaction scheme normally considered is no longer adequate, and there must be reactions occurring in the atmosphere which destroy ozone but which have been neglected in the past".*

A few years later, the very first measurements of nitrogen compounds became available, and it was proposed that NO*x* (mono-nitrogen oxides NO and NO_2) is produced in the stratosphere via the decomposition of nitrous oxide, N_2O:

R5: $$N_2O + O \rightarrow 2NO$$

Then in 1970, Crutzen proposed (Crutzen, 1970) that the presence of NO*x* may have an effect on the concentration profile of ozone in the stratosphere via a catalytic reaction that destroys ozone. Shortly after, Lovelock et al. (Lovelock, et al., 1973) discovered that CFCs, with long atmospheric lifetimes, were accumulating *globally* in the atmosphere. From this vantage point, Molina and Rowland (1974) developed a similar theory that CFCs, which bear similarities to N_2O in that they are both very stable at ground level where they are typically released, may also result in the catalytic destruction of ozone once diffused into the upper atmosphere, where solar radiation is much more intense:

R6: $$XO + O \rightarrow X + O_2$$
R7: $$X + O_3 \rightarrow XO + O_2$$
Net: $$O + O_3 \rightarrow 2O_2$$

Where X (X = NO for the nitrogen radical cycle and X = Cl for the chlorine radical cycle)[4] reacts with ozone to produce XO and O_2, and XO in turn reacts with free radicals of oxygen to reform X that is then free to react with more ozone yet again, i.e. a catalytic reaction. The net result is the same as reaction R4 (the destruction of ozone). When compared to ozone depletion mechanisms investigated by other researchers, Molina found that CFCs could result in greater ozone destruction than the natural mechanisms did (Molina, et al., 1974). At the time, however, the findings were only an unverified hypothesis.

[4] For discussion purposes, the cycle catalysed by hydrogen radicals X = H and/or OH was omitted, since it was found by Crutzen (1969) that this mechanism is not sufficient to explain and control the observed ozone concentrations in the stratosphere (i.e. it plays a part in the whole, but it is not a dominating reaction).

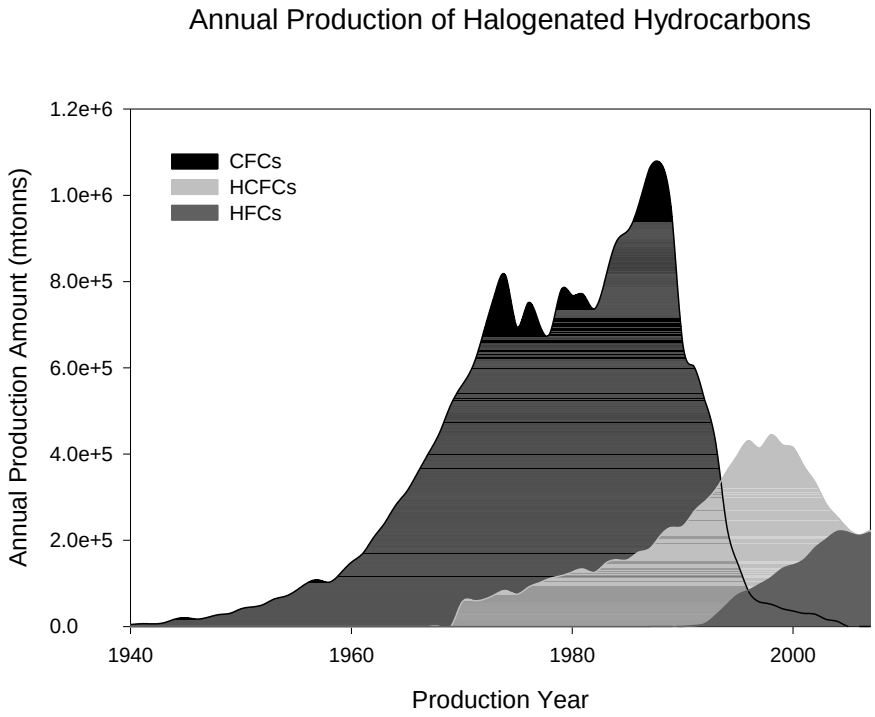

Figure 2-2: Annual production of refrigerants from 1940 through 2007 (AFEAS, 2010).

Although the unproven hypothesis was initially greeted with disbelief and controversy in the scientific community, many people (mainly consumers) began calling for a ban on the production and use of CFCs. As reflected in the production numbers for refrigerants shown in **Figure 2-2** above, increased public scrutiny actually led to an observable change in consumer behaviour after the original publication in 1974. Then, with public concern growing, the U.S. passed a ban that prohibited the manufacturing of CFCs as propellants in nonessential aerosol applications in 1977 (going into effective in 1978), followed by similar independent actions by several other countries (Benedick, 2004). However, without further policy changes to regulate non-aerosol uses (e.g. it is hard to argue that refrigeration is nonessential) the production of CFCs began to grow rapidly again in the early 1980s.

Industry strongly opposed any government sanctions, and publicly denied (Cook, 1994) that the scientific evidence supported the need to reduce CFC outputs. DuPont, the world's largest manufacturer of CFCs[5], went so far as to spearhead the creation of the *Fluorocarbon Program Panel* and, later, the *Alliance for Responsible CFC Policy* to dispute theories that CFCs harmed the environment (Public Citizen, 2011). For a time industrially led research resulted in conflicting models, and several scientists advocating against making any policy decisions before the science could mature (Smith, 1998).

It would be difficult to exaggerate the complexities involved. Ozone itself amounts to considerably less than one part per million of the atmosphere and depends on a myriad of complex physical, chemical and biological processes involving even more minute quantities of other gases (in parts per trillion) and convoluted natural forces such as weather and solar radiation (Benedick, 2004).

[5] In 1985, Du Pont held 50% of the large U.S. market and a 27% global market share, and was the only major producer to have a significant market position in all three major markets, the United States, Europe and Japan. The $600M CFC business was not particularly significant to Du Pont, representing only 2% of sales (Smith, 1998).

To describe such a complex process takes ever more sophisticated computer models. Since policymakers, for instance, require these models to simulate accurately decades into the future, their predictions are often checked against data collected from ground stations, balloons, rockets and satellites whereby further adjustments are made to bring the model predictions back into agreement with the aggregated data.

2.1.2 The Ozone "Hole"

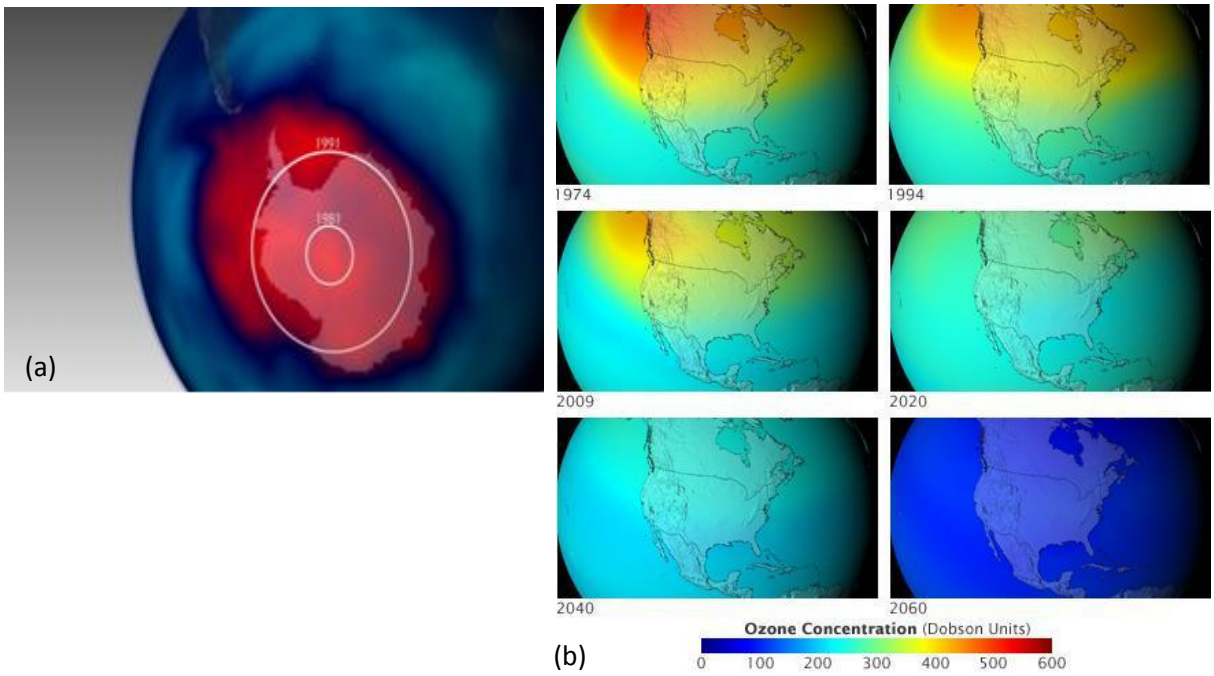

Figure 2-3: (a) A picture of the Antarctic ozone hole over the South Pole on September 14, 2011 (National Environmental Satellite, Data, and Information Service, 2011) and (b) predictions of ozone concentration if CFCs hadn't been banned (NASA, 2009).

Beginning in 1982 Farmer et al. first noticed a dramatic dip (around 40%) in annual ozone readings from a ground station in the Antarctica (UC Berkeley, 2007). It was originally thought that the reading was due to an instrument malfunction, but the following year still saw a drastic decline. Upon reviewing older readings, however, Farman discovered that the decline had really started back in 1977. The observation by Farmer and his team (Farman, et al., 1985) was later verified by NASA in 1984 using data collected from the satellite Nimbus-7 satellite. Although the satellite was continuously taking such readings since its launch in 1978, the processing of the data automatically precluded measurements outside of what scientists considered "reasonable" bounds for ozone (i.e. the data was considered erroneous and thus automatically ignored by the program used to log the data). This discovery soon gained international news coverage, and is now commonly known as the "ozone hole" (as shown in **Figure 2-3** above). Although the exact cause of the ozone hole was not definitively linked to CFCs at the time, the appearance of the phenomena did give a very visible face to the danger of ozone destruction.

The sudden appearance of the ozone hole spurred a public outcry for governments to take action, and resulted in a number of international agreements directly affecting the refrigeration industry. As laid out in the Montreal Protocol of 1987 (Powell, 2002) this included a schedule for the complete phase-out of ozone depleting substances such as CFCs worldwide (as summarized in **Table**

2-1 below). Instead of banning chemicals individually, the treaty allowed chemicals to be controlled as a combined "basket" by weighting each chemical's ozone depleting potential (ODP)[6] against production. A unique strength of the Montreal Protocol was that it was deliberately designed to be flexible so that amendments could be made (e.g. based on new scientific data) without negotiating a new formal treaty. According to the U.S. diplomat and chief negotiator for the Montreal Protocols (Benedick, 2004):

> *Perhaps the most extraordinary aspect of the Montreal Protocol was that it imposed substantial short-term economic costs in order to protect human health and the environment against speculative future dangers—dangers that rested on scientific theories rather than on proven facts.*[7]

The treaty effectively banned the production of CFCs and later HCFCs (which were originally designed to replace CFCs) in order to speed up the recovery of lost stratospheric ozone. Although the ozone layer appears to be recovering in recent years (see **Figure 2-4** below) it is highly unlikely that the Montreal Protocol will be amended to re-allow the use of CFC and HCFC refrigerants in the future. Any new refrigerants, therefore, must have zero ODP.

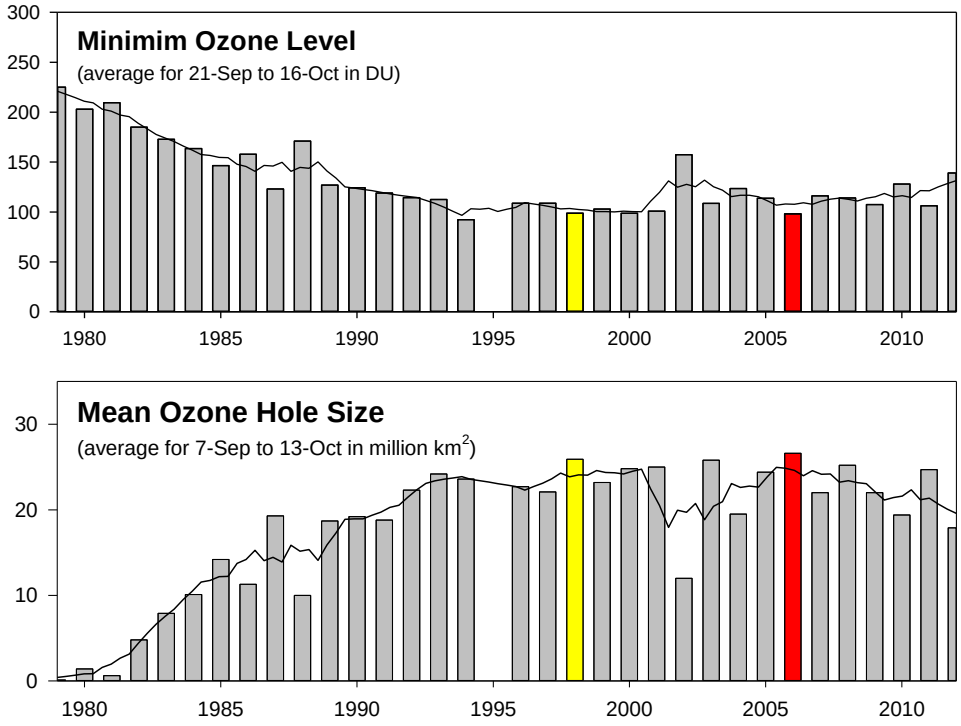

Figure 2-4: Severity of the ozone hole based on NASA data (NASA, 2012).

[6] *Ozone Depletion Potential* (ODP) defines the amount of degradation relative to trichlorofluoromethane (R-11) which has a fixed ODP value of 1.0.

[7] It is interesting to note, however, six months after the Montreal Protocol was initially signed, that the results of an international panel of scientists conclusively proved the ozone depletion theory first proposed by Molina and Rowland—CFCs and halons were now implicated beyond a doubt, including the ozone hole over Antarctica.

Ozone Depleting Substances	Developed Countries	Developing Countries
Chlorofluorocarbons (CFCs)	• Phased out end of 1995[a]	• Total phase out by 2010
Halons	• Phased out end of 1993	• Total phase out by 2010
CCl_4 (Carbon tetrachloride)	• Phased out end of 1995[a]	• Total phase out by 2010
CH_3CCl_3 (Methyl chloroform)	• Phased out end of 1995[a]	• Total phase out by 2015
Hydrochlorofluorocarbons (HCFCs)	• Freeze from beginning of 1996[b] • 35% reduction by 2004 • 75% reduction by 2010 • 90% reduction by 2015 • Total phase out by 2020[c]	• Freeze in 2013 at a base level calculated as the average of 2009 and 2010 consumption levels • 10% reduction by 2015 • 35% reduction by 2020 • 67.5% reduction by 2025 • Total phase out by 2030[d]
Hydrobromofluorocarbons (HBFCs)	• Phased out end of 1995	• Phased out end of 1995
Methyl bromide (CH_3Br) (horticultural uses)	• Freeze in 1995 at 1991 base levels • 25% reduction by 1999 • 50% reduction by 2001 • 70% reduction by 2003 • Total phase out by 2005	• Freeze in 2002 at average 2995-1998 base levels • 20% reduction by 2005 • Total phase out by 2015
Bromochloromethane (CH_2BrCl)	• Phase out by 2002	• Phase out by 2002

a. With the exception of a very small number of internationally agreed essential uses that are considered critical to human health and/or laboratory and analytical procedures.
b. Based on 1989 HCFC consumption with an extra allowance (ODP weighted) equal to 2.8% of 1989 CFC consumption.
c. Up to 0.5% of base level consumption can be used until 2030 for servicing existing equipment, subject to review in 2015.
d. Up to 2.5% of base level consumption can be used until 2040 for servicing existing equipment, subject to review in 2025.
e. All reductions include an exemption for pre-shipment and quarantine uses.

Table 2-1: Summary of Montreal Protocol control measures, including amendments (UNEP (United Nations Environment Programme), 2012).

2.1.3 Global Warming

The problem of global warming due to the greenhouse effect has received far less attention, but the issue is felt by many to be equally important (McLinden, et al., 1988). The greenhouse effect refers to the trapping of solar radiation from the sun by so called "greenhouse gases" in the atmosphere. Global warming then refers to the effect that additional manmade GHGs have on the planet, where it is believed that the increased concentration of these gases can lead to an increase in the average temperature of the earth. Because of this, in 1997, a complimenting treaty called the Kyoto Protocol was adopted by many countries to reduce the emissions of GHGs that have high global warming potentials[8]: namely CO_2, CH_4, NOx, SF_6, HFCs and PFCs (none of which are ODSs). **Figure 2-5** below shows GWP values alongside the ODPs for common refrigerants and candidates.

[8] *Global warming potential* (GWP) is defined as the ratio of the warming caused by a substance to the warming caused by a similar mass of CO_2 over some measured period of time (typically 100 years). The GWP of carbon dioxide (the reference fluid in this case) is therefore fixed at a value of 1.0, while water has a GWP of zero.

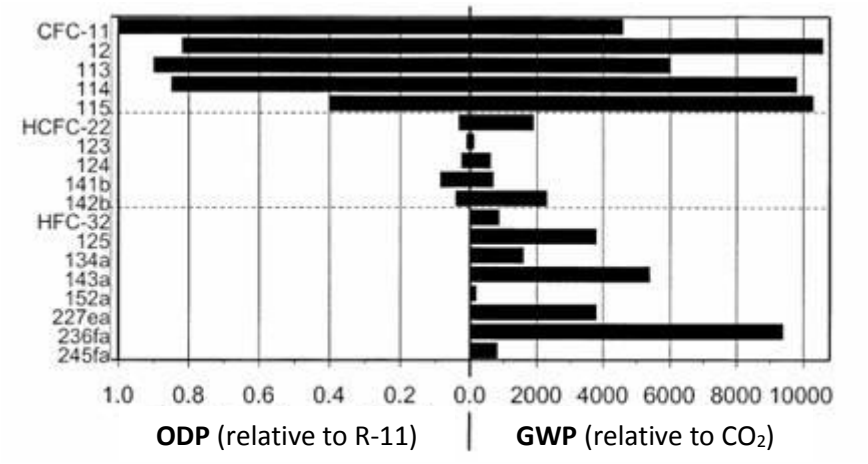

Figure 2-5: ODP versus GWP for common refrigerants and candidates (Calm, 2002).

The goal of the Kyoto Protocol is to reduce total emissions of these 6 greenhouse gases by at least 5% (with respect to their 1990 emissions) over the 2008-2012 period. Unlike the Montreal Protocol, however, which completely bans regulated ODSs, the Kyoto Protocol only limits the use of GHGs. There are also two additional things worth noting. First, the Kyoto Protocol only sets emission targets for “developed“ countries, and provides no clear-cut targets for emerging super-economies like China and India. Secondly, the treaty allows participating countries to buy and sell their agreed allowances of GHGs, largely resulting in a toothless treaty that is increasingly being ignored (leaving big loopholes for abuse). Perhaps the biggest hurtle to a consolidated effort is that the mechanisms effecting climate change are still not fully understood. This alone makes it extremely difficult for countries to make policy decisions based on model results for processes that are too complex to predict confidently. This has led countries such as the United States to withdraw their support, largely leaving the fate of the Kyoto Protocol in the hands of the European Union. So although HFCs (replacing HCFCs, which in-turn have replaced CFCs) have zero ODP, their use is now being challenged by the EU with a directive that bans so-called "F-gas" (fluorochemical) refrigerants in new automobiles that have GWPs exceeding 150 for a 100-yr time integration (Calm, 2008). Because of [this] future refrigerants will likely be limited to those that have a GWP ≤ 150 (while maintaining the requirement of having zero ODP).

Refrigerant contributions to global warming, however, have both a direct and indirect component that must be considered. The direct component is the result of a refrigerant's GWP, while the indirect component is related to the amount of CO_2 released in the process of producing the power needed for operating the refrigeration unit. The fundamental problem is that, in light of environmental concerns such as ozone destruction and global warming, there exist no "ideal" alternatives that can replace halocarbon refrigerants. From CFCs to HCFCs and now to HFCs and PFCs one may ask, *"What is so special about halocarbon refrigerants?"* Such a question can be fundamentally understood by tracing the evolution and development of refrigerants through history.

2.2 Evolution of Refrigerants

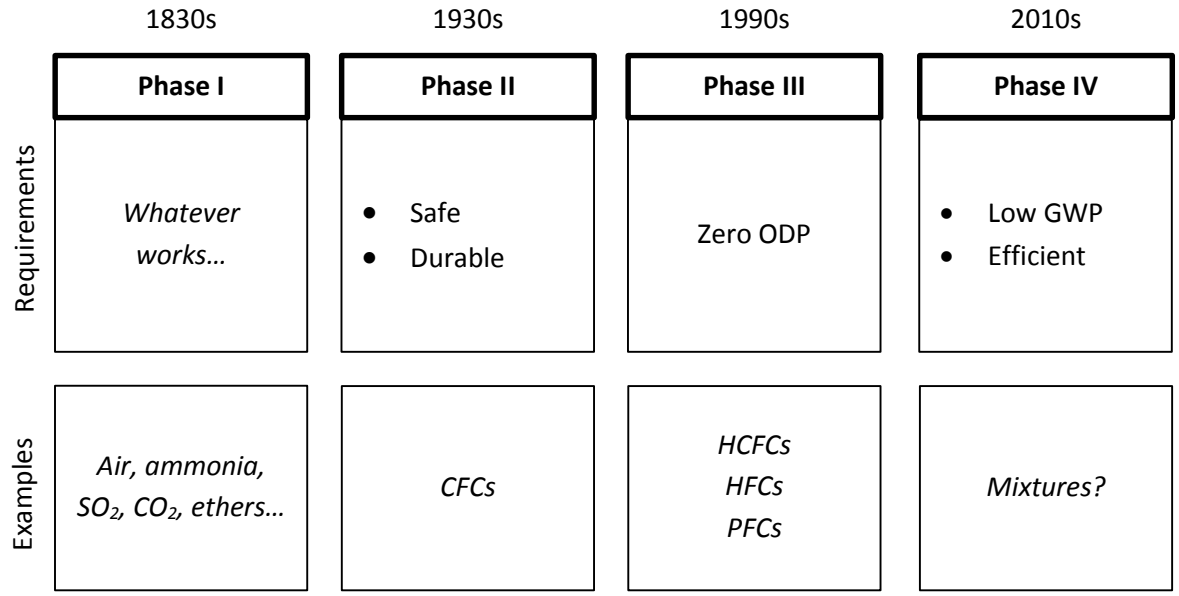

Figure 2-6: Historical perspective on the progression of refrigerants, from early uses to the present, based on the work of Calm (2008).

Modern refrigeration was first introduced by Perkins in the 1830s, who is credited with building the first modern vapour-compression refrigeration cycle, and is the basis for most of the processes still in use today. According to Perkins (Perkins, 1835):

> *Now the object of my invention is so to use a volatile fluid [refrigerant] that the same (having been evaporated by the heat or caloric[9] contained in the fluid about to be reduced in temperature) shall be condensed and come again into the vessel to be again evaporated and carry off further quantities of caloric.*

In other words a volatile refrigerant fluid is used to generate cooling in a closed circuit, where early refrigerants were simply "whatever worked" and was easily available to the user at the time. The first generation of refrigerants, therefore, see **Figure 2-6** above, typically consisted of solvents and other volatile chemicals that were highly flammable, toxic or both. Accidents were frequent and so, during the next 100 years after its introduction, the use of refrigeration was limited to specialty applications like e.g. freezing water into ice.

In order for refrigeration to expand directly into the household, safe and durable refrigerants were first required. This was achieved through the introduction of fluorochemicals during the 1930s, which then dominated the refrigeration industry for next approximately 60 years during the second phase (or generation) of refrigerants. Although non-toxic to humans, these refrigerants were a little too stable and have since been linked to the destruction of the protective ozone layer in the stratosphere (as just discussed in the previous section). This resulted in a shift from CFCs to HCFCs and now to HFCs and PFCs starting in the early 1990s, i.e. the so-called third generation of refrigerants.

[9] For now it is sufficient to equate caloric with the concept of heat. Caloric, or the French word "calorique" as it was first introduced, is explained in further detail in Chapter 3.1, starting on Page 15.

Since refrigeration cycles are also "powered" cycles that e.g. use electricity (primarily generated from the burning of fossil fuels), the focus in the search for the next generation of refrigerants has since been expanded to include energy efficiency too.

2.2.1 Requirements for Working Fluids

There are, therefore, a number of competing characteristics (or properties) that a refrigerant must now meet in today's market. Some of these requirements are essential for modern refrigeration systems, such as those listed in **Table 2-2** below. Others, still, are desired to maintain the operability (and reliability) of such systems, as are listed in **Table 2-3** below.

Essentials for Refrigeration
• **Chemical stability**
• **Safety considerations:** ✓ non-flammable ✓ non-toxic ✓ environmentally benign
• **Thermodynamic properties**

Table 2-2: Necessary requirements for refrigeration systems.

Desirable for Reliability	Desirable for Operability
• **Lubricant solubility**	• **Ease of leak detection**
• **Material compatibility**	• **Amenable to recycling**
• **Low moisture solubility**	• **Ease of handling**
• **Transport properties**	• **Recharging**
• **High dielectric strength**	• **Low cost**

Table 2-3: Desirable requirements for both machinery reliability (left column) and to facilitate operations (right column).

The most essential characteristic of a refrigerant is likely chemical stability, because all other properties would be meaningless if the refrigerant decomposed or reacted during use. Stability, however, can also be a liability that can lead to long atmospheric lifetimes and high GWP values (recall **Figure 2-5**, Page 12). Atmospheric lifetimes need to be long enough to prevent the formation of photochemical smog (and acid rain depending on the compound) but short enough to avert environmental concerns over atmospheric accumulation. Since all halogenated compounds will absorb infrared radiation, the most effective approach to producing low GWP alternatives is to develop compounds with shorter lifetimes. This can be accomplished, for instance, by increasing the hydrogen content of a refrigerant, but this adversely also increases the flammability of the component and in many cases reduces efficiency (which indirectly increases CO_2 production).

It then follows that the task of finding refrigerants that meet all or most (or even some) of these requirements is quite difficult. Future refrigerants, therefore, will likely represent a compromise between some of these conflicting requirements.

2.2.2 The Potential of Mixtures

In the early years of refrigerant development, for instance, Midgley defined only eight elements with appropriate chemical properties that lend themselves to being used in the formulation of refrigerants: carbon, nitrogen, oxygen, sulphur, hydrogen, fluorine, chlorine and bromine (Midgley, Jr., 1937; Midgley, Jr., 1938). All other elements in the periodic table violated one or more of the essential requirements listed in **Table 2-2**—stability, safety or thermophysical properties required for "operations". The majority of the periodic elements, for instance, are metals in their elemental form and combine with other elements to form non-volatile compounds that are fundamentally incapable of being used as working fluids in a vapour compression cycle. Others, still, must now be eliminated in view of the evolving environmental regulations previously outlined. After discarding chlorine and bromine, this leaves only carbon, nitrogen, oxygen, sulphur (which is suspect/debatable), hydrogen and fluorine (in correct proportions with hydrogen) which have the appropriate chemical properties for the purpose. As these are quite definitely not similar enough in their various properties to provide a direct replacement for an existing refrigerant, a mixture of different components (conceivably made of these remaining elements) may well be tailored to meeting all or most of the requirements listed in **Table 2-2** and **Table 2-3**.

3 Vapour-Compression Cycles

Refrigeration is the "cooling" of something or someplace (or system) by lowering its temperature relative to its surroundings (reservoir or sink). This cooling is achieved by first removing "heat" from the system, and is maintained by continuously (or intermittently) removing the heat that is thermally driven back into the system by the second law of thermodynamics, through any material exchanged with the system's environment, or through other means like radiation, electrical energy, etc. In air conditioning, for example, where heat is removed from the warmer environment, the required cooling is not only influenced by the temperature of the warm air outside the system, but also by the humidity of the air that enters to be cooled. Any excess humidity has to first be condensed, which requires the heat of condensation to be removed from the system too.

In the past, this cooling (or refrigeration effect) was achieved by using blocks of ice to absorb heat from their surroundings. This is why, for instance, household refrigerators are sometimes jokingly referred to as *ice boxes*. The harvesting of the ice they originally used, however, was severely limited by seasonal changes and by its storage and transportation during the warmer months of the year. As a result, the practice of harvesting ice began to give way to mechanical devices using chemical refrigerants like e.g. ammonia as early as the 1880s (Briley, 2004). These early industrial refrigerators, therefore, allowed manufactures to continuously produce ice throughout the year, and not just during the winter months. Then after the introduction of CFC refrigerants during the 1930s, the practice of using ice eventually gave way to smaller (household) refrigerators based on a vapour compression cycle to provide the cooling. Most of today's refrigeration systems are still derived from this basic design. The present chapter is therefore devoted to their description.

Some historical context within the developing framework of thermodynamics is first provided. This is then followed by an explanation of the (fully reversible) Carnot refrigeration cycle, which naturally gives way to a description of an actual (real) vapour compression system. The discussion then expands into process modelling (or simulation) aspects of the cycle, and concludes by describing the key thermodynamic properties that influence the performance of refrigerants in such processes.

3.1 Some Historical Context

During the time of Sadi Carnot heat was considered a conserved quantity called *calorique*[10], a finite quantity that behaved much like a fluid. This means that when a material expands upon heating, for instance, that this expansion is due to the space in which the calorique occupies within it. Heat then flows due to the escaping calorique particles from within a crowded heat source (where the calorique particles are fighting for position) into colder heat sinks having much more space to accommodate these same calorique particles. Even the heat resulting from the cannon boring experiments of Benjamin Thompson (Count of Rumford) was thought to have been caused by "liberated" calorique particles that were removed alongside metal shavings produced during boring

[10] Although it is now more commonly known as "caloric", the French spelling is used here in honor of the French chemist Lavoisier who first introduced it as "calorique" (for obvious reasons). While stating that *calorique* need not be considered as a real material, Lavoisier nevertheless included it, along with light (lumineux or luminous), in his revised periodic table of chemical elements in his *Traité Élémentaire de Chimie* of 1789 (Cajori, 1922). The idea of heat (or calorique) as a material became firmly established soon after.

(Count of Rumford, 1798). Since temperature was also known to increase with the amount of heat added, it was thought that the temperature maybe a direct measure of the amount of calorique (or heat) an object contained. Of course, as time went on, evidence contrary to the calorique theory began to challenge this dominant viewpoint of the time.

The boiling of pure water is one such example, for instance, where the liquid water absorbs heat until it begins to boil at 100°C. The uptake of heat causes a change of phase (or state) and not a change of temperature during the transition. If temperature was a direct measure of the amount of heat a material contains, then what causes the phase to change? This observation, for instance, led to the concepts of *heat capacity* and *latent heat*, material specific properties, which are e.g. "stored" in the vapour phase and can be recovered in a condenser that converts the steam back into liquid water.

These observations were difficult to reconcile with the calorique theory of the time, and they have since been rationalized in terms of the fundamental laws of thermodynamics. It is not the heat that is conserved, but it is the quantity $(\delta Q + \delta W)$ that is conserved. This law was observed again, and again and is now simply referred to as the first law of thermodynamics, which describes the internal energy state of a system. This in turn spurred further investigations into the interrelations of heat (Q), work (W) and energy (E). Eventually more patterns were recognized regarding these variables, and the interrelationships were then incorporated into further theories (or laws) that form the foundations of thermodynamics known today (see **Appendix A** for additional details).

3.2 The Carnot Cycle

Carnot was unaware of the fundamental laws (or universal truths) that thermodynamics is now known to be built upon. Instead, interesting enough, his results were based on thought experiments alone, where he drew parallels between how heat engines and water wheels operate. He first conceived of an ideal, frictionless, water wheel in which every single drop of water is successfully converted into usable work. He then envisioned an ideal heat engine that operates much like the ideal water wheel, where all of the heat goes into the motion of the piston. In actual practice, however, besides frictional losses, not all of the water successfully makes it into the trough that rotates the wheel (e.g. some splashes out). Likewise, this led Carnot to postulate that not all of the heat transported in a heat engine goes into the motion of the piston producing usable work i.e. there must be a limit to their efficiency, a condition of the second law thermodynamics. Much as the water wheel is dependent on the height in which the water falls, the efficiency of a heat engine similarly depends on the temperature difference (or driving force) between the hot and cold reservoirs (Magie, 1899):

> *"The motive power of a waterfall depends on its height and on the quantity of the liquid; the motive power of heat depends also on the quantity of caloric used and on what may be termed the height of its fall, that is to say, the difference of temperature of bodies between which the exchange of caloric is made. In the waterfall the motive power is exactly proportional to the difference in level between the high and low reservoirs. In the fall of the caloric the motive power undoubtedly increases with differences in temperature between the warm and cold bodies."*

The parallels Carnot drew from the water wheel, as shown in **Figure 3-1** on the following page, allowed him to gain insight into the key-factors that influence the efficiency of heat engines, which take in heat in order to perform work.

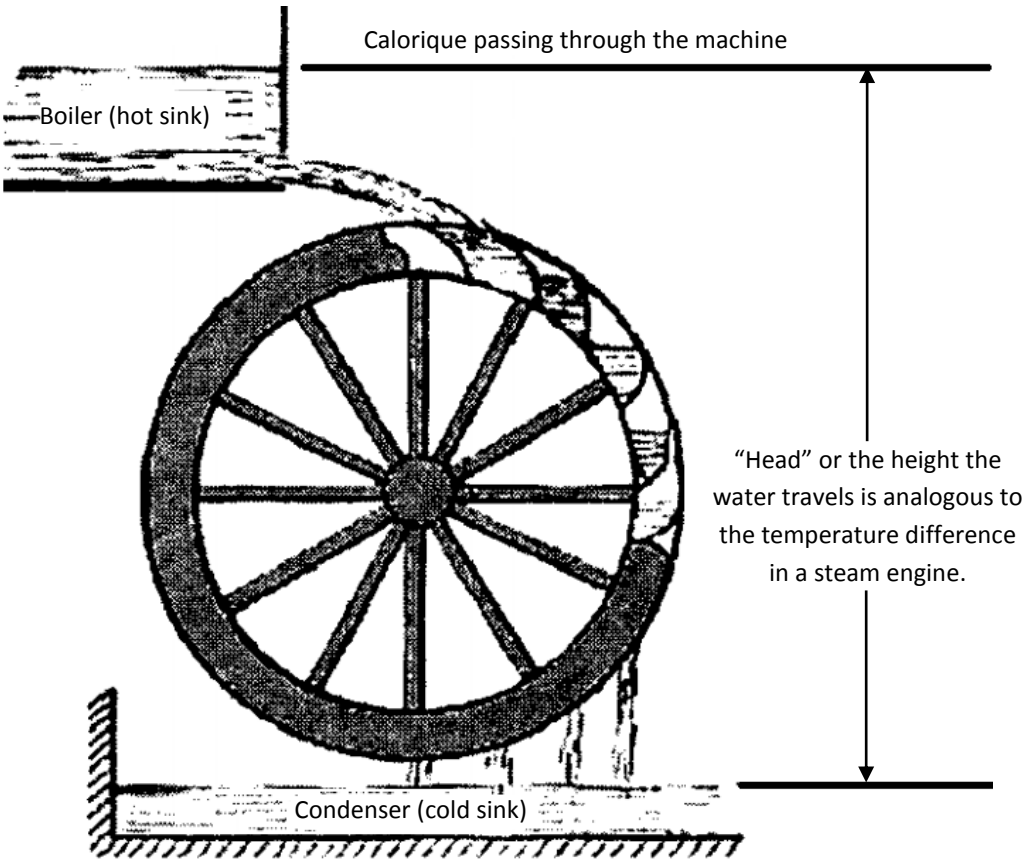

Figure 3-1: Carnot's steam engine/waterwheel analogy (Lienhard, 2008).

3.2.1 Thermal Efficiency

The *thermal efficiency* (η) of a heat engine is therefore described as the amount of work produced (W_{output}) divided by the amount of heat removed from the hot reservoir (Q_{hot}) to produce the work:

$$\eta = \frac{\dot{W}_{output}}{\dot{Q}_{hot}} \approx 1 - \frac{\dot{Q}_{cold}}{\dot{Q}_{hot}}$$
$$\eta_C = 1 - \frac{T_{cold}}{T_{hot}} \qquad (3\text{-}1)$$

where the first law energy conservation equation reduces to $\dot{W}_{output} = (\dot{Q}_{hot} - \dot{Q}_{cold})$. For $\eta = 1$ (100% thermal efficiency) all of the heat $\dot{Q}_{hot}$ absorbed by the working fluid must be used to produce work $\dot{W}_{output}$, without rejecting any wasted heat $\dot{Q}_{cold}$ to the cold reservoir in the process. According to the second law of thermodynamics, however, this is not feasible: some energy is always wasted in the process of using it or converting it into other usable forms like e.g. $\dot{Q}_{hot} \rightarrow \dot{W}_{output}$. Not even for a fully reversible Carnot process, for which the total entropy change is zero, can the thermal efficiency η_C reach 100%, since this would also violate the third law of thermodynamics by requiring $T_{cold} =$

0 K. The alternative of maximising η_C by letting $T_{hot} \to \infty$ is also not realistic. The limiting thermal efficiency of the equivalent Carnot-cycle, therefore, is always less than 100%, and the true thermal efficiency of the actual cycle will (practically) remain below the Carnot value due to further non-idealities (or non reversible opeartions experienced in the real cycle). The actual thermal efficiencies of real heat engines, for instance, rarely exceed 0.35 (Smith, et al., 2001).

3.3 The Refrigeration Cycle

A refrigeration cycle is just a type of vapour compression cycle, which in itself is similar to a heat engine. Instead of taking in heat in order to produce usable work, however, a refrigeration cycle takes in work in order to remove heat. Essentially it is a heat engine run in reverse—a *heat pump*—that requires the use of a working fluid (or refrigerant) according to some very basic principles:

- Boiling the working fluid stores energy.
- Condensing this same fluid gets it back.
- Control is obtained (or maintained) by manipulating the pressure.

Sensible heat from the cold reservoir (i.e. the process-side) gets absorbed at low pressure as latent heat by the evaporating working fluid, and is later rejected to the hot reservoir as the same refrigerant condenses at a higher pressure. The refrigerant is then cooled and returned to its pre-boiling state, and the cycle repeats. As shown in **Figure 3-2** below, this process involves four key-operations that manipulate the fluid's PVT behaviour:

1. **Evaporation** involves moving from state-① to state-② (or to the superheated state-②*) on the pressure-enthalpy diagram of **Figure 3-2** (a). The *cold* refrigerant enters the evaporator at its bubble point pressure at state-①, already partially vaporised at some vapour fraction *x* (sometimes referred to as quality, *q*). Sensible heat is then absorbed from the cold box (i.e. the process-side) as latent heat by the remaining liquid refrigerant as it vaporises. This continues until all of the remaining liquid becomes a vapour at state-② on the saturated vapour (dew point) line. In practice, however, design allowances are often made to *superheat* the vapour to state-②*. Compared to the ideal cycle shown in green of **Figure 3-2** (a), the extra heat taken in by the refrigerant as sensible heat is to protect the compressor from any line losses realised in the actual process, like e.g. the pressure drop across the evaporator and radiative heat losses from the suction line. The formation of condensate would lead to wet-compression that could permanently damage the compressor, or at the very least hinder its performance. The cycle's refrigeration effect (or capacity) is then equivalent to the enthalpy difference between state-① and state-② (or state-②* for the superheated vapour case).

2. **Compression** involves moving from state-② to state-③ on the temperature-entropy diagram of **Figure 3-2** (b) for the idealised cycle, and from state-②* to state-③* in the real process. This change of state is equivalent to the work required to remove the heat absorbed in the evaporator. The move from state-② to state-③ is then equal to the isentropic work required to compress the working fluid in the idealised process, whereas the move to state-③* includes compressor inefficiencies due to e.g. mechanical friction in the actual system (hence the higher discharge temperature); both compression steps end at a superheated vapour state. The change in pressure brings the heated vapour molecules of the fluid closer together for

economical heat transfer in the condenser, where the liquid-liquid bonds broken in the evaporator are reformed upon cooling.

3. **Condensation** involves moving from the superheated vapour state-③ to state-④ on the pressure-enthalpy diagram of **Figure 3-2** (a) for the idealised cycle, and from state-③* to state-④* in the actual process. This change of state is equivalent to the heat dumped (or rejected) to the hot-reservoir, and includes any "extra" heat that is added e.g. due to compressor inefficiencies of the actual process. The sensible heat is first removed from the superheated vapour states of ③ and ③*, followed by the latent heat of vaporisation required to condense the saturated vapour to a saturated liquid at state-④ on the bubble point curve. In some cases the saturated liquid may be subcooled to state-④* in the actual process to ensure that the refrigerant enters the expansion device as a total liquid (which increases the refrigeration effect/capacity by reducing throttling losses). Like in the evaporator of the real process, there also exists a small pressure drop accompanying the flow of fluid across the condenser.
4. **Expansion** involves moving from state-④ to state-① on the pressure enthalpy diagram of **Figure 3-2** (a) for the idealised process, and from state-④* to state-①* in the actual process. This change of state is required to reset the "cycle" back to its original starting position at the inlet conditions to the evaporator. For the idealised process the pressure of the saturated liquid state-④ is let-down to the pressure of the evaporator at state-① (the bubble point pressure of the refrigerant at the temperature of the evaporator). The pressure let-down from state-④* to state-①* in the real process, on the other hand, results in a lower vapour fraction due to the subcooling of state-④* from the condenser (i.e. more liquid is available to vaporise in the evaporator). Both pressure reductions take place using an expansion device like e.g. a valve, and occurs quickly enough so that the process is essentially isenthalpic ($\Delta h = 0$). This restores the refrigerant to its original starting condition at the inlet of the evaporator, poised for vapourisation, and the cycle repeats.

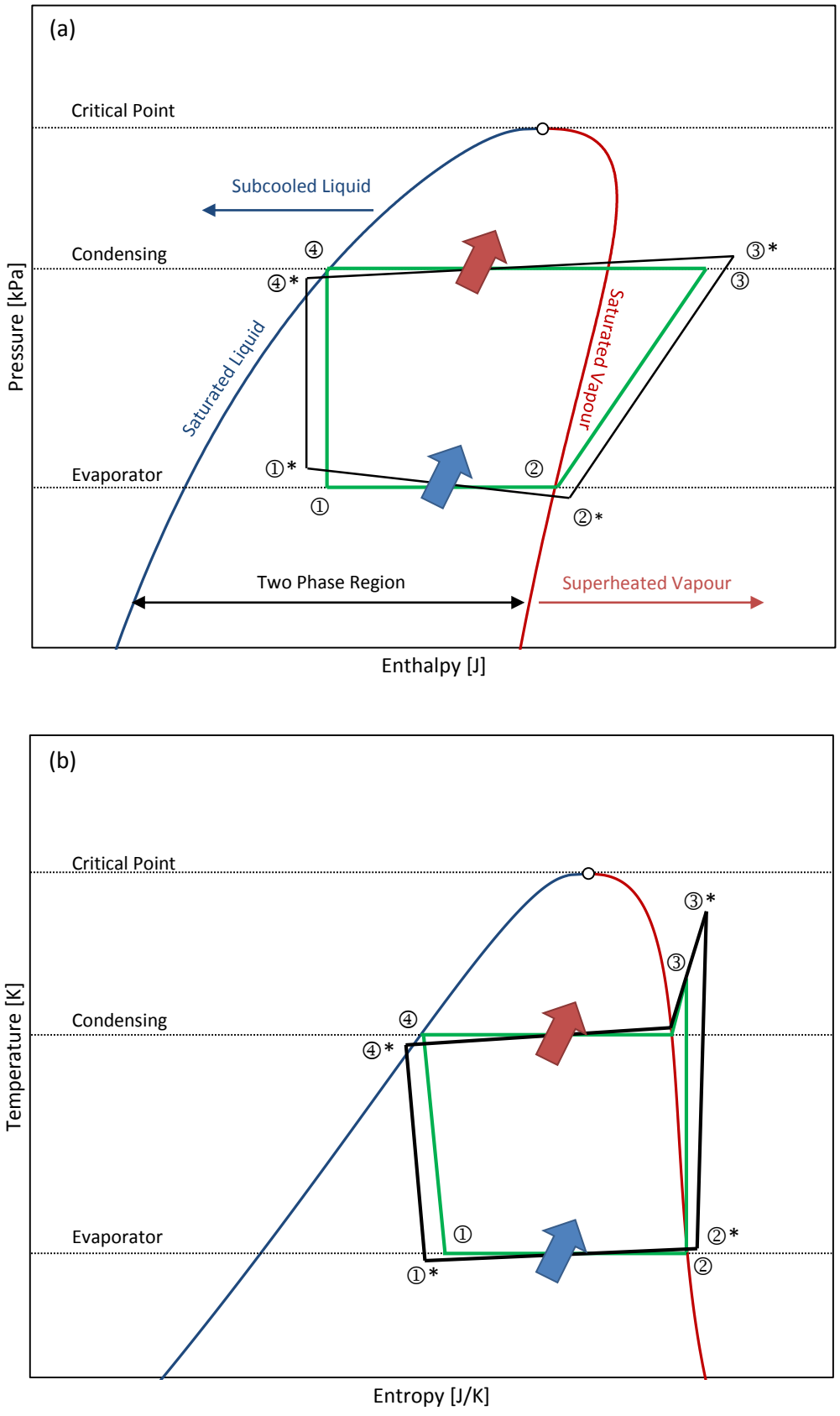

Figure 3-2: Pressure-enthalpy (a) and temperature-entropy diagrams (b), including operating paths for an ideal refrigeration cycle (-----, green line) compared to those of an actual cycle with losses (-----, black line).

3.3.1 Coefficient of Performance

Since refrigeration cycles are just heat engines run in reverse, their cooling performance is just the inverse of the thermal efficiency, called the *coefficient of performance* (COP):

$$COP = \frac{Q_{cold}}{W_{input}} \approx \frac{Q_{hot}}{Q_{cold}} - 1$$

$$COP_C = \frac{T_{cold}}{T_{hot} - T_{cold}} \tag{3-2}$$

$$COP_{ideal} = \frac{Q_{cold}}{W_{s,input}}$$

Heat is absorbed at the lower temperature T_{cold} as Q_{cold} in the evaporator, which requires an external source of energy W_{input}, before it is rejected at the higher temperature T_{hot}. If an actual process operated between $T_{cold} = 5$°C (278.15 K) and $T_{hot} = 35$°C (308.15 K), for instance, then the limiting value of the coefficient of performance could be calculated for a Carnot refrigeration process operating between the same T_{cold} and T_{hot} temperatures, i.e. $COP_C \cong 9.27$, which is only achievable if all steps in the process are fully reversible, i.e. always in equilibrium with the next and preceding steps. The real process, however, will experience a number of irreversibilities e.g. mechanical and thermal inefficiencies in the compression step that cause the actual COP value to be less than the limiting Carnot value, and also less then the ideal value COP_{ideal} assuming isentropic compression $W_{s,input}$). Therefore the higher the COP value the more efficient the refrigeration process is, and the less work it requires to achieve a given cooling effect.

3.4 Practical Simulation of the Refrigeration Cycle

As discussed in the previous chapter, the basic vapour compression cycle consists of four key-operations: evaporation, compression, condensation and expansion. If both the inlet and outlet conditions for each of these unit operations are known, for instance, then simple flash calculations can be used to obtain all the required state information needed to evaluate the performance of any given system. This is typically the case for existing cycles, where readings are directly taken from the working process and then compared against available equipment datasheets (i.e. design-case data). Alternatively, since existing processes rarely operate at design-case conditions, these same equipment data sheets can also be used to build an in depth simulation model of the process. Where detailed modelling equations, e.g. which account for equipment specific geometries and materials of construction etc., can be used to characterize the mass, momentum and energy conservation equations needed to uniquely describe each component of the process. The specification of a typical shell-and-tube heat exchanger, for example, would include most, if not all, of the following information:

- Shell and tube-side fluid properties used to design the exchanger.
- The type and size of tubes, number of passes, materials of construction and baffle details controlling fluid flow.
- The overall heat transfer coefficient (including fouling resistance) used to determine the exchanger's heat duty at the design conditions (including the reported design limits).

The geometric configuration of the equipment fixes the design pressure drop and, by proxy, the mass and momentum balances, while the assumption of several mechanical and thermodynamic parameters fixes the exchanger's thermal performance, i.e. heat transfer coefficients and the surface area required for the heat to exchange.

A detailed process simulation is often required, for instance, for *rating-type problems*. Where the engineer(s) must determine if the existing equipment will be able to handle any new process changes, e.g. like a new refrigerant with properties different from those used for the original design. Although such a scenario is within the present work scope of the project, no experimental apparatus was available to base such a model on. Failing to have a working cycle, i.e. first-hand knowledge of some working process, this project was forced to rely on process descriptions found in the open literature. These descriptions, however, rarely include the required information necessary to completely define detailed process models. Only fundamental model equations, therefore, can be used for each component of the process, where the results can later be "tuned" (at least somewhat) to more closely match limited experimental information. For newer installations this simplification should not impact the overall aim of the project (to identify novel refrigerant replacements), but it should be noted that such an approach is likely limited in accuracy when applied to the analysis of existing systems.

Once a matching process simulation is obtained for some process, it can then be used to predict cases outside of the experimental conditions it was fitted to match. As long as the simulation cases are not too far removed from the fitting conditions, the results should be sufficiently precise in all of but the final stages of the design process, where a more detailed rating would be desired. Since the present scope of work is mainly focused on identifying novel refrigerant replacements, the simulated (or targeted) conditions should not widely change from one working fluid to the next. Although the components of fluids and their compositions will change as independent variables to be optimised, only those fluids that shows similar properties, and thus performance, as the original refrigerant used in the design of the system are of true interest.

The added complexity of including more detailed model equations is, therefore, safely neglected here at present, and can be added at a later date in further research e.g. using the experimental refrigeration testing-apparatus that is currently being developed. Accordingly, only the fundamental equations required to model each component, as depicted in **Figure 3-3** below, are provided in the sub-chapters that follow.

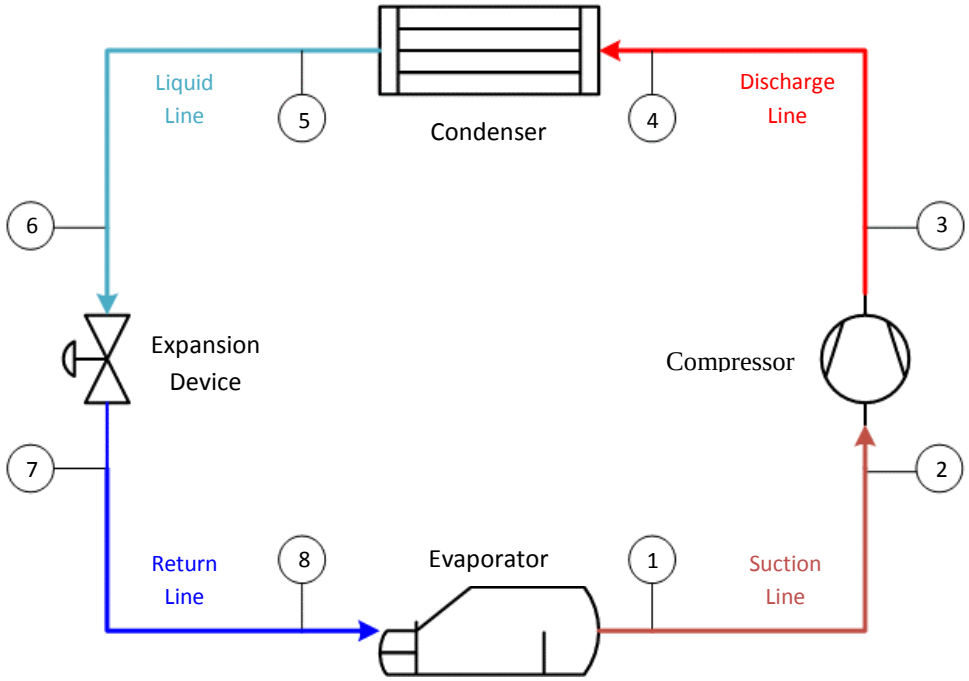

Figure 3-3: General schematic of a vapour compression refrigeration cycle.

3.4.1 Evaporator/Condenser

Heat exchange in vapour-compression cycles takes place mainly in the evaporator (cooling side) and the condenser. Since the main goal of a refrigeration cycle is to remove (or transfer) heat, a sufficiently precise heat exchanger model is essential for evaluating potential alternatives. The heat exchanger model not only impacts the amount of heat transferred, but also the required refrigerant flow rate for a given cooling scenario.

If for example a room has to be cooled using economical feasible heat exchangers, the evaporator temperature has to be significantly below the room temperature and the returning compressed liquid will be significantly warmer than the outside temperature to maintain a sufficient temperature gradient for heat transfer. This means that the boiling temperature at suction pressure must be significantly under the room temperature (but still above 0°C to prevent ice formation) and the dew point at the compression side significantly above the outside temperature (typical temperatures are around 60-70°C).

For the simplified calculation, however, only the basic heating and cooling requirements of the evaporator and condenser are truly necessary. The heat duty of the exchangers are thus calculated using a fundamental enthalpy balance around each unit:

$$\dot{Q} = \dot{m} \cdot [h(T_{out}, P_{out}) - h(T_{out}, P_{out})] \tag{3-3}$$

where $\dot{Q}$ is the rate of heat exchanged in either the evaporator or condenser, $\dot{m}$ is the mass (or molar, $\dot{m}/M_W$) flow rate of the working fluid, and $h(T_{out}, P_{out}) - h(T_{out}, P_{out})$ is the specific enthalpy change for the heat exchanged.

The heat duty of the evaporator, i.e. the cooling capacity of the cycle, then fixes the required refrigerant flow rate for the process at a given set of inlet and outlet conditions for the exchanger. As

a first-pass estimate the pressure drop across the evaporator can be neglected if necessary, while the inlet pressure can be chosen (or iteratively solved) to give a favourable approach temperature for heat transfer purposes, e.g. 10°C below the evaporator temperature. If the outlet temperature is higher than the saturation temperature at that pressure, the refrigerant leaves the evaporator as a superheated vapour, where the amount of superheat can then be determined by subtracting the heat of vaporisation contribution from the overall duty of the evaporator. In practice, however, the evaporator will have a non-zero pressure drop which can later be used to make small adjustments to the calculated duty (including the amount of superheat) required to match available experimental data. Similar parallels can also be made for the condenser, where its duty is equivalent to the amount of heat removed in the evaporator *plus* any heat added during the compression step *minus* line losses (which are typically minimal).

3.4.2 Compressor

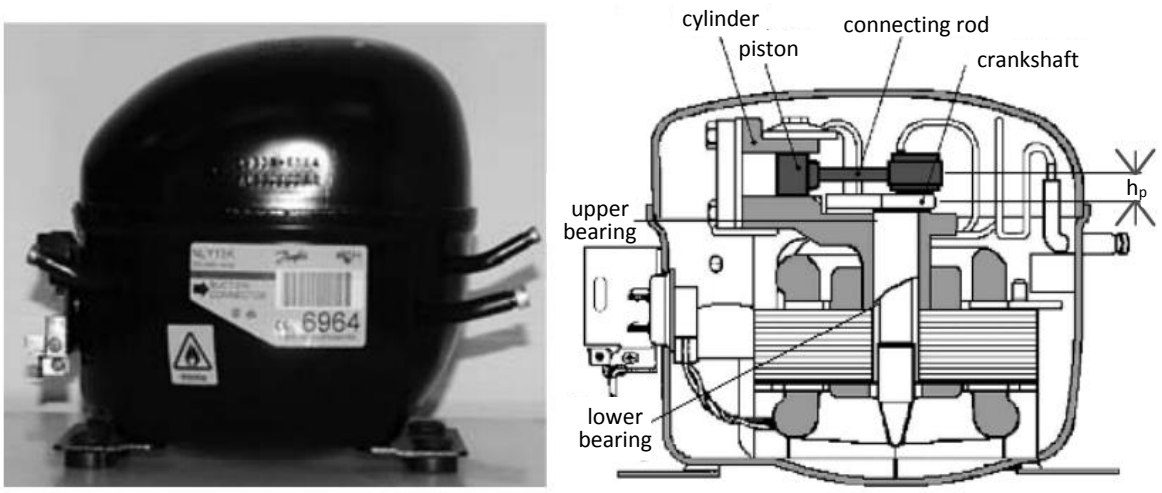

Figure 3-4: Picture and schematic of a typical hermetic reciprocating compressor (Estupinan, et al., 2009).

The compressor is the most complex component of the process. One of the most common types of compressors used in the refrigeration field is the reciprocating, hermetic (sealed) compressor, also known as a piston, or constant volume, compressor. A picture and schematic of this type of compressor is shown in **Figure 3-4** above for a common household refrigerator. The motor and compressor are directly coupled on the same shaft and contained within the same sealed-housing. Lubricating oil is collected at the bottom of the can where it is in free contact with the refrigerant, which also acts to cool the motor windings prior to entering the piston-cylinder assembly (Domanski, et al., 1983). As a first approximation an isentropic model can be used to define a reasonable upper bound for the mechanical efficiency of the processes, i.e. work output divided by the energy input. The results of the reversible (isentropic) process can then be adapted to the real world by applying efficiency factors:

$$POWER\ (technical\ work) = \dot{m}\int_{P_{in}}^{P_{out}} VdP \approx \frac{\dot{m}\Delta h_s}{\eta_s\eta_m} = \frac{\dot{m}[h_s(T^*_{out}, P_{out}) - h(T_{in}, P_{in})]}{\eta_s \cdot \eta_m} \tag{3-4}$$

where η_s and η_m are the isentropic and mechanical efficiencies respectively, and T^*_{out} is the calculated discharge temperature assuming an isentropic compression path moving from $P_{in} \rightarrow P_{out}$. Of course, in practice, compression is not carried out reversibly, i.e. leakage and fluid friction, along with external mechanical and electrical losses, lead to a higher work input being required. The isentropic efficiency term η_s, therefore, is used to move from the compressed isentropic state point (T^*_{out}, P_{out}) to the true discharge state at (T_{out}, P_{out}). The calculated power can be further adjusted by also adding a mechanical efficiency term η_m to correct for motor related losses. In the environment of a process simulator, this type of calculation is typically carried out via iteration to find T^*_{out}. Instead, as an alternative, a compressor can also be viewed as a pressure pump with a given head:

$$HEAD\ (specific\ work) = \int_{P_{in}}^{P_{out}} VdP \approx \frac{\Delta h_s}{\eta_s\eta_m} = \frac{P_{in}V_{in}}{\left(\frac{k-1}{k}\right)}\left[\left(\frac{P_{out}}{P_{in}}\right)^{(k-1)/k} - 1\right] \tag{3-5}$$

where $PV^k = constant$ is applied to the head integral by assuming that $k = c_p/c_v$ remains constant along an isentropic compression path (for an ideal gas). The benefit of this algebraic form is that Δh_s can be explicitly solved for a given P_{out} and inlet conditions, i.e. no iteration is required. Similar efficiency corrections can also be added here, but their absolute values may be different than those determined using the former calculation route. Equation (3-4), however, is the most rigorous of the two methods for calculating isentropic work, since its accuracy is most intimately linked to the correct description of the required caloric properties of the refrigerant (i.e. it is equivalent to using Mollier charts directly, traditional enthalpy-entropy diagrams). The magnitudes of the efficiency factors, therefore, are also functions of the physical properties of the refrigerant. Additional efficiency factors could also be added like e.g. the volumetric efficiency (the actual refrigerant mass flow rate divided by the ideal refrigerant mass flow rate), but they often require detailed knowledge of the process to be correctly determine. By omitting these factors their contributions to the overall efficiency are effectively lumped into the isentropic and mechanical efficiency terms that are used in this work, i.e. $\eta \approx \eta_s\eta_m$. Although not ideal, this approach is sufficiently precise for most modelling scenarios.

3.4.3 Expansion Device

A constant flow area expansion device, sometimes called a capillary tube or flow restrictor, is employed in many of the heating and air conditioning systems in use today. It separates the high pressure side from the low pressure side of the process, and is primarily responsible for maintaining the minimum pressure at the condenser at which all the flowing refrigerant can condense. When the refrigerant passes through this device, it experiences a large and very quick pressure drop which causes the working fluid to partially vaporise according to the pressure (and bubble point temperature) of the evaporator. The flow rate of the refrigerant through the capillary tube is therefore

controlled by the inlet pressure, which in turn is a function of the condenser's performance. If the outside air temperature increases, for instance, than less heat is rejected by the condenser due to the lower temperature difference (or thermal driving force) between the air and the refrigerant. The liquid then enters the capillary with a higher enthalpy, or less subcooling, which acts to reduce the refrigerant's flow rate through the device. Since the compressor's capacity remains unchanged, the pressure builds up in the condenser until a new equilibrium is reached. As the condenser pressure increases it also pulls up the pressure of the evaporator so that a higher mass flow rate is required to maintain the same cooling capacity prior to the change, i.e. to counteract the smaller enthalpy change in the evaporator. In a steady state simulation, however, such a description is not required. It is only mentioned here to highlight the role that the capillary tube plays in the overall balance (or operating conditions) of the system. The same applies to an expansion valve with a constant orifice diameter. In practice, however, the open area for fluid flow through the valve is typically regulated via a process control scheme.

Although a lot of work goes into the design of the expansion device, it represents a relatively minor component from a capital standpoint. Detailed calculations are therefore not necessarily required for this component, even for a rating-type problem. Since the expansion of the gas through the device does not perform any work, and as the device is assumed to be sufficiently insulated from heat transfer to and from the surroundings, the process can be considered adiabatic:

$$H(T_{in}, P_{in}) = H(T_{out}, P_{out}) \tag{3-6}$$

where H_{in} is fixed by the condenser performance, and H_{out} by the evaporator and suction line conditions of the compressor.

3.5 Key Thermodynamic Properties

The relevance of this project's results will then depend on how accurately the thermodynamic properties of potential working fluids can be predicted. Sufficiently precise descriptions of component vapour pressures, heats of vaporisation and heat capacities etc. are essential for obtaining reliable results from process simulation models. Large property errors, for instance, can lead to incorrect rankings of the potential refrigerant replacements. It is therefore important to understand the dominating thermodynamic properties that effect refrigerant performance, pure or mixture:

- The **critical temperature** (T_c) of a refrigerant affects the height of the two-phase region, and defines the upper limit of the dome on the P-H diagram. As the condenser temperature approaches the critical point, for example, the compressor requires more work to compress the same amount of refrigerant due to the higher suction pressure, i.e. increased gas density. This translates into lower COP values for a given cooling capacity and refrigerant. Potential drop-in replacements, therefore, will need to have critical points either similar or higher than the working fluid(s) they are replacing.
- The **normal boiling point** (T_b), on the other hand, defines the lower operational limits of the refrigerant, where the saturated temperature of the boiling liquid in the evaporator must be sufficiently lower than the process-side so that a favourable temperature difference exists to drive the heat exchange. This is just another way of saying that the bubble point pressure must also be greater than that of the process-side to prevent contamination of the refrigerant

from system leaks. Household refrigerators and air-conditioning units, for example, require bubble point pressures greater than 101.325 kPa at the evaporator conditions. If the normal boiling point of the refrigerant is greater than the required evaporator temperature, the fluid cannot be used unless under vacuum (which is typically something, from an operational standpoint, that should be avoided).

- The **latent heat of vaporisation** (Δh_v) of a refrigerant then determines the width of the two-phase region, and is represented as the difference between the saturated liquid and saturated vapour lines of the P-H diagram. The refrigerant's **vapour pressure** (P^s) controls the slope and shape of the bubble point line, while the dew point line is mainly determined from the refrigerants **PVT** behaviour, especially its vapour phase properties. Since the latent heat of vaporisation approaches zero at the critical point, the slope of the saturated vapour enthalpy has no choice but to change in order to intersect with the relatively insensitive slope of the saturated liquid line to complete the bell-curve. High **vapour molar heat capacities**, therefore, tend to skew the two-phase region to the right, which can lead to significant performance losses and undesirable "wet compression" if sufficient superheat is not added in the evaporator to compensate.

4 Review of Equation of State Models

In the present chapter a brief history of the development of equations of state is provided. This chapter begins[11] with a fundamental overview of the basic thermodynamic relationships used in equilibrium calculations, with emphasis on those required for the implementation of equations of state. Following this basic review, the virial equation is shown to be a series expansion of the ideal gas equation, where the virial coefficients relate to the actual intermolecular forces occurring between molecules. The equation of van der Waals and the other related cubic equations of Redlich-Kwong, Soave-Redlich-Kwong and Peng-Robinson are then discussed. The chapter then concludes by describing the key concepts of Wertheim's theory and the SAFT equation of state, which are then used to formulate/describe the PC-SAFT equation (which is employed in this work).

4.1 Fundamentals

Although the focus of the present research is not on phase equilibrium calculations, the method (or approach) used in such calculations determines how other thermodynamic properties like e.g. enthalpy and molar volumes are calculated (which are of direct interest). The methods used to represent fugacity in phase equilibrium relationships, therefore, is of fundamental importance.

As shown (see **Appendix A**) the equality of chemical potentials at equilibrium can be replaced by the so-called isofugacity condition. Mathematically, this can be written for a hypothetical system consisting of phases α through π in equilibrium as,

$$\hat{f}_i^{\alpha}(Final) = \hat{f}_i^{\beta}(Final) = \cdots = \hat{f}_i^{\pi}(Final)$$

where $\hat{f}_i^{\alpha}(Final)$ represents the mixture fugacity $(\wedge)$ of component i in phase α at equilibrium $(Final)$, which is also equal to the mixture (or solution) fugacity of that same component in any other phase. In the case of mixtures, at low pressures the fugacity is nearly identical to the partial pressure of the compound considered (Gmehling, et al., 2012). For practical applications, however, this relationship is not very helpful, since the connection to measurable quantities T, P and the composition (liquid and vapour phases) is missing. Therefore, auxiliary properties such as activity coefficients (γ_i) and fugacity coefficients (φ_i) have since been introduced (see **Appendix A**):

$$\gamma_i \equiv \frac{\hat{f}_i^L}{x_i f_i^{\circ}}$$

$$\varphi_i^L \equiv \frac{\hat{f}_i^L}{x_i P} \quad \text{and} \quad \varphi_i^V \equiv \frac{\hat{f}_i^V}{y_i P} \tag{4-1}$$

When these different definitions for the fugacities are substituted into the isofugacity criterion, two different approaches can be derived for the description of phase equilibria:

[11] This survey originally began with the formulation of the ideal gas equation of state, including historical context; however, since the historical development of this equation is more of an interest-story than prerequisite for discussion purposes, it has been more appropriately placed (for the curious reader) in **Appendix B** instead.

$$\overbrace{\left[y_i\varphi_i^L P = x_i\gamma_i f_i^{\circ}\right]}^{\substack{gamma-phi\\approach}} \equiv \left(\hat{f}_i^L = \hat{f}_i^V\right)$$
$$\left(\hat{f}_i^L = \hat{f}_i^V\right) \equiv \underbrace{\left[x_i\varphi_i^L = y_i\varphi_i^V\right]}_{\substack{equation\ of\ state\\approach}} \quad (4\text{-}2)$$

The first approach is commonly referred to as the gamma-phi (γ-φ) approach, where an activity coefficient model like Wilson, NRTL or UNIQUAC equation is typically used to calculate the activity coefficients for the description of the liquid phase[12], and an equation of state like the van der Waals equation is used to calculate the fugacity coefficients for the description of the vapour phase. The second approach, on the other hand, uses an equation of state like e.g. PC-SAFT to calculate the fugacity coefficients in both phases (φ^L-φ^V) for a substance, which are required to calculate other thermodynamic properties like e.g. H, G and A.

4.2 Equations of State

Foster (Foster, 2011) defines an equation of state (EOS) as "a mathematical model that is capable of describing the Pressure-Volume-Temperature (PVT) behaviour of both the vapour and liquid phase of a pure substance or mixture." This definition, however, excludes the ideal gas equation. Instead, it is much more accurate to say that an *ideal*-EOS is one that is capable of describing the PVT behaviour of real substances (mixture or pure) *which may appear in more than one phase*.

From the formulation of the first equation of state in 1834 to the present day, vast amounts of research has led to numerous equations of state developments. In fact, if you type in the phrase "new equation of state" (including quotes) within Google Scholar you obtain roughly 3,340 search results (Google)! As pointed out by Ramjugernath (Ramjugernath, 2000), given the number of equations of state that have been developed, it is virtually impossible to provide a comprehensive summary. Given the abundance of material available e.g. Walas (Walas, 1985), Sengers et. al (Sengers, et al., 2000), Orbey and Sandler (Orbey, et al., 1998), Kontogeorgis and Folas (Kontogeorgis, et al., 2010), Goodwin et. al (Goodwin, et al., 2010) and Robinson and Chao (Robinson, et al., 1986), just to name a few, it is not the goal to provide an exhaustive survey but to attempt to link the development of equations of state into a cohesive picture for discussion purposes. For convenience, therefore, most of these models may be broadly categorized into one of the following four groups (Gmehling, et al., 2012):

- Viral Equations of State
- High Precision Equations of State
- Cubic Equations of State
- Advanced Equations of State

Of the four groups above, this project focuses on the practical industrial use of the advanced equation of state PC-SAFT. The flow of ideas from this point forwarded, therefore, are limited to only those EOS having historical significance, and to the concepts required for understanding the development of the PC-SAFT equation itself. It then follows that a detailed discussion of high precision (multiparameter)

[12] This approach is covered in detail in previous work by the author (Satola, 2011)

equations of state, although used in property packages such as REFPROP (which is also employed here), is outside the present scope of work, and thus is safely neglected.

4.3 Viral Equation of State (Series Expansion)

As follows from the discussion of intermolecular forces in **Appendix C**, these forces influence all matter and are responsible for the various phases in which matter can appear: gas, liquid, or solid. Since the gas law treats the behaviour of all fluids as *perfect gases* (i.e. ideal behaviour), the ideal gas equation is fundamentally incapable of predicting the condensed phases of liquid or solid. It then follows that this simplified PVT relationship is also incapable describing the phase-split (transition) between phases as well, which is fundamentally important for the description of many industrialised processes such as distillation or refrigeration for instance. These insights, however, are nothing new.

The limitations and inexactness of this equation has been quite well known, even as it applies to gases within its domain of validity. As reportedly shown by Regnault in 1847 (Xiang, 2005), at best, the equation provides only an approximation of the true PVT behaviour for even simple gases such as nitrogen. Observed pressures can either be lower or higher than those calculated from this equation. This equation, however, successfully describes the limiting (ideal) behaviour of all gases as $P \to 0$. The equation, therefore, represents an important starting point used in the development of ever more sophisticated equations of state, ones in which are capable of describing the true behaviour far removed from the ideal limit. One early adaptation of this relationship was the virial equation of state.

One-way to correct for the fundamental inaccuracies incorporated into the ideal gas equation (see **Appendix B**), is to add simple correction terms to it. In this regards the concept of "compressibility" is useful, where the compressibility factor (Z) acts to correct for the calculated ideal gas value:

$$P = Z\left[\frac{nRT}{V}\right] = Z\left[\frac{RT}{\upsilon}\right] \tag{4-3}$$

where $Z = \upsilon_{real}/\upsilon_{ideal}$, υ_{real} is the "actual" molar volume occupied by a substance, and υ_{ideal} is the ideal molar volume for the same substance. Therefore, the compressibility factor for a molecule that behaves "ideally" would have a value of one, or at least a value very close to one (such as for simple gases near atmospheric conditions). This value, however, will move away from one (ideal behaviour) depending on the net effect of the intermolecular forces occurring between the actual molecules. The value of Z, for example, becomes < 1 when the real volume of a molecule is smaller than its ideal volume (compaction caused by forces of attraction), and Z becomes > 1 when it is larger than its expected ideal volume (expansion created by forces of repulsion).

Another way to correct the calculated behaviour of the ideal gas equation is to add correction terms to it, which is essentially what the virial equation does. The viral equation is just a rearrangement of the ideal gas equation in terms of the compressibility factor Z to describe real gases, which is then expanded into an infinite series in powers of either $1/\upsilon$ or pressure:

$$Z = \overbrace{\sum_{n=1}^{\infty} \frac{\mathcal{B}_n}{(\upsilon - \upsilon_0)^{n-1}}}^{=P\left[\frac{\upsilon}{RT}\right]} = \overbrace{\sum_{n=1}^{\infty} \mathcal{B}_n(\rho - \rho_0)^{n-1}}^{\equiv P\left[\frac{1}{\rho RT}\right]} = \overbrace{\sum_{n=1}^{\infty} \mathcal{B}'_n(P - P_0)^{n-1}}^{=P\left[\frac{\upsilon}{RT}\right]} \tag{4-4}$$

$$Z = \overbrace{1}^{\substack{for\ an\\ ideal\ gas\\ reference}} + \overbrace{\left[\frac{\overbrace{\mathcal{B}_2(T)}^{\substack{second\ virial\\ coefficient}}}{\upsilon_{real}} + \frac{\overbrace{\mathcal{B}_3(T)}^{\substack{third\ virial\\ coefficient}}}{\upsilon_{real}^2} + \cdots\right]}^{\substack{corrected\ for\\ real\ gases}} \tag{4-5}$$

$$= 1 + \rho * \mathcal{B}_1(T) + \rho^2 * \mathcal{B}_2(T) + \cdots$$

$$= 1 + P * \mathcal{B}'_1(T) + P^2 * \mathcal{B}'_2(T) + \cdots$$

where $\mathcal{B}_1 = 1$ represents the ideal-gas term in the expansion, and $\mathcal{B}_n$ $(n > 1)$ are functions in temperature called *viral coefficients* (not to be confused with $\mathcal{B}'_n$). Virial coefficients, therefore, are only used to describe the coefficients of the series expanded in terms of molar volume (or equivalently molar density), where it is typically more common to use the notation $B = \mathcal{B}_2$ for the second virial coefficient, $C = \mathcal{B}_3$ for third virial coefficient, $D = \mathcal{B}_4$ for the fourth virial coefficient, etc. It is often more convenient, however, to use pressure as the independent variable in the expansion. So although the parameters $\mathcal{B}'_n$ are not "technically" in themselves virial coefficients, they still may be related to the virial coefficients like $\mathcal{B}_n$ by a set of conversion (or inversion) formulas (Dobbins, et al., 1988); after all, pressure-volume-temperature are interrelated, and therefore the coefficients of these equations must be too.

Since $Z(T, \rho)$ is not generally the same function for all gases, it then follows that the temperature-dependence of the virial coefficients must differ as well. The virial coefficients, therefore, should be a measureable quantity in themselves. Just as the compressibility factors for gases relate to the deviations observed in the ideal gas equation to the behaviour of real gases, the virial coefficients should also be a measure of the actual molecular interactions occurring between real molecules (which has been experimentally verified).

The empirical verification that the virial coefficients are a "type" of measurable quantity, however, is not why the equation receives so much attention. Instead, it is important because it has a rigorous theoretical foundation. It can be derived from statistical mechanics, which provides exact analytical relationships between the virial coefficients and the interactions between molecules in isolated clusters. As stated elsewhere (Sengers, et al., 2000), it is then found that "*B [the second viral coefficient] depends upon interactions between pairs of molecules, C [the third viral coefficient] upon interactions in a cluster of three molecules, D [the fourth viral coefficient] upon interactions in a cluster of four molecules, and so on.*" In fact, the term virial comes from the Latin word "vis" meaning force; thus, the virial coefficients take into account the interaction forces between the molecules (Rao, 2003). Most importantly, the experimental verification of the nature of virial coefficients supports the statistical framework of thermodynamics, which relates what is happening on the microscopic level (individual molecular contacts) to bulk quantities such as work, heat and energy.

Figure 4-1 below shows the experimental second and third virial coefficients for argon, and is used to describe the typical behaviour of the virial coefficients. It then follows that at very low temperatures B is of little importance, and the positive quantities of C and higher coefficients dominate the expression—molecules become sticky—except at high temperatures where molecules may approach ideal gas behaviour and B becomes negative (Poling, et al., 2001). Since the virial equation of state is based on a series expansion, additional terms can always be added to very accurately describe available experimental PVT data. However, the virial equation is typically truncated after the third term due to the difficulty of determining the required higher-order virial coefficients. Furthermore, the equation is only applicable to substances existing in a single phase and is classically only applied to the calculation of properties within the gas phase.

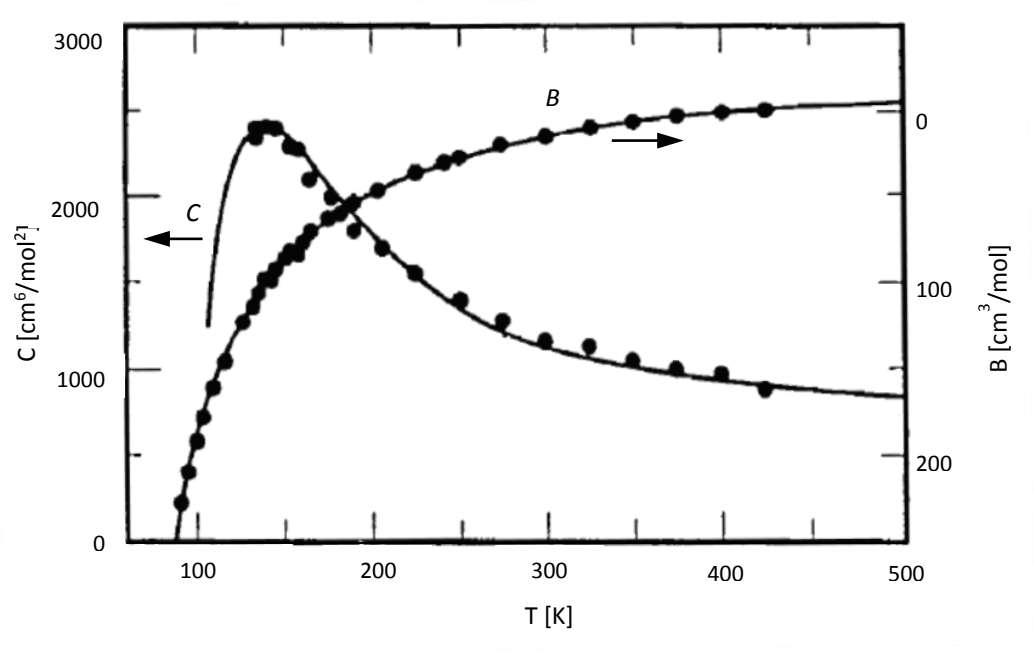

Figure 4-1: Second and third virial coefficients for argon with experimental points and curves calculated from an accurate binary potential energy function (in-kind to **Figure 4-6** starting on Page 48)—based on figure 9-8 from Pitzer (Pitzer, 1995).

4.4 Cubic-Family of Equations of State

Through experimentation (observations) it is quite well known that substances can exist in one of three phases, and which of those phases a substance takes then depends on the intermolecular forces occurring between the molecules of that substance (or mixture) and the state (or conditions) in which the molecules themselves are in. Furthermore, *all* substances have the "opportunity" to exist in anyone of these phases; therefore, *all* substances will experience a phase transition (phase-split) when moving from one phase into the next. Like energy, a substance does not simply cease to exist in one phase and then pop into existence in another—mass *is* a continuum, mass *is* conserved (see **Appendix D**).

4.4.1 Van der Waals (vdW) Equation

Several different routes lead to the infamous van der Waals equation of state, each with their own merit given in explanation. For people interested in the historical developments of such equations, however, it becomes exceedingly "muddy" to sift through these various, and often tidy,

viewpoints. The problem lies in the organization of these explanations (or stories), because tidiness is simply not a characteristic attributed to such developments in this world. The story of van der Waals equation is no less different. Nonetheless, the discussion is (at present) being limited to a derivation which is conveniently based on the ideal gas equation. For an excellent historical narrative on the origins of this equation, however, the works of Klein and Brush (Klein, 1974; Brush, 1974) are highly recommended.

In this regards, the van der Waals equation can then be thought of as a "corrected" form of the ideal gas equation. This equation not only can describe gases, but can also describe the behaviour of a system near its gas-liquid critical point (i.e. it can describe phase transitions)—something which the ideal gas equation and virial equations cannot do. The physicist and mathematician J.D. van der Waals first published his now famous equation in 1873:

$$\overbrace{\left[P+\frac{a}{v^2}\right]}^{\substack{pressure\\ corrected\ for\\ attractive\ forces}} * \overbrace{(v-b)}^{\substack{molar\ volume\\ corrected\ for\\ repulsive\ forces}} = RT \tag{4-6}$$

where a and b are essentially just two empirical parameters that can be fitted to reproduce experimental results; even so, it is possible to give them a physical interpretation. It then follows that parameter b (the so-called *effective molecular volume,* or simply called the *covolume*) corrects for the actual volume of real molecules, and the *attraction parameter* a then corrects for the actual pressure exerted by these same molecules.

The attractive forces then affect the kinetic energy of the molecules (i.e. the ability of each molecule to move and exert pressure). The internal energy of an ideal gas only depends on the temperature, and therefore a correction term is needed for higher densities (such as in liquids). This is why the "corrected" pressure has the form $(P + a/v^2)$. Moreover, actual molecules have finite sizes (e.g. they are often viewed as hard-spheres having a definite volume), and thus the volume available to each of these molecules for motion is reduced by $(v - b)$. Parameter b then represents the volume occupied by each molecule.

The van der Waals equation, for instance, can be rearranged to the following pressure-explicit form $[P = f(v, T)]$:

$$\overbrace{P=\frac{RT}{(v-b)}-\frac{a}{v^2}}^{pressure\ explicit\ form} \tag{4-7}$$

which is a unique function of both the molar volume and the system's temperature. Alternatively, the van der Waals equation can also be written into a polynomial-form in terms of either the molar volume or the compressibility factor:

$$\overbrace{v^3 - \left(b + \frac{RT}{P}\right)v^2 + \left(\frac{a}{P}\right)v - \left(\frac{ab}{P}\right) = 0}^{polynomial\ forms}$$
$$Z^3 - \left(\frac{bP}{RT} + 1\right)Z^2 + \left[\frac{aP}{(RT)^2}\right]Z - \left[\frac{abP^2}{(RT)^3}\right] = 0 \qquad (4\text{-}8)$$

These equations are cubic equations, and therefore allow for more than one solution (i.e. not a unique solution). Therefore, in certain ranges of pressure and temperature, switching from one solution (or root) to the next causes a change in the calculated molar volume or compressibility factor, which is exactly what is required during a phase transition (see **Appendix D**). The S-shaped isotherm witnessed by Thomson in 1871 (Walas, 1985; Rowlinson, 2003)—the continuity of the liquid and vapour phases—can therefore be described using the van der Waals equation of state. Since the van der Waals equation is cubic (of the third degree in volume or of the third degree in compressibility), any subcritical isotherm will then have three real positive roots, whereas any supercritical isotherms will only have one real root. For the subcritical case, it then follows that the smallest root corresponds to the liquid phase (the left side of the envelope) and the largest root corresponds to the vapour phase (the right side of the envelope). These are characteristics of the cubic equation, and are mathematically imposed by the critical point.

4.4.1.1 The Principle of Corresponding States

It then follows that the van der Waals equation is also capable of describing the behaviour of a system near the gas-liquid critical point. Mathematically the critical point is a point of inflection, and may be found by equating the first and second derivatives to zero at the critical volume:

$$\left(\frac{\partial P}{\partial V}\right)_T = \left(\frac{\partial^2 P}{\partial V^2}\right)_T = 0 \qquad (4\text{-}9)$$

This relationship, therefore, can then be applied to the van der Waals equation at the critical point:

$$\left(P_C - \frac{a}{V_C^2}\right)(V_C - b) = RT_C \qquad (4\text{-}10)$$

$$\left(\frac{\partial P}{\partial V}\right)_T = -\frac{RT_C}{(V_C - b)^2} + \frac{2a}{V_C^3} = 0 \qquad (4\text{-}11)$$

$$\left(\frac{\partial^2 P}{\partial V^2}\right)_T = -\frac{2RT_C}{(V_C - b)^3} + \frac{6a}{V_C^4} = 0 \qquad (4\text{-}12)$$

These same equations can then be solved simultaneously to obtain the parameters (a and b) in terms of the critical properties of a substance:

$$a_c = 3P_C V_C^2 = 27R^2 T_C^2 / 64P_C$$
$$b_c = V_C/3 = RT_C/8P_C \qquad (4\text{-}13)$$
$$Z_C = 0.375$$

where the critical compressibility factor Z_C is predicted to be 0.375 *for all fluids*. This is quite high for instance, since an average critical compressibility of 0.257 is obtained from more than one-thousand components within the Dortmund Databank (DDBST GmbH, 2012). The van der Waals equation, therefore, can only expect to give, at best, a qualitative description of the gas-liquid critical point for most substances. In fact, like the ideal gas equation, the van der Waals equation of state is only of historical interest nowadays, since it represents another common starting point for devising ever more reliable, and complex equations of state.

Regardless of the inadequacies of the van der Waals equation, the qualitative nature of the equation was sufficient to draw a conclusion of great significance, the *Principle of Corresponding States*, which is suggested when parameters a and b (which are typically fitted to experimental data) are eliminated from the van der Waals equation in terms of their critical equivalents (a_c and b_c). The result of this operation follows from

$$(P_r + 3/V_r^2)(3V_r - 1) = 8T_r \qquad (4\text{-}14)$$

where the ratios $P_r = P/P_C$, $V_r = V/V_C$, and $T_r = T/T_C$ are called *reduced properties*, and the equation above is then called the reduced van der Waals equation of state. Of course, any equation written in the form $P = f(V, T)$ can likewise be written in terms of reduced properties, i.e. a *reduced equation of state* e.g. written in terms of the dimensionless compressibility factor:

$$Z = f(T_r, P_r) = f(T_r, V_r) = f(P_r, V_r) \qquad (4\text{-}15)$$

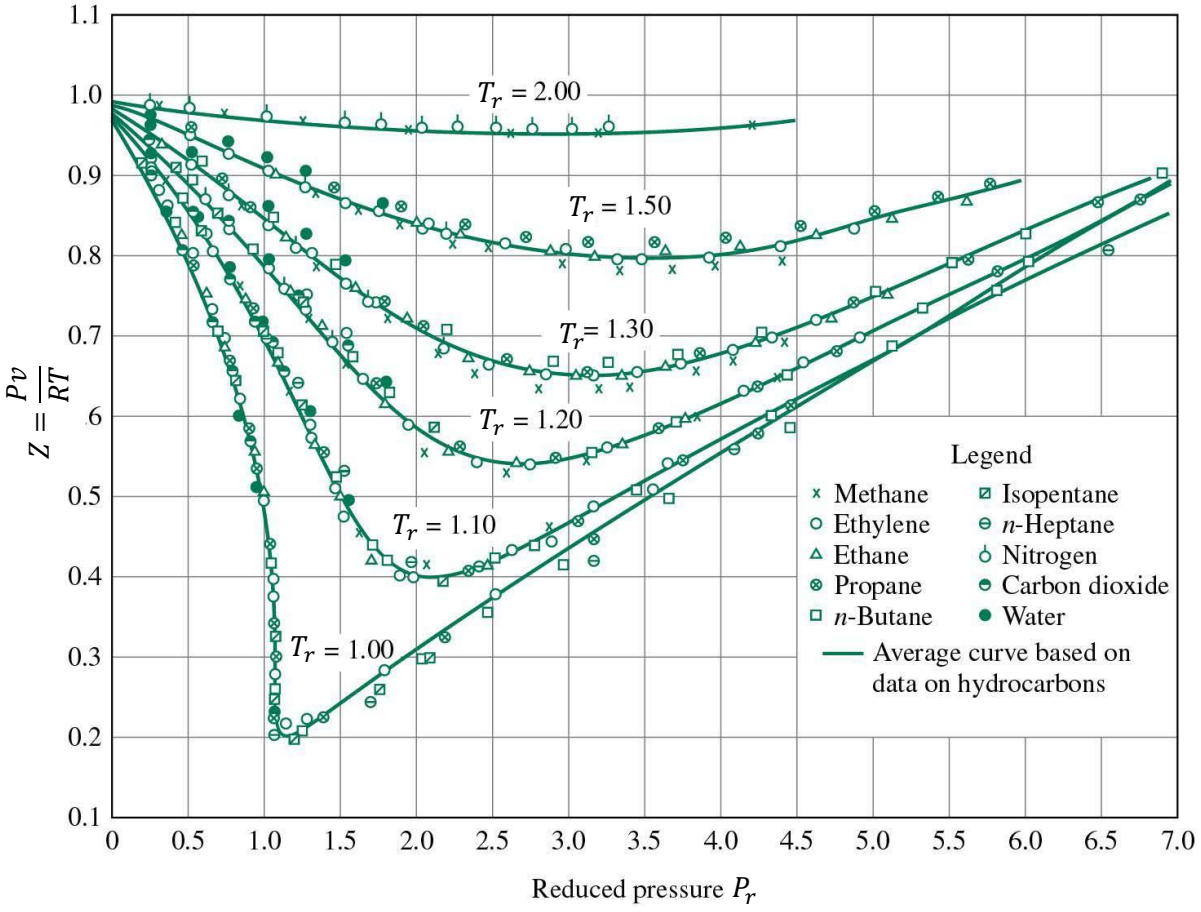

Figure 4-2: Compressibility factor chart for a select number of hydrocarbons, carbon dioxide and water in terms of reduced pressure P_r at various reduced temperatures T_r (Su, 1946).

A reduced EOS, therefore, is applicable *in principle* to any substance, whereby any substances that have the same reduced properties are then said to be in *corresponding states* with each other. This means, for example, that on a plot of Z vs. P_r that the lines of constant T_r should (ideally) be the same for every substance. As shown in **Figure 4-2** above, however, this is clearly only an approximation of the true behaviour of real gases, but is close enough to being correct to be very useful for so-called "quick and dirty" calculations by engineers in the field. It is, in effect, a graphical EOS that only requires the user to know at least two critical constants for the substance(s), i.e. Equation (4-14) is a two-constant EOS. It should be emphasised, however, that the reduced forms of EOS are of course no more accurate than the original forms of the EOS they are based on. The results from several reduced EOS, for instance, in terms of common reduced properties, can often differ widely from each other, while experimental data are often more nearly in accord to the principle of corresponding states than with specific EOS (Walas, 1985). The differences that do arise can then be attributed to intermolecular interactions from e.g. strong permanent dipole moments and/or non-spherical force fields defining non-bonded interactions (see **Appendix C**, Intermolecular Forces). These types of comparisons eventually led researchers to ask whether adding additional parameters to Equation (4-14) would make the corresponding states principle more accurate in newer EOS developments. This led, for instance, to Soave's modification of the Redlich-Kwong EOS by including Pitzer's acentric factor in a newer formulation (discussed later in **Chapter 4.4.3**, Soave-Redlich-Kwong (SRK) Equation, Page 40).

4.4.1.2 Relating the van der Waals and Virial Equation of State

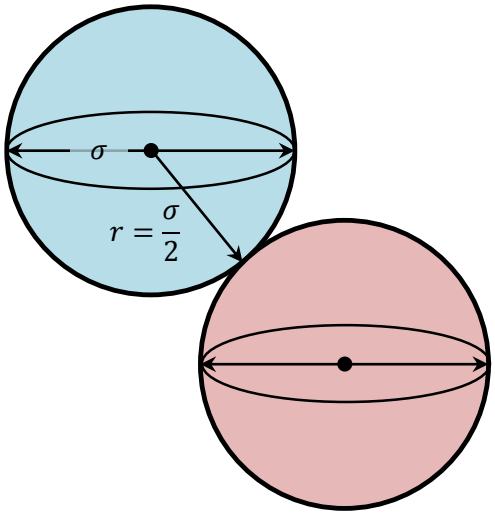

The excluded volume is then equivalent to the volume in which these two molecules (modelled as hard-spheres) occupy:

$$\frac{1}{6}\pi\sigma^3$$

Therefore, the excluded volume per particle is then just half this amount:

$$b = \frac{1}{12}\pi\sigma^3$$

Figure 4-3: Two molecules modelled as hard spheres at closest contact within a sphere of diameter σ.

As already covered, the virial equations come from Taylor expansions about the ideal gas equation. Alternatives, however, can also be obtained by expanding compressibility factor defined by other equations. The second-order expansion of the van der Waals (vdW) equation of state, for instance, results in

$$\left[P + \frac{a}{v^2}\right](v - b) = RT$$

$$\overset{implies}{\Rightarrow} \quad Z_{vdW} = \frac{1}{1 - \frac{b}{v}} - \frac{a}{vRT} = \overbrace{\frac{1}{1 - b\rho}}^{\substack{hard-sphere \\ compressibility}} - \frac{a}{RT}\rho = Z_{hs} - \frac{a}{RT}\rho \qquad (4\text{-}16)$$

where $Z_{hs} = v_{real}/(v_{real} - b) = 1/(1 - b\rho)$ represents the short-range repulsive forces among the molecules of a hard-sphere fluid (an approximation, see **Figure 4-3** above), while the second term accounts for the long-range attractive forces related to the kinetic energy of these same molecules. A Taylor series expansion about this hard-sphere compressibility then leads to the following virial equation for a hard-sphere fluid:

$$Z_{hs} = \frac{1}{1 - b\rho} = 1 + b\rho + (b\rho)^2 + (b\rho)^3 + \cdots \qquad (4\text{-}17)$$

Combining these two expansions then leads to the viral form of the van der Waals equation:

$$Z_{vdW} = 1 + \overbrace{\left(b - \frac{a}{RT}\right)}^{\substack{second\ virial \\ coefficient \\ B_2}} \rho + (b\rho)^2 + (b\rho)^3 + \cdots \qquad (4\text{-}18)$$

Therefore, in the van der Waals model, repulsive forces (approximated here as hard-spheres) and attractive forces occurring between the molecules then compete in their effects on the 2nd virial coefficient. At high temperatures, however, the higher-order virial coefficients that typically dominate the calculated behaviour in this region are then governed by the covolume parameter only (e.g. they have no temperature dependence). Therefore, one can expect the equation to provide poor liquid-phase predictions, which is exactly what is typically observed in most cases. In the low-density limit, however, where the effects of intermolecular forces weaken between molecules, the van der Waals equation correctly collapses to obey the ideal gas law.

4.4.2 Redlich-Kwong (RK) Equation

As mentioned earlier, the principle use of the van der Waals equation has been, like the ideal gas equation, as a starting point for devising more reliable, and ever more complex, equations of state. Redlich and Kwong made one of the first *important* modifications to the van der Waals equation in 1949, which resulted in a substantial quantitative improvement over the original van der Waals equation. The improvement, however, is purely empirical. Redlich himself (O'Connell, et al., 2005) remarked that there is no real theoretical justification for the changes made in the attractive term of the van der Waals equation:

$$\left[P + \frac{a}{\sqrt{T}v(v+b)}\right](v-b) = RT \tag{4-19}$$

where the parameters a and b, like the van der Waals equation, can be regressed to reproduce the behaviour of experimental data, or they can be calculated in terms of the critical properties of a pure substance as

$$\begin{aligned} a_c &= \overset{1/9\left(2^{1/3}-1\right)}{\widetilde{\Omega_a}}\left[\frac{R^2T_C^{2.5}}{P_C}\right] = 0.427480\left[\frac{R^2T_C^{2.5}}{P_C}\right] \\ b_c &= \overset{\left(2^{1/3}-1\right)/3}{\widetilde{\Omega_b}}\left[\frac{RT_C}{P_C}\right] = 0.086640\left[\frac{RT_C}{P_C}\right] \\ Z_C &= 0.333 \end{aligned} \tag{4-20}$$

It then follows that the Redlich-Kwong (RK) equation can, like the vdW EOS, be written in terms of reduced properties:

$$P_r = \frac{3T_r}{v_r - 3\Omega_b} - \frac{9\Omega_a}{v_r\sqrt{T_r}(v_r + 3\Omega_b)} \tag{4-21}$$

The RK equation of state, therefore, is very similar to the van der Waals equation except for the small alteration to the attractive term that adds some temperature-dependence to it, which was intended to address the inadequacies of the van der Waals equation at low and high densities (Valderrama, 2003). In general, the virial coefficients can be obtained from any equation of state by (Tian, et al., 2007)

$$\mathcal{B}_n = \frac{b}{4}\frac{1}{(n-1)!}\left(\frac{\partial^{n-1}Z}{\partial y^{n-1}}\right)_{y=0} \tag{4-22}$$

where $y = b/(4v)$. The second virial coefficient for the Redlich-Kwong equation of state is then

$$\mathcal{B}_2 = b - \frac{a}{R\sqrt{T}} \tag{4-23}$$

which, compared to the virial form of the van der Waals equation (see Equation (4-18)), has a much larger dependence on temperature as is illustrated in **Figure 4-4** below for the case of Argon. Consequently, at low densities, this modification results in a better second virial coefficient for a hard-sphere fluid and thus produces a measurable improvement for substances, like argon, over the van der Waals equation. This minor alteration, however, is still not enough to correct for the poor calculated behaviour of liquid phases, which brings to light the benefit of the aforementioned gamma-phi approach.

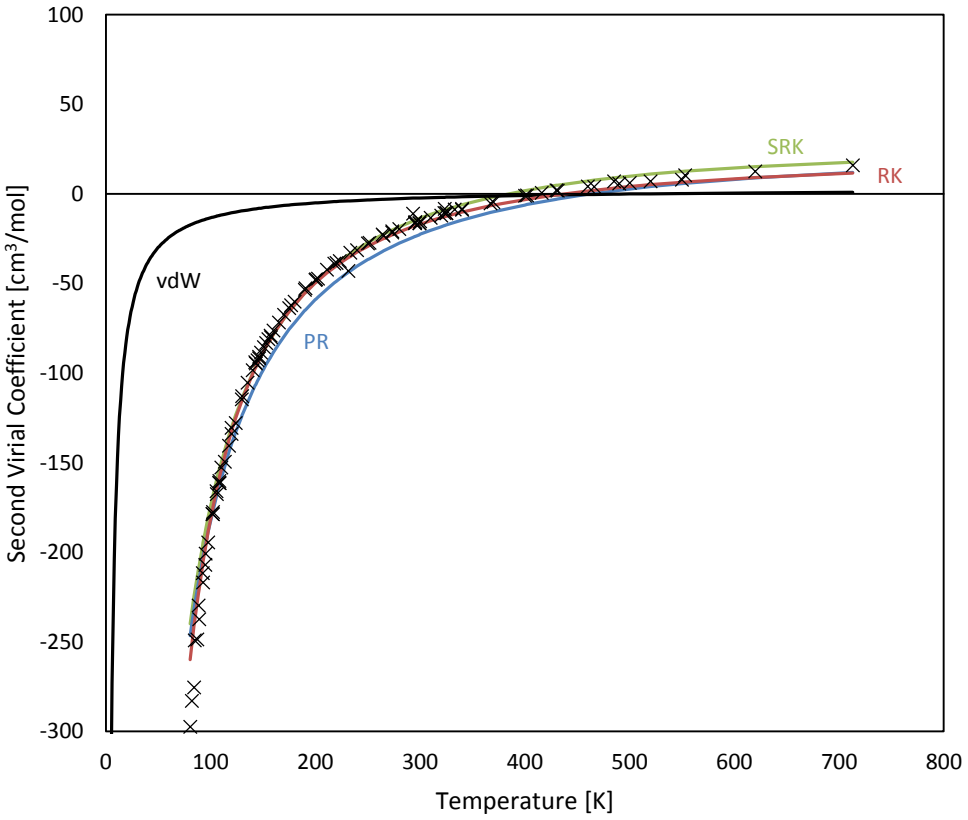

Figure 4-4: Second Virial coefficient data for argon from the DDB, with calculated results from the van der Waals (vdW), Redlich-Kwong (RK), Soave-Redlich-Kwong (SRK) and Peng-Robinson (PR) equations of state using their respective a_c and b_c terms.

4.4.3 Soave-Redlich-Kwong (SRK) Equation

Whether a given equation is properly called a modified Redlich-Kwong or a modified van der Waals equation or something else, is a matter of semantics. The success of the Redlich-Kwong equation of state, however, developed some seventy years after the van der Waals equation, is nonetheless largely responsible for further modifications of the attraction term, a/v^2 in the van der

Waals equation (Prausnitz, et al., 1986). One such modification was given by Soave (Soave, 1972) who replaced the attraction term $a/T^{1.5}$ in the Redlich-Kwong equation with a more general temperature-dependent term represented by $\alpha(T,\omega)$,

$$\left[P + \frac{\alpha(T,\omega)}{v\sqrt{T}(v+b)}\right](v-b) = RT \tag{4-24}$$

where the attraction parameter of the RK equation is modified by the function $\alpha(T,\omega)$, and is dependent on temperature and the *acentric factor* developed by Pitzer et. al (Pitzer, et al., 1955)

$$\omega = -1.0 - \log_{10}\left[\frac{P_{sat}(T_r = 0.7)}{P_C}\right] \tag{4-25}$$

Furthermore, the modified function $\alpha(T,\omega)$ was fitted to better reproduce the vapour pressure data of hydrocarbons:

$$\alpha(T_r,\omega) = a\left[1 + \left(1 - \sqrt{T_r}\right)(0.480 + 1.574\omega - 0.176\omega^2)\right]^2 \tag{4-26}$$

It then follows that this modification limits the range of applicability of the SRK equation, where only compounds similar to hydrocarbons can be predicted with any degree of confidence (i.e. non-polar and slightly polar compounds). Also, unlike the equations of van der Waals and Redlich-Kwong, the SRK equation depends upon a third constant, the acentric factor (ω). Since this modification was developed to match experimental vapour pressure data at a reduced temperature of 0.7 (Foster, 2011), it then follows that the method is further limited to the reduced temperature range of around 0.6 to 1 (which typically leads to satisfactory results of vapour). At the critical point, however, the value of this modification reduces to a value of one, and therefore has no effect on the calculation. The two parameters (a and b) can then be written in terms of critical properties as

$$\begin{aligned} a_c &= \Omega_a\left[\frac{R^2T_C^2}{P_C}\right] = 0.427480\left[\frac{R^2T_C^2}{P_C}\right] \\ b_c &= \Omega_b\left[\frac{R^2T_C^2}{P_C}\right] = 0.086640\left[\frac{R^2T_C^2}{P_C}\right] \\ Z_c &= 0.333 \end{aligned} \tag{4-27}$$

where Ω_a and Ω_b are equivalent to the values found in the Redlich-Kwong equation. At the critical point, therefore, even if these two parameters are fitted to experimental data to reproduce correct critical pressures and critical temperatures, the critical volumes (or equivalently the critical compressibility factors) will be forced into further error just like the equations of van der Waals and Redlich-Kwong. The addition of the acentric factor in Soave's modification only has a measurable effect away from the critical point.

4.4.4 Peng-Robinson (PR) Equation

In 1976, Peng and Robinson (PR) proposed the following equation of state:

$$\left[P + \frac{\alpha(T,\omega)}{v(v+b)+b(v-b)}\right](v-b) = RT \tag{4-28}$$

where, just like Soave, they replaced the attraction parameter in the Redlich-Kwong equation with a more general temperature-dependent term $\alpha(T,\omega)$. Their correlation of this function to the vapour pressure of hydrocarbons, however, resulted in coefficients that are slightly different from those obtained by Soave:

$$\alpha(T_r,\omega) = a\left[1 + \left(1 - \sqrt{T_r}\right)(0.3746 + 1.54226\omega - 0.269926\omega^2)\right]^2 \tag{4-29}$$

At the critical point, this leads to

$$\begin{aligned} a_c &= \Omega_a\left[\frac{R^2T_C^2}{P_C}\right] = 0.45724\left[\frac{R^2T_C^2}{P_C}\right] \\ b_c &= \Omega_b\left[\frac{R^2T_C^2}{P_C}\right] = 0.07780\left[\frac{R^2T_C^2}{P_C}\right] \\ Z_c &= 0.307 \end{aligned} \tag{4-30}$$

where the critical compressibility of the equation is closer to the average of the true values of many substances ($\bar{Z}_C \cong 0.257$). It then follows that the equation should be more capable near the critical point than its predecessors. Therefore, the largest difference between the equations of Peng-Robinson (PR) and the modification made by Soave (SRK) is to the functional form of the equation of state itself (i.e. the denominator of $\alpha(T,\omega)$). Although not obvious from direct observation, this change to the pressure-volume relationship addresses the inadequacies of the RK and SRK equations to correctly calculate reasonable liquid densities. In this regards, the PR equation proves superior for medium sized hydrocarbons and compounds with intermediate acentric factor values. For compounds with small acentric factors, however, the SRK model proves to be a better option (Foster, 2011; Sengers, et al., 2000).

4.4.5 Concluding Remarks

Arguably, the van der Waals equation represents the single largest contribution to the development of cubic equations of state, and one of the most significant advancements in the history of equations of state development in general. Van der Waals was the first to show that the phase-split of a substance naturally lends itself to a description obtained using an equation cubic in form. Since cubic equations have analytical solutions, they are very attractive for use in process simulators, which require repeated property calculations within iterative loops. Furthermore, the terms of the van der Waals equation relate to measurable interactions occurring on the microscopic level. This, no doubt, firmly established the idea that in order for an equation of state to be accurate these effects need to be accounted for—molecules of real substances are not perfect gases, intermolecular forces influence them. In the van der Waals and related equations, the specifics of these forces are lumped into the repulsion parameter b and the attraction parameter a (typically written in terms of the function α).

All of the cubic equations cited in **Chapter 4.4**, for instance, have retained the van der Waals repulsion term, $RT/(v-b)$, but use a different attraction term to adjust predictions made at

saturated conditions. Apart from the van der Waals equation, this attractive term is typically characterised as the function of temperature α, which has steadily increased in complexity from the relatively simple $\alpha = 1/\sqrt{T}$ in the Redlich-Kwong equation. These modifications were made in order to improve the predictions of component vapour pressures, especially for polar compounds (Goodwin, et al., 2010). The complexity of the α-functions, however, can only be expected to compensate for the inadequacies of these equations so much, which is why the parameters a and b typically need to be fitted to experimental data in order to obtain reliable results. In terms of "cubic" equations of state development, it is very doubtful that there will be any *major* advancement in the future of such equations. To selectively quote (Walas, 1985):

> *…many other equations of varying merit were proposed over the years. Almost every one of these has been shown, or claimed, to be superior in some respects to earlier ones—because of a sound theoretical basis, or in some particular range of temperature and pressure, or for some particular substances, or for the evaluation of some particular thermodynamic property, or for being easier to use, or because the inventor had become interested in the topic. Most of these equations have not been accepted, not always because they were inferior, but simply because they were not superior.*

4.4.5.1 Handling Mixtures

Until now, the discussion has primarily been limited to the representation of pure components; however, these same equations are also capable of representing fluid mixtures when appropriate methods are used. Although there are unlikely to be any major developments to the actual PVT models currently favoured (e.g. Redlich-Kwong and Peng-Robinson), the methods for modelling multicomponent mixtures using these equations is still at the centre of much research. As pointed out by (Foster, 2011; Sengers, et al., 2000), the establishment of appropriate mixing and combining rules are often more important than the actual PVT relationship embodied within a particular EOS itself.

One approach is to replace the pure component parameters of the equation of state with parameters characteristic of the mixture. The mixture, therefore, can be thought of as a hypothetical "pure" fluid, where some composition-dependent function (the *mixing rule)* is used to weight the pure component parameters of each component according to their concentration in the mixture (Foster, 2011). The simplest mixing rule is to take a linear average of the pure component parameters of each species, but then this neglects taking into account the fundamental concept of pairwise interactions (Wei, et al., 2000). The next level of complexity is to introduce a quadratic dependence on the concentration of the mixture components. In terms of the parameters of the van der Waals and related equations, this is given by

$$a_m = \sum_i \sum_j x_i x_j a_{ij}$$
$$b_m = \sum_i \sum_j x_i x_j b_{ij} \qquad (4\text{-}31)$$

where a_{ii} and b_{ii} are equivalent to the constants of the equation for pure component i, and a_{ij} and b_{ij} $(i \neq j)$ are the cross parameters relating to pairwise interactions. These cross parameters are then determined using by using a *combining rule*; customarily, the geometric mean is used for the cross-attraction parameter a_{ij} and the arithmetic mean was used for the cross-repulsion parameter b_{ij} (Valderrama, 2003). Interaction parameters were then introduced to enable the direct correlation of specific experimental data using equations of state by modifying the combining rules defining the cross-parameters:

$$a_{ij} = \sqrt{a_i a_j}\left(1 - k_{ij}\right)$$
$$b_{ij} = \frac{1}{2}\left(b_i + b_j\right)\left(1 - \beta_{ij}\right) \tag{4-32}$$

where k_{ij} and β_{ij} are then the interaction parameters typically fitted to experimental (or predicted) phase equilibrium data. Although not necessary, these modifications (known as the Berthelot-Lorentz combining rules) retain the quadratic concentration dependence of the equation of state parameters, and have the "feel good" factor of retaining its relationship to the "exact" mixing rules provided by statistical mechanics for the virial coefficients (van Ness, et al., 1981). Case in point, the second virial coefficient for a mixture $\widehat{\mathcal{B}}_2$ is given by

$$\widehat{\mathcal{B}}_2 = \sum_i \sum_j y_i y_j \mathcal{B}_{ij} \tag{4-33}$$

where $\mathcal{B}_{ij}$ is the cross 2nd virial coefficient, and the y's are used to reaffirm the fact that the virial equation is only applicable to gases. Therefore, by comparison, the virial form of the van der Waals equation of state (Equation (4-18) then implies that the quadratic mixing rules for a_m and b_m are consistent with the theoretically exact virial equation. It is for this reason, that these (quadratic) mixing rules are also known as the *van der Waals one-fluid mixing rule*s.

There exist, of course, many other mixing and combing rules, including alternative methodologies of how to incorporate the concentration dependence[13]. However, the PC-SAFT equation of state that this project will be using only uses the so-called "classical" mixing and combining rules that were just discussed; therefore, further elaboration on the topic is not warranted here. Instead, the books of Orbey and Sandler (Orbey, et al., 1998) and Kontogeorgis and Folas (Kontogeorgis, et al., 2010) are recommended for further self-indulgence.

4.5 Advanced Equations of State

As pointed out by Walas (Walas, 1985) "the adequacy of any relation in describing a particular phenomenon depends on how completely the pertinent variables are identified." There are not only forces of attraction and repulsion that must be accounted for, but differences in the sizes and shapes of molecules, their relative positions to other surrounding molecules, charge characteristics and other factors that also influence the true PVT behaviour of substances. The cubic equations of state of the previous section "lumped" these specific contributions into the attractive and repulsive parameters

[13] If you type in the phrase *"new mixing rule" OR "new combining rule"* within Google Scholar, for instance, you obtain almost 700 search results (Google)!

for simplicity. Another approach, however, is to take a specific accounting of the interacting forces on the molecular level by assuming pair-wise additivity, and then to sum across the number of molecular pairs (or contacts) to determine the overall energy of the system.

The thermodynamic properties of fluids interacting through pair-wise forces are typically determined from knowledge of two-body distribution functions. An analytical form of these functions is, unfortunately, only available for a very limited number of systems (e.g. pairs of particles interacting through a hard sphere potential). The problem becomes even more complicated if there are many-body forces or if, for example, the intermolecular potential is not spherically symmetric.

Perturbation theories provide a means by which the properties of a system (e.g. the distribution functions, free energy or pressure) can be represented as a perturbation/agitation from those of a reference system with known properties. Such approaches therefore represent some of the most versatile, accurate and powerful theories to date. Wertheim's work on associating and polymeric fluids and its implementation as an equation of state in the statistical associating fluid theory (SAFT) is one such approach. SAFT and related advanced equations of state like the PC-SAFT equation then constitute a major advancement towards a theoretical framework for modelling the behaviour of fluids by specifically accounting for the intermolecular forces involved. In this section, therefore, a review of these methods and supporting information is provided.

4.5.1 Statistical Mechanics and Intermolecular Forces

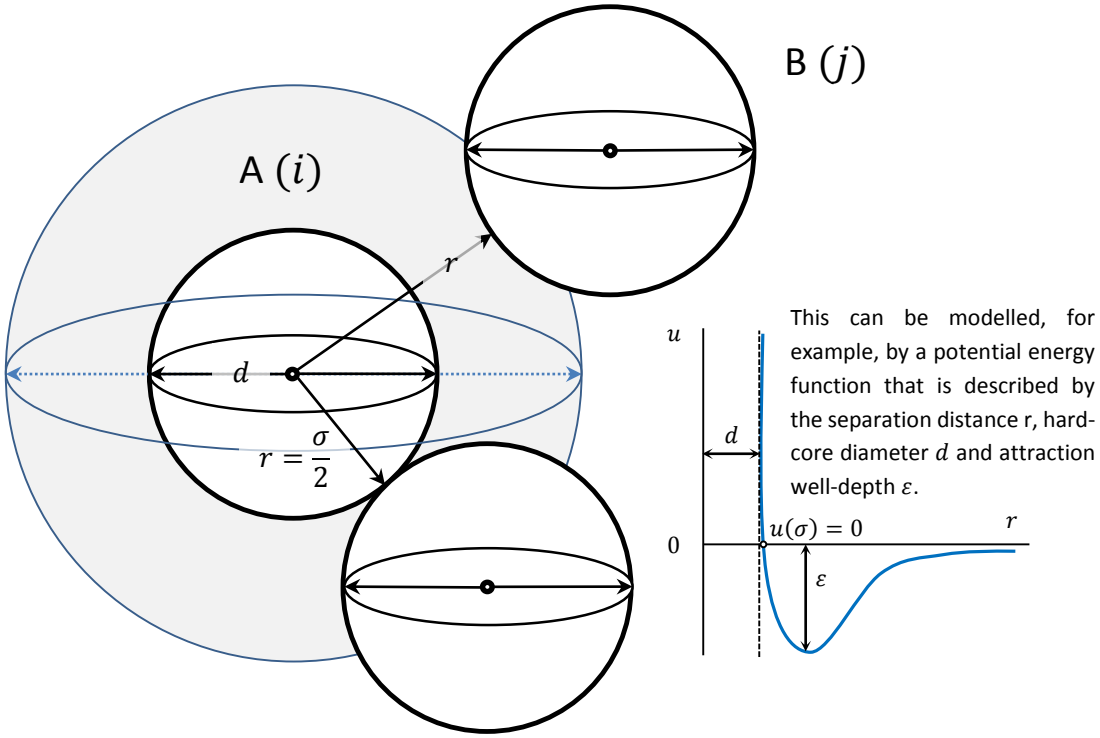

Figure 4-5: Two interacting molecules (A and B, or i and j, etc.). The central molecule *i* has a hard-core diameter d (which is equivalent to σ in this case) and is separated by a central distance r from the other interacting molecule j.

The forces of attraction and repulsion are relatively common concepts. The former holds molecules together, while the later keeps them from mutual destruction. These same forces of course depend on the total energy of the system, which is a function of both the kinetic energy and the potential energy of the interacting molecules (or particles). The kinetic energy (positive by definition) is a function of vibrational, rotational and translational energies of the molecules (or the atoms forming the molecules), and can absorb energy from the force-field effects of attraction and repulsion due to e.g. van der Waals interactions (see **Appendix C**). An accurate equation of state, therefore, is likely one that can sufficiently describe these forces. This can be done, for instance, through statistical mechanics using potential energy functions that relate to these same forces on a microscopic level:

$$F = -\frac{du(r)}{dr} \tag{4-34}$$

where F is the net force acting between two molecules, and is calculated by integrating the potential energy function u, whose gradient describes the relative position of the molecules (such as the angles of orientation) and the intermolecular forces occurring between them (dependent only on the distance r for a one-dimensional case). Such an approach, for example, can be used to derive both the van der Waals EOS and the virial EOS, which represents an important justification of the approach. The virial coefficients, for instance, are measurable quantities, i.e. thermodynamicists are not just doing a whole bunch of math for no reason (there is actually some physical justification for it).

Molecules not only interact in pairs, but also as triplets, quartets, etc., which contribute to the observed deviations from ideality that correspond, for instance, to the coefficients of the virial EOS (see **Chapter 4.3**, Page 31). For the second virial coefficient this is (Walas, 1985):

$$\mathcal{B}_2 = -2\pi N_A \int_0^\infty [exp(-u(r)/kT) - 1] r^2 dr \qquad (4\text{-}35)$$

where N_A is the Avogadro number, k is the Bolzmann constant, and the integrand between brackets (formally known as the Mayer *f*-function). The potential energy functions used in expressions like these, however, are entirely empirical. Some have been developed on rational grounds, others partly because they lead to integral relations that are convenient for theoretical studies (Walas, 1985). It was found by London (London, 1937), for instance, that attraction potentials vary inversely as the sixth power of the separations, whereas some higher but not specific power is involved with repulsion potentials. A widely used function incorporating these observations was proposed by Mie (Mie, 1903):

$$u(r) = ar^{-n} - br^{-6} \qquad (4\text{-}36)$$

where a, b and n are positive constants and where n > 6 (to represent repulsive forces). For instance, a special case with $n = 12$ was introduced by Lennard-Jones (Jones, 1924) and has been widely employed. Besides the Lennard-Jones potential, two potentials are especially useful in theoretical work:

(1) The *hard-sphere potential*, which assumes that attractive forces are absent and that repulsive forces are infinite when the molecules touch and zero at finite separation. There is only one parameter.
(2) The *square-well potential*, where a hard-sphere repulsion term is retained, and a constant attraction potential over finite distance is included. Since there are three parameters (ε, σ and g), use of the square-well potential can result in very flexible correlations.

Many other potentials are also possible; for instance, a few of the simpler ones are given in **Figure 4-6** below, and are similar (in form) to those used to describe the effects of gravity on a planetary scale. The ones shown have either 0, 1, 2, or 3 parameters that can be fitted to capture the characteristic behaviour of data. Many modern and advanced equations of state like the SAFT equation and its variants employ such functions.

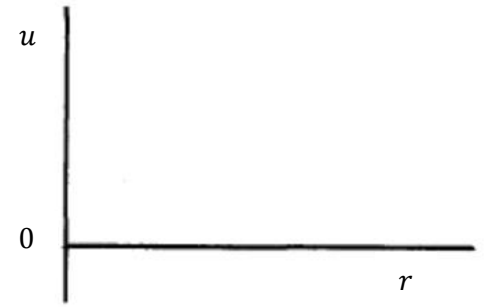

(a)

Ideal gas, no intermolecular forces:

$$u = 0$$

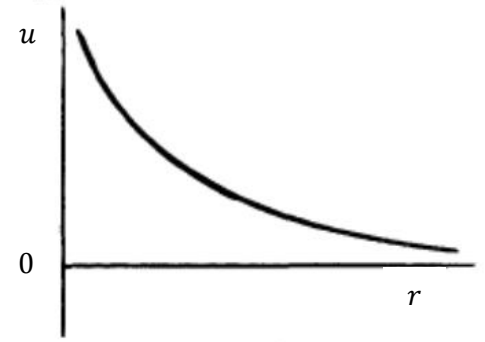

(b)

Point of repulsion is at the centres of the molecules:

$$u = ar^{-\alpha}$$

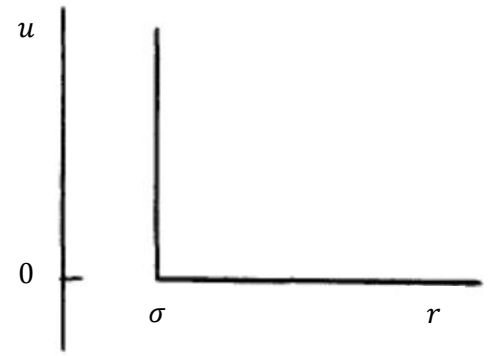

(c)

Hard-sphere potential. Point of repulsion is at molecular surface:

$$u = \begin{cases} \infty & r < \sigma \\ 0 & r > \sigma \end{cases}$$

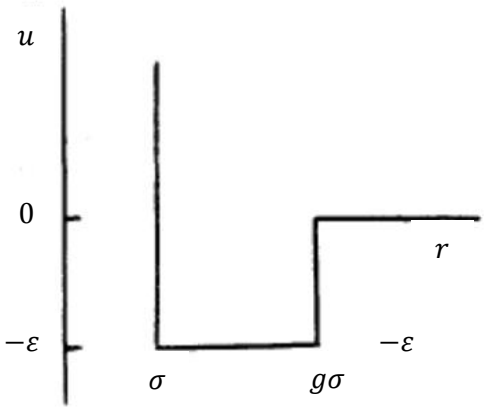

(d)

Square-well potential. Point of repulsion at surface, with constant attraction over a limited distance:

$$u = \begin{cases} \infty & r < \sigma \\ -\varepsilon & \sigma < r < g\sigma \\ 0 & r > g\sigma \end{cases}$$

Figure 4-6: Some commonly used potential energy functions (Walas, 1985).

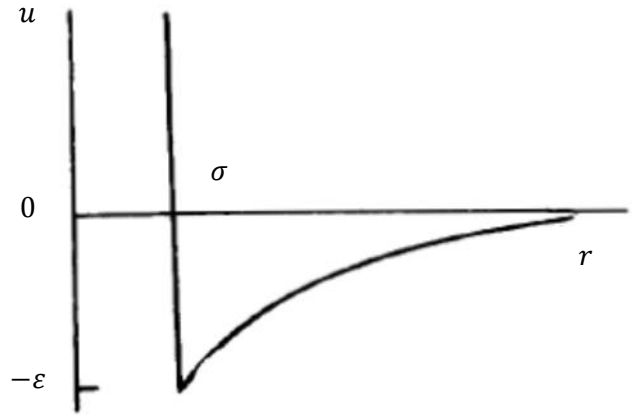

(e)

Sutherland potential. Point of repulsion at surface, attraction varies with distance:

$$u = \begin{cases} \infty & r < \sigma \\ -\varepsilon \left(\frac{\sigma}{r}\right)^{\alpha} & r > \sigma \end{cases}$$

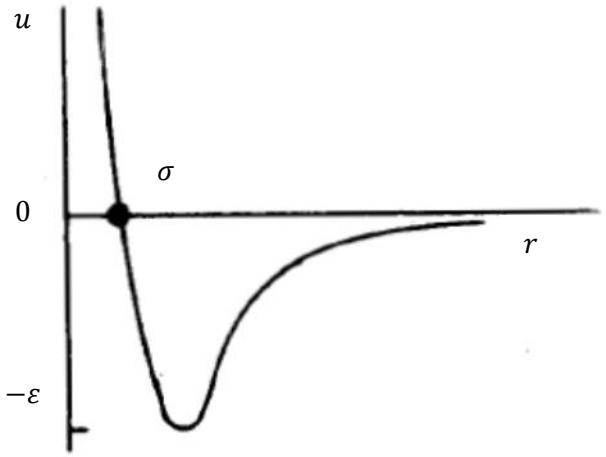

(f)

Bireciprocal, of which the Lennard-Jones is a special case:

$$u = a\left(\frac{\sigma}{r}\right)^{\alpha} - b\left(\frac{\sigma}{r}\right)^{\beta}$$

$$u_{LJ} = 4\varepsilon\left[\left(\frac{\sigma}{r}\right)^{12} - \left(\frac{\sigma}{r}\right)^{6}\right]$$

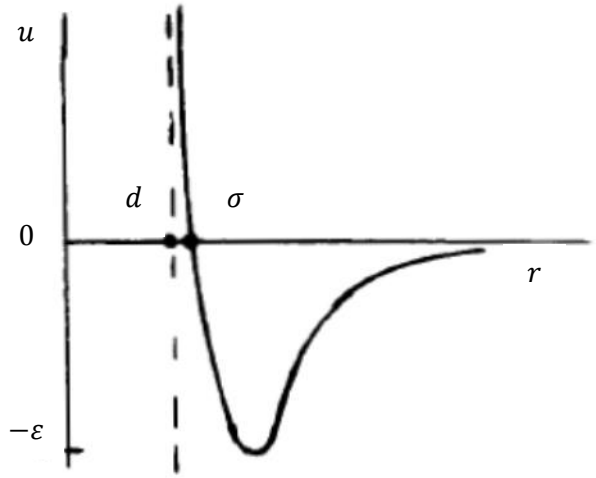

(g)

Kihara potential. Point of repulsion is a hard core of diameter d, which is smaller than the molecular diameter, σ:

$$u = \begin{cases} \infty & r < d \\ 4\varepsilon\left[\left(\frac{\sigma - d}{r - d}\right)^{12} - \left(\frac{\sigma - d}{r - d}\right)^{6}\right] & r \geq d \end{cases}$$

Figure 4-6 (*continued*).

4.5.1.1 In the Beginning there was Andersen

The work of Andersen (Andersen, 1975) was among the first treatments of associating fluids using statistical mechanics, and has influenced many of the association fluid theories currently in use today (Goodwin, et al., 2010). Anderson postulated that the potential between two interacting molecules, which can depend on both their position and orientation to each other, can be approximated by

$$u(r) = u_0(r) + u_{HB}(r) \tag{4-37}$$

$$u_o(r) = \begin{cases} \infty & \text{for } r < \sigma \\ 0 & \text{for } r > \sigma \end{cases} \tag{4-38}$$

where u_o is the reference potential and u_{HB} is the hydrogen-bonding contribution to the overall potential u.[14] This is an example, for instance, of how *perturbation theory* can be applied to simplify and solve a more complex problem. This is done by using a simple base-system for which an exact mathematical solution is known as the starting reference, whereby additional terms are added to make "perturbing" adjustments to the initial reference state (point or system).

For a binary fluid consisting of hard spheres of the same diameter σ and single association sites, such is in the case of Andersen, for example, the reference is described by a hard-sphere potential that is known (see **Figure 4-6** (c) on Page 48) with the point of repulsion at the molecular surface, i.e. the interacting molecules are assumed to have a hard-sphere core of diameter σ. At very short distances, therefore, molecules are prevented from interacting when $r < \sigma$, which is just a mathematical way of preventing the simultaneous association of more than two molecules at a time. Saturation, therefore, is reached at the dimer level as illustrated in **Figure 4-7** below, where the reference state (for $r > \sigma$) is adjusted according to the hydrogen-bonding contribution to the overall potential energy describing the bonding/interaction of association.

[14] Both generalised and specific notations are used for variables of interacting molecules. The pairwise potential energy of two interacting molecules 1 and 2, for example, can be written as $u(r)$, $u(r_{12})$ or simply $u(1,2)$. The former is convenient when the discussion is limited to pairwise interactions, while the later two cases are needed to differentiate interactions with e.g. an additional molecule 3. When generalised notation is used, however, it is meant for any two interacting molecules e.g. $u(i,j)$; the form used depends on context.

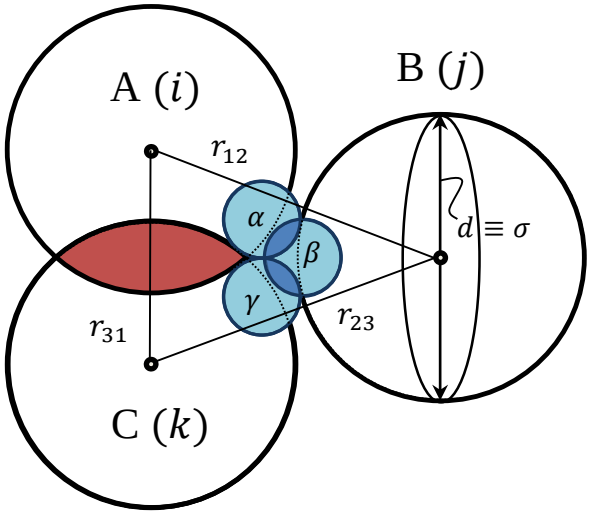

The black lines represent the boundary of the hard-core reference potential $u_0(i,j)$ while the small blue spheres represent the association sites, where the hard-core diameter equals the collision diameter ($d = \sigma$). If molecules 1 and 2 are in a bonded state (overlap of the association sites), the site of molecule 3 cannot overlap that of either molecule 1 or molecule 2 without experiencing a hard sphere overlap with molecule 1 or molecule 2. Thus, three-molecule bonding and higher is forbidden in this case, i.e. steric hindrance (represented by the shaded region in red).

Figure 4-7: Illustration of steric inhibition of bonding beyond the dimer level.

If $u_{HB}(1,3) \neq 0$ and $u_{HB}(2,3) \neq 0$, for instance, this would mean that the distance between molecules 1 and 2 is less than the hard-core radius and $u_o(1,2) = \infty$; two molecules cannot occupy the same space at the same time. The integrand, or Mayer f-function, is then given by

$$f(1,2) = exp(-u(1,2)/kT) - 1 \tag{4-39}$$

where,

$$\begin{aligned} f_0(1,2) &= exp(-u_0(1,2)/kT) - 1 \\ f_{HB}(1,2) &= exp(-u(1,2)/kT) - exp(-u_0(1,2)/kT) \end{aligned} \tag{4-40}$$

Therefore if r is less than the hard-core radius for the molecules, then $u_0(1,2) \longrightarrow \infty$ so that $u_0(1,2) = -1$. This concept of limiting the level of bonding for interacting molecules, i.e. steric inhibition, is a key element of Wertheim's theory of association.

4.5.1.2 Wertheim's Theory of Association

Wertheim essentially took Mayer's cluster theory (Mayer, et al., 1941)—a power series expansion of the partition function in terms of density—and simplified it by deriving approximations using both perturbation theory and integral equations (Goodwin, et al., 2010). In the first paper (Wertheim, 1984) Wertheim begins by stating that "a model potential [that is] capable of representing a wide variety of physical circumstances is the following:"

$$u(1,2) = u_0(1,2) + \sum_{\alpha}\sum_{\beta} u_{\alpha\beta}\left|\boldsymbol{r}_2 + \boldsymbol{d}_\beta(\boldsymbol{\Omega}_2) - \boldsymbol{r}_1 - \boldsymbol{d}_\alpha(\boldsymbol{\Omega}_1)\right| \tag{4-41}$$

where $i = 1, 2, \ldots$ is shorthand for the position $\mathbf{r}_i$ of the molecular centre of mass and the orientation $\boldsymbol{\Omega}_i$ of molecule i; $\mathbf{d}_\alpha$ and $\mathbf{d}_\beta$ then represent vectors from the molecular centres to the interaction sites α and β. This equation represents the foundation, i.e. the specific model, on top of which Wertheim's theory of association is developed. The later term, of course, is much more complex then the reference

contribution to the overall potential, and accounts for a number of different orientations and positions (hence the use of vectors); fortunately, Wertheim was able to make a number of simplifications based on steric considerations (Goodwin, et al., 2010).

Wertheim introduced Andersen's idea of steric inhibition by using Equation (4-38) to represent the hard (or infinitely repulsive) cores of interacting molecules with diameters σ. The simplest model for association, therefore, assuming identical molecules with identical association sites α and β, has the form

$$u_{\alpha\beta}(1,2)\begin{cases}\ll 0 & \text{for } x < a\\ = 0 & \text{for } x > a\end{cases}, \quad x = |\mathbf{r}_2 + \mathbf{d}(\Omega_2) - \mathbf{r}_1 - \mathbf{d}(\Omega_1)| \tag{4-42}$$

where, to ensure steric saturation, d must satisfy (according to **Figure 4-7** on the previous page):

$$[(\sigma - a)/2] < d \equiv |\mathbf{d}| < (\sigma/2) \tag{4-43}$$

The boundaries of the molecules in **Figure 4-7** then represent the boundary of the hard-core potential $u_0(i,j)$, while the small blue spheres represent the association sites α, β, etc. If molecule-2 is bonded to molecule-1, then molecule-3 is unable to bond to either of these molecules without experiencing a hard sphere overlap with one or the other (the red-shaded region of the figure). This, like the work of Andersen, ensures that the bonding stops at the dimer level (any higher is physically not possible). Strong short-ranged sites of association, therefore, are located at the hardedge of the molecules (at a distance $a = \sigma$).

In the second paper (Wertheim, 1984) Wertheim cleaned-up the muddy results of Equation (4-43) and transformed it into something more user friendly by applying a first-order perturbation theory to approximate the behaviour of association. In so doing, he was able to establish a direct relationship between the change in the residual Helmholtz energy due to association and the fluid density. This resulted in the fluid (or monomer) density related to an integral approximation characterizing the strength of association. His approach yielded

$$\frac{A^{Assoc.}}{kT} = \frac{A - A_0}{kT} = N\left(\ln X - \frac{X}{2} + \frac{1}{2}\right)$$
$$X = \frac{\rho_0}{\rho} \tag{4-44}$$

where N is the total number of monomeric units, whether bonded or not, ρ_0 is the density of monomer segments, ρ is the total density of segments, and X is the fraction of segments that are non-bonded, determined from

$$\rho(1) = \rho_0(1)\left[1 + \int g_0(1,2) f_A(1,2) \rho_0(2) d2\right] \tag{4-45}$$

where $g_0(1,2)$ is the pair distribution of the reference fluid, and $f_A(1,2)$ is the Mayer *f*-function of the association interaction $u_A(1,2)$ (where $u_A \equiv u_{\alpha\beta}$) over all possible positions and orientations of molecules-1 and 2, i.e. it is a spatially inhomogeneous fluid. The following assumptions were then made to obtain a simplified expression:

(1) Spatial uniformity, e.g. in a lattice-like structure, which makes $g_0(1,2)$ a function of the hard sphere diameter only ($g_0 = f(\sigma)$) instead of the relative positions of molecules-1 and 2.
(2) That the association potential $u_A(1,2)$ can be approximated by a square well potential of depth ε_{HB}.
(3) The association sites were limited to a small range of distances near the hard-sphere diameter ($a = \sigma$).

These assumptions result in

$$\frac{\rho_0}{X} = \rho_0 + \rho_0^2 g_0(\sigma) exp(\varepsilon_{HB}/kT)K \xrightarrow{yields} X = \frac{1}{1 + \rho_0 g_0(\sigma) exp(\varepsilon_{HB}/kT)K} \quad (4\text{-}46)$$

where K is the volume available for bonding. As Sengers et. al. (Sengers, et al., 2000) explains,

> *"in subsequent papers in the series, Wertheim extended his analysis to multiple association sites (Wertheim, 1986) and to systems undergoing polymerization (Wertheim, 1986). His key contribution was to show that it is possible to obtain the properties of an associating or chain fluid based on knowledge of the thermodynamic properties (the Helmholtz energy and structure) of the monomer fluid. This is the basis of the now well-known Wertheim thermodynamic perturbation theory, and in turn, the basis of all SAFT equations of state. Interestingly, in this series of four papers, Wertheim did not present a single calculated result or any numerical tests of his proposed theories."*

4.5.2 Statistical-Association-Fluid-Theory (SAFT) Equation of State

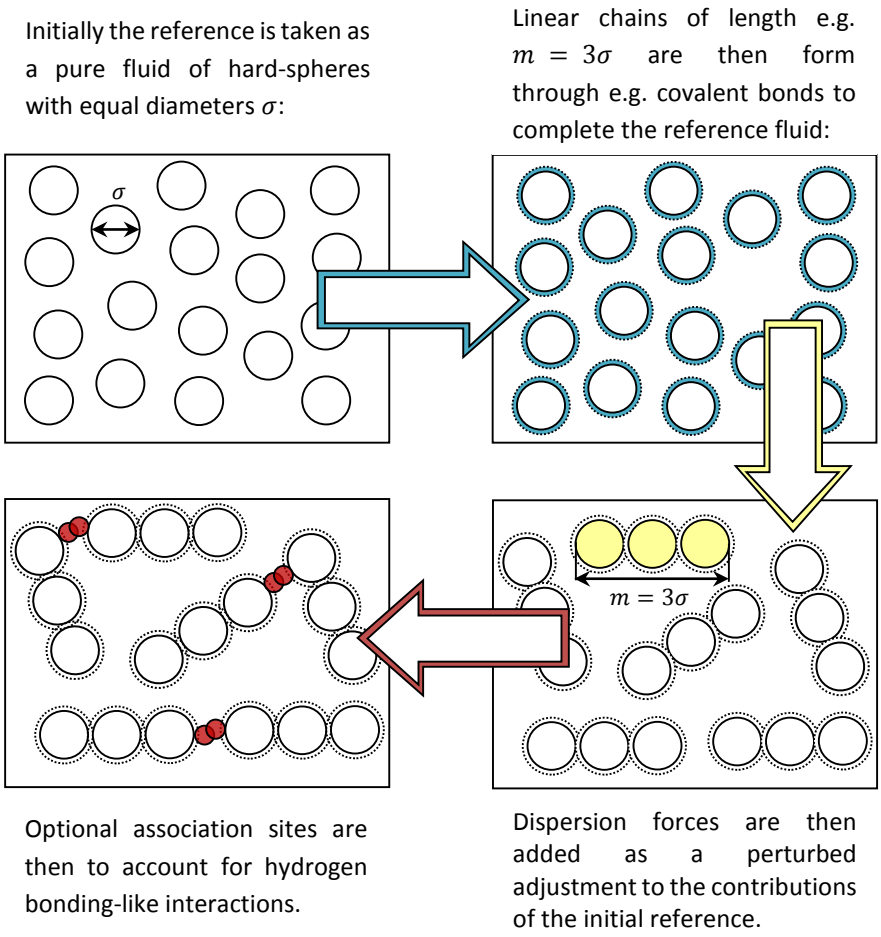

Figure 4-8: Illustration of the perturbation scheme for a pure fluid within the framework of the SAFT equation.

Wertheim's work was later incorporated into the *statistical-association-fluid-theory* (SAFT) equation of state by Chapman and co-workers in 1989 (Chapman, et al., 1989), where Wertheim's theory was extended to mixtures of hard-spheres and chain molecules by replacing the association sites (or bonds) with covalent, chain-forming bonds that form monomers (spherical segments) with short ranged attractive sites limited by steric hindrance. In this case, as illustrated in **Figure 4-8**, the Helmholtz energy is then written as the sum of four separate contributions:

$$\frac{A}{NkT} = \frac{A^{Ideal}}{NkT} + \underbrace{m\left(\frac{A_0^{hs}}{NkT} + \frac{A_0^{disp}}{NkT}\right)}_{\equiv \frac{A^{Ref}}{NkT}} + \frac{A^{Chain}}{NkT} + \frac{A^{Assoc}}{NkT} \tag{4-47}$$

where A^{Ideal} is the ideal free energy, A^{Ref} is the free energy reference term due to the monomer-monomer repulsion and dispersion interactions (where m is the number of segments per chain), A^{Chain} the contribution due to the formation of bonds between monomeric segments, and $A^{Assoc.}$ the contribution due to association. A^{Chain} and A^{Assoc}, therefore, are treated as perturbations of the spherical-segment reference fluid which is approximated by a repulsive hard-sphere term and an attractive dispersion term (Tan, et al., 2008).

The main reason that SAFT and related approaches are held in such high regards is because they are built upon statistical mechanical perturbation theory, which is based on some reference system (or unperturbed system) for which everything is explicitly known. Typically, this knowledge comes from molecular simulation results or from the solution of some integral equation of a potential energy function. It then follows that the perturbation terms A^{Chain} and $A^{Assoc.}$ (Wertheim's contributions) effectively correct (or perturb) the calculated behaviour of the reference fluid to match more closely the true real behaviour of real fluids.

Systematic improvements, therefore, and extension of the theory are then possible by evaluating modifications against the theoretical predictions obtained from computer simulations for the same model. If the tested modifications do not correlate well with these simulation results, then new modifications can be sought. Many such modifications, for instance, have been proposed to the original SAFT model over the years. At present, however, the discussion is being limited to the PC-SAFT equation for which the current project will employ.

4.5.3 Perturbed-Chain SAFT (PC-SAFT) Equation of State

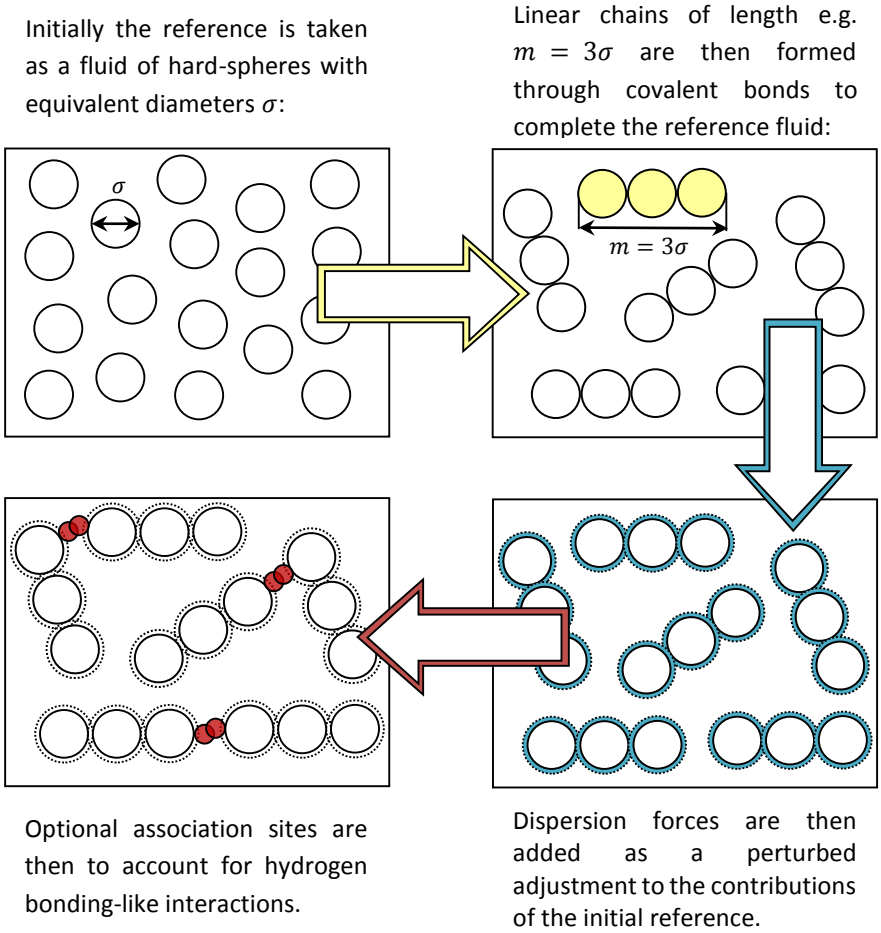

Figure 4-9: Illustration of the perturbation scheme for a pure fluid within the framework of the PC-SAFT equation.

In contrast to the SAFT equation of state, the PC-SAFT approach (or variation) considers a hard-chain reference system instead of a hard-sphere reference that includes dispersion forces. A new dispersion term, as the name suggests, is thus derived for chain molecules by treating it as a perturbed

adjustment to the hard-chain reference fluid. The main focus of the original PC-SAFT publication (Gross, et al., 2000), for instance was the derivation of the new dispersion expression for chain molecules, and thus only applies to non-associating components which are dominated by dispersive forces e.g. like in the case of alkanes. Unlike the SAFT equation, the total Helmholtz energy is then determined by

$$\frac{A}{NkT} = \frac{A^{Ideal}}{NkT} + \underbrace{m\left(\frac{A_0^{hs}}{NkT} + \frac{A_0^{Chain}}{NkT}\right)}_{\equiv \frac{A^{Ref}}{NkT}} + \frac{A^{disp}}{NkT} + \frac{A^{disp}}{NkT} + \cdots \tag{4-48}$$

where A^{hs} corresponds to the free energy of a reference hard-sphere-chain fluid, where the monomer fluid at this point is a fluid of hard-spheres, and A^{Chain} describes the chain perturbation contribution (usually taken to the second-order). According to Goodwin et. al. (Goodwin, et al., 2010):

> *the chain perturbation "…is based on an earlier theory for square-well chain molecules (Gross, et al., 2002) and is determined from a Taylor series expansion fitted to the vapour-liquid phase envelopes of pure alkanes (Gross, et al., 2001). This fitting greatly enhances the accuracy of the approach in comparison with experimental systems, but unfortunately means that it is no longer straight forward to define the underlying intermolecular potential of the model and so comparison against computer simulations cannot be used in the assessment of further theoretical developments."*

In subsequent versions of the PC-SAFT equation, additional terms were added to include explicit expressions for molecular association (Gross, et al., 2002) and multi-polar contributions that include dipole-dipole (Gross, et al., 2006), quadrupole-quadrupole (Gross, et al., 2004; Gross, 2005), and dipole-quadrupole (Vrabec, et al., 2008) effects. Detailed expressions are provided in the cited references, however, and will not be discussed here; instead, at present, it is sufficient to limit the discussion to the original PC-SAFT equation.[15]

4.5.3.1 The Potential Energy Function

Since the PC-SAFT equation uses a reference fluid of molecular chains composed of spherical segments, a pair potential to describe the segment-segment interactions is then required. In this regards, the work of Chen and Kreglewski (Chen, et al., 1977) is used:

$$u(r) = \begin{cases} \infty & r < (\sigma - s_1) \\ 3\varepsilon & (\sigma - s_1) \leq r < \sigma \\ -\varepsilon & \sigma \leq r < \lambda\sigma \\ 0 & r \geq \lambda\sigma \end{cases} \tag{4-49}$$

where $u(r)$ is a modified square-well pair potential, r is the radial distance between two segments, σ is the temperature-independent segment diameter, ε denotes the depth of the potential well, and λ

[15] This is also done out of necessity, since the PC-SAFT version implemented by Aspen Plus (which is used later in this project) does not include any multi-polar contributions, which may be required to correctly represent e.g. quadrupoles such as carbon dioxide and R-32.

is the reduced well width, where it is assumed that $s_1/\sigma = 0.12$ (to account for soft repulsion).[16] Integration of the step potential then leads to the so-called temperature-dependent hard segment diameter $d_i(T)$ of component i,

$$d_i(T) = \sigma_i \left[1 - 0.12\ exp\left(-\frac{3\varepsilon_i}{kT}\right)\right] \tag{4-50}$$

Therefore, instead of describing the reference fluid in terms of the temperature-independent hard-segment diameter σ, soft repulsion is accounted for in terms of the temperature-dependent effective segment diameter $d_i(T)$.

4.5.3.2 Hard-Chain Reference Equation of State

Like almost all the variations of SAFT, Gross and Sadowski opted to use the same chain and dispersion terms used in the original SAFT model proposed by Chapman et al. (Chapman, et al., 1989). In the PC-SAFT version, however, hard-sphere chains are used to define the reference fluid itself instead of as a perturbation of the reference as in the original SAFT EOS. Therefore, regardless of the order of this contribution, the equation of state (based on Wertheim's theory) developed by Chapman et al. (Chapman, et al., 1989) is still used here to describe the hard-spheres (homonuclear) chains of the reference fluid:

$$\begin{aligned} \frac{A^{Chain}}{NkT} &= \sum_i x_i m_i \frac{A^{hs}}{N_s kT} - \sum_i x_i (m_i - 1)\ ln\ g_{ii}^{hs}(d_{ii}) \\ &= \bar{m}\frac{A^{hs}}{N_s kT} - \sum_i x_i (m_i - 1)\ ln\ g_{ii}^{hs}(d_{ii}) \end{aligned} \tag{4-51}$$

where $\bar{m} = \sum_i x_i m_i$ is the mean segment number of the system, A^{hs} the hard-sphere contribution to the reference fluid, and $g_{ii}^{hs}(d_{ii})$ represents the average radial distribution function of the hard-sphere fluid in terms of the effective segment diameter. In this case, the expressions of Boublik (Boublík, 1970) and Mansoori et al (Mansoori, et al., 1971) are used to represent the mixture of hard-spheres for the reference system (derived from the Carnahan-Starling equation of state (Carnahan, et al., 1969)),

$$\frac{A^{hs}}{N_s kT} = \frac{1}{\zeta_0}\left[\frac{3\zeta_1\zeta_2}{(1-\zeta_3)} + \frac{\zeta_2^3}{\zeta_3(1-\zeta_3)^2} + \left(\frac{\zeta_2^3}{\zeta_3^2} - \zeta_0\right)\ln(1-\zeta_3)\right] \tag{4-52}$$

$$g_{ij}^{hs}(\sigma_{ij}) = \frac{1}{(1-\zeta_3)} + \left(\frac{d_i d_j}{d_i + d_j}\right)\frac{3\zeta_2}{(1-\zeta_3)^2} + \left(\frac{d_i d_j}{d_i + d_j}\right)^2 \frac{2\zeta_2^2}{(1-\zeta_3)^3} \tag{4-53}$$

with ζ_n defined as

[16] *Soft repulsion* is introduced, because molecules have a collision diameter of σ only when they collide at infinitely slow speed (i.e. the zero temperature limit). Increasing temperature, therefore, will result in a lower collision diameter (Gross, et al., 2001). Conceptually, therefore, it is somewhat like a system of interacting balloons with hard-cores.

$$\zeta_n = \frac{\pi}{6}\rho \sum_i x_i m_i \, d_i^n \qquad n \in \{0,1,2,3\} \tag{4-54}$$

It then follows that the reference fluid is characterized by three pure component parameters: the size parameter σ, the segment energy parameter ε, and chain length m, i.e. the number of segments in the molecule.

4.5.3.3 Dispersion Perturbation Theory for Pure Chain Molecules

The remaining terms of the total Helmholtz energy, just like in SAFT, are then treated as perturbed adjustments of the repulsive interactions defined by the reference fluid. Instead of adding dispersion interactions to hard-spheres and then forming chains as a perturbation in SAFT (refer back to **Figure 4-8**), the chain dispersion is added as a perturbation to the hard-sphere chains forming the reference fluid in PC-SAFT (see **Figure 4-9** below).

The dispersion contribution of the chain interactions (i.e. the attractions) are then treated according to the perturbation theory of Barker and Henderson (Barker, et al., 1967; Barker, et al., 1967), which is expressed as an inverse temperature expansion around the free energy of the reference system:

$$\frac{A^{Disp.}}{NkT} = \overbrace{\frac{A_1}{NkT}}^{\substack{first-order\\ contributions}} + \overbrace{\frac{A_2}{NkT}}^{\substack{second-order\\ contributions}} \tag{4-55}$$

which is typically truncated after the second term (Henderson, 1974) due to numerical considerations[17]. A_1 and A_2 then represent the first-and second-order perturbation terms respectively. Although this theory was originally developed for spherical molecules, Gross and Sadowski (Gross, et al., 2000) were able to extend it to chain molecules since each chain-segment is in itself spherical. Therefore, the total chain-chain interaction between molecules is then given as the sum of all the individual segment-segment interactions of the molecules (Gross, et al., 2000).

$$\frac{A_1}{NkT} = -2\pi\rho\left(\frac{\varepsilon}{kT}\right)\sigma^3 \overbrace{\int_1^\lambda \tilde{u}(x) g_{\alpha\beta}^{hc}(m; x, \rho) x^2 \, dx}^{I_1 = f(m,\eta)} \tag{4-56}$$

$$\frac{A_2}{NkT} = -\pi\rho m \underbrace{\left(kT\frac{\partial\rho}{\partial P^{hc}}\right)}_{\left(1+Z^{hc}+\rho\frac{\partial Z^{hc}}{\partial\rho}\right)^{-1}} \left(\frac{\varepsilon}{kT}\right)^2 \sigma^3 \overbrace{\frac{\partial}{\partial\rho}\left[\rho\int_1^\lambda \tilde{u}(x)^2 g_{\alpha\beta}^{hc}(m; x, \rho) x^2 \, dx\right]}^{I_2 = \frac{\partial(\eta I_1)}{\partial\eta}} \tag{4-57}$$

where $x = r/\sigma$ is the reduced radial distance around a sphere, $\tilde{u}(x) = u(x)/\epsilon$ is the reduced potential function, and $g_{\alpha\beta}^{hc}(m; x, \rho)$ is the site-site radial distribution function of the chains, which

[17] According to the work of Nezbeda (Nezbeda, 2001) "it was established already long time ago that the perturbation expansion is fast converging if the structure of the reference and considered fluids are nearly identical (very similar)."

represents the radial distribution function for a segment α of one chain and a segment β of another chain separated by the radial distance $x_{\alpha\beta} = x$ (Gross, et al., 2000). The compressibility term of the second-order contribution to the dispersion term, in this case, can then be obtained for pure chain fluids using Equation (4-51)**:**

$$\left(1 + Z^{hc} + \rho\frac{\partial Z^{hc}}{\partial\rho}\right) = m\frac{8\eta - 2\eta^2}{(17-\eta)^4} + (1-m)\frac{20\eta - 27\eta^2 + 12\eta^3 - 2\eta^4}{[(1-\eta)(2-\eta)]^2} \tag{4-58}$$

where $\eta \equiv \zeta_3$ is the volume occupied by the molecules (the packing fraction), and represents a reduced segment density. Furthermore, for convenience, the abbreviations I_1 and I_2 are introduced for the integrals of the first-and second-order perturbations, where an approximation obtained from the work of Chiew (Chiew, 1991) for the site-site radial distribution function of the reference fluid is employed

$$g^{hc}(m; x, \rho) = \frac{1}{m^2}\sum_{\alpha}^{m}\sum_{\beta}^{m} g_{\alpha\beta}^{hc}(m; x, \rho) \tag{4-59}$$

Defining relatively simple and yet physically plausible perturbation integrals to solve these equations then represents the most difficult problem for the entire perturbation theory. Furthermore, from the definition of the integrals above, it is evident that the reference contributions and perturbation contributions are interrelated, of which can lead to the density dependence of the integrals exhibiting rather complex and unpredictable behaviour (Nezbeda, 2001). To compensate for these artefacts, the integrals have been replaced by a power series in density (assuming that the temperature dependence of $g^{hc}(m; x, \rho)$ is moderate, and can therefore be neglected):

$$I_1(\eta, m) = \sum_{i=0}^{6} a_i(m)\eta^i \tag{4-60}$$

$$I_2(\eta, m) = \sum_{i=0}^{6} b_i(m)\eta^i \tag{4-61}$$

where the coefficients of the power series (a_i and b_i) are functions of the chain length m, and represent additional (empirical) terms added to the equation of state given by

$$a_i(m) = a_{0i} + \frac{m-1}{m}a_{1i} + \frac{m-1}{m}\frac{m-2}{m}a_{2i} \tag{4-62}$$

$$b_i(m) = b_{0i} + \frac{m-1}{m}b_{1i} + \frac{m-1}{m}\frac{m-2}{m}b_{2i} \tag{4-63}$$

where the model constants a_{0i}, a_{1i}, a_{2i}, b_{0i}, b_{1i}, and b_{2i} of these equations are obtained by fitting the simplified integrals of Equations (4-60) and (4-61) to the integrals of Equations (4-56) and (4-57) for a square-well potential using the radial distribution function proposed by Chiew (see Equation (4-59)). Although this procedure can be, in principle, performed using the step potential given by Equation (4-49), practical results often require the incorporation of information describing the true behaviour of actual substances. The reasons for this are given by Gross and Sadowski (Gross, et al., 2000); stated verbatim as

(1) There are uncertainties in the dispersion properties, namely in the assumed perturbing potential $u(x)$ as well as approximations in $g^{hc}(r)$.
(2) Errors introduced in the reference equation of state can be corrected to a certain extent.
(3) The molecular model assuming molecules to be chains of spherical segments might be oversimplified.

The model constants, therefore, are then fitted to pure-component experimental data. To account for the chainlike shape of the molecules in the dispersion term, it then follows that the elongated molecules of the series of n-alkanes are best suited here as model substances, where methane is assumed to be of spherical shape and is used to determine the boundary case of $m = 1$ (where only the constants a_{0i} and b_{0i} are relevant). The fitting results are given in **Table 4-1**, and are considered to be universal, since the entire ranges for the parameters m and η are effectively covered during regression of experimental data[18].

i	a_{0i}	a_{1i}	a_{2i}	b_{0i}	b_{1i}	b_{2i}
0	0.910563	-0.308402	-0.090615	0.724095	-0.575550	0.097688
1	0.636128	0.186053	0.452784	2.238279	0.699510	-0.255757
2	2.686135	-2.503005	0.596270	-4.002585	3.892567	-9.155856
3	-26.54736	21.41979	-1.724183	-21.00358	-17.21547	20.64208
4	97.75921	-65.2558853	-4.130211	26.85564	192.6723	-38.80443
5	-159.5915	83.31868	13.77663	206.5513	-161.8265	93.62677
6	91.29777	-33.74692	-8.672847	-355.6023	-165.2077	-29.66691

Table 4-1: Universal Model Constants for Equations (4-62) and (4-63) displayed to 7 significant figures— (Gross, et al., 2001).

4.5.3.4 Handling Mixtures

Like **Chapter 4.4**, the PC-SAFT equation can be extended to mixtures by using suitable mixing and combining rules for the pure component parameters. These new parameters will then be characteristic of the "hypothetical" pure fluid that is the mixture. According to Gross and Sadowski (Gross, et al., 2000), "comparisons with simulation data of short-chain mixtures showed that the chain structure does not introduce any significant additional error to the one-fluid mixing rule." Applying the van der Waals one-fluid mixing rules to Equations (4-56) and (4-57), the perturbation terms gives

$$\frac{A_1}{NkT} = -2\pi\rho I_1(\bar{m},\eta) \sum_{i}^{nComp} \sum_{j}^{nComp} x_i x_j m_i m_j \left(\frac{\varepsilon_{ij}}{kT}\right) \sigma_{ij}^3 \tag{4-64}$$

$$\frac{A_2}{NkT} = -\pi\rho\bar{m}\left(1 + Z^{hc} + \rho\frac{\partial Z^{hc}}{\partial\rho}\right)^{-1} I_2(\bar{m},\eta) \sum_{i}^{nComp} \sum_{j}^{nComp} x_i x_j m_i m_j \left(\frac{\varepsilon_{ij}}{kT}\right)^2 \sigma_{ij}^3 \tag{4-65}$$

where the power series of I_1 and I_2 (Equations (4-60) and (4-61)) are calculated using the mean segment number $\bar{m}$ of the mixture,

[18] m varies between $m = 1$ for spherical molecules (in this case represented by methane) and $m = \infty$ for infinitely long chains (represented by the series of n-alkanes), and the packing fraction ($\eta \equiv \zeta_3$) ranges between $\eta = 0$ for an ideal gas and $\eta \leq 0.74$ for the closest packing of segments (Gross, et al., 2001).

$$\bar{m} = \sum x_i m_i \tag{4-66}$$

and the van der Waals one-fluid mixing rules, which are typically abbreviated as

$$m^2 \left(\frac{\varepsilon}{kT}\right)^y \sigma^3 = \sum_i^{nComp} \sum_j^{nComp} x_i x_j m_i m_j \left(\frac{\varepsilon_{ij}}{kT}\right)^y \sigma_{ij}^3 \qquad y\epsilon\{1,2\} \tag{4-67}$$

where m is replaced with $\bar{m}$. The cross parameters relating to pairwise interactions are then described using the Lorentz-Berthelot combining rules:

$$\sigma = \sqrt[3]{\frac{m^2 \left(\frac{\varepsilon}{kT}\right)^{y=1} \sigma^3}{m^2 \varepsilon}} \tag{4-68}$$

$$\sigma_{ij} = \frac{1}{2}(\sigma_i + \sigma_j)$$

$$\varepsilon = \frac{m^2 \left(\frac{\varepsilon}{kT}\right)^{y=2} \sigma^3}{m^2 \left(\frac{\varepsilon}{kT}\right)^{y=1} \sigma^3} \tag{4-69}$$

$$\varepsilon_{ij} = \sqrt{\varepsilon_i \varepsilon_j}(1 - k_{ij})$$

where one binary interaction parameter, k_{ij}, in the energy term is introduced so that predictions made using the PC-SAFT equation can be regressed to reproduce the behaviour of specific experimental datasets. Therefore, the binary interaction parameter can serve as an indication of any inadequacies or shortcomings that the PC-SAFT equation may have. As the defects grow, the k_{ij} values will become far removed from zero. This can be important, for instance, in cases where the exclusion of multipolar terms may lead to significant deviations like in the case of mixtures containing CO_2. At present, however, additional terms beyond those in the original PC-SAFT equation (Gross, et al., 2001) are not discussed; instead, they will only be considered on an as needed basis once a working version of the PC-SAFT equation is developed for testing purposes.

5 Evaluation of PC-SAFT Model

The present chapter evaluates the assumption that the PC-SAFT equation can describe all required fluid phase properties with a sufficient degree of accuracy. Large uncertainties in some or all property predictions, for instance, would most certainly lead to false conclusions about how a refrigerant would perform in a given vapour compression process. A very high precision representation of the working fluid is essential for process model calculations during the final stage of design, but is probably not required for fluid ranking during the design process.

The *REF*erence fluid *PROP*erties package (REFPROP) used in ASPEN Plus® (AspenTech, 2012) is based on the most accurate equations of state and models currently available, and provides thermodynamic and transport properties for a total of 97 components and several mixtures and includes many of the working fluids currently used by the refrigeration industry. The equations of state for the description of pure component thermodynamic properties in REFPROP are mainly:

- modified Benedict-Webb-Rubin equation of state (pressure explicit)
- Helmholtz equations of state (explicit in Helmholtz energy),
- extended corresponding states models that require only a limited number of parameters (for fluids with limited data).

For mixtures an excess Helmholtz energy model is then used, where experimentally based values of the mixture parameters are available for hundreds of mixtures.

REFPROP then represents a collection (or package) of a selected model for each fluid and their mixtures within its database. Given the high precision of REFPROP to describe such fluids, with uncertainties typically below 1% for most conditions and as low as 0.1% in some cases, it is used here as the baseline (best-case scenario) for the evaluation of the PC-SAFT equation of state, and then later for fitting PC-SAFT parameters for select components.

5.1 Introduction

The PC-SAFT equation requires at least three pure-component parameters to calculate all thermodynamic properties of each component present in a fluid:

- m, segment chain-length that forms the component
- σ, temperature-independent segment diameter
- ε, segment dispersion energy, i.e. the depth of the potential well

The physical meaning of these parameters are depicted in **Figure 5-1** below.

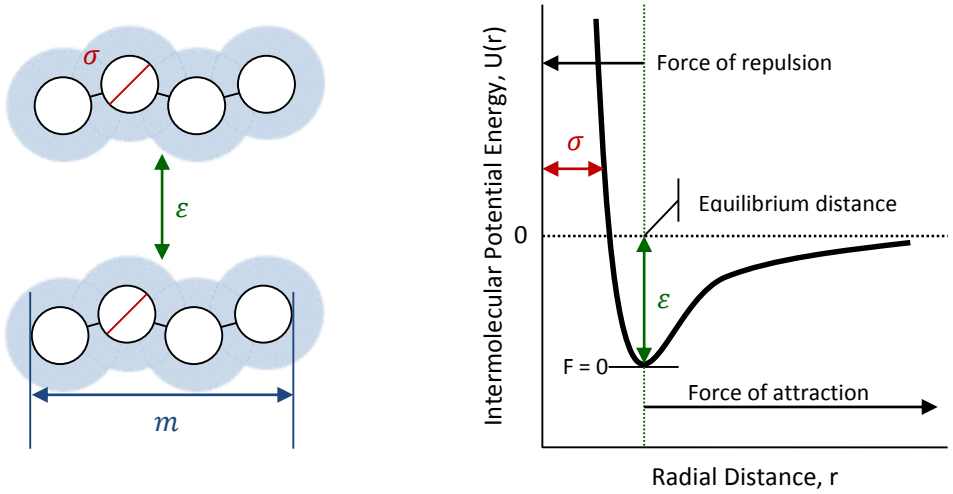

$$\text{Force}\,(r) = -\frac{\mathrm{d}U(r)}{\mathrm{d}r}$$

The distance r is then described by all three pure component PC-SAFT parameters via the radial distribution function of hard-spheres (hs) previously given as Equation (4-53) on Page 57:

$$g_{ij}^{hs} = f\left(\sigma_{ij}, \varepsilon_{ij}, d_{ij}(m_i, m_j)\right)$$

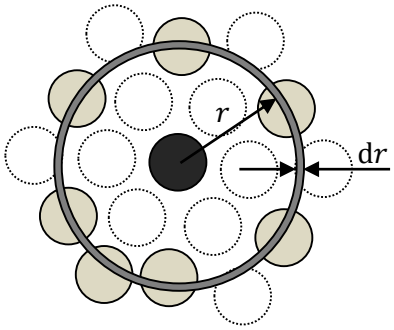

Figure 5-1: Reference schematic for the parameters of a PC-SAFT mixture.

Further parameters are required in case of polar or associating components. These parameters can either be directly fitted to available experimental data of sufficient quality, or to appropriately accurate results of a predictive model or correlation. This latter approach is used here, whereby the three pure-component parameters of the PC-SAFT equation are fitted to the predictions of saturated vapour pressure, liquid density and heat of vaporization obtained using the REFPROP package. For the case of mixtures one additional PC-SAFT parameter (k_{ij}) can also be used to correct the dispersion interaction between unlike species (ε). The fitting of the mixture parameter, however, requires quality mixture information for each component-pair. This is clearly not practical for the large scale optimisation that is proposed in this work, and the mixture parameter is therefore neglected here out of necessity ($k_{ij} = 0$). In case of sufficiently similar compounds this usually does not lead to unrealistic results.

By choosing an equation of state to represent thermodynamic properties, a wide range of fluid properties are guaranteed to display thermodynamic consistency with each other. The question then becomes, *are the results obtained using the PC-SAFT equation sufficiently accurate?* Pure component and mixture evaluations are therefore presented next for some common refrigerants, followed by concluding remarks concerning the applicability of the PC-SAFT equation to the present project.

5.2 Pure Components

Fluid	Model	Source	Range of Applicability		
			T [K]	**P** [MPa]	$\boldsymbol{\rho}$ [kg/m^3]
R-12	Helmholtz	(Marx, et al., 1992)	116.10 (T_{tp}) – 525	0 – 200	0 – 1829.4
R-22	Helmholtz	(Kamei, et al., 1995)	115.73 (T_{tp}) – 550	0 – 60	0 – 1721.6
R-32	MBWR	(Tillner-Roth, et al., 1997)	136.34 – 435	0 – 70	0 – 1429.3
R-115	Helmholtz	(Lemmon, et al., 2010)	173.75 (T_{tp}) – 550	0 – 60	0 – 614.78
R-125	MBWR	(Lemmon, et al., 2005)	172.52 (T_{tp}) – 500	0 – 60	0 – 1691.1
R-134a	Helmholtz	(Tillner-Roth, et al., 1994)	169.85 (T_{tp}) – 455	0 – 70	0 – 1591.7
R-143a	MBWR	(Lemmon, et al., 2000)	161.34 (T_{tp}) – 650	0 – 100	0 – 1332.0
R-290	MBWR	(Lemmon, et al., 2009)	85.53 – 650	0 – 1000	0 – 908.37
R-600	Helmholtz	(Bücker, et al., 2006)	134.90 (T_{tp}) – 575	0 – 200	0 – 805.57
R-601	Helmholtz	(Span, et al., 2003)	143.47 (T_{tp}) – 600	0 – 100	0 – 959.6

Table 5-1: Equations of state currently implemented in REFPROP for a selection of pure fluids, where T_{tp} is the triple point temperature of the fluid.

PC-SAFT parameters were fitted to REFPROP predictions for each of the fluids listed in **Table 5-1** above. A simple objective function that calculates the root-mean-squared-deviation (RMSD) in saturated vapour pressure, liquid density and heat of vaporization at the boiling point was used for all regressions:

$$O.F. = f(m, \varepsilon/K, \sigma) = RMSD = \sqrt{\frac{1}{n}\sum \frac{P^* - P_{ref}}{P_{ref}}} \tag{5-1}$$

Where n is the number of property values used for the fitting, P^* the property value calculated using PC-SAFT and P_{ref} for that of REFPROP.

The objective function was minimized using the Simplex Nelder-Mead method (Nelder, et al., 1965) by accessing and controlling Aspen Plus as a COM object via VBA in Excel.[19] Although the built-in Data Regression System of Aspen Plus (DRS) could have also been used in this case, it is the experience of the author that the Simplex methodology consistently yields superior results compared to the maximum likelihood method that Aspen Plus employs in the DRS. A summary of the regression results is provided in **Table 5-2** below, including the property values used for the fitting from REFPROP (with non-zero differences between the results obtained using PC-SAFT and REFPROP given in parentheses). As the number of degrees of freedom (3 parameters) is equal to the number of data points, a perfect fit should be expected.

[19] The routines developed to interface with Aspen Plus were integrated into the Thermodynamic Research Utilities for Excel (TRUx) utility that the author has been developing. It currently consists of roughly 50,000+ non-blank lines of code (1,000+ pages) containing about 1.5+ million non-blank characters (300,000+ words). As it stands, at a high typing speed of 80 words per minute, it would physically take 2.5+ days of continuous typing to write! Although it is outside the scope to cover the program in detail, a brief overview is provided in **Appendix E**.

Fluid	O.F.	m	σ	ε/k	T_b	ρ_b	$\Delta h_{v,b}$
		----	[Å]	[K]	[K]	[kg/m^3]	[kJ/kmol]
R-12	0	2.1470	3.6053	210.18	243.398	1487.02	20092.2
R-22	0	2.3461	3.1899	195.07	232.340	1409.18	20211.3
R-32	6.79E-07	2.1474	2.9355	201.86	221.499	1212.93	19865.0
R-115	0	2.7284	3.5251	171.88	233.932	1546.63	19365.4
R-125	0	3.0853	3.1308	157.48	225.061	1513.60	19695.4
R-134a	0	3.0550	3.0801	176.49	247.076	1376.67	22137.5
R-143a	0	2.3209	3.3690	187.33	225.909	1166.39	19045.5
R-290	2.69E-07	1.9224	3.6683	213.23	231.036	580.895	18767.2
R-600	0	2.2176	3.7713	229.65	272.650	601.271	22417.7
R-601	9.47E-08	2.5798	3.8140	237.01	309.214	609.724	25798.7

Table 5-2: Fitted PC-SAFT molecular parameters (this work) for selected components.

Although the fitting results of **Table 5-2** provide a near perfect match at the normal boiling point conditions (T = T_b and P = 101.325 kPa) for each refrigerant, the important T-s and T-h diagrams show large deviations at other temperatures. **Figure 5-2** below, for instance, shows a temperature-entropy (a) and a temperature-enthalpy diagram (b) for the evaluated refrigerants. To simplify the results for discussion, dimensionless coordinates were used in both figures. Both entropy (s*) and enthalpy (h*) were normalized to the calculated conditions obtained from each respective model at 273.15 K (arbitrarily chosen):

$$s^* = \frac{s - s_l^0}{s_v^0 - s_l^0} \tag{5-2}$$

$$h^* = \frac{h - h_l^0}{h_v^0 - h_l^0} \tag{5-3}$$

This normalizes the width of the two-phase dome, and is therefore also suitable for qualitatively assessing the impact of the domes' shape on the coefficient of performance for each refrigerant. The superheated-vapour irreversibilities of a real vapour compression system are then described by T-s* while the throttling-induced capacity losses are described by T-h*. If a simple Carnot cycle is imagined that uses the same condensing and evaporating temperatures for each fluid, for instance, then it can be concluded that these losses will be minimized (COP is maximized) for R-12 compared to all other refrigerants depicted in **Figure 5-2**.[20] R-12 simply has the largest dome of those evaluated, which is qualitatively why it has historically been such a good refrigerant.

[20] R-115 is only needed later in Chapter 5.3 for defining the mixture R-502. These results, therefore, have been purposely omitted from **Figure 5-2** so that the curves for the remaining refrigerants could be easily distinguished from each other.

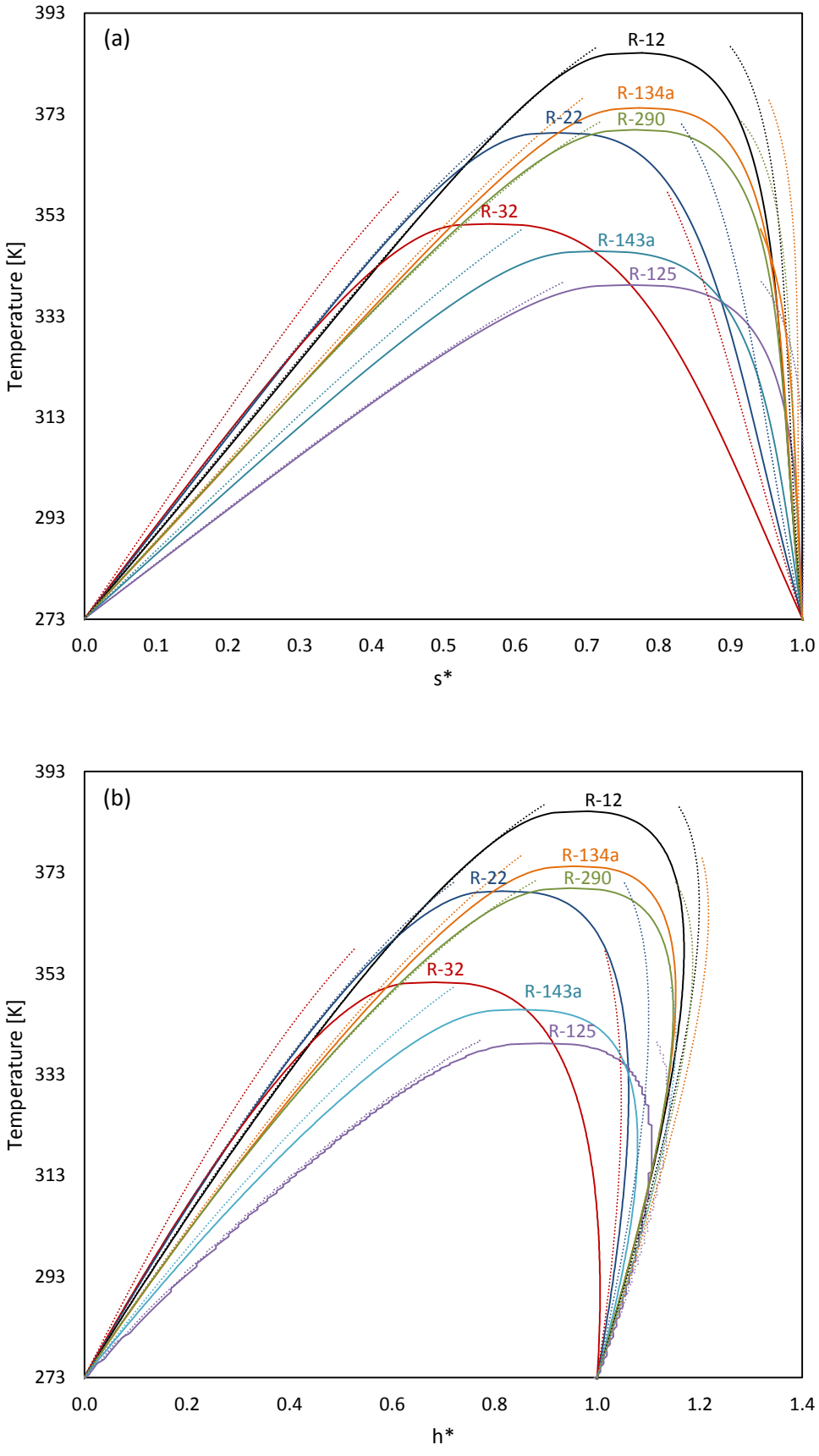

Figure 5-2 Dimensionless temperature-entropy (a) and temperature-enthalpy (b) diagrams calculated using REFPROP (solid lines) and PC-SAFT (dotted lines) for a selection of pure-component refrigerants.

Although the results obtained using the fitted parameters of PC-SAFT are quite poor compared to the calculations made using REFPROP, the general character of the results is still similar in nature. From a design standpoint, however, these deviations would lead to incorrect mass flow rates and state conditions along the actual vapour-compression path of the refrigerant. To understand the reason for these differences it is most useful to trace the calculation of the enthalpy departure. This is done in the following subsection for R-32, which has the largest deviations in caloric properties from the values calculated using REFPROP (best-case).

5.2.1 Enthalpy Departure

In practice the effects of temperature and pressure (or volume) on various thermodynamic properties are of great interest. This is especially true for the case of refrigerant design, where these effects must be understood and balanced against specific process requirements. The calculation of enthalpy, like any of the other auxiliary thermodynamic properties covered in **Appendix A**, requires a reference state that can differ from program to program. In Aspen Plus the reference state is that of an ideal gas at 298.15 K and 101.325 kPa and the enthalpy at this reference state is the enthalpy of formation from their most stable state at the same conditions. This means that the enthalpy of a compound at any given temperature and pressure can then be calculated as the sum of three different quantities[21] (depicted in **Figure 5-3** on the following page):

1. **DHFORM:** the enthalpy change involved in reacting the elements at 298.15 K and 101.325 kPa at their reference state (vapour, liquid or solid) conditions to form the compound at 298.15 K and 101.325 kPa at ideal gas conditions, so that the enthalpy description is also consistent with respect to chemical reactions.
2. Enthalpy change involved in taking the compound from 298.15 K to the system temperature at 101.325 kPa and ideal gas conditions, i.e. the integral of the ideal heat capacity correlation (CPIG or CPIGDP parameters):

$$\int_{298.15}^{T} c_p^{ig}(T)dT \tag{5-4}$$

   This is then added to the value of DHFORM to obtain the enthalpy contribution from the ideal gas at the system temperature as **HIG**:

$$HIG(T) = DHFORM + \int_{298.15}^{T} c_p^{ig}(T)dT \tag{5-5}$$

3. **DH:** the difference in enthalpy between the ideal gas at system temperature and 101.325 kPa and the real gas at this temperature and system pressure. This depends on the property method used to calculate the residual part (e.g. REFPROP or PC-SAFT).

[21] Further (different) paths of enthalpy calculation are also optionally available in Aspen Plus and most other process simulation programs. So although the vapour enthalpy departure is typically used for the equation of state approach (as is shown below in **Figure 5-3**), an alternative route could be to use the liquid enthalpy departure instead with the heat of vaporization (that could even be described by a separate correlation).

In Aspen Plus this is referred to as either DHV (vapour state), DHL (liquid state) or DHS (solid state which is not of interest here).

The shape of the enthalpy two-phase dome is therefore controlled solely by the enthalpy departure (or residual contribution) that is calculated using the selected thermodynamic model.

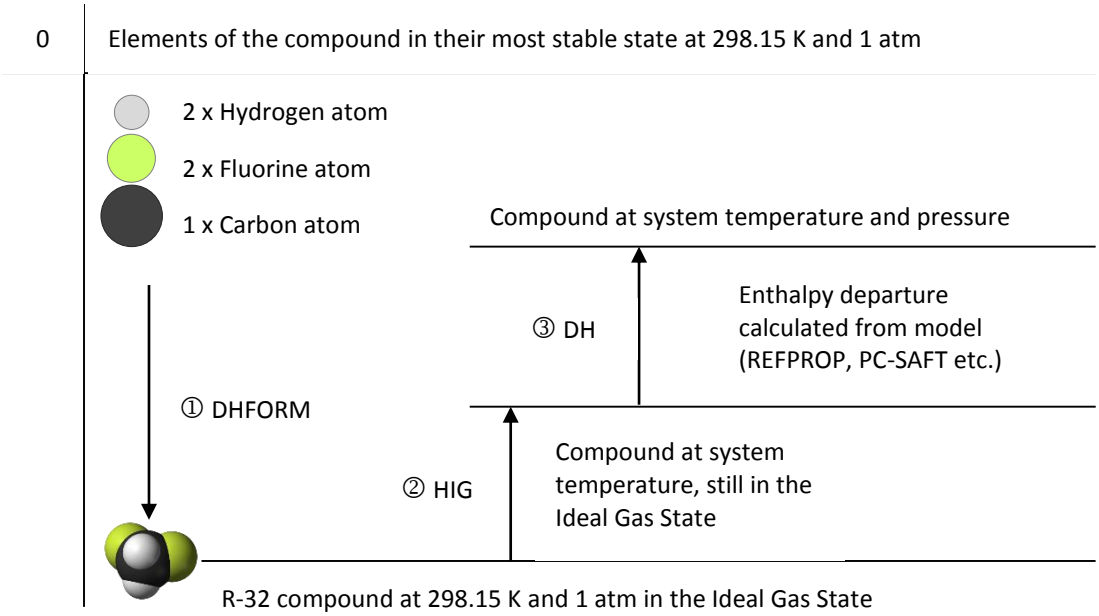

Figure 5-3 Enthalpy calculation procedure used by Aspen Plus, using R-32 as an example.

To mathematicians properties like enthalpy (and all other auxiliary properties) represent a special class of functions that are "homogeneous of the first degree." This is just a conceited way of saying that their values are interrelated through the total and partial derivatives of the properties and the intensive thermodynamic properties that influence their behaviour (i.e. mass, temperature and pressure only). The total differential of the specific enthalpy for a closed system (constant mass) can therefore be written as

$$dh = \underbrace{\left(\frac{\partial h}{\partial T}\right)_P dT}_{C_p dT} + \left(\frac{\partial h}{\partial P}\right)_T dP \tag{5-6}$$

where the second term is the enthalpy departure (or residual contribution) and the first partial derivative, $\left(\frac{\partial h}{\partial T}\right)_P$, is readily identified as the molar heat capacity *at constant pressure* (a function of temperature only), leaving a relationship that describes $\left(\frac{\partial h}{\partial P}\right)_T$ to be desired. By taking the partial derivative of the functional form of enthalpy given by equation (A-17) with respect to pressure one obtains the following:

$$\overbrace{h = Tds - Pdv}^{\text{Eq. (A-17)}} \longrightarrow \left(\frac{\partial h}{\partial P}\right)_T = T\left(\frac{\partial s}{\partial P}\right)_T - P\left(\frac{\partial v}{\partial P}\right)_T \tag{5-7}$$

Combining this with the Maxwell relationship $-\left(\frac{\partial s}{\partial P}\right)_T = \left(\frac{\partial v}{\partial T}\right)_P$ Equation (5-7) then leads to the enthalpy departure described by two separate terms: one that corrects for temperature and the other for both temperature and pressure (which is influenced by the PVT-behaviour described by the equation of state that is being used):

$$dh = C_p dT + \left[v - T\left(\frac{\partial v}{\partial T}\right)\right] dP \tag{5-8}$$

Since HIG in Aspen Plus already describes the enthalpy difference of the ideal gas between 298.15 K and the system temperature, the enthalpy at any given temperature and pressure is then calculated as

$$\begin{aligned} h(T,P) &= \Delta H^0 + \int_{298.15}^{T} C_p^{ig}(T)dT + \int_0^P \left[v - T\left(\frac{\partial v}{\partial T}\right)\right] dP \\ &= DHFORM + HIG(T) + DH(T,P) \end{aligned} \tag{5-9}$$

Although the standalone REFPROP program employs a different reference state and ideal gas heat capacity correlation than what is used by Aspen Plus (which is built directly into the external REFPROP program for each fluid model), a "black-box" check shows that Aspen Plus actually does some trickery and renormalizes the results obtained from the external REFPROP package.[22] The REFPROP calculations obtained using Aspen Plus are therefore forced to be consistent with the calculation procedure outlined in **Figure 5-3** above. Therefore, within this framework, the differences in the calculation of enthalpy between one model and the next can only result from the calculation of DH (which is different for each thermodynamic model used). This is not to say that the calculation of HIG is unimportant, but that its effect cancels out if each model uses the same CPIG parameters and equation to calculate the ideal gas reference state (which is the case in Aspen Plus).

[22] The documentation on the Aspen Properties System (APS) goes to great lengths to describe the differences between the reference states used by Aspen Plus and those employed in the external REFPROP package, but nowhere in all of [this] do they mention that they are actually renormalizing the results obtained from REFPROP so that they are consistent within the existing framework of the APS. Looking through the REFPROP documentation by NIST, it appears that Aspen Tech simply provided a cut-and-paste of information that is no longer relevant. It just goes to show that it is always wise to double check the calculation procedures used by process simulators (i.e. they should not be treated as a "black-box").

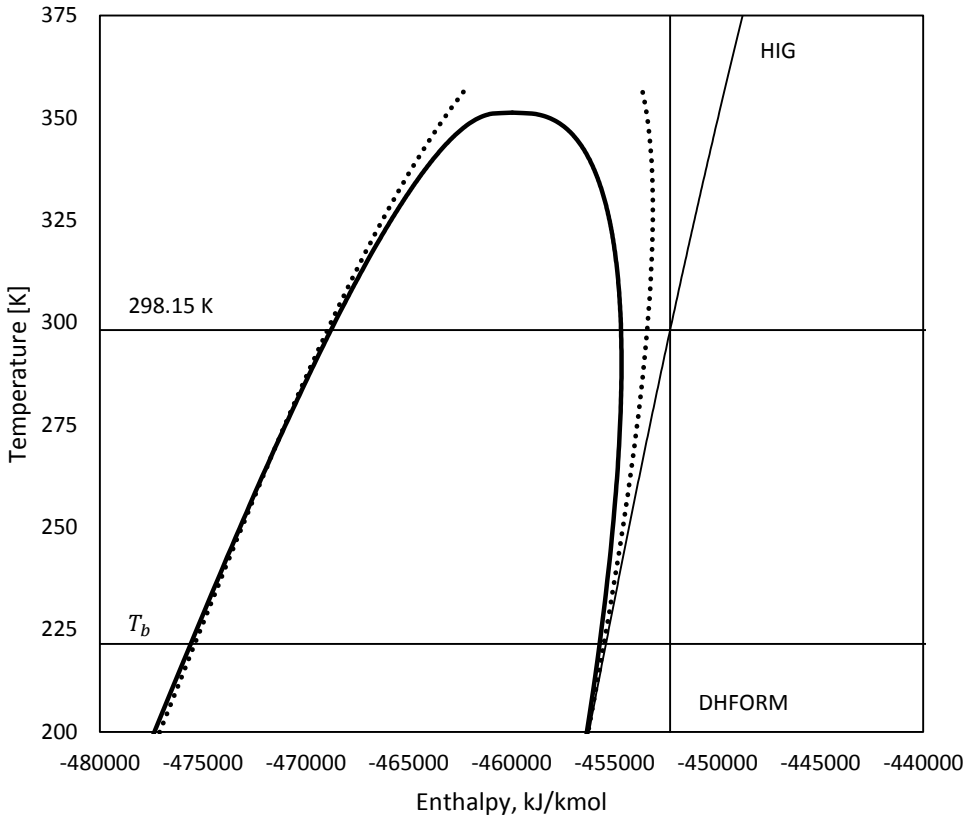

Figure 5-4 Calculated pressure-enthalpy diagram for R-32 using REFPROP (solid line) and PC-SAFT using fitted parameters (dotted line).

Figure 5-4 above depicts the pressure-enthalpy diagram for the case of R-32, along with the separate contributions used in the calculation of enthalpy. Far enough away from the critical point the vapour is in a close to ideal state and so the pressure correction of the enthalpy departure largely drops away. The slope of the vapour curve is thus primarily a function of the integral of the ideal heat capacity correlation used in the calculation of HIG (represented by the difference between the DHFORM and HIG lines of the figure). As the critical region is approached, however, the slope of the vapour curve begins to deviate more strongly as the vapour becomes denser, while in the case of the liquid the effect of temperature on the liquid density is much smaller by comparison (**Figure 5-5** a). This is why the shape of the two-phase dome is most strongly determined by the character of the vapour phase, where the latent heat of vaporization (Δh_v, or DHVL) is then just the enthalpy difference between the two saturation curves at any given temperature. Since Δh_v approaches zero at the critical point, the slope of the saturated vapour enthalpy has no choice but to change in order to intersect with the relatively insensitive slope of the saturated liquid line (thereby completing the shape of the bell-curve).

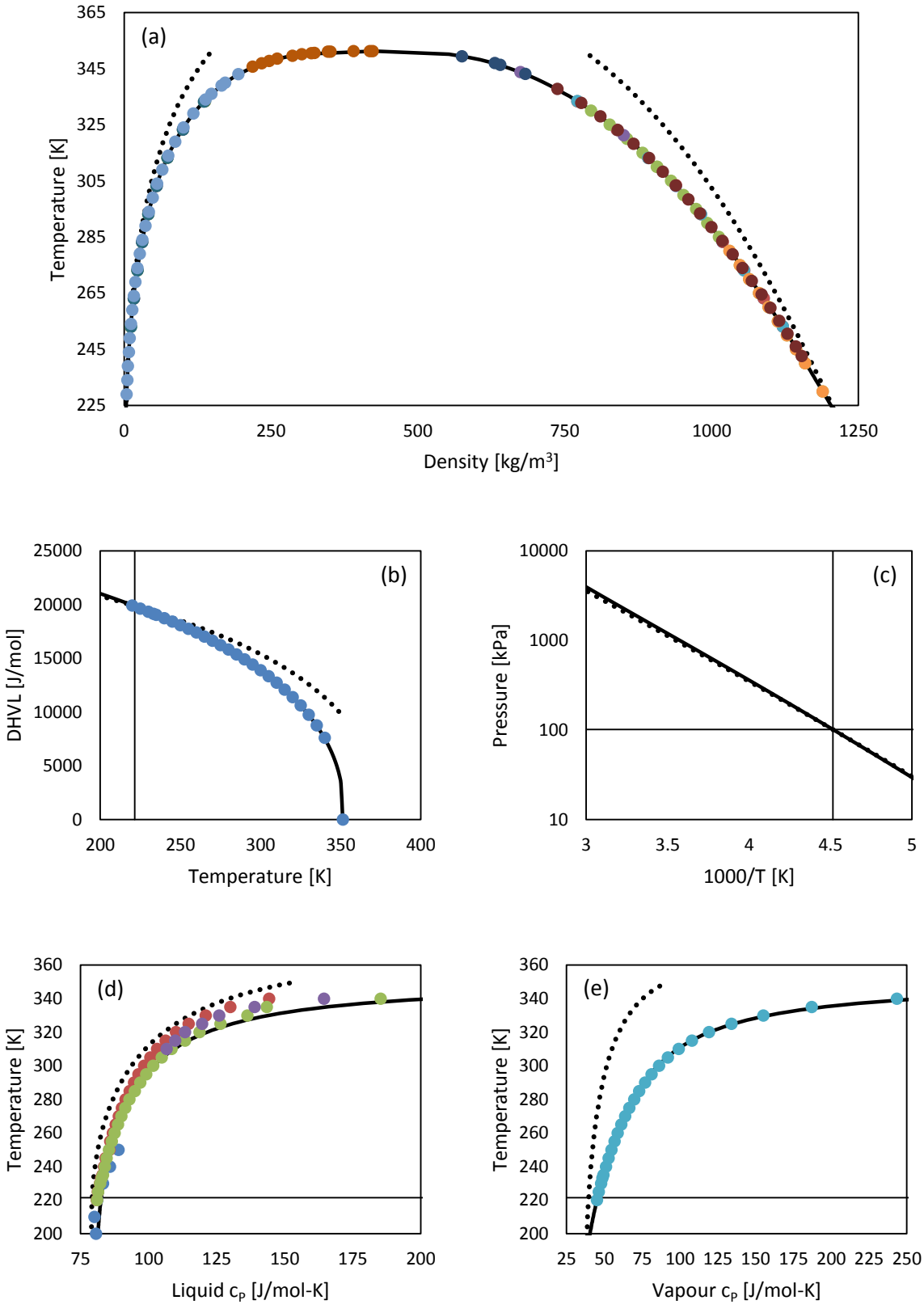

Figure 5-5: Performance of REFPROP (solid line) and PC-SAFT (dotted line) against select experimental data from the DDB (DDBST GmbH, 2012) for R-32: saturated densities (a), heat of vaporization (b), saturated vapour pressure (c), liquid heat capacity (d) and vapour heat capacity (e). Intersecting lines are at the normal boiling point fitting conditions for R-32 (T_b = 221.5 K and 101.325 kPa).

Since HIG is used both in the calculation of the saturated vapour and saturated liquid enthalpy values, its effect gets cancelled out during the calculation of Δh_v which is depicted against some experimental data in **Figure 5-5** (b) above. As the figure shows, there exists only a single point in which the PC-SAFT equation correctly predicts the heat of vaporization: the normal boiling point that was used to fit the PC-SAFT parameters (T_b = 221.5 K). Below this point the PC-SAFT under predicts Δh_v, while above T_b it over predicts Δh_v. Since the heat of vaporisation is directly linked to the saturated vapour pressure by the Clausius-Clapeyron equation:

$$\frac{dP^S}{dT} = \frac{\Delta h_v}{T(v^V - v^L)} \tag{5-10}$$

this translates into an over prediction of the saturated pressure (P^S) below T_b, as shown in **Figure 5-5** (c) above, and an under prediction of P^S above T_b. The under prediction of P^S above T_b may imply that the PC-SAFT equation is predicting stronger intermolecular forces than REFPROP, which in turn results in the PC-SAFT equation predicting lower heats of vaporisation above the normal boiling point. Or, in other words, the effect of error in Δh_v on PC-SAFT is mostly compensated by the error in $(v^V - v^L)$ at higher temperatures. Therefore in order for the PC-SAFT equation to correctly capture both the heat of vaporisation and the liquid density (or volume) at the normal boiling point, as per the fitting procedure, the PC-SAFT equation has no choice but to adjust the saturated vapour volume (or density) prediction to do so. As can be seen in **Figure 5-5** (a) above, the PC-SAFT equation incorrectly predicts the vapour volume even at low temperatures near T_b. So although the PC-SAFT equation can be fitted to the heat of vaporization at a single point (such as T_b in this case) it does not necessarily mean that the specific heat capacities of either the liquid and/or vapour phases are correctly represented too. As a result differences of about 12% and 34% are observed in **Figure 5-5** (d) and **Figure 5-5** (e) for both the specific heat capacities of the saturated liquid and vapour phases respectively compared to REFPROP.

The shape of the enthalpy-dome is therefore directly related to the ability of the equation of state to correctly describe the PVT (or VLE) behaviour of the fluid. So although the discussion was limited to R32, the results can be easily generalized for all fluids in this case. An analytical comparison using the PC-SAFT equation can only be meaningful, therefore, if the relative errors are more or less consistent across all of the fluids.

5.2.2 Physical Significance

It is important to recognize that the ability of the PC-SAFT equation to correctly represent pure component properties, besides the equation form itself, is dependent on both the conditions at which the parameters are regressed to match and the objective function that is used for the fitting. **Figure 5-6** below, for example, shows multiple calculation results for R-32 using the PC-SAFT equation and separate parameters that were regressed to REFPROP predictions at different temperatures. The results of the upper dotted line are the "original" results obtained using the standard fitting procedure at the normal boiling point, while the results of the lower dotted line were obtained using the same fitness function but at a much higher reduced temperature, T_r = 0.91 (319.65 K). Both parameter sets underestimate the heat of vaporisation of R-32 below their respective fitting conditions, and overestimate the phase equilibrium behaviour beyond these points. This type of under-over prediction around the single state point used to fit the parameters seems to be fairly consistent for the selected components (as was already shown in **Figure 5-2** on Page 66).

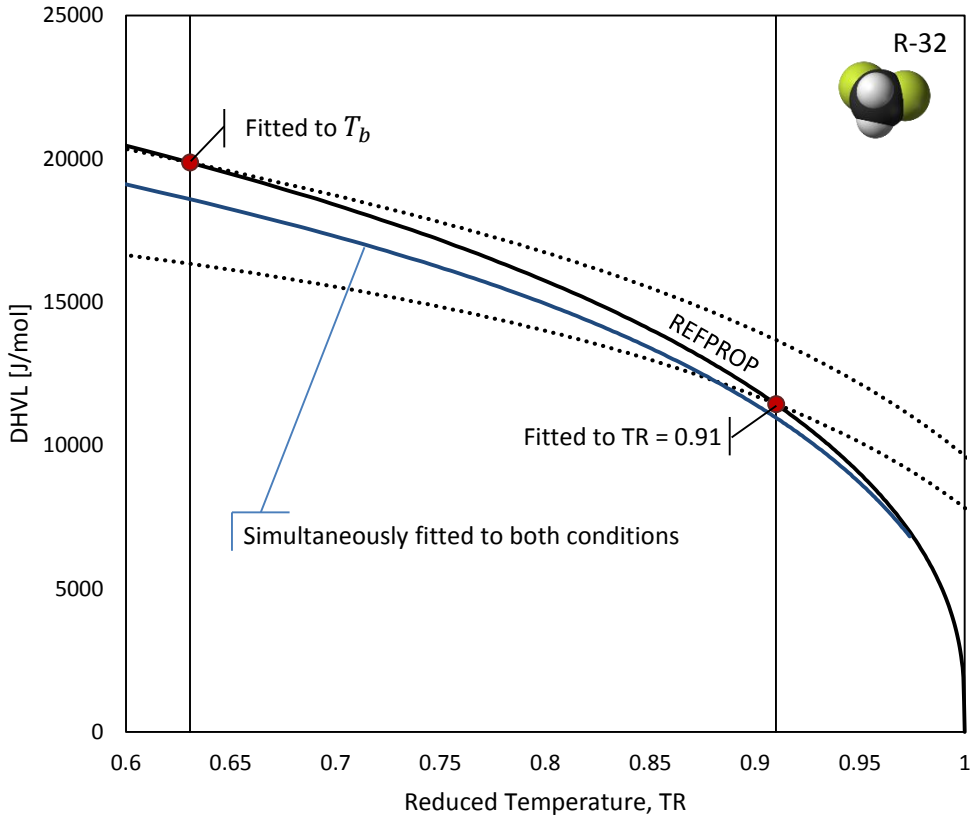

Figure 5-6: The fitting results of PC-SAFT parameters for R-32, regressed to REFPROP predictions at different conditions.

Although inaccuracies in the PC-SAFT equation are unlikely to be wholly avoided, it is probably better to have underestimations in a design-case scenario. Overdesigned equipment, for instance, can most often still achieve the design objective(s) without major equipment modifications, whereas under designs (from overestimations) will likely require complete replacements that cost both precious time and money. Underestimations, in this case, for R-32 can only be forced for the majority of reduced temperatures, up to T_r values of around 0.98, by simultaneously regressing the PC-SAFT parameters to both conditions (blue line of **Figure 5-6** above). Doing so, however, undermines the theoretical framework of the PC-SAFT equation.

Figure 5-7 below, for example, shows the extreme case of individually fitting PC-SAFT parameters over a wide range of temperatures ($0.63\ (T_b) \leq T_r \leq 0.98$). As the fitting temperature is increased the segment number (or shape) of the R-32 molecule becomes smaller, or more "gas-like", in order to sufficiently describe the behaviour at the higher fitting temperatures, while at the same time both the segment diameter and the dispersion energy parameter also increase. Although it is tempting to introduce temperature-dependent parameters into the PC-SAFT equation, i.e. given the near perfect matches at each fitted temperature, the results would no longer make physical sense. Higher intermolecular dispersion interactions are most often associated with larger molecules, not smaller fatter molecules as is the case here. The standard fitting procedure is therefore likely to be only ever guaranteed, with confidence, for reduced temperatures in the vicinity of the normal boiling point of the pure components (which is typically $T_r \cong 0.6 – 0.8$ for most components), with significant errors then expected for T_r > 0.95 (which should be outside the operating range of most, if not all, refrigerants).

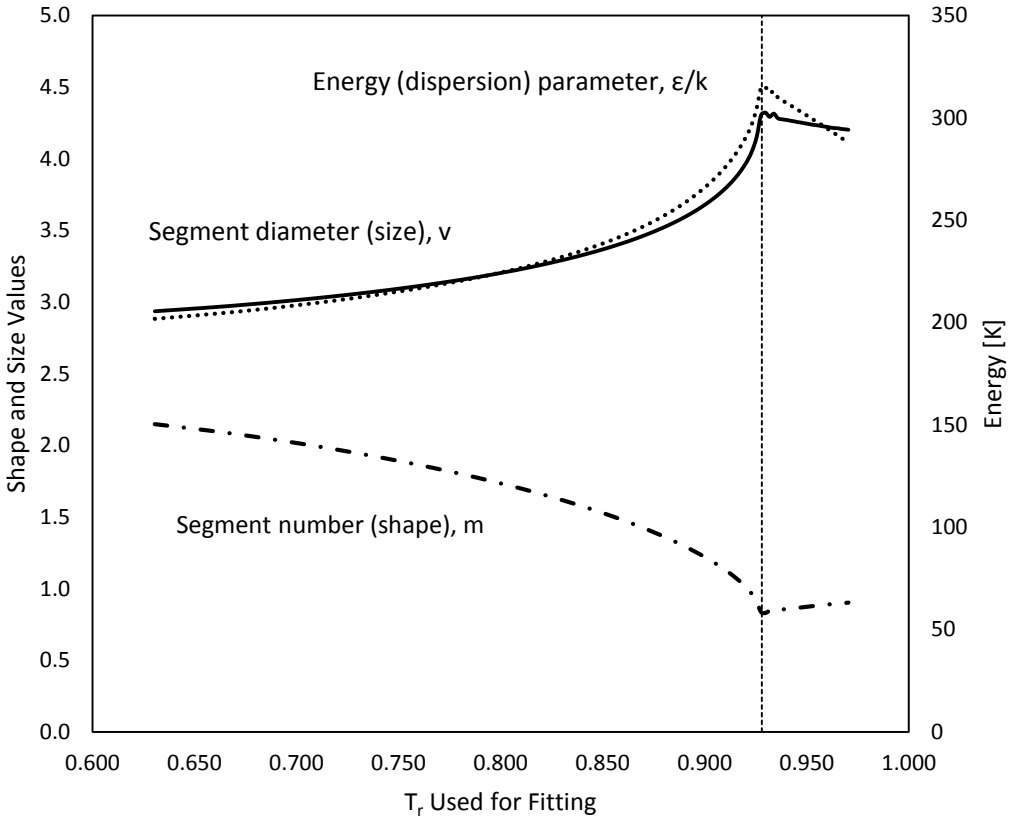

Figure 5-7: PC-SAFT parameters for R-32 fitted to a range of reduced temperatures T_r.

The main advantage of using the PC-SAFT equation is that the model parameters are well-behaved and suggest predictable trends within specific component families. It was shown, for instance, that the parameters for n-alkanes can qualitatively be related to the molecular weight of the component by (Gross, et al., 2001):

$$(m/M) = q_{02} + q_{12}\left[\frac{M - M_{CH_4}}{M}\right] + q_{22}\left[\frac{M - M_{CH_4}}{M}\right]\left[\frac{M - 2 \cdot M_{CH_4}}{M}\right] \tag{5-11}$$

$$\sigma = q_{01} + q_{11}\left[\frac{M - 16.04}{M}\right] + q_{21}\left[\frac{M - 16.04}{M}\right]\left[\frac{M - 2 \cdot 16.04}{M}\right] \tag{5-12}$$

$$(\varepsilon/k) = q_{03} + q_{13}\left[\frac{M - 16.04}{M}\right] + q_{23}\left[\frac{M - 16.04}{M}\right]\left[\frac{M - 2 \cdot 16.04}{M}\right] \tag{5-13}$$

with coefficients for n-alkanes given in **Table 5-3**.

j	units	0	1	2
q_{j1}	Å	3.7039	-0.3226	0.6907
q_{j2}	mol/g	0.06233	-0.02236	-0.01563
q_{j3}	K	150.03	80.68	38.96

Table 5-3: Parameters for Equations (5-11) – (5-13).

Figure 5-8, for example, shows well-defined trends for a number of components when the fitted PC-SAFT parameters are grouped into similar component families. The clear linear trend of the n-alkanes of **Figure 5-8** (a) are well represented by the predicted values obtained using Equations (5-11) – (5-13) and the parameters of **Table 5-3** (which are specific to straight-chain alkanes). Although similar trends are also evident for the branched alkanes of **Figure 5-8** (b), cycloalkanes of **Figure 5-8** (c) and halocarbons of **Figure 5-8** (d), better predictions would require that the parameters of **Table 5-3** be separately refitted for each component family. Even then, the predictive approach is likely to fail in certain cases, such as in halo alkanes where the position of the halogenated components may need to be more accurately accounted for (or the steric effects of the branched alkanes). Although not wholly accurate, equivalent predictions made for straight chain alkanes for given molecular weights are likely in the vicinity of the true values for many potential refrigerants. The predictions can therefore be used as a first approximation/check of the parameter fitting results within the project.

The mathematical complexity of the PC-SAFT equation, for instance, may lead to cases of multiple solutions. To test the uniqueness of the fitting solution, starting values for the PC-SAFT parameters were randomised for the case of R-32: segment number ($0.5 \leq m \leq 5$), segment diameter ($1.0 \leq \sigma \leq 5$) and the energy parameter ($1.0 \leq \varepsilon/k \leq 500$). From over 125 unique starting values, four unique parameter sets were found using the standard fitting procedure, i.e. they all satisfied (or nearly satisfied) the fitting criteria. The parameter results are shown in **Table 5-4** below, where cases (2) – (4) are easily eliminated due to severe calculation failures away from the normal boiling point condition used to fit the parameters. The results obtained using the parameters of case (1), on the other hand, give no such errors to base such a decision on, and qualitative comparisons such as **Figure 5-9** are only useful if experimental or predicted data of sufficient quality is available for comparison (which is typically not the case). Instead, given the predictable trends of the parameters of the PC-SAFT equation, the results of case (1) can safely be discarded based on their values alone. The segment number, for instance, is less than one (smaller than methane) and is simply physically unrealistic in this case. Furthermore their values are far removed from the equivalent alkane predictions using Equations (5-11) – (5-13): $m \approx 2.222$, $\sigma \approx 3.664$ and $\varepsilon/k \approx 216.15$ (or an absolute average deviation, AAD, of approximately 770%). At the very least such cases with high deviations of the fitted parameters from their predicted n-alkane equivalent values make the fitting results suspect. In such cases a closer evaluation of the fitting results is likely required.

R-32	O.F.	m	σ	ε/k
Original	6.79E-07	2.1474	2.9355	201.86
(1)	0	0.2769	6.8259	265.00
(2)	5.65E-01	0.6931	10.061	607.39
(3)	7.58E-01	1.1076	1.4009	400.80
(4)	8.31E-01	4.3035	4.8134	418.10

Table 5-4: Multiple solution cases for R-32 using the standard fitting procedure.

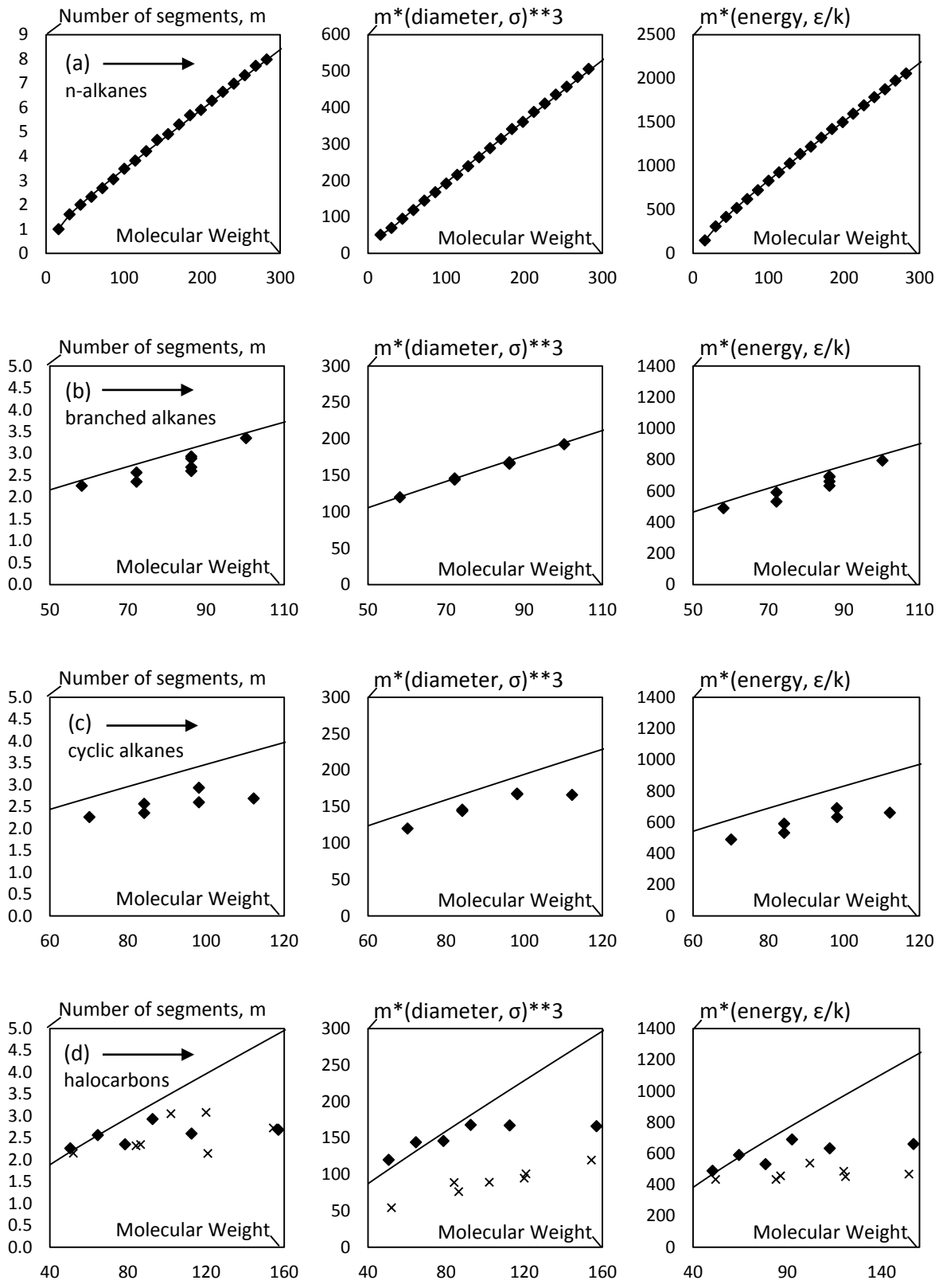

Figure 5-8: Shows fitted parameter values from Gross, et al. (♦), select values obtained from this work (x) and predictions using Equations (5-11) – (5-13) and **Table 5-3** parameters for straight alkanes (a), branched alkanes (b), cyclic alkanes (c) and halocarbons (d).

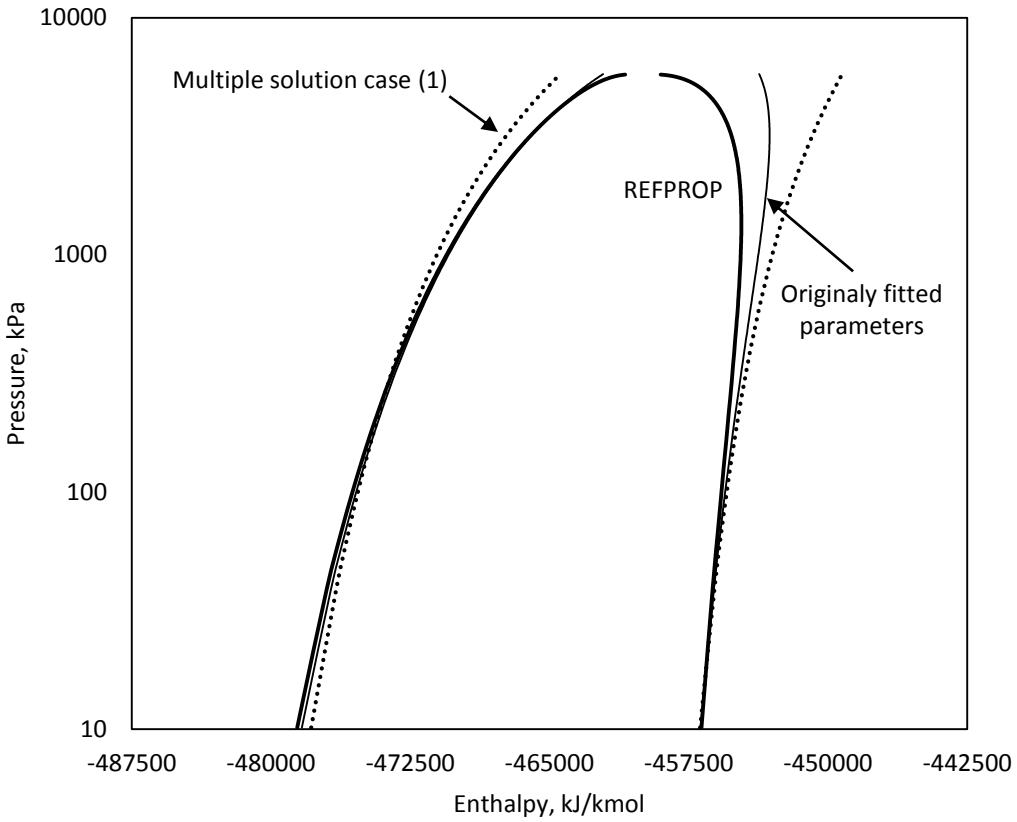

Figure 5-9: Shows REFPROP predictions for R-32 (bold line), and results obtained using the PC-SAFT equation and two separate parameter sets both equally satisfying the fitting condition, i.e. a case of multiple solutions.

5.2.3 Overall Performance

The ability of the PC-SAFT equation to sufficiently describe working cycles is of key interest. To compare the consistency of results, both REFPROP and PC-SAFT were used to simulate a hypothetical refrigeration process over a wide range of conditions. In this case the condenser temperature was varied while maintaining a constant temperature difference of 30°C between the bubble point of the evaporator and the dew point of the condenser. To make the results "somewhat" more realistic, the following operating conditions were also imposed:

- 5°C superheat to prevent wet compression, including a pressure drop of 10 kPa through the evaporator to promote fluid flow.
- 80% isentropic efficiency for the compressor.
- 5°C subcooling to ensure 100% liquid into the valve, including a pressure drop of 50 kPa through the condenser to promote fluid flow.
- Isenthalpic expansion through the valve.
- 1 ton of refrigeration (or approximately 3513.89 W) was maintained at each increment of the condenser temperature by allowing the refrigerant flow rate to vary.

It is important to note that the performance evaluations are in part dependent on these assumptions. As an alternative, the temperature difference (or degree of cooling) could have been varied by keeping the evaporator temperature constant while increasing the condenser temperature. This approach, however, would eventually lead to unrealistic pressure ratios for the compressor and expansion valve

as the temperature difference becomes large. Instead, by maintaining a constant 30°C temperature difference, a feasible (although maybe not optimal) cycle is guaranteed for every temperature increment.

Aspen Plus simulations were performed using the PC-SAFT equation and the fitted parameters of **Table 5-2**. Results are grouped by similar component types on Pages 79 – 81 in **Figure 5-10** for methane based refrigerants, **Figure 5-11** for the ethane derivatives and **Figure 5-12** for hydrocarbons. Key points from these figures are also summarized in **Table 5-5** below for convenience. Since most of the simulated cases using REFPROP predict a maximum COP value of around T_r = 0.91, a practical range of interest for using the PC-SAFT equation is therefore 0.6 – 0.8 < T_r < 0.95. In all cases there is a slight over prediction of the pressure ratios for the valve (PRV), and a slight under prediction for the pressure ratios of the compressor (PRC). Due to the tendency of the PC-SAFT equation to overestimate the critical point, higher COP values and lower refrigerant mass flow rates are predicted compared to calculation results obtained using REFPROP. Overall, the simulation results obtained using the PC-SAFT equation seem reasonable for T_r < 0.95.

Fluid	**T_r at Optimum COP**		**Relative Errors (%) at T_r = 0.95**			
	REFPROP	PC-SAFT	MFLOW	PRC	PRV	COP
R-12	0.91	0.91	(-2.9)	(-0.28)	0.31	1.0
R-22	0.91	0.92	(-5.8)	(-0.42)	0.48	2.4
R-32	0.92	0.96	(-15)	(-2.5)	2.7	7.2
R-125	0.91	0.92	(-3.6)	0.20	(-0.16)	1.1
R-134a	0.91	0.92	(-7.6)	(-0.42)	0.50	2.7
R-143a	0.92	0.94	(-11)	(-1.7)	1.9	4.6
R-290	0.91	----	(-3.0)	(-0.49)	0.53	1.0
R-600	0.91	0.91	(-4.6)	(-0.57)	0.63	1.3
R-601	0.90	0.91	(-6.3)	(-0.42)	0.49	1.7

Table 5-5: Summary of key performance indicators for select components in the process.

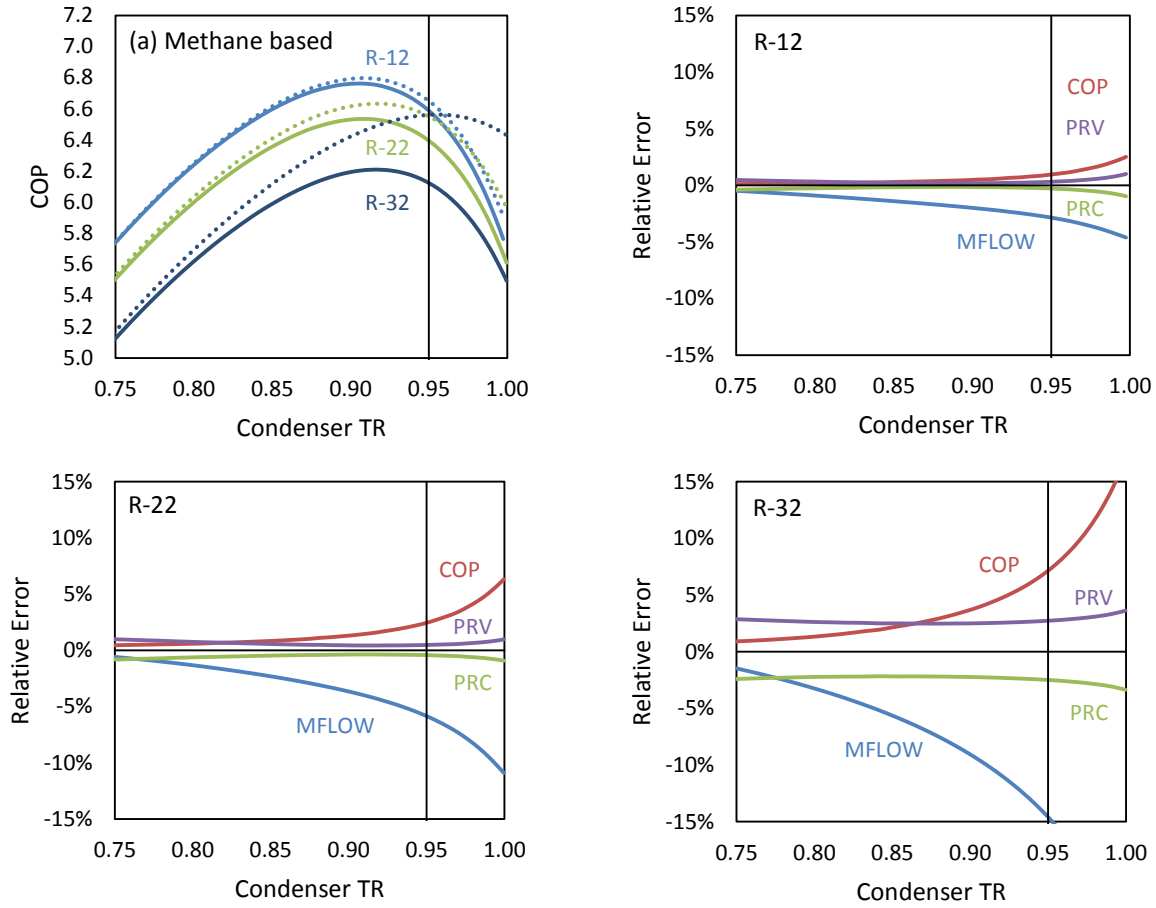

Figure 5-10: Overall performance results using the PC-SAFT equation and fitted model parameters (dotted lines) are compared against results obtained using REFPROP (solid lines) for selected methane-based halocarbons (a). Including individual process errors for PC-SAFT relative to REFPROP for each component.

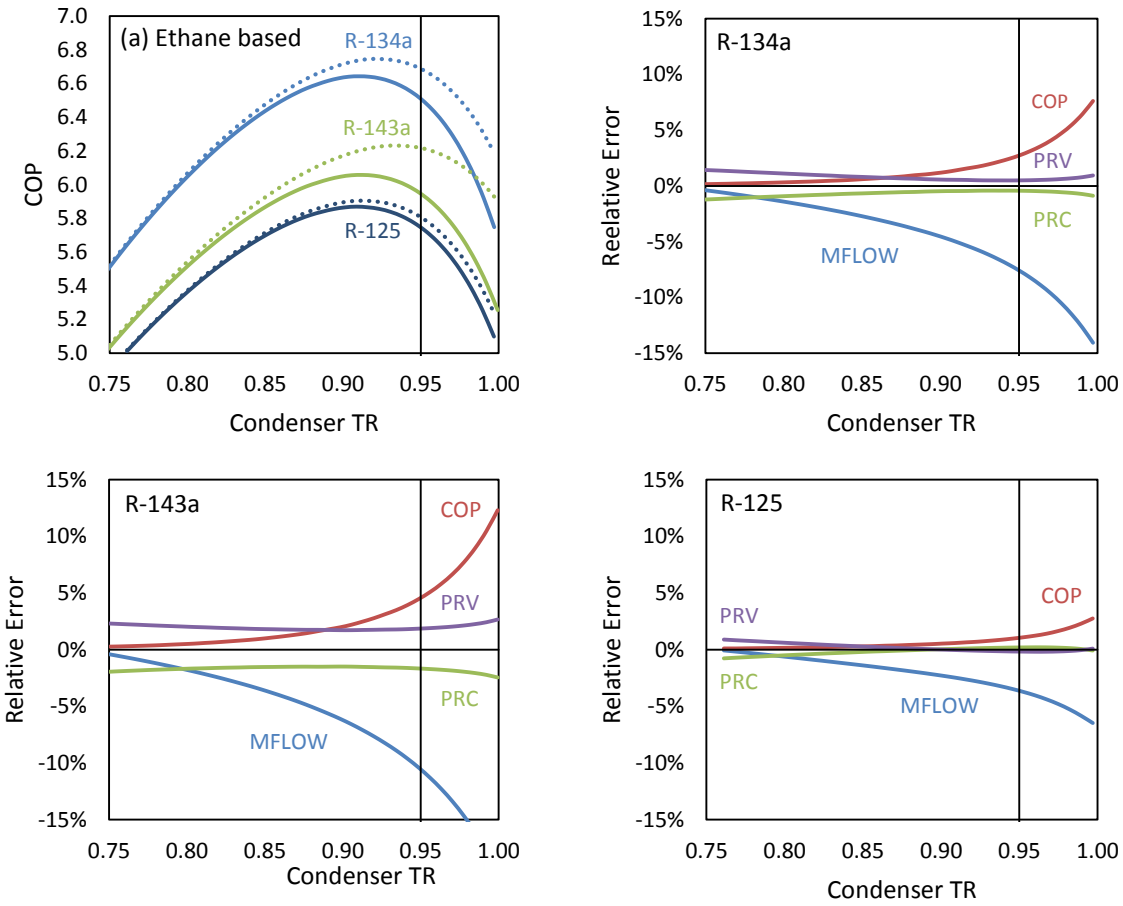

Figure 5-11: Overall performance results using the PC-SAFT equation and fitted model parameters (dotted lines) are compared against results obtained using REFPROP (solid lines) for selected ethane-based halocarbons (a). Including individual process errors for PC-SAFT relative to REFPROP for each component.

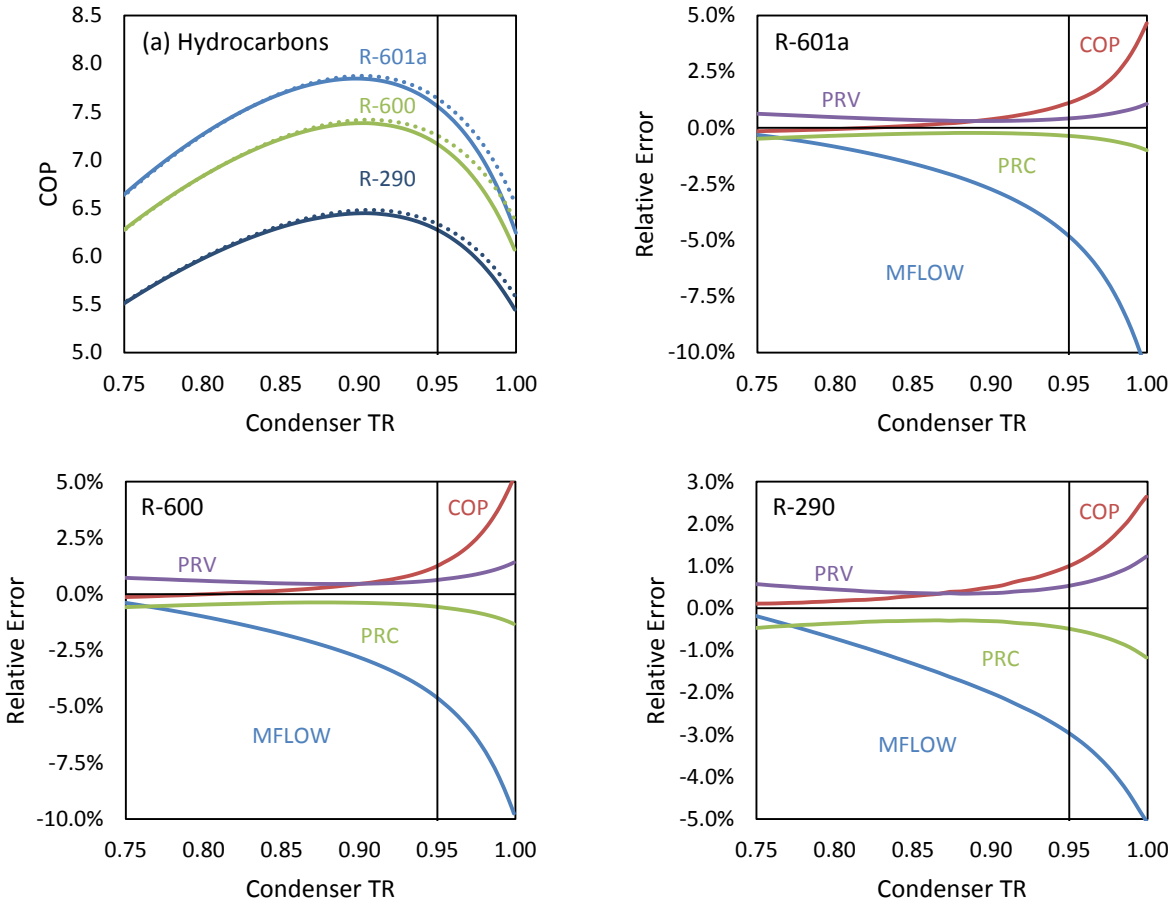

Figure 5-12: Overall performance results using the PC-SAFT equation and fitted model parameters (dotted lines) are compared against results obtained using REFPROP (solid lines) for selected hydrocarbons (a). Including individual process errors for PC-SAFT relative to REFPROP for each component.

5.3 Mixtures

Fluid	Type	Blend Components	Composition	Replaces
R-404a	Zeotrope	R-125/-143a/-134a	44/52/4	R-502
R-407c	Zeotrope	R-32/-125/-134a	23/25/52	R-22
R-410a	Zeotrope	R-32/-125	50/50	R-22
R-507a	~Azeotrope	R-125/-143a	50/50	R-502
R-502	Azeotrope	R-22/-115	48.4/51.2	-------

Table 5-6: Commonly used HFC refrigerant blends, where mass fraction is given for the composition.

The PC-SAFT parameters that were fitted in the preceding section are now used to evaluate the performance of the PC-SAFT equation of state to represent mixture behaviour for some common R-22 and R-502 replacements. The blend components and their compositions are listed in **Table 5-6** above, including whether or not the replacement blend forms an azeotrope or near azeotrope (~azeotrope, or so-called azeotropes). R-502, for example, is a binary refrigerant mixture at the azeotropic composition of its two components R-22 and R-115, so that it behaves just like a pure component. Most mixture refrigerants, however, exhibit a temperature variation (or glide) during a phase change at constant pressure, i.e. the dew points and bubble points do not match at every isobar. Refrigerant blends that have temperature glides of about < 0.1 °C are typically identified as near

azeotropic mixture refrigerants, while larger temperature glides such as in the majority of those listed in **Table 5-6** are denoted as zeotropes (which is most often the case).

5.3.1 R-502 Replacements

The azeotropic blend R-502 was (pre 1996) widely used in commercial refrigeration industry for low and medium (evaporator) temperature single-stage applications, and operated over a wide range of evaporating (-40°C to -4°C; 233.15 K to 269.15 K) and condensing (21°C to 55°C; 294.15 K to 328.15 K) temperatures (Sundaresan, 1992). It is important to note, however, that although R-502 is an "azeotropic refrigerant" that the true azeotropic point of the mixture (and others like it) changes as a function of the fluid's state, i.e. its temperature and pressure. As illustrated by **Figure 5-13** (a), for instance, the azeotropic composition of the blend is found to occur at T ≅ 320.97 K (T_r = 0.905), but even away from this point the Pxy behaviour of the blend is relatively flat so that it behaves, practically, like a pure component refrigerant. This leads to nearly flat isotherms for the R-502 mixture, as shown in **Figure 5-13** (b). Compared to the base-line predictions made using REFPROP (solid lines) the results obtained using the PC-SAFT equation (dotted lines) predict near perfect ideal behaviour for the system chlorodifluoromethane [R-22] (1) + chloroperfluoroethane [R-115] (2), i.e. the Pxy predictions of **Figure 5-13** (a). Furthermore the PC-SAFT equation only predicts an azeotropic point at the lower isotherms, but even this is grossly overestimated compared to the baseline predictions obtained using REFPROP. Better VLE predictions would likely require at least the inclusion of the k_{ij} parameter, but this would also require the existence of suitable VLE data for regression purposes (which, as previously discussed, is outside the scope of the present project). Even so, inaccuracies in describing the VLE behaviour of the mixture only lead to small deviations in the P-H diagram of **Figure 5-13** (b). Results, therefore, are likely sufficiently precise for a first-pass design/estimation as long as the reduced temperature range is kept, like for the pure component cases, below 0.95.

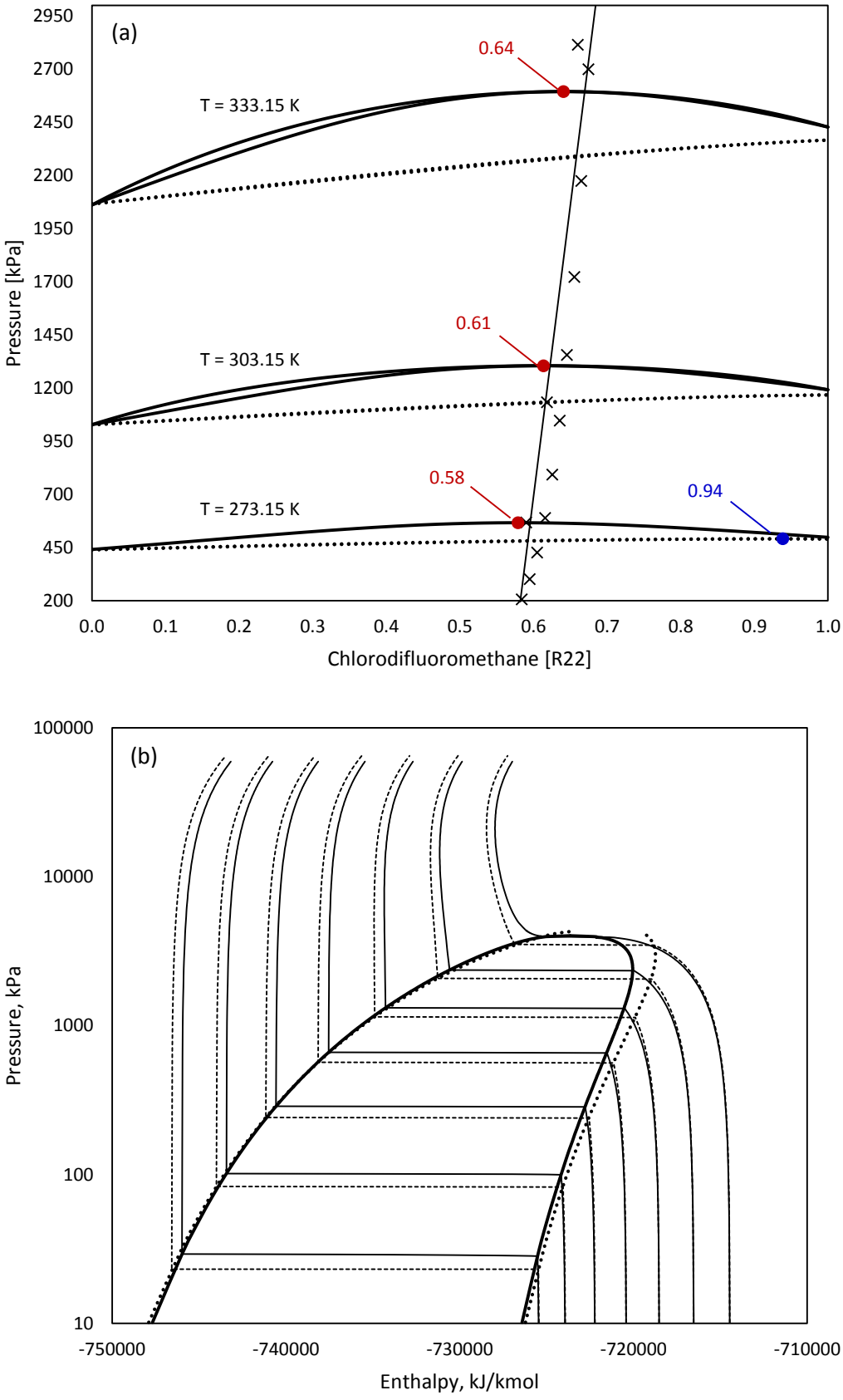

Figure 5-13: Predicted isothermal Pxy data using REFPROP (solid lines) and the PC-SAFT equation (dotted lines) for the system chlorodifluoromethane [R-22] (1) + chloroperfluoroethane [R-115] (2), including azeotropic data from the DDB (a). A P-H diagram including isotherms for R-502 is also shown (b).

Fluid	x_i	M_W		T_b		T_c		P_c	
		[g/mol]	Rel. %	[K]	Rel. %	[K}	Rel. %	[kPa]	Rel. %
R-502	----	111.6	----	227.8	----	354.7	----	4017	----
R-22	0.6300	86.47	(77.5)	232.3	(102)	369.3	(104)	4975	(124)
R-115	0.3700	154.5	(138)	233.9	(103)	353.1	(99.5)	3126	(77.8)
R-404a	----	97.60	(87.4)	226.9	(99.6)	345.2	(97.3)	3729	(92.8)
R-125	0.3578	120.0	(123)	225.1	(99.2)	339.5	(98.3)	3595	(96.4)
R-134a	0.0383	102.0	(105)	247.1	(109)	374.3	(108)	4064	(109)
R-143a	0.6039	84.04	(86.1)	225.9	(99.6)	346.3	(100)	3759	(101)
R-507a	----	98.86	(88.6)	226.4	(99.4)	343.7	(96.9)	3705	(92.2)
R-125	0.4118	120.0	(121)	225.1	(99.4)	339.5	(98.7)	3595	(97.0)
R-143a	0.5882	84.04	(85.0)	225.9	(99.8)	346.3	(101)	3759	(101)

Table 5-7: Select properties for R-502 and its replacements, including values for the individual components of each blend. Relative percentages for each property compared to its parent mixture are given in parentheses, e.g. R-502 is the parent of R-507a, while R-404a is the parent of R-143a.

The R-502 mixture replacements therefore combine two or more components to give similar properties and behaviours to the original mixture. **Table 5-7** above lists a number of key properties for each of the blends and their components including relative amounts (percentages) with respect to the parent mixture. The molecular weight of R-507a is therefore 88.6% of the original 111.6 g/gmol of R-502, i.e. the parent to R-507a, while its individual components are 121% (R-125) and 85% (R-143a) of the final 98.86 g/gmol of the R-507a mixture replacement (which in turn is the parent to each of its sub-components). Other properties of the table are similarly read. Both R-507a and R-404a closely match the T_b (normal boiling point) and T_c (critical temperature) of the original R-502 mixture refrigerant, while larger deviations are observed for the P_c (critical pressure) and M_W (molecular weight) of the original refrigerant. While the exact shape of the dimensionless T-h* diagram is incorrectly captured by the PC-SAFT equation, see **Figure 5-14** below, the character of the predictions is very similar to those obtained using REFPROP, i.e. comparable results should be expected.

So in a drop-in replacement scenario both R-507a and R-404a would require more refrigerant to obtain the same cooling effect as a system using R-502, since the width of the enthalpy domes are slightly smaller. If a choice had to be made between the two replacements, however, R-507a would likely be the better choice since it is a near-azeotropic mixture with only two components (less complex). Considering **Table 5-8** below, however, the temperature glide of R-404a is very modest and its performance should be similar to R-507a. In this regards, likely do to the near-azeotropic behaviour of the replacements, both the temperature glides (ΔT) predicted by REFPROP and PC-SAFT are in close agreement with each other. In fact, given the relative property errors of **Figure 5-15** (a) on Page 86, both R-507a and R-404a are practically indistinguishable. Therefore parallel results are obtained when using the refrigerant replacements in the same hypothetical process used to evaluate the pure component cases (see **Chapter 5.2.3**, Overall Performance, Page 77) as shown in **Figure 5-15** (b). By comparing **Figure 5-15** (a) to **Figure 5-15** (b) it can easily be shown how the errors in property predictions translate to a working process. The mass flow rate (MFLOW) required to yield 1 ton of refrigeration capacity, for instance, is lower in all cases due to the overestimation of the heats of vaporisation (Δh_v). Nonetheless, the overall predicted COP values using the PC-SAFT equation to model the hypothetical process are in fair agreement with those predicted using REFPROP. Only in the

final stages of the design are more accurate property predictions required, e.g. larger RHOV deviations from using the PC-SAFT equation may lead to incorrect equipment and line sizes.

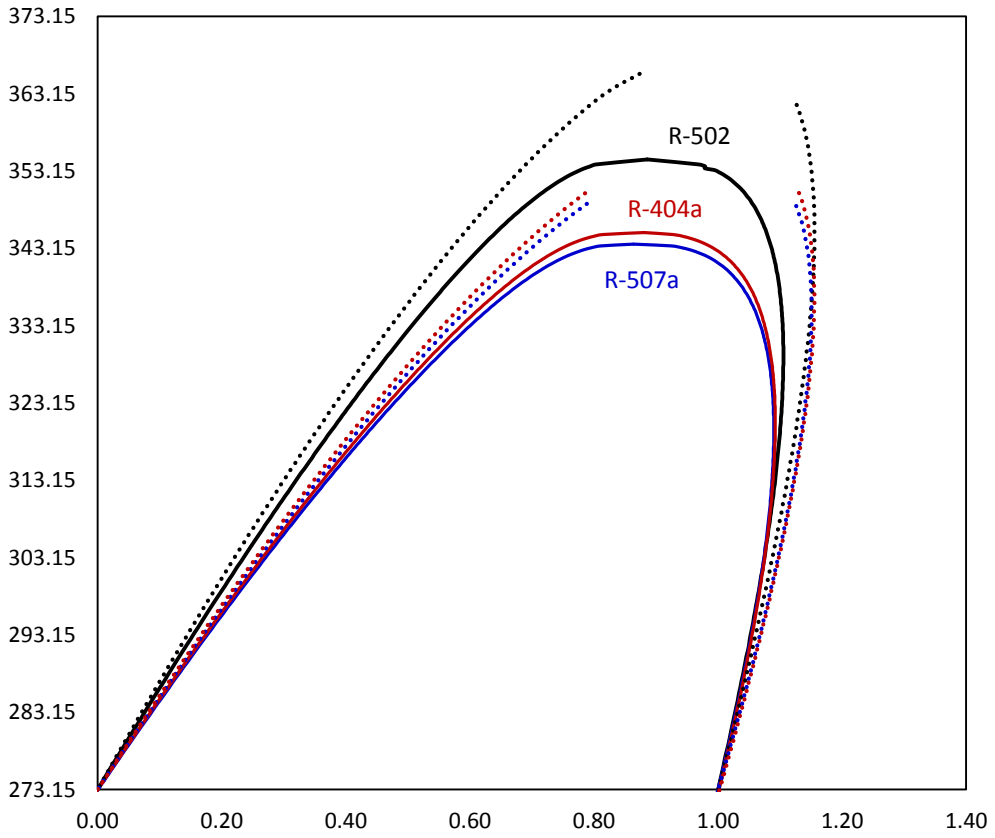

Figure 5-14: Dimensionless temperature-enthalpy diagram calculated using REFPROP (solid lines) and PC-SAFT (dotted lines) for the original R-502 mixture refrigerant and its mixture replacements R-507a (binary) and R-404a (ternary).

Fluid	T1	T2 (T_b)	T3	T4	T5	T6	T7
	[K]	[K]	[K]	[K]	[K]	[K]	[K]
R-502							
• TBUB	204.18	227.81	251.76	275.71	299.66	323.62	347.57
• T_r	0.5757	0.6423	0.7099	0.7774	0.8449	0.9125	0.9800
• ΔT	0.4917	0.2607	0.1164	0.0375	0.0052	0.0002	0.0004
	(0.0004)	(0.0081)	(0.0283)	(0.0619)	(0.0951)	(0.1049)	(0.0877)
R-404a							
• TBUB	204.14	226.93	249.20	271.48	293.75	316.02	338.30
• T_r	0.5914	0.6574	0.7219	0.7864	0.8510	0.9155	0.9800
• ΔT	0.9228	0.7511	0.6245	0.5198	0.4235	0.3213	0.1749
	(1.0197)	(0.8557)	(0.7372)	(0.6438)	(0.5624)	(0.4787)	(0.3709)
R-507a							
• TBUB	203.41	226.41	248.51	270.60	292.70	314.80	336.89
• T_r	0.5917	0.6586	0.7229	0.7872	0.8514	0.9157	0.9800
• ΔT	0.0008	0.0094	0.0256	0.0452	0.0658	0.0869	0.1092
	(0.0008)	(0.0065)	(0.0268)	(0.0552)	(0.0907)	(0.1239)	(0.1126)

Table 5-8: Temperature glides (ΔT) for R-502 and its replacements at different bubble point (TBUB) and reduced temperatures (T_r), including the normal boiling point temperature (T_b) for each fluid, using REFPROP and the PC-SAFT equation (values in parentheses).

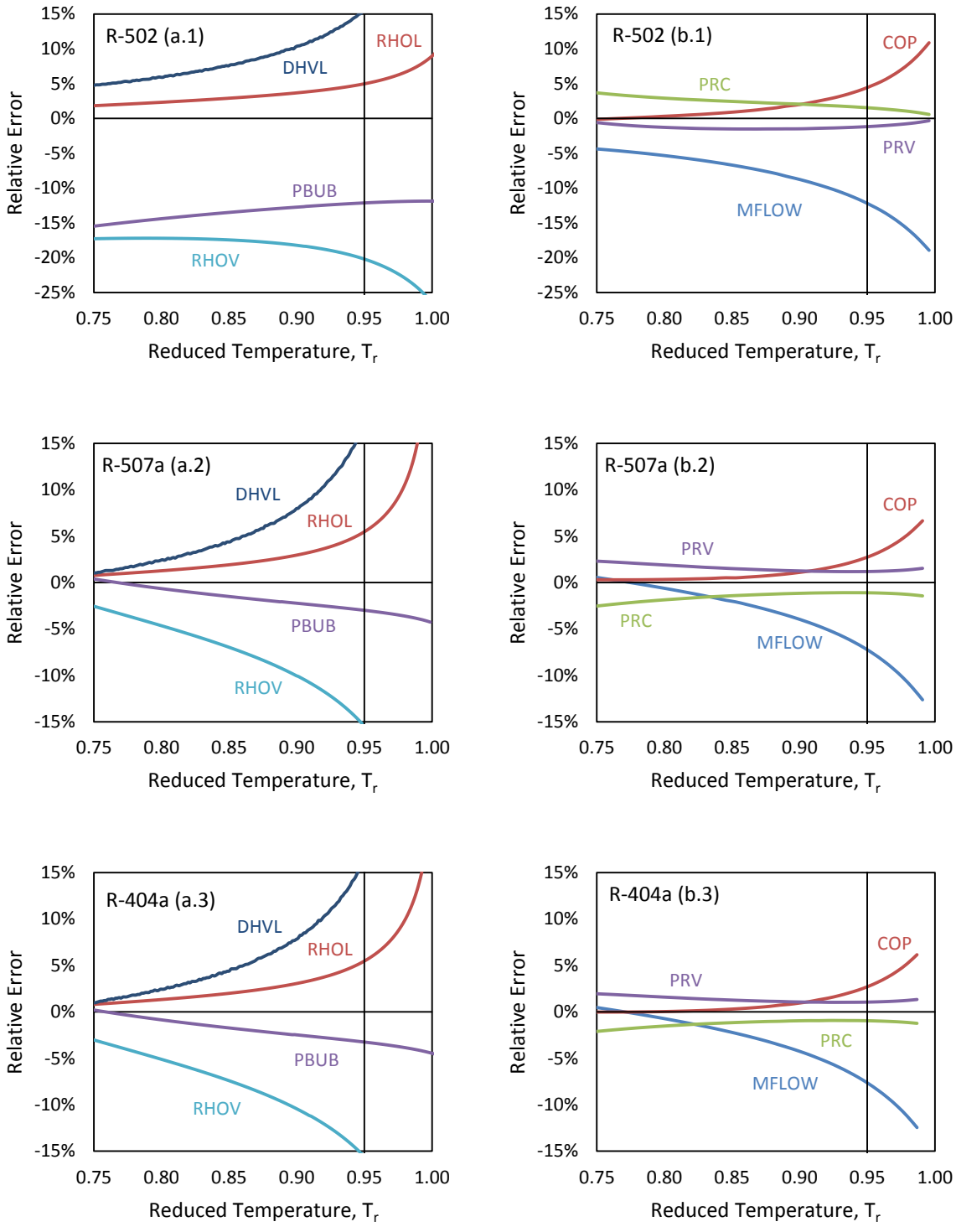

Figure 5-15: Relative errors based on REFPROP predictions obtained using the PC-SAFT equation and fitted parameters for R-502 and its replacements R-507a and R-404a (a), including relative process errors for some hypothetical process at different reduced temperatures for each fluid (b).

5.3.2 R-22 Replacements

Fluid	x_i	M_W		T_b		T_c		P_c	
		[g/mol]	Rel. %	[K]	Rel. %	[K]	Rel. %	[kPa]	Rel. %
R-22	----	86.47	----	232.3	----	369.3	----	4975	----
R-407c	----	86.20	(99.7)	229.5	(98.8)	359.2	(97.2)	4629	(93.1)
R-32	0.3811	52.02	(60.3)	221.5	(96.5)	351.6	(97.9)	5830	(126)
R-125	0.1796	120.0	(139)	225.1	(98.1)	339.5	(94.5)	3595	(77.7)
R-134a	0.4393	102.0	(118)	247.1	(108)	374.3	(104)	4064	(87.8)
R-410a	----	72.59	(83.9)	221.7	(95.4)	344.5	(93.3)	4902	(98.5)
R-32	0.6976	52.02	(71.7)	221.5	(99.9)	351.6	(102)	5830	(119)
R-125	0.3024	120.0	(165)	225.1	(102)	339.5	(98.5)	3595	(73.3)

Table 5-9: Select properties for R-22 and its replacements, including those for the individual components of each blend. Relative percentages for each property compared to its parent (mixture, or pure in this case) are given in parentheses, e.g. R-22 is the parent of R-407c, which in turn is the only parent of R-134a.

R-22 is a HCFC refrigerant that is most commonly associated with household HVAC systems, which can operate over a wide range of evaporating temperatures starting at around -35°C (238.15 K) and condensing temperatures ranging from 35°C to 55°C (208.15K to 328.15 K) for most cooling scenarios. R-407c is a ternary replacement, while R-410a is a binary replacement. Both of which are zeotropes, having much larger temperature glides than those of the preceding section (i.e. the R-502 replacements). As can be seen from **Table 5-12** above, the thermodynamic properties of R-407c most closely match those of R-22 than the alternative R-410a binary mixture replacement, but this matching also requires the mixing of a wider range of normal boiling points to achieve this. In this case, therefore, larger temperature glides can be expected for the R-407c case as is shown in **Table 5-10** below. The temperature glides predicted using the PC-SAFT equation are in close agreement with those predicted using REFPROP.

So in a drop-in replacement scenario it would depend on the operating range of the process. There are substantial differences in the shape and sizes of the dimensionless T-h* domes of **Figure 5-16**. The critical point of R-407c occurs at about T_r = 0.97, while that of the R-410a mixture replacement occurs at about T_r = 0.93 (both with respect to the critical temperature of R-22). The ternary mixture of R-407c therefore has a wider range of applicability, and would also require less refrigerant to achieve the same cooling effect due to its higher molecular weight (which typically trends alongside the required heat of vaporization). In fact, the differences of R-410a are likely large enough to cause various issues in such a scenario. It is highly likely, based on experience, that a process that was first designed for R-22 would require at least some component modifications (maybe even a complete redesign). For newly designed systems only the change of COP is important, but for existing systems the properties of the replacement need to be as close to the original as possible to avoid complications with the existing equipment. Overall, like for the R-502 replacements, the relative property errors of **Figure 5-17 (a)** translate into reasonable relative errors for the hypothetical process using the PC-SAFT equation, as shown in **Figure 5-17 (b)**, i.e. only in the final stages of the design process would more accurate property predictions be required.

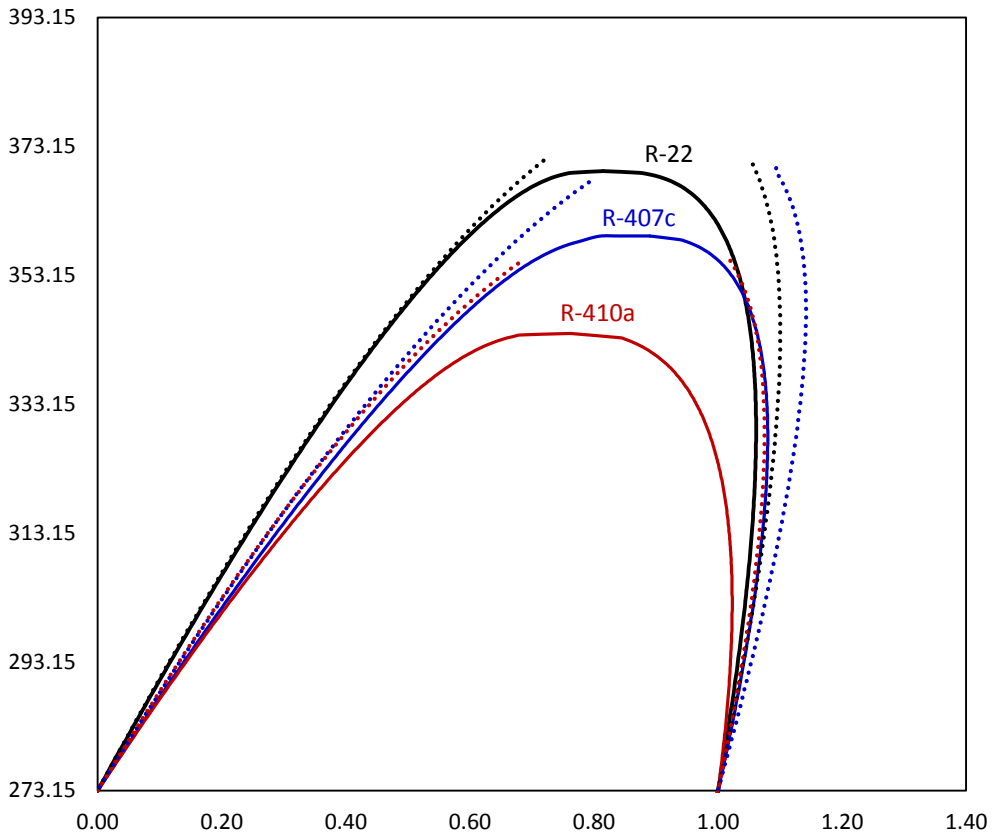

Figure 5-16: Dimensionless temperature-enthalpy diagram calculated using REFPROP (solid lines) and PC-SAFT (dotted lines) for the original R-22 refrigerant and its mixture replacements R-407C (ternary) and R-410a (binary).

Fluid	**T1**	**T2 (T_b)**	**T3**	**T4**	**T5**	**T6**	**T7**
	[K]	[K]	[K]	[K]	[K]	[K]	[K]
R-407c							
• TBUB	208.63	229.52	254.02	278.51	303.01	327.50	352.00
• T_r	0.5808	0.6390	0.7072	0.7754	0.8436	0.9118	0.9800
• ΔT	7.3494	6.9982	6.5415	5.9929	5.2753	4.2290	2.2632
	(7.7513)	(7.2842)	(6.7095)	(6.0656)	(5.2988)	(4.3307)	(2.9876)
R-410a							
• TBUB	199.81	221.71	244.89	268.07	291.25	314.43	337.61
• T_r	0.5800	0.6436	0.7108	0.7781	0.8454	0.9127	0.9800
• ΔT	0.0824	0.0787	0.0861	0.1004	0.1154	0.1176	0.0721
	(0.0309)	(0.0379)	(0.0501)	(0.0634)	(0.0677)	(0.0617)	(0.0456)

Table 5-10: Temperature glides (ΔT) for R-22 replacements at different bubble point (TBUB) and reduced temperatures (T_r), including the normal boiling point temperature (T_b) for each fluid, using REFPROP and the PC-SAFT equation (values in parentheses).

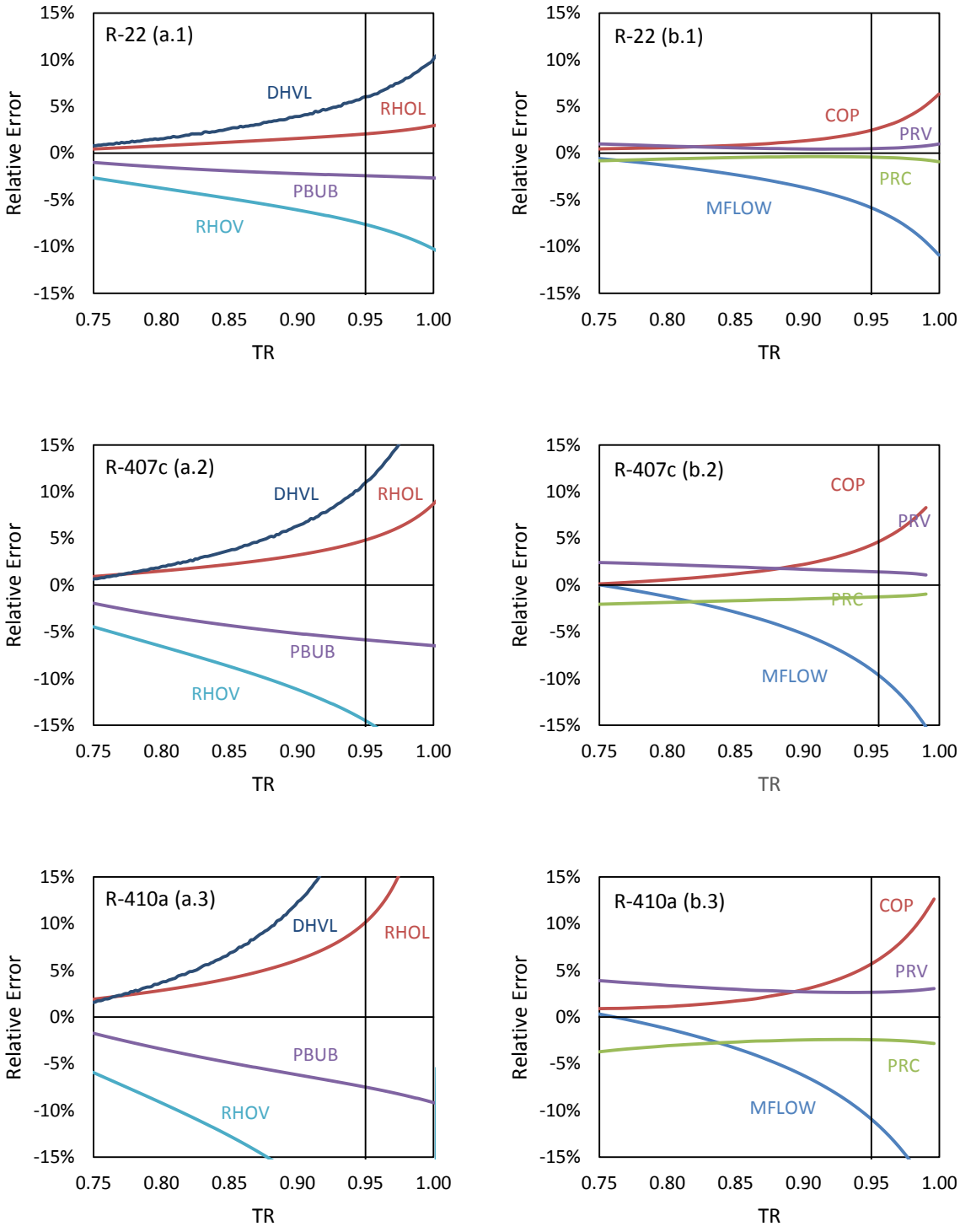

Figure 5-17: Relative errors based on REFPROP predictions obtained using the PC-SAFT equation and fitted parameters for R-22 and its replacements R-407c and R-410a (a), including relative process errors for some hypothetical process at different reduced temperatures for each fluid (b).

5.3.3 Overall Performance

Fluid	x_i	T_r at Optimum COP			Relative Errors (%) at T_r = 0.95		
		REFPROP	PC-SAFT	MFLOW	PRC	PRV	COP
R-502	----	0.91	0.93	(-12)	1.5	(-1.2)	4.4
R-22	0.6300	0.91	0.92	(-5.8)	(-0.42)	0.48	2.4
R-115	0.3700	0.91	0.91	(-0.79)	0.21	(-0.22)	(-0.30)
R-404a	----	0.92	0.93	(-7.2)	(-1.1)	1.2	2.7
R-125	0.3578	0.91	0.92	(-3.6)	0.20	(-0.16)	1.1
R-134a	0.0383	0.91	0.92	(-7.6)	(-0.42)	0.50	2.7
R-143a	0.6039	0.92	0.94	(-11)	(-1.7)	1.9	4.6
R-507a	----	0.92	0.93	(-7.6)	(-1.0)	1.1	2.7
R-125	0.4118	0.91	0.91	(-3.6)	0.20	(-0.16)	1.0
R-143a	0.5882	0.92	0.94	(-11)	(-1.7)	1.9	4.6
R-22	----	0.91	0.92	(-5.8)	(-0.42)	0.48	2.4
R-407c	----	0.93	0.95	(-9.1)	(-1.3)	1.4	4.3
R-32	0.3811	0.92	0.96	(-15)	(-2.5)	2.7	7.2
R-125	0.1796	0.91	0.91	(-3.6)	0.20	(-0.16)	1.0
R-134a	0.4393	0.91	0.92	(-7.6)	(-0.42)	0.50	2.7
R-410a	----	0.93	0.95	(-11)	(-2.4)	2.6	5.7
R-32	0.6976	0.92	0.96	(-15)	(-2.5)	2.7	7.2
R-125	0.3024	0.91	0.91	(-3.6)	0.20	(-0.16)	1.0

Table 5-11: Summary of key performance indicators for select mixtures in some process.

Like for the pure component cases, Aspen Plus simulations were performed using the PC-SAFT equation and the fitted parameters of **Table 5-2** and the mixture compositions of **Table 5-6**. Results reflect the simulation results of **Figure 5-15** (b) and **Figure 5-17** (b). Key points from these figures are also summarized in **Table 5-12** above for convenience. Compared to the pure component cases of the previous section, the maximum COP values for each mixture refrigerant occur at $T_r \approx 0.92$ for most cases, and are typically above the largest maximum COP value for the sub-components. Estimations obtained using the PC-SAFT equation are then slightly higher. The overall predicted performance of the process using the PC-SAFT equation, however, seems to be somewhat reasonable, e.g. relative COP errors of less than five percent at T_r = 0.95 for all but the R-410a mixture replacement. The differences between the predicted T_r at the maximum (or optimum) COP of the process are larger in the case of the mixtures, but this error does not seem to compound in the reported relative errors at T_r = 0.95. Therefore, like for the pure component cases, a practical range of interest for using the PC-SAFT equation is also $0.6 - 0.8 < T_r < 0.95$.

In all cases there is a slight over prediction of the pressure ratios for the valve (PRV), and a slight under prediction for the pressure ratios of the compressor (PRC). Due to the tendency of the PC-SAFT equation to overestimate the critical point, higher COP values and lower refrigerant mass flow rates are predicted compared to calculation results obtained using REFPROP. Overall, the simulation results obtained using the PC-SAFT equation seem reasonable for $T_r < 0.95$, i.e. there does not seem to be a significant worsening of the results for the case of mixtures compared to the pure component cases.

5.3.4 Mixture Optimization

Like other more conventional equations of state, the PC-SAFT equation in itself is only capable of describing the behaviour of pure fluids. For the case of mixtures, therefore, suitable mixing and combining rules for the pure component parameters to characterise a "hypothetical" pure fluid that is the mixture (recall **Chapter 4.5.3** starting on Page 55). The parameters that describe the azeotropic mixture R-502, for example, using the previously fitted pure component parameters for each species of the mixture in **Table 5-2**, are therefore calculated as,

$$\bar{m} = \sum x_i m_i$$

$$= 0.63 * (2.3461) + 0.37 * (2.7284) \cong 2.4875$$

$$\sigma = \sqrt[3]{\frac{\sum_i \sum_j x_i x_j m_i m_j \left(\frac{\varepsilon_{ij}}{kT}\right)^{y=1} \sigma_{ij}^3}{\bar{m}\varepsilon}} \cong 3.3278$$

$$\sigma_{ij} = \frac{1}{2}(\sigma_i + \sigma_j) = \begin{bmatrix} 3.1899 & 3.3575 \\ 3.3575 & 3.5251 \end{bmatrix}$$

where, as an example, $\sigma_{12} = \frac{1}{2}(3.1899 + 3.5251) \cong 3.3575$

$$\varepsilon = \frac{\sum_i \sum_j x_i x_j m_i m_j \left(\frac{\varepsilon_{ij}}{kT}\right)^{y=2} \sigma_{ij}^3}{\sum_i \sum_j x_i x_j m_i m_j \left(\frac{\varepsilon_{ij}}{kT}\right)^{y=1} \sigma_{ij}^3} \cong 184.99$$

$$\varepsilon_{ij} = \sqrt{\varepsilon_i \varepsilon_j} * (1 - k_{ij}) = \begin{bmatrix} 195.0736 & 183.1075 \\ 183.1075 & 171.8754 \end{bmatrix}$$

where, as an example, $\varepsilon_{12} = \sqrt{195.0736 * 171.8754} * (1 - 0) \cong 183.1075$

The mixing rules thus determine equivalent parameters used in place of the pure component parameters, while the combining rules are needed to account for the cross-interactions of these same parameters. Similar calculations can be performed for the remaining mixtures; results are summarized in **Table 5-12** below, including fitted PC-SAFT parameters for each mixture using a pseudo pure-component based on methane (values shown in parentheses). This means that the ideal gas heat capacity is fixed to the value of methane for the fitted pseudo pure components of each mixture. This is at best, therefore, only a qualitative assessment, since the ideal gas heat capacity substantially influences the shape of the two-phase region.[23]

[23] It should be noted that characterising a fluid using only PC-SAFT parameters is not possible without first establishing a link between these parameter values and c_p^{ig} as a function of temperature (Lampe, et al., 2014).

Fluid	m	σ	ε/k
R-502	2.4875	3.3278	184.99
	(2.4451)	(3.3551)	(182.64)
R-507a	2.6357	3.2524	174.08
	(2.6776)	(3.2407)	(172.37)
R-404a	2.6225	3.2544	175.34
	(2.7688)	(3.2097)	(169.46)
R-407c	2.7146	3.0439	180.03
	(3.8911)	(2.7836)	(143.59)
R-410a	2.4310	3.0047	184.47
	(3.2607)	(2.9910)	(151.47)

Table 5-12: PC-SAFT molecular parameters calculated for the pseudo-mixture using the fitted pure component parameters of **Table 5-2**, compared against pseudo pure-component parameter fits for each mixture (given in parentheses).

For the case of zeotropes, for instance, the pure pseudo-component parameters are unable to capture the fluid phase equilibrium behaviour of the mixture correctly. They are only applicable in homogeneous phases and not between phases with different composition. One cannot, therefore, simply use the mixing and combining rules to map a mixture to the PC-SAFT parameters of an existing fluid, i.e. it has no physical meaning. That's why fitting the parameters for a pseudo-component (based on methane) only matches the behaviour closely for those mixtures that consist of similar components, or those that act like azeotropes. Instead, for the case of zeotropes, one must first fit PC-SAFT parameters for the individual pure components of the mixture, and then solve for the mixture concentrations to match the properties of the refrigerant to be replaced, and not simply its PC-SAFT parameters.

5.3.5 Proof of Concept

It then becomes necessary to test the suitability of using the PC-SAFT equation to identify novel refrigerant replacements. To do this a relevant database of pure component PC-SAFT parameters is required. Since no such database exists within the Aspen Plus property manager, i.e. containing parameters for components of interest, one had to first be created. This was accomplished by fitting PC-SAFT parameters using the same regression procedure that was previously employed (**Chapter 5.2** starting on Page 64) for each component described by REFPROP. The regression results for the fitted components[24] are summarized in **Table F-1** of **Appendix F**, and represent the "pool" of components that could be used to evaluate potential replacements, for example, R-22. The component identifiers for the pure component database were then mapped to those components within the Aspen Plus property manager (so-called Aspen alias names) so that constraints could be imposed to limit the number of components to those close to, or near in character to, R-22:

- $22 \leq M_W \leq 173$ g/gmol (or -75/+100% of R-22 M_W = 86 g/gmol)
- $209 \leq T_b \leq 256$ K (or ±10% of R-22 T_b = 232 K)
- $332 \leq T_c \leq 406$ K (or ±10% of R-22 T_c = 369 K)
- $3483 \leq P_c \leq 6468$ kPa (or ±30% of R-22 P_c = 4975 kPa)

[24] Since Aspen Plus employs NIST/REFPROP version 8, some of the newer components e.g. some siloxanes and R-161 (fluoroethane) could not be fitted. Although a different fitting procedure could have resulted in parameters for these missing components, it was decided to limit the study to those fitted using the same procedure.

These restrictions resulted in 32 components from a cross-database of approximately 10,000 components, which was further limited to a final pool of 23 components after excluding, because of environmental and safety concerns, those containing any chlorine, bromine and/or arsenic. Of these final 23 components, only 11 are available from the REFPROP regressions (see **Table 5-13** on the next page). One can then use the binomial coefficient (BC, sometimes read as "n choose k") to return the number of combinations that can be made from a set of n items taken (or chosen) k at a time, regardless of order:

$$BC = \binom{n}{k} = \frac{n!}{k!\,(n-k)!} \tag{5-14}$$

For a system of 11 components (n = 11) the total number of potential combinations from two, three and four components (k = 2, 3 and 4) is then 55, 165 and 330 respectively. The concentrations for these component combinations (or blends) were then fitted to REFPROP predictions of R-22 using a similar fitting procedure used to fit the pure component PC-SAFT parameters, i.e. the same fitness function. Discarding those blends in which the procedure resulted in the fitting of one or more components with mole fractions < 0.01 resulted in a final list of potential replacements consisting of 15 binary, 34 ternary and 66 quaternary blends. An example from each of these three cases is given in **Table 5-14** below for discussion, where the full list of results can be found in **Table F-2** of **Appendix F**, followed by plots of the P-H domes and heats of vaporisation for each of the cases in **Figure 5-18**.

Name	M_W	T_b	T_c	P_c	ρ_b	$\Delta h_v\ (T_b)$	Lifetime[1,a]	ODP[2,a]	GWP[3,a]
	[g/gmol]	[K]	[K]	[kPa]	[kg/m3]	[J/mol]	[years]	-----	[100-yr]
Chlorodifluoromethane [R-22]	86.47	232.3	369.4	4975	1409	20211	11.9	0.04	1790
Difluoromethane [R-32]	52.02	221.5	351.6	5830	1213	19865	5.2	0	716
Carbonyl sulfide (COS)	60.07	223.0	378.3	6302	1174	18558	5.7[a]	-----	27[b]
Pentafluoroethane [R-125]	120.02	225.1	339.5	3595	1514	19695	28.2	0	3420
Propylene [R-1270]	42.08	225.5	365.0	4620	610	18470	0.001	0	< 20
1,1,1-Trifluoroethane [R-143a]	84.04	225.9	346.3	3759	1166	19046	47.1	0	4180
Propane [R-290]	44.10	231.0	370.0	4246	581	18767	0.041	0	~ 20
Cyclopropane	42.08	241.7	398.0	5540	698	21728	0.44	0	~ 20
1,1,1,2-Tetrafluoroethane [R-134a]	102.03	247.1	374.3	4064	1377	22137	13.4	0	1370
Propyne	40.06	248.0	402.4	5624	695	21004	0.001[c]	0[c]	< 20[c]
Dimethyl ether [RE-170]	46.07	248.3	400.0	5370	735	21263	0.015	0	-----
1,1-Difluoroethane [R-152a]	66.05	249.1	386.4	4516	1011	21791	1.5	0	133

Note: All atmospheric lifetime [1], ODP [2] and GWP [3] values are taken from the work of Calm (Calm, et al., 2011) unless otherwise noted.
[1] Is a measure of the time required to restore (natural) atmospheric equilibrium.
[2] Is the relative amount of ozone depletion it can cause compared to R-11 (whose ODP is standardised to 1).
[3] Is a relative measure of how much heat a greenhouse gas traps in the atmosphere (here values are reported using a 100 yr. time interval).
a. (Ulshöfer, et al., 1997)
b. (Brühl, et al., 2012)
c. Reported values for propylene are used.

Table 5-13: Final pool of components used to define potential blend replacements for R-22, including relevant pure component properties.

	Blend Components	O.F.	Compositions (Moles) / [Mass]	T_b [K]	ρ_b [kg/m3]	$\Delta h_{v,b}$ [J/mol]
	R-22	----	----	232.34	1409.18	20211.3
(a)	R-152a/-125	0.0146	(27.0/73.0) [16.9/83.1]	229.04	1404.67	20680.0
(b)	R-32/-125/-134a	0.0019	(21.1/24.3/54.6) [11.5/30.4/58.1]	232.34	1409.18	21640.0
(c)	R-143a/-125/{COS}/-134a	0.0015	(8.5/35.9/10.0/45.6) [7.0/41.9/5.8/45.3]	232.33	1409.16	21190.0

Table 5-14: The examples of R-22 replacement blends, where the compositions were fitted to REFPROP predictions of the normal boiling point (T_b at 101.325 kPa), liquid density at T_b (ρ_b) and the heat of vaporisation at T_b ($\Delta h_{v,b}$) for R-22.

The enthalpies for each of the optimisation cases of **Table 5-14** were adjusted so that the P-H domes of **Figure 5-18** would overlap that of R-22 (the target of the optimisation). This allows the shapes of the potential replacement blends to be compared against the REFPROP predictions of R-22, which agree fairly well considering that the concentrations for the replacement blends were fitted using only the normal boiling point conditions of R-22. Above the fitting conditions each of the cases results in an under prediction of the vapour pressure as shown by the saturated liquid lines of the P-H domes. Considering the Clausius-Claperyron (5-10, Page 72) this translates into smaller slopes. Since the differences in the enthalpies of vaporisation are slightly above those of the targeted R-22 for most conditions of each case, the differences between the liquid and vapour molar volumes for each of the replacement blends must generally be larger than that of R-22 because of the temperature glides, i.e. compositional changes of the blend components during vaporisation. Each of the replacement blends must also, therefore, have high vapour molar heat capacities given that the two-phase region is slightly skewed to the right, which could cause significant performance losses and undesirable "wet compression" if sufficient superheat is not added or available in the evaporator to compensate.

Still it is interesting to note that the procedure resulted in the identification of components matching those, discussed previously, of R-407c (marketed as a replacement for R-22): R-32/-125/-134a. The commercial variant is made of 23/25/52 by mass, while the optimised concentrations from the procedure (this work) resulted in 11.5/30.4/58.1 instead. Although not exact they are close, and give similar P-H shapes as shown in **Figure 5-18**. In so observing it is important to note that the concentrations for the commercial variant were likely chosen to give the best performance at the typical operating conditions of an actual process, where the concentrations of case (b) were instead fitted to the normal boiling point conditions of R-22.

To identify the fittest results, therefore, the compositions of potential blend replacements (see **Table F-2** of **Appendix F**) need to be optimised using a working process model instead.

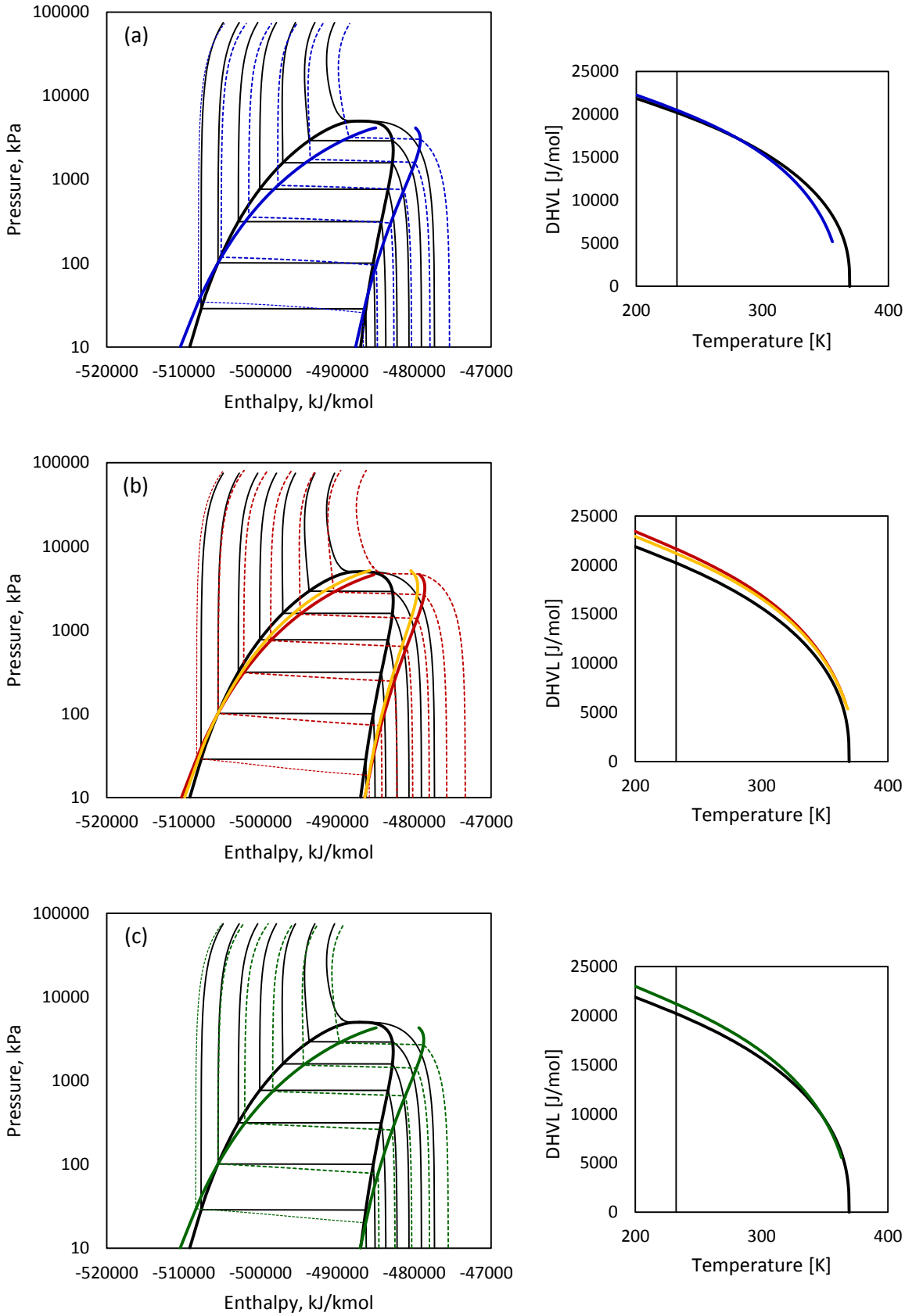

Figure 5-18: Pressure-enthalpy and heats of vaporisation (Δh_v) are plotted for R-22 using REFPROP (black lines) and PC-SAFT equation using the fitted concentrations for the blends of

6 Model Development and Optimisation

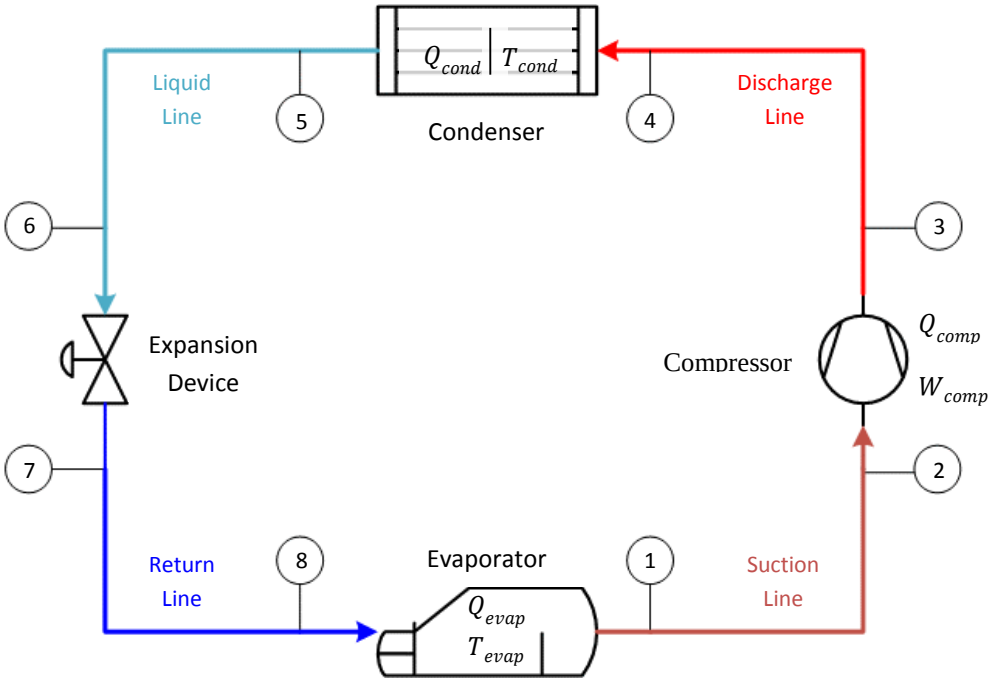

Figure 6-1: Schematic diagram of vapour-compression liquid chiller.

In the previous chapter, the PC-SAFT equation was evaluated for its ability to describe all required fluid phase properties with a sufficient degree of accuracy. It was shown that, while not exactly precise, the equation is able to sufficiently describe those properties necessary for a first-pass design/estimation of a refrigeration process for reduced temperatures below 0.95 (which, for the intended application, is typically the case). An optimisation procedure was then used to identify potential R-22 replacements using two, three and four component blends, where the final "pool" of available components was limited to those close in character to R-22. The concentrations for each blend combination were then optimised using the PC-SAFT equation and the required pure component model parameters that were also fitted in this work (see **Table F-1** on Page 168 of **Appendix F**). The final concentrations that give the best performance, however, are in large part dependent on the actual process in which they are to be used. Better still is to identify the final blend compositions for the potential refrigerant replacements using a real process, i.e. an integrated approach.

The present chapter, therefore, describes the development (and validation) of a process model that reproduces the real operating performance of an existing refrigeration system. The validated model is then used to optimise potential blend compositions to give similar operating performance as the refrigerant that is currently used in the real process.

6.1 Model Development

Knowledge of some working refrigeration cycle is then required. Originally, a complementary research project that involves the design and commissioning of a new experimental refrigeration apparatus was to be used for this purpose, but was not completed in time to be used in the present

research. Once the apparatus is complete, however, it can still be employed to evaluate potential refrigerant blends identified by the present research. Open literature, therefore, was investigated for a suitable substitute instead. Most available articles, however, only depict graphical trends of calculated quantities, and fail to correctly include supplementary tables that include recorded values taken from all available sampling points (which are needed for evaluation purposes). Redundant measurements, for instance, are often curiously excluded so that measurement errors cannot be checked, or determined, with any degree of confidence. The most promising literature sources are those listed in **Table 6-1** on the next page, with available sampling points relating to the labels of **Figure 6-1** above.

Of the available candidates listed in **Table 6-1**, option 1 was chosen simply due to the number of measurements reported by the author. These state-point measurements are required, for instance, in order to correctly account for the irreversibilities associated with each component of the real process. Losses can arise, for example, due to finite-rates of heat exchange between the refrigerant and coolant, losses associated with the performance of the compressor, and line losses due to fluid flow and heat transfer with the surroundings. Fluid phase properties of the refrigerant, with respect to operating conditions of the process, are also deterministic of the losses for each component of the process (or unit).

Option 1 contains the experimental results for three different unit configurations: unit B was modified from unit A by swapping in a new condenser with a greater heat transfer, and unit C was modified from B by using a more efficient compressor. All three configurations use R-22 as the working fluid, but the process model of unit C produced the best results, i.e. the predictions made using the model are in close agreement with the available measurements. The discussion, therefore, is limited to the description of only this process model. **Table 6-2** (next page), therefore, provides the measured temperature and pressure data for each state point of option 1 C, including the saturated temperature, molar enthalpy and entropy for each point of the process calculated using the standalone REFPROP package[25]. If the measured temperature is above the saturated temperature, then the stream exists as a superheated vapour above its bubble point e.g. streams 1 – 4, while temperatures below this value exist as a subcooled liquid below its dew point. **Table 6-3** presents the reported heat and work values related to each section of the process, and are compared against the heat and work values calculated via an Aspen Plus model of the process (corresponding to the caloric data of **Table 6-2**). The following discussion is based on the results in these tables, and has been broken into separate sections for each component of the process below: the evaporator, compressor, condenser and expansion device.

[25] The REFPROP DLL (dynamic link library) was integrated into the author's project code. So although the absolute values may not agree with those obtained using Aspen Plus, the deviations of these values will still give comparable results for the calculation of work (W) and heat (Q) quantities obtained from Aspen Plus. Recall that Aspen Plus uses a different reference state in its calculation of caloric properties such as enthalpy and entropy (see **Chapter 5.2.1**, Enthalpy Departure, Page 62).

	Fluid(s)	1	2	3	4	5	6	7	8	W	Q_E	F_a	F_b	F_c	T_E^{in}	T_E^{out}	T_C^{in}	T_C^{out}	References
1.	R22	●	●	●	●	●	●		●	✓	✓		✓	✓	✓	✓	✓	✓	(Lee, 2010)
2.	R22, 407c	●	●	●	●	●			●	✓	✓	✓	✓	✓	✓	✓	✓	✓	(Lee, et al., 2002)
3.	R12, 22, 134a, 290/134a		○	●		○				✓	✓				✓	✓	✓	✓	(Kim, et al., 1994)
4.	R22			●	○					✓	✓	✓				✓	✓		(Domanski, et al., 1983)
5.	R404a	●	●	●	●	●	●		●	✓	✓	✓			✓	✓	✓	✓	(Kizilkan, et al., 2010)
6.	R22	●	●	●			●	●		✓	✓								(Padmanabhan, et al., 2013)
7.	R134a	●	○	○	○	●	○	○	○	✓	✓	✓	✓	✓	✓	✓	✓	✓	(Rigola, et al., 1996)
8.	R12	●	○	○	○	●	○	○	○	✓	✓	✓	✓	✓	✓	✓	✓	✓	(Rigola, et al., 1996)

State points 1 thru 8 as labeled in **Figure 6-1** on the previous page:

- Solid shaded circe ● indicates that both temperature and pressure are recorded at the sampling point.
- Empty filled circle ○ indicates that either the temperature or pressure is recorded (but not both).
- A red marker indicates when a sampling point exists, but the author(s) choose not to publish their values.

W = compressor power

Q_E = evaporator (or refrigerant) capacity

F = measured flow rate of refrigerant (a), process-side flow rate of the evaporator (b) and the heat-transfer-fluid (HTF) of the condenser (c).

T_E = inlet (in) and outlet (out) temperatures for the process-side fluid of the evaporator

T_C = inlet (in) and outlet (out) temperatures for the heat-transfer-fluid (HTF) of the condenser

Table 6-1: List of experimental systems from open literature that include all required state points.

	State Point	T	P	T_{sat}	h_{calc} (T, P)	s_{calc} (T, P)
		[K]	[kPa]	[K]	[kJ/kg]	[kJ/kg-K]
1.	Evaporator outlet	278.55	527	274.90	408.4	1.758
2.	Compressor inlet	279.25	522	274.61	409.0	1.761
3.	Compressor outlet	>> 345.95	<!> 1536	313.21	445.9	1.789
4.	Condenser inlet	344.55	1506	312.41	445.1	1.788
5.	Condenser outlet	306.35	1479	311.67	240.7	1.138
6.	Expansion valve inlet	306.25	1476	311.59	240.6	1.137
7.	Evaporator inlet	278.45	598	278.90	206.3	1.022
		>> 278.45	<!> 589.61	278.45	206.3	1.022

Absolute uncertainties for R22 using REFPROP are 0.1% in density, 1% in heat capacity, and 0.3% in the speed of sound, except in the critical region. The uncertainintty in vapor pressure is 0.2%.
Experimental T = ± 0.03°C
Experimental P = ± 0.15
>> Indicates that the value was used as a design setpoint for the model
<!> Indicates that the valve is iteratively solved to meet a design setpoint for the model
Points in red are values from the physical measurement that were herin disputed as invalid.

Table 6-2: Thermodynamic properties measured (Lee, 2010) and calculated at various state points using REFPROP.

	Component	Duty	Work	COP	Q_{calc}	W_{calc}
		[kW]	[kW]	----	[kW]	[kW]
1.	Evaporator	>> 357.85	0		357.85	0
2.	Suction line	1.315	0		1.331	0
3.	Compressor	-1.799	>> 79.86		-1.151	79.86
4.	Discharge line	-1.722	0	**4.5**	-1.712	0
5.	Condenser	-435.257	0		-435.903	0
6.	Liquid line	-0.277	0		-0.275	0
7.	Expansion valve	0	0		0	0
	Total	**-79.89**	**79.86**		**-79.86**	**79.86**

Experimental flowrate = ± 0.5, which implies ± 1 error in reported (measured) Q values
Experimental power consumption ± 0.5
>> Indicates that the value was used as a design-setpoint for the model

Table 6-3: Thermodynamic properties measured (Lee, 2010) and calculated at various state points using Aspen Plus.

6.1.1 Evaporator (Cooling Capacity) Model

The testing conditions of the evaporator included setting the temperature of the process side (chilled water) so that it entered and left the evaporator at 285.45 ± 0.5 K and 280.55 ± 0.5 K (or 12 ± 0.5± 0.5°C and 7 ± 0.5°C). The flow rate of the process side was then measured and used to determine that the experimental cooling capacity of the cycle is 357.85 kW, including superheat, as is listed in **Table 6-3** on the previous page. The duty of the evaporator is then used to determine the amount of refrigerant necessary to chill the process side. The experimental temperature and pressure at the stream leaving the evaporator are then used as input-specifications for the process model, while the flow rate is iterated until the specified evaporator duty is obtained. This results in a predicted R-22 flow rate of 88.78 kmol/hr (or 7676.51 kg/hr) for the actual cycle, with a stream quality (or vapour fraction) of 0.17 entering the evaporator. This is assuming that the inlet to the evaporator is actually ~590 kPa and not 598 kPa as reported (which is explained in 6.1.4 Expansion Device). The refrigerant flow rate, unfortunately, cannot be checked against the actual physical measurement since the author chose not to report its value in the article.

The refrigerant, therefore, enters the evaporator as a partially vaporised liquid and exits as a superheated vapour. It takes approximately 352.07 kW to completely vaporise the remaining liquid in the entering stream to its dew point at 527 kPa and 274.90 K (or 1.75 °C), where an additional 5.7837 kW is then required to superheat the vapour to the final exit temperature of 278.55 K (or 5.4 °C). This is equivalent to an actual superheat of 3.65 K, which is lower than the 5 K set point used by the author. Although no details of the process control are provided, it could be that since unit B was modified from unit A by swapping in a new condenser with a greater heat transfer, and unit C was modified from B by using a more efficient compressor, that the evaporator maybe slightly under capacity and/or the controlling scheme is less than ideal. The added superheat is needed, in part, to compensate for the suction line losses leading to the inlet of the compressor.

6.1.2 Compressor Model

The test conditions for the compressor then involved compressing a superheated vapour from 522 kPa at point 2 to 1536 kPa at point 3, or a pressure ratio of approximately 2.94. At the very least a compressor model requires that the discharge pressure (or pressure ratio) be specified, where the actual power required to compress the working fluid then depends on both the isentropic and mechanical efficiencies of the compressor, besides, of course, the fluid-specific properties of the refrigerant that is used. Since the calculated discharge temperature for a fully isentropic process is only 335.13 K (or 62 °C) the compressor's isentropic efficiency was then iteratively solved to exactly match the reported 345.95 K (or 72.8 °C) at point 3. This resulted in an isentropic efficiency of 74.55 %, with an indicated horsepower of 78.7085 kW. The compressor's mechanical efficiency then had to be adjusted so that the calculated power matched the reported 79.86 kW ± 0.5% reading of the wattmeter. This resulted in a mechanical efficiency of 98.56 %, and accounts for -1.1515 kW of wasted power leaving the system as wasted heat, and is in line with the use of a high efficiency motor (which are typically used in larger-scale applications such as this to reduce operational costs). Since no wet compression was predicted for this step, the actual superheat of 3.65 K from the evaporator (although less than the 5 K set point) also appears be sufficient.

6.1.3 Condenser (Heat Rejection) Model

The testing conditions of the condenser included setting the temperature of the heat transfer fluid (cooling water) so that it entered and left the condenser at 303.15 ± 0.5 K and 308.15 ± 0.5 K (or 30 ± 0.5± 0.5°C and 35 ± 0.5°C). The flow rate of the cooling water was then measured and used to determine the -435.5 kW that was reported as the condenser's duty, including subcooling, as listed in **Table 6-3** on Page 100. Since the required refrigerant flow rate has already been fixed based on the evaporator duty, the condenser model only needs to account, i.e. remove or reject, all of the heat absorbed from the process side plus any additional heat added from the compression step/inefficiencies (less line losses). The calculated duty from the process model, therefore, is predicted to be approximately -435.9 kW. Although the author chose not to report the physical measurement of the cooling flow rate, the calculated duty from the process model almost exactly matches the reported duty (with only 0.4 kW in difference).

The refrigerant, therefore, enters the condenser as a superheated vapour and exits as a subcooled liquid. It takes approximately -349.53 kW to bring the entering stream to its bubble point at 1479 kPa and 311.67 K (or 38.5 °C), where an additional -12.351 kW is then removed to subcool the liquid to the final exit temperature of 306.35 K (or 33.2 °C). This is equivalent to an actual subcooling of -5.32 K, which is higher than the 5 K set point used by the author. It could be that the combination of the new condenser with a greater heat transfer and a more efficient compressor resulted in a slightly oversized condenser and/or an un-optimised process control strategy. The added subcooling is needed, in part, to compensate for the superheat added in the evaporator and to reduce the required refrigerant flow rate of the process by reducing the amount of liquid that vaporises through the expansion device.

6.1.4 Expansion Device

Of all the components of the refrigeration cycle, the expansion device is typically the easiest to model by assuming that the pressure let-down occurs rapidly without much heat exchange with the surroundings. This is often a good assumption, where the pressure change across the device can then be modelled as an adiabatic flash across a valve. By specifying an outlet valve pressure of 598 kPa, however, as published in the journal article, this assumption results in a calculated exit temperature of 278.9 K (or 5.8 °C), which is 0.45 higher than the reported 278.45 K (or 5.3 °C) inlet measurement for the evaporator, i.e. the enthalpy of the stream is no longer consistent with the reported conditions for the inlet stream of the evaporator. Some of the difference could be attributed to the distance between the exit of the expansion device and the sample location at the inlet of the evaporator, but this distance is typically small enough that the heat lost between the pipeline and surroundings is often negligible (which is why, with good reason, they are routinely presumed to operate adiabatically). Alternatively it could be that the error in the pressure sensor and/or temperature probe is larger than reported, e.g. from faulty instrument(s), or the author could have simply been mistaken in the values that were reported. If you assume, for instance, that the author meant to report the pressure as ~589 kPa instead of the 598 kPa reported in **Table 6-2** (in red), then an adiabatic flash across the valve results in a temperature of 278.44 K (which is within the reported experimental error of ± 0.03 °C). This plausible explanation, however, fails to explain the same errors found in the other unit configurations A and B (not shown here). As a result it seems much more likely that the actual pressure sensor was in error and should be disregarded in favour of the predicted value (assuming the temperature reading at the same point can be accepted as originally reported).

The correct outlet pressure for the valve, therefore, can be obtained by iteration until the reported temperature of 278.45 K is obtained. This results in an outlet pressure of 589.61 kPa, with a vapour fraction of 0.17 that forces the required refrigerant flow rate to increase from 73.7 kmol/hr (if the entire stream was subcooled as was originally reported) to 88.78 kmol/hr to cover the fractional loss previously achieved from the vaporisation of the entire stream.

6.2 Model Validation

The process model, however, is only as good as its predictions relate to the working process. The values of physical measurements used in building the model, for instance, contain at least some type of error—*should the physical measurements be believed or predictions made using the process model? On what basis are such decisions made?* The reconciliation of available measurement data and the validation of process models goes hand-in-hand. Not only is process knowledge required to define a process model, but the process model itself is often required to back-check (or reconcile) measured variables against available redundant measurements with respect to the fundamental material and energy balances of the process.

In this case, for instance, physical measurements were only taken from the real process once the system reached steady state for at least one hour before a set of four readings were taken, at 20 minute intervals, before averaging to obtain the reported values in **Table 6-2** and **Table 6-3**. The effects of random errors due to small dynamic (normal) variations of the process should thus be limited, and steady-state operation can thus be safely assumed so that the refrigerant flow leaving one component is the same as that entering the next. Given the non-rigorous modelling approach herein adopted, and the choice of using REFPROP to reliably provide all required physical property information for R22, significant discrepancies between predicted process variables and their physical measurements should primarily be limited to those having systematic (or gross) errors e.g. from process leaks. The reported outlet pressure to the expansion device in the preceding sub-chapter, for example due to failure or incorrect calibration of the pressure sensor, was rejected based on ill-reconciliation with model results and the remaining process variables, while other differences are even smaller and as a consequence not worth mentioning further. The overall performance of the process model, however, exactly matches the 4.5 COP of the real process, and although the calculated 88.7 kmol/hr (or 7676.51 kg/hr) of refrigerant cannot be validated it does seem reasonable. The very fact that the process model closely describes the physical measurements from the real process is validation enough, where any major differences between the calculated and reported results have been suitably explained.

6.3 Model Generalisation

Although the process model had been developed and validated at the test conditions for R-22, what is needed is a general model that can to a certain degree predict the realistic performance of similar but different working fluids. If the properties of the new working fluid differ too greatly from those of R-22, then a more detailed model would likely be required e.g. manufacture performance maps would have to be integrated into the compressor model so that its performance for specific sets of suction conditions, i.e. molecular weight of the fluid, pressure, temperature, compressibility and isentropic exponent at the inlet of the compressor, could be determined with sufficient accuracy (Stephenson, 2011). Such an analysis, however, requires detailed knowledge of the working process which is not available for the current system. Therefore, instead, pure component properties of the blend components for potential R-22 replacements were kept close to those of R-22 (see 5.3.5 Proof

of Concept on Page 92), so that it can be assumed that potential R-22 blend replacements are close enough in character to the original refrigerant, i.e. that a first-pass process model of the real process will result in calculations that are sufficiently meaningful. The final component concentrations of the potential blend replacements (see **Table F-2** of **Appendix F**, Page 172) will be presented in the following chapter, where the component concentrations have been re-optimised using the process model and the following set of conditions (based on the base-line model results just discussed):

- The inlet temperature to the evaporator is kept at 278.45 K (or 5.3 °C) to promote heat transfer between the refrigerant and chilled water, and is maintained by adjusting the let-down pressure of the valve, i.e. the inlet pressure to the evaporator.
- The duty of the evaporator is kept at 357.85 kW (including 3.65 K of superheat) with a pressure drop of -62.61 kPa, and is maintained by adjusting the refrigerant flow rate.
- The suction line loss is assumed constant at 1.331 kW, with a pressure drop of -5 kPa.
- The isentropic and mechanical efficiency of the compressor are kept constant at 74.55% and 83.71 % respectively, and the discharge temperature is kept at 345.95 K (or 40.1 °C) by adjusting the compressor discharge pressure.
- The discharge line loss is assumed constant at -1.712 kW, with a pressure drop of -30 kPa.
- The pressure drop across the condenser is kept at -27 kPa (including 5.32 K of subcooling).
- The liquid line loss is assumed constant at -0.275 kW, with a pressure drop of -3 kPa.

This set of conditions allows the process model to change the operating set points, i.e. pressure and mass flow rate or refrigerant, so that the process always achieves the desired performance. The model now can be used to optimise component blend concentrations in the process using the PC-SAFT equation.

6.4 Model Optimisation

Recall that the overall objective of the present research project is to develop a methodology to identify potential refrigerant replacements, which fall into one of two categories. Replacements for existing systems i.e. in the truest sense of the word, or for new installations. These two cases are discussed separately in the following sub-chapters below.

6.4.1 Drop-in Replacements

The search for so-called “drop-in replacements” is the most difficult. In such a case it is desired that existing equipment be re-used with little to no modification, while maintaining equivalent (or near-matching) system performance. Since the equipment was designed using the physical property information of the original refrigerant, one of the simplest ways to safeguard the operation of the existing cycle is to identify replacements that have similar properties to the refrigerant that is now going to be replaced. Such an approach, for instance, was used in the preceding chapter to identify potential R-22 replacement blends based on how well they match (at atmospheric pressure) the boiling point, liquid density and the heat of vaporisation of R-22 (see **Chapter 5.3.5,** Proof of Concept, Page 92). A better option, still, is to instead optimise the compositions of potential blends to the working process in which they are to be used. In such a case a sufficiently precise process model of the existing cycle is required for optimisation purposes.

A more integrated design approach, therefore, is attempted using the process model that was developed earlier in the present chapter for an existing cycle that uses R-22. Instead of directly using only property constraints to minimise an objective function, the performance of the process model will also be used to fit the final concentrations for components of potential blends. A simple objective function like that used to fit pure component PC-SAFT parameters was again used:

$$O.F. = f(x_i) = RMSD = \sqrt{\frac{1}{n}\sum \frac{P^* - P_{ref}}{P_{ref}}} \quad (6\text{-}1)$$

Where n is the number of property values used for the fitting, P^* the property value calculated using PC-SAFT and P_{ref} for that of REFPROP. Here the word "property" is loosely used, and can either refer to a thermodynamic and/or transport property of the refrigerant (typical convention) or could represent a calculated quantity from the process model e.g. the coefficient of performance, or COP, of the process. The final choice of which properties to include in the objective (or fitness) function will then, of course, have an impact on the relevance of the final fitting results i.e. the component mole fractions of potential refrigerant replacements.

To test the responsiveness of fitting potential blend compositions to the actual process, a simple fitness function consisting of the COP for the real process and the liquid heat capacity of R-22 (both calculated via REFPROP) were initially used. The liquid heat capacity of the mixture (CPLMX) is used here to "somewhat" limit the results to those close in character to R-22, while allowing the COP to fluctuate a little more freely than it would if it was used as the sole fitness-objective. A low CPLMX value, for instance, typically increases the quality of the refrigerant after it flashes through the expansion device i.e. the vapour fraction $VF \to 0$ leaving more liquid refrigerant available for vaporisation, which then requires less refrigerant (and thus power) to obtain the necessary 357.85 kW of cooling that the real process commands. The calculated COP is then necessary to keep the results on-par with the overall performance of the existing process. The number of adjustable parameters, therefore, are only ever equal to the number of fitness-objectives for the case of three-components, i.e. functions of two adjustable mole fractions. The fitness function, however, is likely only applicable to systems of two-components in this case since both CPLMX and COP are interrelated, where three or more component systems are then expected to have more flexibility then the problem demands i.e. to satisfy both the 4.481 COP of the real process and the 103.67 J/mol-K of the existing R-22 refrigerant used in the objective function. This point is not raised to invalidate the analysis, but to make clear the potential limitations of the objective function as it currently stands.[26]

The process optimisation was then performed using a near identical procedure to **Chapter 5.3.5** (Proof of Concept, Page 92). The only difference is that the component concentrations for potential blend replacements are now fitted using the process model of the real process, instead of just fitting to the calculated pure component properties of R-22 using REFPROP. The process optimisation results were then filtered by removing those solutions in which one or more mixture-

[26] The number of properties included in the optimisation function (O.F.) may need to be chosen based on the number of components in the system: two-components (one adjustable mole fraction) needs a single fitness-objective, three-components (two adjustable mole fractions) needs two fitness-objectives and so forth. This is not a strict rule, however, since the problem is non-linear in nature, where these "rules" may not necessarily apply (i.e. they are only true for linear problems).

components have mole fractions < 0.01 i.e. the optimisation routine was likely forcing $x_i \to 0$ in these cases (which should be ignored). Even so, there are a number of results that have a fitness of zero (perfect matches), but only for blends having three or more components as expected e.g. 80% of these higher-ordered systems resulted in a perfect match. This just reaffirms the notion that these many component systems have too much flexibility for the problem, i.e. objective function, as it is currently defined. The focus of the results, therefore, is accordingly limited to binary systems alone; the fittest of these are summarised in **Table 6-4** below:

	Blend Components	**O.F.**	**Compositions**	**COP**	**CPMXL**
			(Moles) / [Mass]	----	[J/mol-K]
	R-22	----	----	4.48	103.7
1.	R-143a/{COS}	0.0023	(31.5/68.5) [39.1/60.9]	4.47	103.4
2.	{Cyclopropane}/{Propyne}	0.0063	(28.8/71.2) [29.8/70.2]	4.50	102.8
3.	RE-170/{COS}	0.0075	(80.0/20.0) [75.4/24.6]	4.50	104.7
4.	R-125/{COS}	0.0126	(21.7/78.3) [35.6/64.4]	4.53	105.0
5.	R-1270/{COS}	0.0150	(49.2/50.8) [40.5/59.5]	4.42	101.9
6.	R-1270/-32	0.0165	(49.4/50.6) [44.1/55.9]	4.53	105.8
7.	R-290/{COS}	0.0187	(38.7/61.3) [31.7/68.3]	4.41	101.4
8.	R-1270/{Propyne}	0.0208	(20.6/79.4) [21.4/78.6]	4.35	103.3
9.	R-290/-32	0.0211	(40.3/59.7) [36.3/63.7]	4.54	106.4
10.	RE-170/-32	0.0211	(82.5/17.5) [80.7/19.3]	4.52	106.6

Table 6-4: Fittest binary replacement blends, where the component compositions were fitted to the COP of the process and the liquid heat capacity (at constant pressure) of R-22 at the inlet conditions of the expansion valve.

These result in **Table 6-4**, however, cannot *all* be considered relevant answers. A number of the potential solutions contain carbonyl sulphide (COS), for instance, but are unlikely to be entertained by industry due to safety, e.g. since COS is reactive and oxygenated, and environmental concerns from its sulphur content. Although the pool of components used for the optimisation was initially restricted to eliminate the inclusion of such substances, COS was accidently included due to an oversight before the optimisation was performed (COS is therefore labelled in red, to read as "cautionary"). Given the favourable results in comparison to the more traditional compounds, the results of mixtures containing COS are also listed instead of completely disregarded out of hand (but are largely ignored in subsequent analysis as being irrelevant). Although it is predicted that the potential substitutes of **Table 6-4** closely match the operating COP of the existing cycle, there is still no guarantee that these results would function as suitable replacements if directly substituted into the actual process. There are additional questions, in general, that should be addressed:

- Is the existing piping network sufficient for the new refrigerant at the predicted rates?
- How will the compressor (and the new refrigerant) handle the required pressure change?
- Are the evaporator and condenser appropriately sized?
- Can the expansion valve handle the capacity? Is it in the range of controllability??

To aid in resolving these types of questions a more detailed (rating-based) analysis is truly required. This, however, as explained earlier, requires comprehensive knowledge of the process that is not available for the case at hand; even so, comparisons against other process variables e.g. as shown in **Figure 6-2** can still be used to some extent gauge their potential performance. The closer these variables operate to the operating conditions of the existing R-22 refrigerant the better.

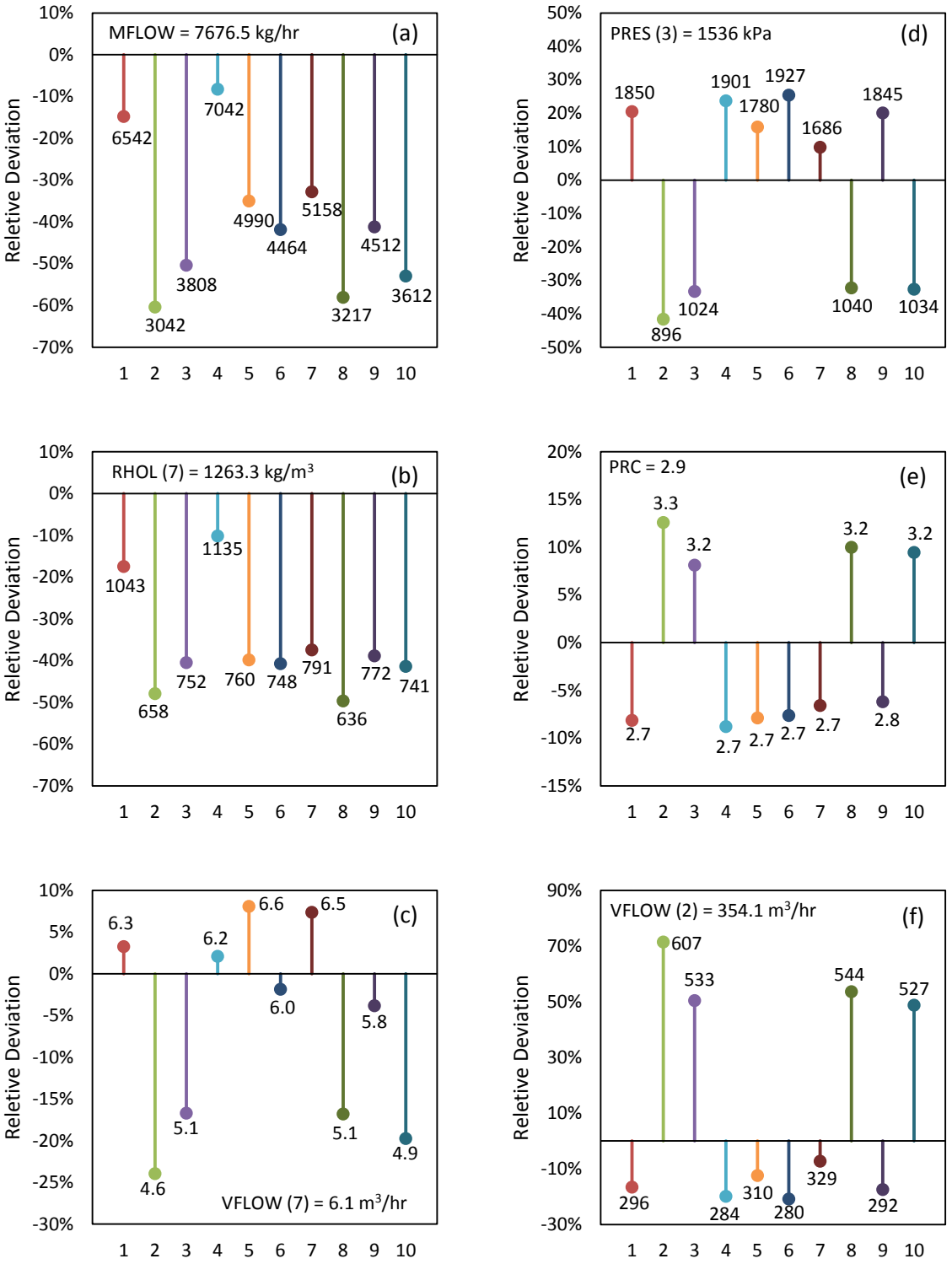

Figure 6-2: Relative deviations in refrigerant mass flow rate (a), liquid density entering the evaporator (b), liquid volumetric flow rate entering the evaporator (c), discharge pressure (d), pressure ratio (e) and the vapour volumetric flow rate at the compressor suction (f) for selected potential blends compared against existing R-22 values.

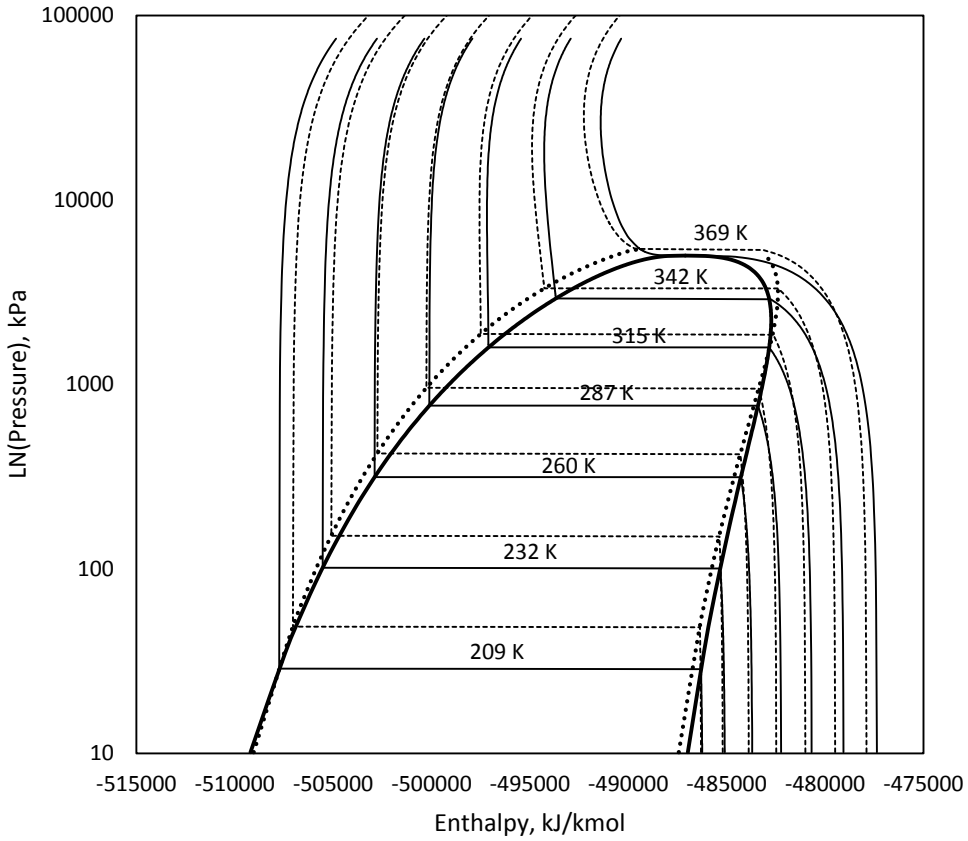

Figure 6-3: Pressure-enthalpy plotted for R-22 using REFPROP (black lines) and PC-SAFT equation using fitted concentrations from **Table 6-4** for the binary system 1,1,1-trifluoroethane [R-143a] (1) + carbonyl-sulfide (2).

The fittest result in **Table 6-4**, which closely reproduces the behaviour of R-22 as shown in **Figure 6-3** above, may not necessarily be the best overall result. If liquid flow through the evaporator is assumed, for instance, then properties such as the pressure, mass flow rate and density (or similarly the volumetric flow rate) of the potential refrigerant also become factors in accounting the conservation of energy via the Bernoulli's Equation e.g. for incompressible flow through a horizontal pipe corrected for energy loss:

$$\overbrace{\frac{P_1}{\rho g}+z_1+\frac{v_1^2}{2g}}^{\text{Energy per weight of fluid upstream}}=\overbrace{\frac{P_2}{\rho g}+z_1+\frac{v_2^2}{2g}}^{\text{Energy per weight of fluid downstream}}+\overbrace{h_f}^{\text{Energy loss correction}} \qquad (6\text{-}2)$$

$$\Delta P=\frac{\rho}{2}(v_2^2-v_1^2)+h_f(L,D_i,\bar{v},\sigma,\dots)$$

where P is the pressure, ρ is the fluid mass-density, v the average fluid velocity, g the gravitational constant and h_f the empirical correction factor describing the energy loss between the up and downstream points (a function of pipe geometry and fluid specific properties). [27] The effects of

[27] Strictly speaking viscosity σ has a large impact on the pressure drop calculation through the empirical correction factor h_f, which takes into account the flow regime of the fluid (which in turn heavily depends on σ). The effects of this are ignored here, however, out of necessity, since Aspen Plus does not include an option-switch to force the calculation of σ using the PC-SAFT equation.

pressure, in this case, can largely be ignored since constant pressure drops were assumed throughout the process model. They are, however, still important for determining if the existing pipes, tubes and their fittings have the appropriate pressure rating for the new operation (if such detailed knowledge of the process exists). The direct substitution of cyclopropane (1) + propyne (2) into the real process, for example, could conceivably result in fluid flow problems such as hammering (pulsing or the sudden starting-and-stopping of fluid flow) due its reduced mass flow rate (MFLOW) and a disproportionate reduction in the liquid density (RHOL (7) of stream seven) as depicted in **Figure 6-2** on Page 108. If one now considers the performance of the compressor, instead, then properties such as the volumetric flow rate at the suction point of the compressor (VFLOW (2)), pressure ratio across the compressor (PRC) and the suction/discharge pressures of the compressor (PRES (2) and PRES (3) respectively) become important. In order to obtain potential blend replacements that can simultaneously match the myriad of properties of **Figure 6-2**, additional fitness-objectives are thus required (although their inclusion will likely result in more binary solutions having sub-optimal COP values e.g. like blends 7-and-8 of **Table 6-4**).

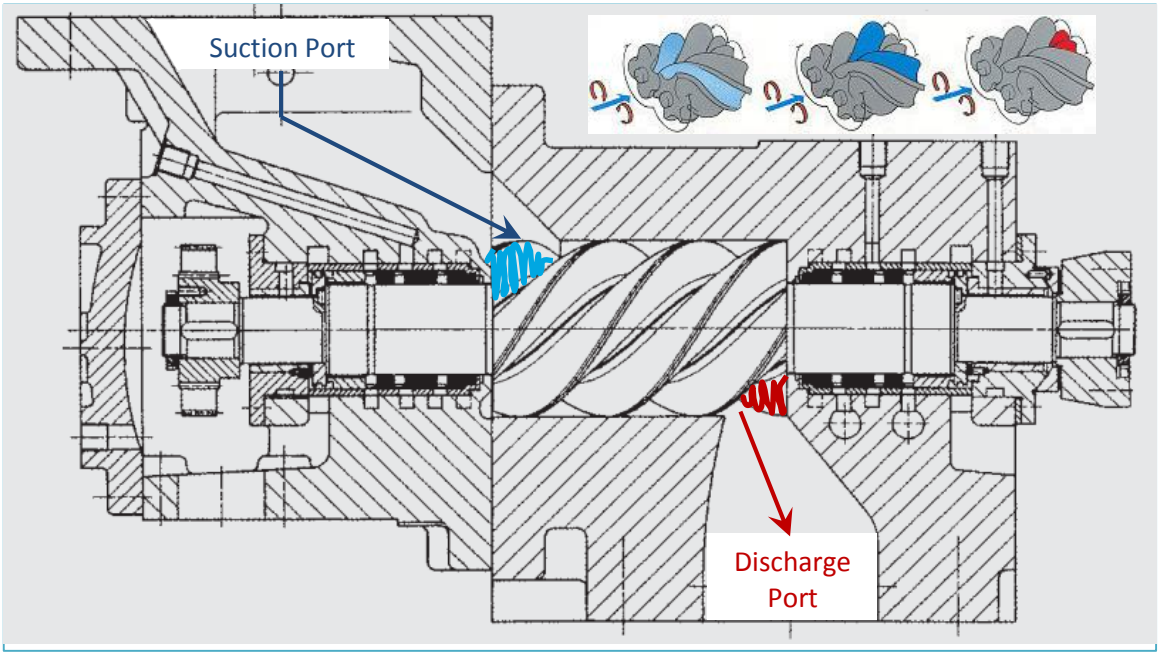

Figure 6-4: Horizontal section of a twin-screw compressor.

Systems with three or more components should exhibit more flexibility to satisfy additional constraints. The real process, for instance, uses a twin-screw compressor with a displacement of 380 m^3/hr. Since compressors are typically the largest sources of entropy generation (or lost work) in a refrigeration cycle, it was desired to expand the previous objective function (which was used to primarily test the responsiveness of the process) to also include process-objectives to address the operability of the compressor. Unlike typical reciprocating compressors (as previously described in **Chapter 3.4.2**, Page 25) screw compressors are fixed-volume machines that have no valves that handle the suction and discharge of the gas, but instead accept a certain volume of suction gas in a cavity and reduces this volume a specific amount before discharge (a general schematic is provided in **Figure 6-4** above for discussion purposes). They function, therefore, like positive displacement machines that operate with some advantages over the more common reciprocating-type compressors (Wennemar, 2009):

- The suction volume flow and power consumption grow linearly with the compressor speed, at constant discharge pressure.
- The suction volume flow is nearly constant for variation of pressure ratio or gas molecular weight with no surging limit.
- The achievable pressure ratio per compressor stage does not depend on the gas molecular weight but is limited mostly by the allowable discharge temperature or by mechanical limits.

Therefore, unlike reciprocating compressors, screw compressors do not have a dead volume that re-expands (a source of entropy generation/lost-work) during the suction phase i.e. the suction and discharge of the gas is connected to the suction and discharge lines respectively via fixed-ports in the compressor casing as depicted in **Figure 6-4**, with a fixed *built-in volume ratio*[28] that is determined by the casing's geometry.

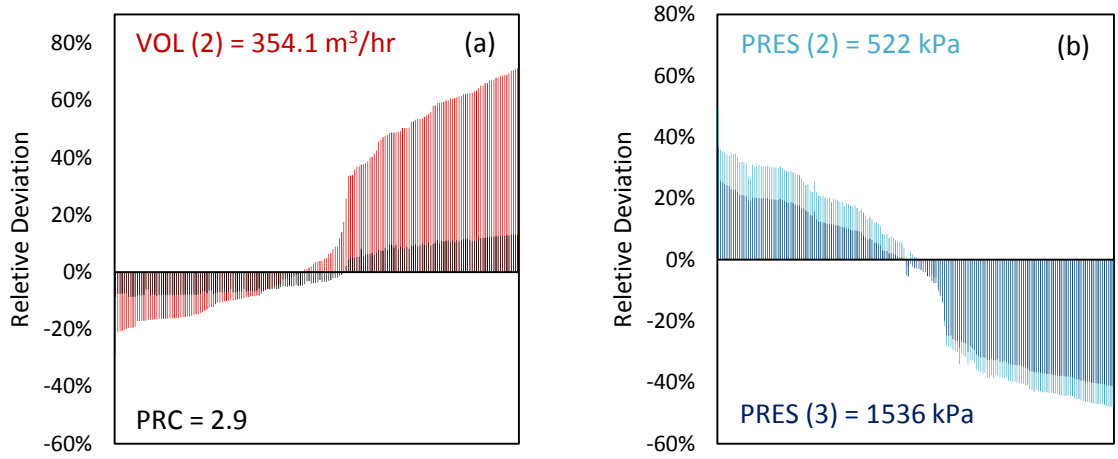

Figure 6-5: Relative errors in the suction volume rate and the pressure ratio across the compressor (a), and the suction and discharge pressures of the compressor (b) for ternary systems fitted in the previous sub-chapter (6.4.1.1 Binary Replacements).

The operability of the existing compressor, therefore, is not only a function of the discharge pressure and pressure ratio of the compression step, but also of the suction volume of the compressor. **Figure 6-5** above, for instance, shows the relative errors in these properties for the ternary systems that were just fitted to COP and CPLMX. In these cases about half the results show suction volumes in excess of the current required 354 m^3/hr of R-22 (which itself is about 7% under the 380 m^3/hr design-displacement for the compressor), while 80% of these systems resulted in a fitness of zero. It is tempting, therefore, in this case, to expand the previous objective function to include V2, but this may not be the best choice. Regardless of the predicted suction volume required for a specific blend, the casing of the existing compressor may not be rated to handle the pressures and/or pressure ratios for blends far removed from its current operating conditions. The allowable pressure difference for the compressor, for instance, is typically limited by the allowable shaft stresses and the load on its bearings (Wennemar, 2009). It is likely, therefore, more important to match the discharge pressure (P3) and pressure ratio (PRC) of the existing process instead of just V2 (which, to some extent, depends on the type of motor used to drive the compressor). This can be accomplished, for instance, by adding

[28] The *built-in volume ratio* is defined as the ratio of the volume in cavity when the suction port closes to the volume in cavity when the discharge port uncovers.

both the suction and discharge pressures to the previous objective function, instead of just P3 (or P2) and PRC directly. The choice of using P3/P2 (i.e. PRC) or V2 should largely be a moot point, given that these variables are directly linked via the PVT behaviour of the working fluid, but it was found that the overall pressure profile of the process could be better matched by indirectly specifying both P2 and P3 instead. This, of course, is just the solution route chosen in this work.

The previous objective function was then extended to include the compressor suction and discharge pressures as additional fitness-objectives, i.e. in addition to CPLMX and COP. Instead of again testing all possible component combinations, however, the optimisation was limited to the filtered results from the previous optimisation, i.e. blends fitted to the COP of the existing process with $x_i > 0.01$. This was done to eliminate unnecessary computing time for infeasible solutions, and should not impact the overall fitting results presented in **Table F- 3** of **Appendix F**, after again removing those results that have one or more component mole fractions < 0.01 (which, as before, should be ignored). The most promising drop-in binary and ternary mixture replacements for the existing process are presented in the appropriate sub-chapters that follow. Quaternary mixture results were prudently ignored, since every potential mixture replacement of this kind contained carbonyl sulfide as a mixture component (results are, however, included in **Table F- 3** of **Appendix F** for the curious).

6.4.1.1 Binary Replacements

The ten fittest results for binary replacements are presented in **Table 6-5** above. Potential blend replacements are ordered according to COP (with respect to the value of the objective function) and preference given to mixtures that do not contain carbonyl sulphide. So although the mixture R-1270 (1) + cyclopropane (2) has a lower objective function value than the mixture R-32 (1) + R-134a (2), the latter is listed first in the table since it has the higher COP value. Furthermore, although the mixture COS (1) + R-134a (2) has one of the highest COP values while also having the lowest objective function value, it is listed last since it contains carbonyl sulphide. Refrigerants R-32, COS, R-125, propylene, R-143a and R-290 are so-called “low boilers” with respect to R-22, while cyclopropane, R-134a, R-152a, and RE-170 are the “high boilers”. As can be seen from the list, therefore, all potential replacements consist of one low boiler and one high boiler (which mix to give something close to R-22). Most of the mixtures that made the list contain R-32, and with the exception of cyclopropane (1) + R-134a (2) consistently show better performance than those with other low boilers. This is also observed in previous work sponsored by the US Environmental Protection Agency, which analysed potential R-22 replacements (Radermacher, et al., 1991). Known substitutes for R-22 can also be seen in **Table 6-5** (highlighted yellow) in positions 1-2 and 7, which gives further confidence to the procedure that was used to generate the results. This is quite surprising since the implementation of the PC-SAFT equation within Aspen Plus does not include any of the newer modifications to account for dipolar interactions e.g. R-32. It was reported elsewhere, for instance, that the mixture R-32 (1) and R-125 (2) shows the best results at the mass percentage 80/20 near the azeotropic point (pressure-maximum) of the mixture (Arcaklioglu, et al., 2005), whereas this work predicts a weight percentage of roughly 87/13 for the mixture while under predicting the azeotropic point by ~8%. **Figure 6-6** (f), for instance, shows the predicted VLE obtained using the PC-SAFT equation compared against available data from the DDB. Except for **Figure 6-6** (d) and (e) the predictions, overall, look sufficiently adequate i.e. the correct character of the mixtures is being captured with sufficient accuracy for comparisons. Still other known replacement blends do not show-up such as R-432a and

R-33a (R-1270/-170 and -290 respectively), but enough cross-observations have been made to show that at least some of the results have some physical basis.

Further comparisons can be made using **Figure 6-7** below, which shows the relative deviation in selected properties for the different binary blends of **Table 6-5** compared to R-22 that is currently used in the existing process. Considering that results 1-2 and 7 represent known replacements for R-22, all the proposed blends can be labelled “plausible”. Apart from directly substituting the proposed mixtures into the working process, there is no real way to tell how they will perform without more process specifics i.e. detailed rating-based simulations. From a practical standpoint, however, results 6 and 7 can likely be considered as the worst case scenarios because of their high negative deviations in the volumetric flow rate at the compressor’s suction point (a screw-type with a fixed volume uptake). Although a variable speed drive could somewhat compensate for these lower suction volumes it would depend on the specifics of the compressor in practice e.g. the point at which vibration begins compromises the operability and/or reliability of the compressor. Given that the aim of the project was to identify “new and novel refrigerant mixture replacements,” then results 3-5 warrant further investigation due to their favourable predicted process performance (compared to 8 and 9 which fall below the 4.48 COP of the existing cycle). It is interesting to note, however, that the best performance predicted was for the mixtures containing COS.

	Blend Components	O.F.	Compositions	COP	CPMXL	Lifetime	ODP	GWP
			(Moles) / [Mass]	----	[J/mol-K]	[years]	----	[100-yr]
	R-22	----	----	4.48	103.7	11.9	0.04	1790
1	R-32/-134a	0.092	(52.2/47.8) [35.7/64.3]	4.62	120.9	9.1	0	1029
2	R-152a/-32	0.1409	(52.0/48.0) [57.9/42.1]	5.5	104.3	3.3	0	413
3	RE-170/-32	0.157	(51.7/48.3) [48.7/51.3]	5.58	99.8	2.5	0	346
4	R-32/{Propyne}	0.2017	(48.7/51.3) [55.2/44.8]	5.91	94	2.5	0	2.5
5	{Cyclopropane}/R-134a	0.2166	(93.7/6.3) [86.0/14.0]	4.69	113.5	1.3	0	105
6	R-143a/-32	0.3185	(32.9/67.1) [44.2/55.8]	4.51	111.3	19	0	1856
7	R-32/-125	0.3705	(93.8/6.2) [86.8/13.2]	5.55	99	6.6	0	884
8	R-125/{Cyclopropane}	0.1385	(19.7/80.3) [41.2/58.8]	4.23	124.9	5.9	0	690
9	R-1270/{Cyclopropane}	0.0792	(56.1/43.9) [56.1/43.9]	4.11	115.5	0.2	0	20
10	{COS}/R-134a	0.0437	(62.6/37.4) [49.6/50.4]	4.73	108	8.6	0	529

Table 6-5: Fittest binary replacement blends, where the component compositions were fitted to the COP of the process, the liquid heat capacity (at constant pressure) of R-22 at the inlet conditions of the expansion valve, and the inlet/outlet operating pressures of the existing compressor.

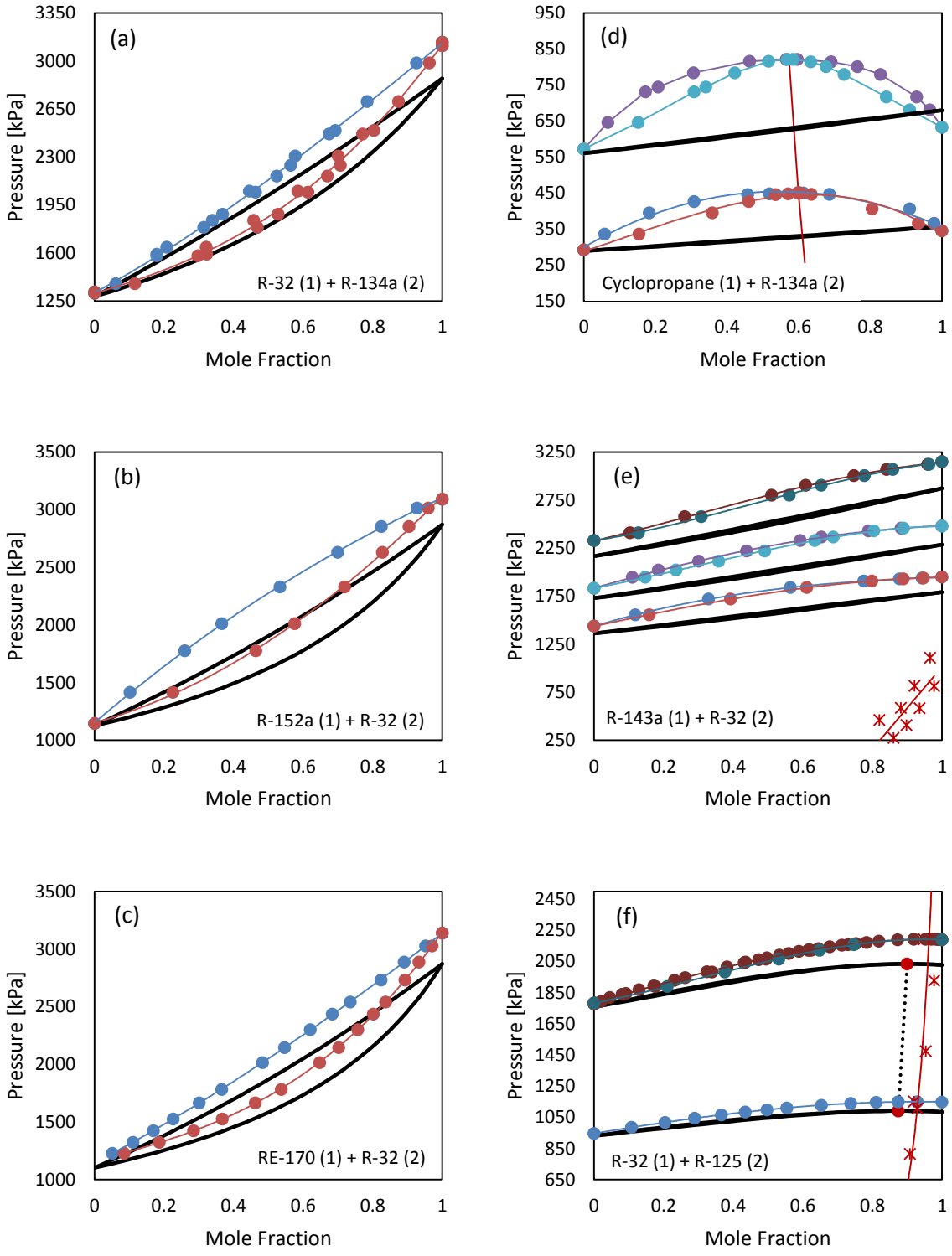

Figure 6-6: Predicted VLE data for selected binaries of **Table 6-5** using the PC-SAFT equation (this work) compared against available experimental data from the DDB (DDBST GmbH, 2012).

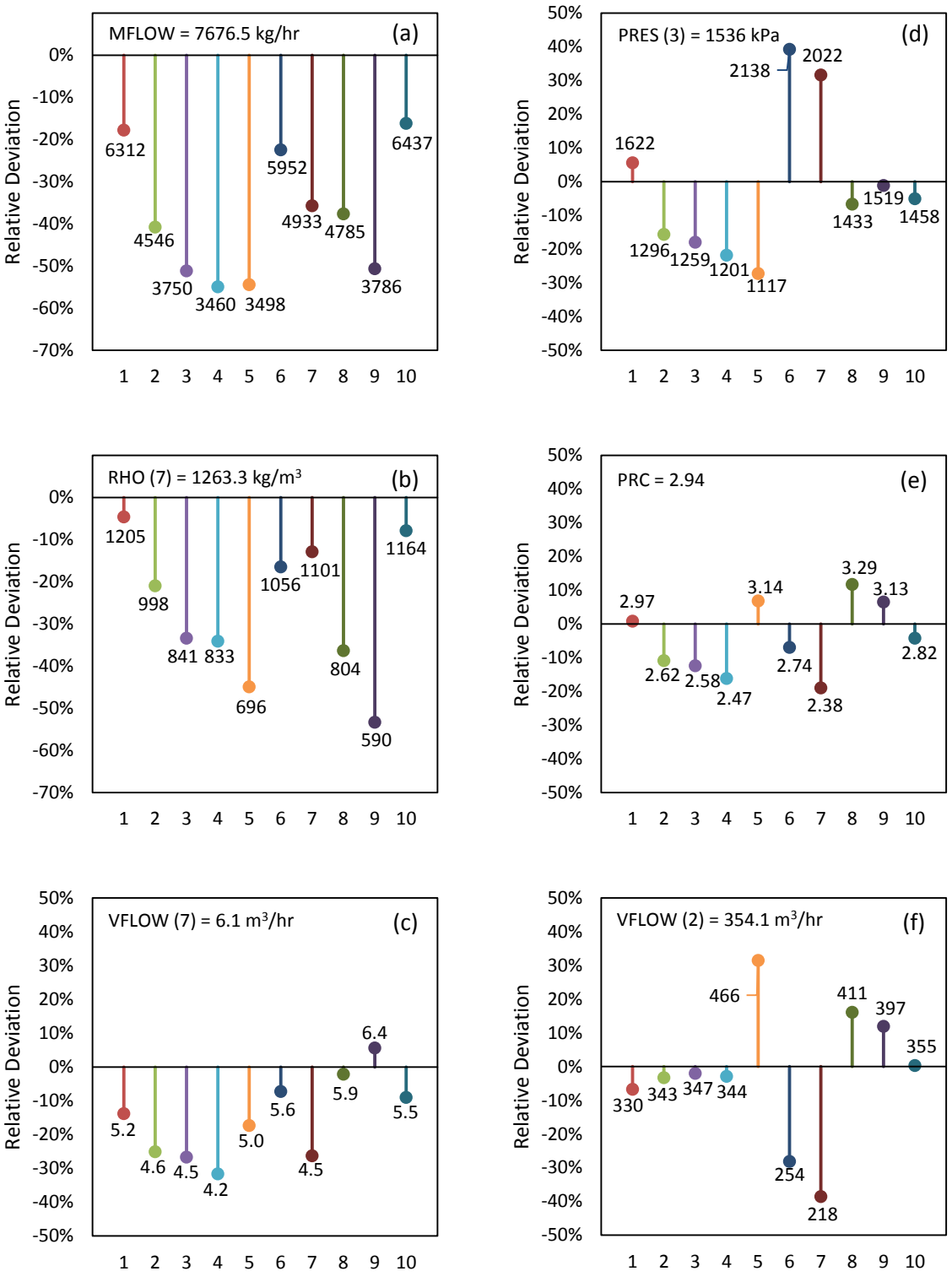

Figure 6-7: Relative deviations in refrigerant mass flow rate (a), liquid density entering the evaporator (b), liquid volumetric flow rate entering the evaporator (c), discharge pressure (d), pressure ratio (e) and the vapour volumetric flow rate at the compressor suction (f) for selected potential binary blends compared against existing R-22 values.

6.4.1.2 Ternary Replacements

The ten fittest results for ternary replacements are presented in **Table 6-6** above. Potential blend replacements are again ordered according to COP (with respect to the objective function value) and preference given to mixtures without carbonyl sulphide. Each potential replacement, like for the binary cases, are then mixtures of both low and high boiling components. Unlike the binaries, however, none of the results are recognized as "known" R22 replacements such as R-32/-125/-134a, or other alternative combinations containing known R-134a substitutes such as R-290 and/or R-32 mixtures with R-600/600a, which were not included in the pool of components used to generate potential mixture combinations (based on the criteria used in **Chapter 5.3.5**, Proof of Concept, Page 92). Dipolar interactions may also be more important in describing ternary combinations e.g. in describing the mixture of dipolar molecules R-32/-125/-134a. In **Figure 6-8** below, compared to the binary results discussed previously, there are larger negative deviations with respect to the required refrigerant mass flow rate and the density of the liquid refrigerant entering the evaporator, while at the same time having smaller deviations in key compressor variables such volumetric flow rate at the suction and discharge points of the compressor. Although every ternary mixture listed in **Table 6-6** can be considered both novel and new, results 1-3 could likely be considered amongst the fittest due to their low relative deviations in the suction volumetric flow, but result 9 may be the most forgiving due to its higher COP e.g. it could handle somewhat more refrigerant mass flow while maintain a COP ≥ 4.48 from the existing cycle.

	Blend Components	O.F.	Compositions	COP	CPMXL	Lifetime	ODP	GWP
			(Moles) / [Mass]	----	[J/mol-K]	[years]	----	[100-yr]
	R-22	----	----	4.48	103.7	11.9	0.04	1790
1	R-290/-32/{Propyne}	0.014	(37.7/37.6/24.7) [36.1/42.4/21.5]	4.51	106.2	2.0	0	282
2	R-1270/-32/{Propyne}	0.0145	(48.2/21.3/30.5) [46.5/25.4/28.0]	4.49	106.1	1.1	0	168
3	RE-170/-1270/-32	0.0229	(31.7/42.3/26.0) [31.8/38.8/29.5]	4.53	107.9	1.4	0	195
4	R-290/-32/{Cyclopropane}	0.0312	(33.4/32.1/34.5) [32.0/36.4/31.6]	4.57	109.7	1.8	0	243
5	R-143a/-32/{Propyne}	0.0319	(31.5/29.6/38.9) [46.1/26.8/27.1]	4.6	109.6	16.4	0	1536
6	R-1270/-32/{Cyclopropane}	0.0325	(40.5/18.5/41.0) [38.8/21.9/39.3]	4.57	109.9	1.1	0	149
7	R-32/-125/{Propyne}	0.0499	(32.0/22.2/45.8) [27.0/43.2/29.8]	4.71	112.4	8.1	0	998
8	R-143a/-32/{Cyclopropane}	0.0535	(22.2/24.1/53.8) [34.7/23.3/42.1]	4.7	113.5	11.9	0	1111
9	R-32/{Propyne}/-134a	0.069	(49.5/12.5/38.0) [37.0/7.2/55.8]	4.85	114.9	7.7	0	878
10	R-32/{COS}/-134a	0.0433	(5.3/56.8/37.9) [3.7/45.2/51.2]	4.73	108.9	8.6	0	573

Table 6-6: Fittest ternary replacement blends, where the component compositions were fitted to the COP of the process, the liquid heat capacity (at constant pressure) of R-22 at the inlet conditions of the expansion valve, and the inlet/outlet operating pressures of the existing compressor.

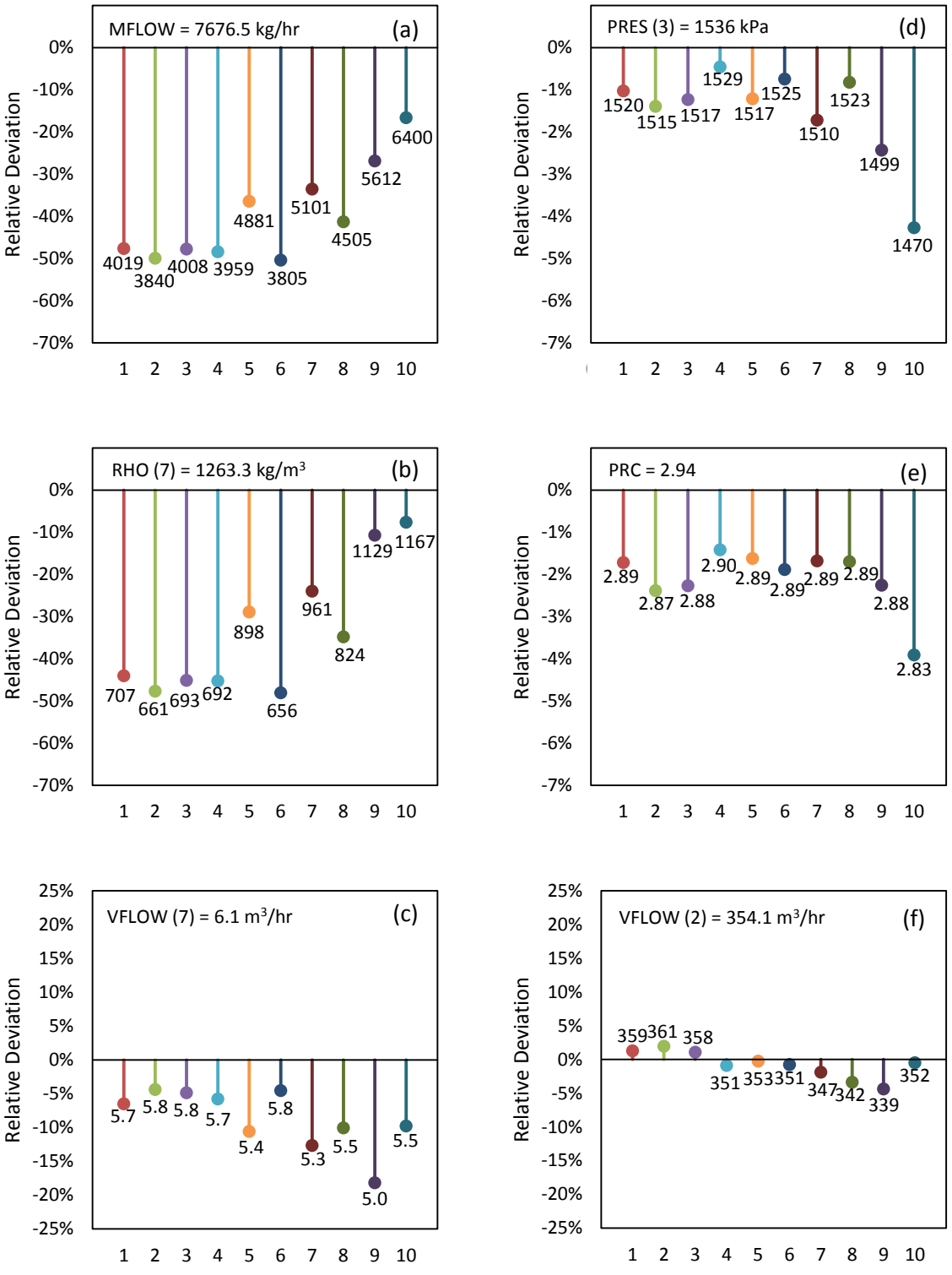

Figure 6-8: Relative deviations in refrigerant mass flow rate (a), liquid density entering the evaporator (b), liquid volumetric flow rate entering the evaporator (c), discharge pressure (d), pressure ratio (e) and the vapour volumetric flow rate at the compressor suction (f) for selected potential ternary blends compared against existing R-22 values.

6.4.2 New Installations

For "new" installations there are relatively few considerations since all major process components can be specifically designed for the new refrigerant i.e. using its specific properties. In this case, therefore, the process model of the existing cycle was optimised to maximise the COP of the existing process by adjusting mixture compositions for every possible combination of the pool-components (defined previously in **Chapter 5.3.5**, Proof of Concept). **Table 6-7** above contains *all* of the fitting results after removing mixture optimums with one or mole component mole fractions < 0.01 and/or with COPs < the current 4.48. If a new system was designed to provide the same amount of cooling as the existing process, then any one of the listed refrigerant mixture replacements should result in a smaller system with a higher COP. Dimensionless PH diagrams for the fittest three results, for instance, are shown in **Figure 6-9** (a) below, along with curves for R-22 and R-12 for comparison. Each of these new mixtures out performs R-22 due to the larger heats of vaporisation they command and higher critical temperatures. Moreover they are able to reduce flash losses across the expansion valve due to their low liquid heat capacities as shown in **Figure 6-9** (c): less material is required achieve the same amount of cooling resulting in less work and therefore higher attainable COP for the process. This is why, for instance, R-12 provides such a low COP even though it also has a larger heats of vaporisation compared to R-22. The new installations will, however, operate at slightly higher pressures as shown in **Figure 6-9** (b), but nothing extreme from a design standpoint. It is also worthy of noting that the mixture R-32 (1) + R-152a (2) has been already found to outperform R22 with respect to COP and volumetric capacity for (Pannock, et al., 1991), which gives some credence to the potential mixtures identified in this work. Only mixture results 2 and 3 had experimental data available for comparison, which also agree with the character of the mixtures predicted with the PC-SAFT equation as shown in **Figure 6-10** below.

	Blend Components	O.F.	Compositions	COP	CPMXL	Lifetime	ODP	GWP
			(Moles) / [Mass]	----	[J/mol-K]	[years]	----	[100-yr]
	R-12	----	----	3.22	125.3	100	0.82	10900
	R-22	----	----	4.48	103.7	11.9	0.04	1790
1	R-32/{Propyne}	0.1558	(79.8/20.2) [83.7/16.3]	6.42	92.1	4.1	0	575
2	RE-170/-32	0.1601	(15.3/84.7) [13.8/86.2]	6.24	94	4.4	0	606
3	R-152a/-32	0.1622	(13.3/86.7) [16.4/83.6]	6.16	95.3	4.7	0	639
4	R-152a/-32/{Cyclopropane}	0.1635	(6.1/83.5/10.4) [7.7/83.8/8.5]	6.12	95.6	4.5	0	608
5	R-32/{COS}/{Cyclopropane}	0.1643	(78.7/13.5/7.8) [78.2/15.5/6.3]	6.09	92.2	4.9	0	569
6	R-32/{Cyclopropane}	0.1645	(87.5/12.5) [89.7/10.3]	6.08	94.9	4.6	0	629
7	R-32/{COS}	0.1645	(76.7/23.3) [74.0/26.0]	6.08	89.7	5.3	0	555
8	{COS}/{Propyne}	0.1664	(88.1/11.9) [91.7/8.3]	6.01	83.9	5.0	0	26

Table 6-7: Potential refrigerant blends, where the compositions have been optimised to maximise COP at real process operating conditions.

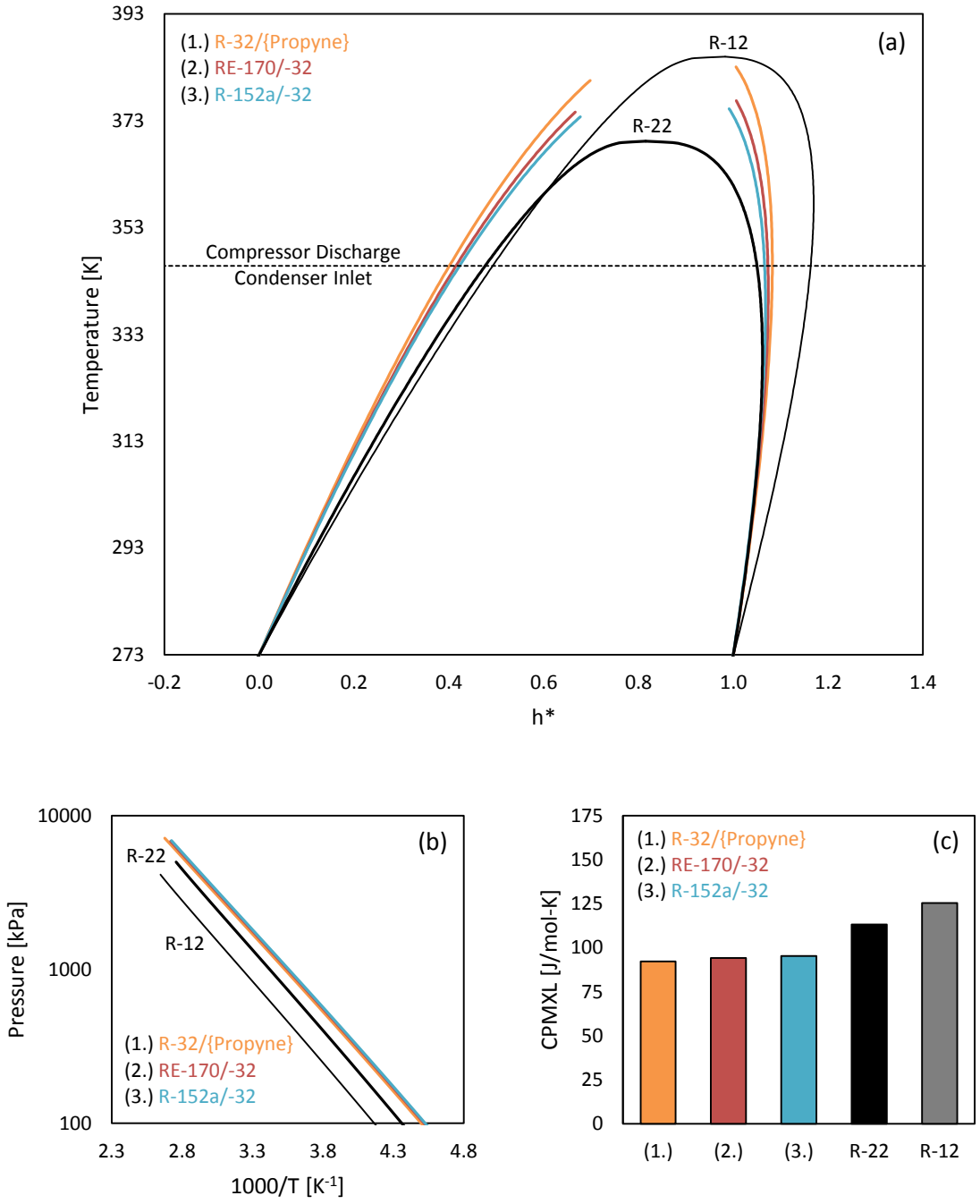

Figure 6-9: Dimensionless temperature-enthalpy (a), saturated vapour pressure (b) and liquid mixture heat capacity (c) diagrams calculated using REFPROP for components R-12 and R-22, and the PC-SAFT equation (using parameters fitted in this work) for results 1-3 of **Table 6-7**.

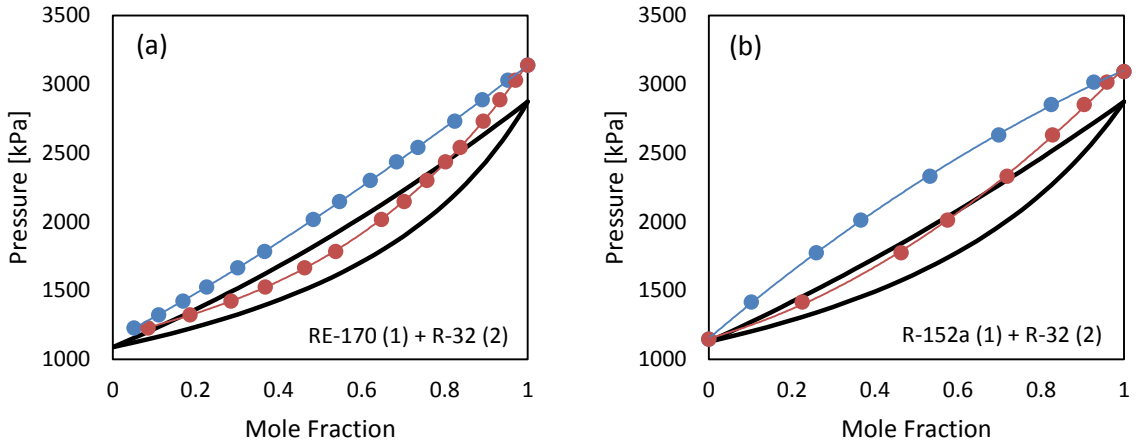

Figure 6-10: Predicted VLE data for select binaries of **Table 6-7** using the PC-SAFT equation (this work) compared against available experimental data from the DDB (DDBST GmbH, 2012).

7 Conclusions

In this study the viability of a *co*ntinuous-*m*olecular-*t*argeting approach towards finding novel refrigerant replacements was investigated. The novelty of this project, therefore, was to combine the component-selection(s) and evaluation steps into a single optimisation problem by using the PC-SAFT equation of state to describe all residual thermodynamic properties required for process calculations (versus performing experimental measurements for every potential refrigerant-replacement). Since the PC-SAFT equation uses physically based molecular-parameters, the model parameters can be e.g. bounded and optimized to give the best overall process performance for a given refrigeration cycle, and then these same (realistic) parameters can be used to identify potential blends. This, however, requires a suitable component-mapping procedure to identify pure components from the PC-SAFT parameters that were optimised for the pseudo-mixture. Another approach, which was herein later adopted, is to instead develop a database (or pool) of pure component PC-SAFT parameters that can be used to predefine various component combinations, leaving only the component concentrations of the mixture to be adjusted and optimised to satisfy specific property and/or design-specifications for some working process (new or existing). The real benefit of using the PC-SAFT equation, in such a way, then becomes that only a very limited amount of pure-component information is required for the initial fitting of PC-SAFT parameters, which can then later be used to describe the full range of residual thermodynamic properties needed for process calculations (and optimisation of the concentration space).

7.1 Concluding Remarks

- The ability of the PC-SAFT equation to represent pure component properties was evaluated by fitting the pure component parameters σ, m and ε/K to predictions made using REFPROP (at the normal boiling point for each component, T_b). Although there will always be a certain "loss in translation" when regressing the calculation results of one model with that of another, the high-precision of REFPROP (for select fluids) implies that any differences in these cases are due solely to the inadequacies of the PC-SAFT equation itself.

  - The enthalpy departure calculation route was traced to elucidate such differences in **Chapter 5.2.1** Enthalpy Departure (Page 67). It was shown that even for cases of a "perfect fit", where the saturated vapour pressure, liquid density and heat of vaporisation data points used in the fitting procedure were regressed exactly, that it does not necessarily mean that other thermodynamic properties such as e.g. the specific heat capacities of either the liquid and/or vapour phases are correctly represented too (although all required residual thermodynamic properties are calculated using the PC-SAFT equation of state).

  - For the case of pure-components, the PC-SAFT equation only has three degrees of freedom (requiring three data points) for fitting purposes. The equation is forced, therefore, to sacrifice the calculation of other properties not directly used in the fitting procedure in order to successfully match those that are. An analytical comparison using the PC-SAFT equation can only be meaningful, therefore, if the relative errors are more or less consistent across all of the fluids of interest. For the relatively simple molecules of typical refrigerants, herein studied, this fortunately appears to be the case as was shown in e.g. **Figure 5-2** on Page 66.

- It is also important to stress that the ability of the PC-SAFT equation to correctly represent pure component properties (and thus mixture properties as well), besides the equation form itself, is also dependent on both the conditions at which the parameters are regressed to match and the objective function that is used in the fitting procedure.

  - **Figure 5-6** on Page 73, for instance, shows multiple calculation results for R-32 using the PC-SAFT equation and separate parameters that were regressed to REFPROP predictions at different temperatures. Although it is not too surprising that different parameters should yield different results (even for the same pure fluid), the "physical basis" of using the PC-SAFT equation in the present work begins to break down in view of such behaviour, i.e. so-called "physical" parameters should be independent of temperature. As was shown in **Figure 5-7** on Page 74, this is clearly not the case.

- The ability of the PC-SAFT equation to represent mixture properties was also evaluated by examining the calculated behaviour of some common mixture replacements for R-502 (azeotropic mixture) and R-22 (pure-component). The pure-component PC-SAFT parameters that were previously fitted to REFPROP predictions (at T_b) were used for the analysis, along with the standard mixing and combining rules defined in **Chapter 4.5.3.4** Handling Mixtures (Page 60), where the inclusion of binary interaction parameters were neglected out of necessity ($k_{ij} = 0$). Mixture evaluations, therefore, were carried out without any empirical adjustments.

  - For mixtures with limited temperature glides, i.e. mixtures with behaviours closest to pure-components (azeotropes and near-azeotropes), it was found that the prediction of key-thermodynamic properties is not grossly effected by inaccuracies in the VLE (PVT) behaviour of the mixture for reduced temperatures of approximately T_r < 0.95. This is fortunate, since pure or pure-acting (azeotropic and near-azeotropic mixtures) are often preferred over refrigerant mixtures with large temperature glides.

- Like other more conventional equations of state, the PC-SAFT equation itself is only capable of describing the behaviour of pure fluids, where suitable mixing and combining rules for the pure component parameters are needed to characterise a "hypothetical" pure fluid that is the mixture. A truly *co*ntinuous-*m*olecular-*t*argeting approach towards finding novel refrigerant replacements, therefore, requires an appropriate mapping procedure to move from the "hypothetical" pure fluid that is the mixture to the pure components that make up the mixture.

  - For zeotropes, however, one cannot simply use the mixing and combining rules to map a mixture to the PC-SAFT parameters of existing pure-fluids as shown in **Chapter 5.3.4** Mixture Optimization (Page 91), i.e. the physical meaning of the equation begins to breakdown without the inclusion of additional adjustable parameters. This, unfortunately, largely prohibits the use of the PC-SAFT equation in a truly a *co*ntinuous-*m*olecular-*t*argeting approach.

  - Instead of e.g. bounding and optimising model parameters to give the best overall process performance for a given refrigeration cycle, it was alternatively proposed to adjust and optimise the concentrations of mixture components to satisfy specific property and/or design-specifications for some working process (existing or for a new

installation). This methodology was verified in **Chapter 5.3.5** Proof of Concept (Page 92).

- Potential mixture replacements for R-22 were identified for an existing refrigeration cycle that was modelled in **Chapter 6.1** Model Development (Page 97), and for newer installations where the cycle-components could be designed around the properties of the new mixture. A database of pure-component PC-SAFT parameters was used to statistically define the various component combinations for optimisation, where the components in the available pool (or databank) were limited to those close in character to R-22 (to limit e.g. temperature glide and non-ideal mixture behaviour).
  - Besides eliminating components with behaviours much different from R-22, the pool of components can be further constrained by removing any so-called "bad actors", i.e. hazardous or environmentally harmful substances like those containing e.g. chlorine and/or bromine (known ozone depleting substances).
  - A number of potential binary and ternary drop-in replacements was identified and summarised in **Table 6-5** and **Table 6-6** (Page 114 and Page 118 respectively), where each potential replacement resulted in a predicted coefficient of performance greater than or equal to the COP of the existing cycle using R-22, $COP \geq 4.48$. The results seem promising since e.g. three out of the ten (binary) results of **Table 6-5** are known R-22 replacements; no known ternary replacements were identified for the existing process.
  - For the case of newer installations, however, which can be designed to accommodate the specific thermophysical properties of the intended refrigerant, the process model of the existing cycle was simply optimised to maximise its COP. Those mixtures with COP > 4.48 are summarised in **Table 6-7** (Page 121).
- Although this procedure was applied to refrigeration using the PC-SAFT equation of state, it is also important to note that the functionality developed for this project can be adapted to other equations and to other application-areas important to industry.

8 Recommendations for Future Work

- Although this project has resulted in the identification of many potential refrigerant mixture blends, it is unlikely that the optimised component concentrations represent anything more than first-pass estimates of the required final values. VLE data should be used to fit and evaluate the inclusion of binary interaction parameters on the optimisation procedure developed during this project.
- A custom PC-SAFT user model should also be developed (or integrated) for future work.
  - Although the PC-SAFT equation can be used to describe all residual thermodynamic properties required for process calculations, Aspen Plus did not take full advantage of this fact when they programmed the equation of state into the property manager of Aspen Plus. Liquid and vapour thermal conductivities, for instance, which are required for more detailed rating-based calculations of e.g. heat exchangers, cannot be calculated using the version of PC-SAFT implemented in Aspen Plus. To fully unlock *all required* thermodynamic properties (for all situations) will require a user-defined version of the PC-SAFT equation. Once developed, the user-model can then also be adapted to test newer SAFT-based equations of state.
  - Existing tools such as e.g. gPROMS should be used for this purpose instead of programming the PC-SAFT equation into Aspen Plus from scratch, i.e. integration of existing functionality is the preferred approach.
- The optimisation procedure used in this work to identify potential refrigerant replacement mixtures should also be experimentally evaluated.
  - Alisha K. Shadrach (UKZN) is currently building an experimental refrigeration testing-apparatus that can be used for this purpose. As in the project, a process simulation model can be developed for the cycle, and then optimised using the same procedures developed in this work.

9 References

[1.] **Achenie L.E.K., Gani R. and Venkatasubramanian V.** Computer Aided Molecular Design: Theory and Practice [Book]. - Amsterdam : Elsevier, 2003. - Computer-Aided Chemical Engineering, 12.

[2.] **AFEAS** Production and Sales of Fluorocarbons: Production, Sales, and Atmospheric Release of Fluorocarbons Through 2007 [Online] // Alternative Fluorocarbons Environmental Acceptability Study (AFEAS). - 2010. - 2013. - http://www.afeas.org/overview.php.

[3.] **Alberty R.A.** Legendre Transforms in Chemical Thermodynamics [Journal] // Chemical Reviews. - 1994. - 6 : Vol. 94. - pp. 1457-1482.

[4.] **Alberty R.A.** Use of Legendre Transformations in Chemical Thermodynamics [Journal] // Pure & Applied Chemistry. - 2001. - 8 : Vol. 73. - pp. 1349-1380.

[5.] **Andersen H.C.** The Structure of Liquids [Journal] // Annual Review of Physical Chemistry. - 1975. - 1 : Vol. 26. - pp. 146-166.

[6.] **Apostolakou A. and Adjiman C. S.** Chapter 12: Refrigerant Design Case Study [Book Section] // Computer Aided Molecular Design: Theory and Practice / book auth. Achenie Luke E.K., Gani Rafiqul and Venkatasubramanian Venkat. - [s.l.] : Elsevier, 2002. - Computer-Aided Chemical Engineering, 12.

[7.] **Arcaklioglu Erol, Cavusoglu Abdullah and Erisen Ali** An Algorithmic Approach Towards Finding Better Refrigerant Substitutes of CFCs in Terms of the Second Law of Thermodynamics [Journal]. - [s.l.] : Energy Conversion and Management, 2005. - Vol. 46. - pp. 1595-1611.

[8.] **AspenTech** Aspen Plus v7.3 (25.0.4987). - [s.l.] : AspenTech, 2012.

[9.] **Bardow Andre, Steur Klaas and Gross Joachim** A Continuous Targeting Approach for Integrated Solvent and Process Design Based on Molecular Thermodynamic Models [Journal]. - [s.l.] : Computer Aided Chemical Engineering, 2009. - Vol. 27.

[10.] **Bardow Andre, Steur Klaas and Gross Joachim** Continuous-Molecular Targeting for Integrated Solvent and Process Design [Journal]. - [s.l.] : Industrial Engineering & Chemical Research, 2010. - 6 : Vol. 49. - pp. 2834-2840.

[11.] **Barker J. and Henderson D.** Perturbation Theory and Equation of State for Fluids. II. A Successful Theory of Liquids [Journal] // J. Chem. Phys.. - 1967. - 11 : Vol. 47. - pp. 4714-4721.

[12.] **Barker J. and Henderson D.** Perturbation Theory and Equation of State for Fluids: The Square-Well Potential [Journal] // Journal of Chemical Physics. - 1967. - 8 : Vol. 47. - pp. 2856-2861.

[13.] **Barnett M.K.** A Brief History of Thermometry [Journal] // Journal of Chemical Education. - 1941. - 8 : Vol. 18. - pp. 358-364.

[14.] **Benedick Richard Elliot** The Improbable Montreal Protocol: Science, Diplomacy, and Defending the Ozone Layer [Online] // American Meteorological Society. - 2004. - 2013. - http://www.ametsoc.org/atmospolicy/PolicyCaseStudies.html.

[15.] **Boublík T.** Hard-Sphere Equaiton of State [Journal] // Journal of Chemical Physics. - 1970. - 1 : Vol. 53. - pp. 471-472.

[16.] **Briley G.C.** A History of Refrigeration [Journal] // ASHRAE Journal. - 2004. - 11 : Vol. 46. - pp. 31-34.

[17.] **Brühl C. [et al.]** The Role of Carbonyl Sulphide as a Source of Stratospheric Sulphate Aerosol and its Impact on Climate [Journal]. - [s.l.] : Atmos. Chem. Phys., 2012. - Vol. 12. - pp. 1239-1253.

[18.] **Brush S.G.** The Development of the Kinetic Theory of Gases [Journal] // Archive for History of Exact Sciences. - 1974. - 1 : Vol. 11. - pp. 1-88.

[19.] **Brush S.G.** The Kinetic Theory of Gases: An Anthology of Classic Papers with Historical Commentary [Book]. - London : Imperical College, 2003. - 978-1860943485.

[20.] **Bücker D. and Wagner W.** Reference Equations of State for the Thermodynamic Properties of Fluid Phase n-Butane and Isobutane [Journal] // J. Phys. Chem. Ref. Data. - 2006. - 2 : Vol. 35. - pp. 929-1019.

[21.] **Cajori Florian** On the History of Caloric [Journal]. - [s.l.] : Isis, April 1922. - 3 : Vol. 4. - pp. 483-492.

[22.] **Calm J.M.** Options and Outlook for Chiller Refrigerants [Journal]. - [s.l.] : International Journal of Refrigeration, 2002. - Vol. 25. - pp. 705-715.

[23.] **Calm J.M.** The Next Generation of Refrigerants--Historical Review, Considerations, and Outlook [Journal] // Ecolibrium. - 2008. - 7 : Vol. 31. - pp. 24-33.

[24.] **Calm James M. and Hourahan G. C.** Physical, Safety, and Environmental Data for Current and Alternative Refrigerants [Conference] // 23rd International Congress of Refrigeration. - Prague : [s.n.], 2011.

[25.] **Carnahan N. and Starling K.** Equation of State for Nonattracting Rigid Spheres [Journal] // Journal of Chemical Physics. - 1969. - Vol. 51. - pp. 635-636.

[26.] **Ceyer S.T.** Lecture 1: Atomic Theory of Matter [Online]. - 2005. - 15 October 2011. - http://ocw.mit.edu/courses/chemistry/5-112-principles-of-chemical-science-fall-2005/video-lectures/. - MIT Open Courseware.

[27.] **Chapman W.G., Gubbins K.E. and Jackson G.** SAFT: Equation of State Solution Model for Associating Fluids [Journal] // Fluid Phase Equilibria. - 1989. - Vol. 52. - pp. 31-38.

[28.] **Chen S.S. and Kreglewski A.** Applications of the Augmented van der Waals Theory of Fluids. I. Pure Fluids [Journal] // Berichte der Bunsengesellschaft für Physikalische Chemie. - 1977. - 10 : Vol. 81. - pp. 1048-1052.

[29.] **Chiew Y.C.** Percus-Yevick Integral Equation of Theory for Athermal Hard-Sphere Chains [Journal] // Molecular Physics. - 1991. - 2 : Vol. 73. - pp. 359-373.

[30.] **Churi Nachiket and Achenie Luke E.K.** Novel Mathematical Programming Model for Computer Aided Molecular Design [Journal]. - [s.l.] : Ind. Eng. Chem. Res., 1996. - Vol. 35. - pp. 3788-3794.

[31.] **Cook David W.** Ethereal Conflict: The Formation, Promotion, and Defense of the United States' Negotiating Position for the Montreal Protocol on Substances that Deplete the Ozone Layer [Online] // Conflict Information Consortium. - University of Colorodo at Boulder, February 1994. - 2013. - http://www.colorado.edu/conflict/full_text_search/AllCRCDocs/94-56.htm.

[32.] **Count of Rumford Benjamin** An Inquiry Concerning the Source of the Heat Which is Excited by Friction. By Benjamin Count of Rumford, F.R.S. M.R.I.A. [Journal]. - London : Philosophical Transactions of the Royal Society of London, 1798. - pp. 80--102.

[33.] **Crutzen P. J.** The Influence of Nitrogen Oxides on the Atmospheric Ozone Content [Journal] // Q.J.R. Meteorol. Soc.. - 1970. - Vol. 96. - pp. 320-325.

[34.] **Crutzen P.J.** Determination of Parameters Appearing in the "Dry" and the "Wet" Photochemical Theories for Ozone in the Stratosphere [Journal] // Tellus. - 1969. - 3 : Vol. 21. - pp. 368-388.

[35.] **DDBST GmbH** Dortmund Data Bank, Version 2012 [Software]. - Oldenburg : [s.n.], 2012.

[36.] **de Villiers Adriaan Jacobus** Evaluation and Improvement of the sPC-SAFT Equation of State for Complex Mixtures [Report] : PhD Thesis / Chemical Engineering ; Stellenbosch University. - Stellenbosch : [s.n.], 2011.

[37.] **Dobbins R.A., Mohammed K. and Sullivan D.A.** Pressure and Density Series Equations of State for Steam as Derived from the Haar–Gallagher–Kell Formulation [Journal] // Journal of Physical and Chemical Reference Data. - 1988. - 1 : Vol. 17. - pp. 1-8.

[38.] **Domanski Piotr and Didion David** Computer Modeling of the Vapor Compression Cycle With Constant Flow Area Expasion Device [Report]. - Washington, DC : U.S. National Bureau of Standards, 1983.

[39.] **Duvedi A. P. and Luke E.K. Achenie** Designing Environmentally Safe Refrigerants Using Mathematical Programming [Journal] // Chemical Engineering Science. - 1996. - 15 : Vol. 51. - pp. 3727-3739.

[40.] **Estupinan Edgar A. and Santos Ilmar F.** Modelling Hermetic Compressors Using Different Constraint Equations to Accommodate Multibody Dynamics and Hydrodynamic Lubrication [Journal] // J. of the Braz. Soc. of Mech. Sci. & Eng.. - [s.l.] : BCM, 2009. - 1 : Vol. XXXI. - pp. 35-46.

[41.] **Falk G.** Entropy, a Resurrection of Caloric: A Look at the History of Thermodynamics [Journal] // European Journal of Physics. - 1985. - 2 : Vol. 6. - pp. 108-115.

[42.] **Farman J.C., Gardiner B.G. and Shanklin J.D.** Large losses of total ozone in Antarctica reveal seasonal ClOx/NOx interaction [Journal] // Nature. - 1985. - Vol. 315. - pp. 207-210.

[43.] **Foster A.** An Improved Group Contribution Volume Translated Peng-Robinson Equation of State [Report] : MSc (Eng.) / Department of Chemical Engineering ; University of KwaZulu-Natal. - Durban : University of KwaZulu-Natal, 2011.

[44.] **Gani Rafiqul** CAMD: Computer Aided Molecular Design - Examples of Applications [Report]. - Lyngby : CAPEC, Department of Chemical Engineering, 2004.

[45.] **Gani Rafiqul** Chapter 14: Case Studies in Chemical Product Design - Use of CAMD Techniques [Book Section] // Chemical Product Design: Toward a Perspective Through Case Studies / book auth. Ng Ka M., Gani Rafiqul and Dam-Johansen Dam. - [s.l.] : Elsevier, 2007. - Computer-Aided Chemical Engineering, 23.

[46.] **Giunta C.J.** Atoms in Chemistry: From Dalton's Predecessors to Complex Atoms and Beyond [Book]. - Washington, DC : American Chemical Society, 2010. - 9780841225572.

[47.] **Gmehling J. [et al.]** Chemical Thermodynamics for Process Simulation [Book]. - Weinheim : Wiley-VCH, 2012. - 1st. - 978-3-527-31277-1.

[48.] **Goodwin A.R., Sengers J. and Peters C.J.** Applied Thermodynamics of Fluids [Book]. - Cambridge : Royal Society of Chemistry, 2010. - 1st : Vol. VIII. - 978-1-84755-806-0.

[49.] **Google** Google Scholar: Search Results for "New Equation of State" [Online]. - 19 October 2011. - http://scholar.google.co.za/scholar?hl=en&q=%22New+Equation+of+State%22&btnG=&as_sdt=1%2C5&as_sdtp=.

[50.] **Google** Google Scholar: Search Results for '"New Mixing Rule" OR "New Combining Rule"' [Online]. - 11 November 2011.

[51.] **Gross J.** An Equation-of-State Contribution for Polar Components: Quadrupolar Molecules [Journal] // AIChE Journal. - 2005. - 9 : Vol. 51. - pp. 2556-2568.

[52.] **Gross J. and Sadowski G.** Application of Perturbation Theory to a Hard-Chain Reference Fluid: An Equation of State for Square-Well Chains [Journal] // Fluid Phase Equilibria. - 2000. - 2 : Vol. 168. - pp. 183-199.

[53.] **Gross J. and Sadowski G.** Application of the Perturbed-Chain SAFT Equation of State to Associating Systems [Journal] // Industrial & Engineering chemistry Research. - 2002. - 22 : Vol. 41. - pp. 5510-5515.

[54.] **Gross J. and Sadowski G.** Perturbed-Chain SAFT: Development of a new Equation of State for Simple, Associating, Multipolar and Polymeric Compounds [Book Section] // Supercritical Fluids as Solvents and Reaction Media / ed. Brunner G.. - Amsterdam, The Netherlands : Elsevier Science, 2004.

[55.] **Gross J. and Sadowski G.** Perturbed-Chain SAFT: An Equation of State Based on a Perturbation Theory for Chain Molecules [Journal] // Industrial Engineering & Chemical Research. - 2001. - 4 : Vol. 40. - pp. 1244-1260.

[56.] **Gross J. and Vrabec J.** An Equation-of-State for Polar Components: Dipolar Molecules [Journal] // AIChE Journal. - 2006. - 3 : Vol. 52. - pp. 1194-1204.

[57.] **Henderson D.** Perturbation Theory for a Mixture of Hard Spheres and Square-Well Molecules [Journal] // Journal of Chemical Physics. - 1974. - 3 : Vol. 61. - pp. 926-931.

[58.] **Hinshelwood C.N. and Pauling L.** Amedeo Avogadro [Journal] // Science. - 1956. - 3225 : Vol. 124. - pp. 708-713.

[59.] **Hunt B.G.** The Need for a Modified Photochemical Theory of the Ozonosphere [Journal] // American Meteorological Society. - 1966. - Vol. 23. - pp. 88-95.

[60.] **Jones J.E.** On the Determination of Molecular Fields. II. From the Equation of State of a Gas [Journal] // Proceedings of the Royal Society of London, Series A.. - 1924. - 738 : Vol. 106. - pp. 463-477.

[61.] **Kamei A., Beyerlein S. W. and Jacobsen R. T.** Application of Nonlinear Regression in the Development of a Wide Range Formulation for HCFC-22 [Journal] // International Journal of Thermophysics. - 1995. - Vol. 16. - pp. 1155-1164.

[62.] **Karunanithi Arunprakash T. and Achenie Luke E.K.** Chapter 4: Solvent Design for Crystallization of Pharmaceutical Products [Book Section] // Chemical Product Design: Toward a Perspective Through Case Studies / book auth. Ng Ka M., Gani Rafiqul and Dam-Johansen Kim. - [s.l.] : Elsevier, 2007. - Computer-Aided Chemical Engienering, 23.

[63.] **Kim M. S., Mulroy W. J. and Didion D. A.** Performance Evaluation of Two Azeotropic Refrigerant Mixtures of HFC-134a With R-290 (Propane) and R-600a (Isobutane) [Journal] // ASME Journal of Energy Resources Technology. - 1994. - Vol. 116. - pp. 148-154.

[64.] **Kizilkan Onder, Kabul Ahmet and Yakut Ali Kemal** Exergetic Performance Assessment of a Variable-speed R404a Refrigeration System [Journal] // International Journal of Energy Research. - 2010. - 6 : Vol. 34. - pp. 463-475.

[65.] **Klein M.** The Historical Origins of the van der Waals Equation [Journal] // Physica. - 1974. - 1 : Vol. 73. - pp. 28-47.

[66.] **Kontogeorgis G.M. and Folas G.K.** Thermodynamic Models for Industrial Applications: From Classical and Advanced Mixing Rules to Association Theories [Book]. - Chichester : Wiley, 2010. - 1st. - 978-0-470-69726-9.

[67.] **Lampe M. [et al.]** Simultaneous Optmization of Working Fluid and Process for Organic Rankine Cycles Using PC-SAFT [Journal] // Ind. Eng. Chem. Res.. - 2014. - 21 : Vol. 53. - pp. 8821-8830.

[68.] **Lampe Matthias [et al.]** Computer-aided Molecular Design of ORC Working Fluids using PC-SAFT [Book Section] // Proceedings of the 8th International Conference on Foundations of

Computer-Aided Process Design / book auth. Eden Mario R., Siirola John D. and Towler Gavin P.. - [s.l.] : Elsevier, 2014. - Computer-Aided Chemical Engineering, 34.

[69.] **Lee D.-Y. [et al.]** Experimental Investigation on the Drop-in Performance of R407C as a Substitute for R22 in a Screw Chiller with Shell-and-Tube Heat Exchangers [Journal] // International Journal of Refrigeration. - 2002. - 5 : Vol. 25. - pp. 575-585.

[70.] **Lee Tzong-Shing** Second-Law Analysis to Improve the Energy Efficiency of Screw Liquid Chillers [Journal] // Entropy. - 2010. - 3 : Vol. 12. - pp. 375-389.

[71.] **Lek-utaiwan P. [et al.]** Integrated Design of Solvent-Based Extractive Separation Processes Including Experimental Validation [Book Section] // 19th European Symposium on Computer Aided Process Engineering / book auth. Jezowski Jacek and Thullie Jan. - [s.l.] : Elsevier, 2009. - Computer-Aided Chemical Engineering, 26.

[72.] **Lemmon E. W. and Jacobsen R. T.** A New Functional Form and New Fitting Techniques for Equations of State with Application to Pentafluoroethane (HFC-125) [Journal]. - [s.l.] : Journal of Physical and Chemical Reference Data, 2005. - 1 : Vol. 34. - pp. 69-108.

[73.] **Lemmon E. W. and Jacobsen R. T.** An International Standard Formulation for the Thermodynamic Properties of 1,1,1-Trifluoroethane (HFC-143a) for Temperatures From 161 to 450 K and Pressures to 50 MPa [Journal]. - [s.l.] : Journal of Physical and Chemical Reference Data, 2000. - 4 : Vol. 29. - pp. 521-552.

[74.] **Lemmon E. W. and McLinden M. O.** Thermodynamic Properties of Propane. III. A Reference Equation of State for Temperatures from the Melting Line to 650 K and Pressures up to 1000 MPa [Journal]. - [s.l.] : Journal of Chemical and Engineering Data, 2009. - 12 : Vol. 54. - pp. 3141-3180.

[75.] **Lemmon E.W., Huber M.L. and McLinden M.O.** Reference Fluid Thermodynamic and Transport Properties (REFPROP) [Software] = NIST Standard Reference Database 23, Version 9.0 / prod. (NIST) National Institute of Standards and Technology. - Bolder : United States of America, 2010.

[76.] **Lienhard John H.** How Invention Begins: Echoes of Old Voices in the Rise of New Machines [Book]. - [s.l.] : Oxford University Press, USA, 2008.

[77.] **London F.** The General Theory of Molecular Forces [Journal] // Trans. Faraday Soc.. - 1937. - Vol. 33. - pp. 8b-26.

[78.] **Lovelock J. E., Maggs R. J. and Wade R. J.** Halogenated Hydrocarbons in and Over the Atlantic [Journal] // Nature. - 1973. - Vol. 241. - pp. 194-196.

[79.] **Magie W. F.** Harper's Scientific Memoirs VI. The Second Law of Thermodynamics: Memoirs by Carnot, Clausius and Thomson [Book]. - New york : Harper & Brothers, 1899. - Vol. 6.

[80.] **Mansoori G.A. [et al.]** Equilibrium Thermodynamic Properties of the Mixture of Hard Spheres [Journal] // Journal of Chemical Physics. - 1971. - 4 : Vol. 54. - pp. 1523-1525.

[81.] **Marx V., Pruss A. and Wagner W.** Neue Zustandsgleichungen fuer R12, R22, R11 und R113: Beschreibung des thermodynamishchen Zustandsverhaltens bei Temperaturen bis 525 K und Druechken bis 200 MPa [Book]. - Dusseldorf : VDI Verlag, 1992. - Series 19 (Waermetechnik/Kaeltetechnik), No. 57.

[82.] **Mayer J.E. and Montroll E.** Molecular Distribution [Journal] // Journal of chemical Physics. - 1941. - 2 : Vol. 9. - pp. 2-16.

[83.] **McLinden M. O. and Didion D. A.** The Search for Alternative Refrigerants - A Molecular Approach [Conference] // International Refrigeration and Air Conditioning Conference. - 1988. - Paper 69.

[84.] **Midgley, Jr. Thomas** From the Periodic Table to Production [Journal]. - [s.l.] : Industrial and Engineering Chemistry, 1937. - 2 : Vol. 29. - pp. 241-244.

[85.] **Midgley, Jr. Thomas** Man-Made Molecules [Journal] // Industrial and engineering Chemistry. - 1938. - 1 : Vol. 30. - pp. 120-122.

[86.] **Mie G.** Zur kinetischen Theorie der einatomigen Körper [Journal] // Annalen der Physik. - 1903. - 8 : Vol. 316. - pp. 657-697.

[87.] **Mitrofanov Igor [et al.]** The Solvent Selection Framework: Solvents for Organic Synthesis, Separation Processes and Ionic Liquid Solvents [Book Section] // 22nd European Symposium on Computer Aided Process Engineering / book auth. Bogle Ian D.L. and Fairweather Michael. - [s.l.] : Elsevier, 2012. - Computer-Aided Chemical Engineering, 30.

[88.] **Molina M.J. and Rowland F.S.** Stratospheric Sink for Chlorofluoromethanes: Chlorine Atom Catalysed Destruction of Ozone [Journal] // Nature. - 1974. - Vol. 249. - pp. 810-812.

[89.] **Morrisette P.M.** The Evolution of Policy Responses to Stratospheric Ozone Depletion [Journal] // Nat. Resources J.. - 1989. - Vol. 29. - pp. 793-820.

[90.] **Müller I.** A History of Thermodynamics: The Doctrine of Energy and Entropy [Book]. - Berlin : Springer, 2007. - 1st. - 978-3642079641.

[91.] **Müller R.** A Brief History of Stratospheric Ozone Research [Journal] // Meteorologische Zeitschrift. - 2009. - 1 : Vol. 18. - pp. 3-24.

[92.] **Nannoolal Y.** Development of a Group Contribution Method for the Prediction of Non-Electrolyte Organic Compounds [Report] : MSc (Eng.) / Chemical Engineering ; University of KwaZulu-Natal. - Durban, ZA : University of KwaZulu-Natal, 2004.

[93.] **NASA** Ozone Hole Watch: Images, Data, and Information for the Southern Hemisphere [Online] // Ozone Hole Watch. - Goddard Space Flight Center, 2012. - 2013. - http://ozonewatch.gsfc.nasa.gov/.

[94.] **NASA** Researchers Cool Gas to Record Low [Online]. - 11 November 2003. - 22 Feburary 2009. - http://www.nasa.gov/vision/earth/technologies/biggest_chill.html.

[95.] **NASA** The Ozone Layer If CFCs Hadn't Been Banned [Online] // NASA Earth Observatory. - 21 May 2009. - 2011. - http://earthobservatory.nasa.gov/IOTD/view.php?id=38685.

[96.] **National Environmental Satellite, Data, and Information Service** Antarctic Ozone Hole Reaches Annual Maximum [Online]. - 13 October 2011. - 6 November 2011. - http://www.nnvl.noaa.gov/MediaDetail.php?MediaID=861&MediaTypeID=1.

[97.] **Nave C.R.** PvT Surface for a Substance which Contracts Upon Freezing [Online] // HyperPhysics. - 20 October 2011. - http://hyperphysics.phy-astr.gsu.edu/hbase/thermo/pvtsur.html. - Georgia State University.

[98.] **Nelder J. A. and Mead R.** A Simplex Method for Function Minimization [Journal]. - [s.l.] : The Computer Journal, 1965. - 4 : Vol. 7. - pp. 308-313.

[99.] **Nezbeda I.** On Molecular-Based Equations of State: Rigor Versus Speculations [Journal] // Fluid Phase Equilibria. - 2001. - 1 : Vol. 182. - pp. 3-15.

[100.] **O'Connell J.P. and Haile J.M.** Thermodynamics: Fundamentals for Applications [Book]. - Cambridge : Cambridge UP, 2005. - Cambridge Series in Chemical Engineering. - 978-0521588188.

[101.] **Orbey H. and Sandler S.I.** Modeling Vapor-Liquid Equilibria: Cubic Equations of State and Their Mixing Rules [Book]. - New York : Cambridge University Press, 1998. - 1st. - 9780521620277.

[102.] **Padmanabhan Venkataramana Murthy V and Palanisamy Senthil Kumar** Exergy Efficiency and Irreversibility Comparison of R22, R134a, R290 and R407C to Replace R22 in an Air Conditioning System [Journal] // Journal of Mechanical Science and Technology. - 2013. - 3 : Vol. 27. - pp. 917-926.

[103.] **Pannock Jürgen and Didion David** Performance of Chlorine-Free Binary Zeotropic Refrigerant Mixtures in a Heat Pump [Report]. - [s.l.] : U.S. Environmental Protection Agency, 1991.

[104.] **Pearson S.F.** Refrigerants - Past, Present and Future. Review Article [Journal] // Bull. IIR. - 2004. - 3 : Vol. 33. - pp. 5-26.

[105.] **Perkins Jacob** Improvements in the Apparatus and Means for Producing Ice and in Cooling Fluids [Patent]. - London, UK, 14 August 1835.

[106.] **Pitzer K.S. [et al.]** The Volumetric and Thermodynamic Properties of Fluids. II. Compressibility Factor, Vapor Pressure and Entropy of Vaporization [Journal] // Journal of the American Chemical Society. - 1955. - 13 : Vol. 77. - pp. 3433-3440.

[107.] **Pitzer K.S.** Thermodynamics [Book]. - New York : McGraw-Hill, 1995. - 3rd. - 978-0070502215.

[108.] **Poling B.E., Prausnitz J.M. and O'Connell J.P.** The Properties of Gases and Liquids [Book]. - New York : McGraw-Hill, 2001. - 5th. - 978-0070116825.

[109.] **Powell Richard L.** CFC Phase-out: Have We Met the Challenge? [Journal] // Journal of Fluorine Chemistry. - 2002. - Vol. 114. - pp. 237-250.

[110.] **Prausnitz J.M., Lictenthaler R.N. and Azevedo E.G.** Molecular Thermodynamics of Fluid-Phase Equilibria [Book]. - Englewoods Cliffs, NJ : Prentice Hall PTR, 1986. - 2nd. - 978-0135995648.

[111.] **Public Citizen** Regulation: The Unsung Hero in American Innovation [Online] // Public Citizen. - Public Citizen's Congress Watch, 13 September 2011. - 2013. - http://www.citizen.org/regulation-innovation.

[112.] **Radermacher Reinhard and Jung Dongsoo** Theoretical Analysis of Replacement Refrigerants for R22 for Residential Uses [Report]. - [s.l.] : US Environmental Protection Agency, 1991.

[113.] **Ramjugernath D.** High Pressure Phase Equilibrium Studies [Report] : PhD (Eng.) Thesis / Department of Chemical Engineering ; University of KwaZulu-Natal. - Durban : University of KwaZulu-Natal, 2000.

[114.] **Rao Y.V.C.** Engineering Thermodynamics Through Examples [Book]. - [s.l.] : Universities Press, 2003. - 978-8173714238.

[115.] **Rigola J. [et al.]** Numerical Study and Experimental Validation of a Complete Vapor Compression Refrigerating Cycle [Conference] // International Refrigeration Conference. - Purdue University : [s.n.], 1996.

[116.] **Rigola J. [et al.]** Numerical Study of a Single Stage Vapor Compression Refrigerant Unit Using Non-Contaminant Refrigerants [Conference] // International Refrigeration Conference. - Purdue University : [s.n.], 1996.

[117.] **Robinson Robert L. and Chao Kwang-chu** Equations of State: Theories and Applications [Book]. - Washington, D.C. : American Chemical Society, 1986. - 9780841209589.

[118.] **Rowland R.S. and Molina M.J.** Chlorofluoromethanes in the Environment [Journal] // Reviews of Geophysics. - 1975. - 1 : Vol. 13. - pp. 1-35.

[119.] **Rowlinson J.S.** The Work of Thomas Andrews and James Thomson on the Liquefaction of Gases [Journal] // Notes and Records of the Royal Society of London. - 2003. - 2 : Vol. 57. - pp. 143-159.

[120.] **Samson Perry** Evolution of the Atmosphere: Composition, Structure and Energy [Online] // Global change. - University of Michigan, 2011. - 01 06 2013. - http://www.globalchange.umich.edu/globalchange1/current/lectures/Perry_Samson_lectures/evolution_atm/.

[121.] **Satola Brian J.** The Development of a Hybrid Activity Coefficient Model Utilizing the Solution of Groups Concept [Report] : MSc (Eng.) / Department of Chemical Engineering ; University of KwaZulu-Natal. - Durban : University of KwaZulu-Natal, 2011.

[122.] **Satola Brian J.** The Language of Thermodynamics [Online] // Chemical Engineering Junkie (ChEJunkie) Website. - 24 March 2013. - 22 June 2013. - http://www.chejunkie.com/thermodynamics/the-language-of-thermodynamics/.

[123.] **Seider Warren D. [et al.]** Product and Process Design Principles: Synthesis, Analysis and Design [Book]. - [s.l.] : Wiley, 2008. - 3.

[124.] **Sengers J.V. [et al.]** Equations of State for Fluids and Fluid Mixtures Part 1 [Book] / ed. 1st. - Amsterdam : Elsevier, 2000. - 978-0-444-50384-8.

[125.] **Smith B.** Ethics of Du Pont's CFC Strategy 1975-1995 [Journal] // Journal of Buisness Ethics. - 1998. - 5 : Vol. 17. - pp. 557-568.

[126.] **Smith J. M., van Ness H. C. and Abbott M. M.** Introduction to Chemical Engineering Thermodynamics [Book]. - [s.l.] : McGraw-Hill, 2001. - 6th Edition.

[127.] **Smith William R. [et al.]** Refrigeration Cycle Design for Refrigerant Mixtures by Molecular Simulation [Journal]. - [s.l.] : Collect. Czech. Chem. Commun., 2010. - 4 : Vol. 75. - pp. 383-391.

[128.] **Soave G.** Equilibrium Constants from a Modified Redlich-Kwong Equation of State [Journal]. - [s.l.] : Chemical Engineering Science, 1972. - 6 : Vol. 27. - pp. 1197-1203.

[129.] **Solomon S. [et al.]** Contribution of Working Group I to the Fourth Assessment Report of the Intergovernmental Panel on Climate Change, 2007 [Online] // Intergovernmental Panel on Climate Change. - IPCC, 2007. - 14 08 2013. - http://www.ipcc.ch/publications_and_data/ar4/wg1/en/faq-1-3.html.

[130.] **Span R. and Wagner W.** Equations of State for Technical Applications. II. Results for Nonpolar Fluids [Journal] // International Journal of Thermophysics. - [s.l.] : Springer, 2003. - 1 : Vol. 24. - pp. 41-109.

[131.] **Span R.** Multiparameter Equations of State: An Accurate Source of Thermodynamic Property Data [Book]. - Berlin : Springer-Verlag, 2000.

[132.] **Srinivasan J.** Sadi Carnot and the Second Law of Thermodynamics [Journal] // Resonance. - 2001. - 11 : Vol. 6. - pp. 42-48.

[133.] **Stephenson G.** Integrate Compressor Performance Maps into Process Simulation [Journal] // AIChE. - 2011. - 6 : Vol. 107. - pp. 42-47.

[134.] **Su Gouq-Jen** Modified Law of Corresponding States for Real Gases [Journal]. - [s.l.] : Ind. Eng. Chem., 1946. - 8 : Vol. 38. - pp. 803-806.

[135.] **Sundaresan S. G.** Near Azeotrope Refrigerants to Replace R-502 in Commercial Refrigeration. [Conference] // International Refrigerantion and Air Conditioning. - 1992.

[136.] **Tan S.P., Hertanto A. and Radosz M.** Recent Advances and Applications of Statistical Associating Fluid Theory [Journal] // Industrial & Engineering Chemistry Research. - 2008. - 21 : Vol. 47. - pp. 8063-8082.

[137.] **Tian J. and Gui Y.** Equations of State for Fluids: Empirical Temperature Dependence of the Second Virial Coefficients [Journal] // J. Phys. Chem. B.. - 2007. - 37 : Vol. 111. - pp. 10970-10974.

[138.] **Tillner-Roth R. and Baehr H. D.** An International Standard Formulation for the Thermodynamic Properties of 1,1,1,2-Tetrafluoroethane (HFC-134a) for Temperatures From 170 K to 455 K and Pressures up to 70 MPa [Journal]. - [s.l.] : Journal of Physical and Chemical Reference Data, 1994. - 5 : Vol. 23. - pp. 657-729.

[139.] **Tillner-Roth R. and Yokozeki A.** An International Standard Equation of State for Difluoromethane (R-32) for Temperatures from the Triple Point at 136.34 K to 435 K and Pressures up to 70 MPa [Journal]. - [s.l.] : Journal of Physical and Chemical Reference Data, 1997. - 6 : Vol. 26. - pp. 1273-1328.

[140.] **UC Berkeley** Ozone Depletion: Uncovering the Hidden Hazard of Hairspray [Online]. - 2007. - 12 06 2013.

[141.] **UK National Physical Laboratory** What are Thermophysical Properties? (FAQ - Thermal) [Online] // UK National Physical Laboratory. - 18 January 2012. - 30 March 2014. - http://www.npl.co.uk/reference/faqs/what-are-thermophysical-properties-(faq-thermal).

[142.] **Ulshöfer V. S. and Andreae M. O.** Carbonyl Sulfide (COS) in the Surface Ocean and the Atmospheric COS Budget [Journal]. - [s.l.] : Aquatic Geochemistry, 1997. - 4 : Vol. 3. - pp. 283-303.

[143.] **UNEP (United Nations Environment Programme)** Summary of Control Measures Under the Montreal Protocol [Online]. - 2012. - 12 June 2013. - http://ozone.unep.org/new_site/en/Treaties/treaties_decisions-hb.php?sec_id=6,7,8,9,10,11,12,13,14,15,16,17,18,19,20,21,22,23,24.

[144.] **United States Environmental Protection Agency** Phaseout of Class I Ozone-Depleting Substances [Online]. - 19 August 2010. - 4 November 2011. - http://www.epa.gov/ozone/title6/phaseout/classone.html.

[145.] **United States Environmental Protection Agency** Phaseout of HCFCs (Class II Ozone-Depleting Substances) [Online]. - 19 August 2010. - 4 November 2011. - http://www.epa.gov/ozone/title6/phaseout/classtwo.html.

[146.] **Valderrama J.O.** Reviews: The State of the Cubic Equaitons of State [Journal] // Ind. Eng. Chem. Res.. - 2003. - 8 : Vol. 42. - pp. 1603-1618.

[147.] **van Ness H.C. and Abbott M.M.** Classical Thermodynamics of Nonelectrolyte Solutions: With Applications to Phase Equilibria [Book]. - New york : McGraw-Hill, 1981. - 2nd. - 978-0070670952.

[148.] **Vrabec J. and Gross J.** Vapor-Liquid Equilibria Simulation and an Equation of State Contribution for Dipole-Quadrupole Interactions [Journal] // Journal of Physical Chemistry B. - 2008. - 1 : Vol. 112. - pp. 51-60.

[149.] **Walas S.M.** Phase Equilibria in Chemical Engineering [Book]. - [s.l.] : Butterworth-Heinemann, 1985. - 978-0750693134.

[150.] **Wei Y.S. and Sadus R.J.** Equations of State for the Calculation of Fluid-Phase Equilibria [Journal] // AIChE Journal. - 2000. - 1 : Vol. 46. - pp. 169-196.

[151.] **Welch Charles** CFCs [Online] // The Ozone Hole. - Solcomhouse, July 2011. - August 2013. - http://www.theozonehole.com/cfc.htm.

[152.] **Wennemar Jürgen** Dry Screw Compressor Performance and Application Range [Conference] // 38th Turbomachinery Symposium. - Houston : Texas A&M University, 2009. - Vol. 38.

[153.] **Wertheim M.S.** Fluids with Highly Directional Attractive Forces. I. Statistical Thermodynamics [Journal] // Journal of Statistical Physics. - 1984. - 1-2 : Vol. 35. - pp. 19-34.

[154.] **Wertheim M.S.** Fluids with Highly Directional Attractive Forces. II. Thermodynamic Perturbation Theory and Integral Equations [Journal] // Journal of Statistical Physics. - 1984. - 1-2 : Vol. 35. - pp. 35-47.

[155.] **Wertheim M.S.** Fluids with Highly Directional Attractive Forces. III. Multiple Attraction Sites [Journal] // Journal of Statistical Physics. - 1986. - 3-4 : Vol. 42. - pp. 459-476.

[156.] **Wertheim M.S.** Fluids with Highly Directional Attractive Forces. IV. Equilibrium Polymerization [Journal] // Journal of Statistical Physics. - 1986. - 3-4 : Vol. 42. - pp. 477-492.

[157.] **Wikipedia** [Online] // Wikipedia. - November 2011. - http://wiipedia.org/.

[158.] **Xiang H.W.** The Corresponding-States Principle and its Practice: Thermodynamic, Transport and Surface Properties of Fluids [Book]. - Amsterdam : Elsevier Science, 2005. - 978-0-444-52062-3.

Appendix A[29]

The Language of Thermodynamics

The historical development of thermodynamics has been paved by many people throughout history. Mostly through the process of trial and error, i.e. the scientific method, we have come to accept certain observations as being *universal* (or always true). Eventually these observations were later tied/linked together using mathematics, which has resulted in a framework of theorems, equations and abstract symbols that can be playfully dubbed "the language of thermodynamics".

An important step is to be able to use this common language to interpret, relate and predict the behaviour of the world around us whilst obeying these universal-*truths*. In practice these truths are incorporated, amongst many other applications, into external models that can accurately represent the real behaviour of mixtures. Given the importance of this language, a brief fundamental review is provided below.

A.1. Historical Context

Much of the foundations can be traced back to the necessity of coal mining, which began to supplant wood as the primary source of "heat" during the late 1800's. After readily accessible coal deposits near the surface became depleted, surface quarries were eventually developed into underground mines that began to flood as veins were pursued ever deeper i.e. below water tables. This saw the re-invention of the steam engine into a practical (modern day) device capable of pumping water out of the mines (Müller, 2007; Falk, 1985).

Although the harnessing of boiling water to produce mechanical motion goes back some 2000, the first generation of these engines were highly inefficient (< 5%). This was not really a deterrent since they themselves were used to mine the very fuel that they consumed, but as these machines were applied to other industries serious attention was placed on improving their design (Müller, 2007; Srinivasan, 2001). Steam engines were very much viewed as a necessity of the *Civilized-World*. The following quite by Carnot says it best (Magie, 1899):

> *"Everyone knows that heat can produce motion. That it possesses vast motive power no one can doubt, in these days when the steam engine is everywhere well known... The study of these engines is of great interest, their importance enormous, their use is continually increasing, and they seem destined to produce a great revolution in the civilized world."*

[29] The material of this appendix is a revised and updated version of material that was originally published in the author's MSc (Eng.) report titled, *The Development of a Hybrid Activity Coefficient Model Utilizing the Solution of Groups Concept* (Satola, 2011). Additional updates, extensions and musings can also be found on the author's personal website (Satola, 2013).

A.2. The Fundamental Foundation

Thinking for efficiencies drove people to study the interrelations of heat (Q), work (W) and the *abstract* concept called energy (E). Eventually patterns were identified regarding these variables, and the interrelationships were incorporated into the fundamental theories forming the foundations of thermodynamics as it is known today.

A.2.1. First Law of Thermodynamics

As touched upon earlier, our collective knowledge has resulted in the acknowledgement of certain truths that we now consider universal. One such universal-truth is the *conservation of energy* principle, which consists of a series of observations:

- Energy can be stored
- Energy can be moved between matter
- Energy can be transformed (but not destroyed)

These simple statements constitute what is known as the *First Law of Thermodynamics*, and can be mathematically written as

$$\mathrm{E}_{\mathrm{stored}} = \mathrm{E}_{\mathrm{in}} - \mathrm{E}_{\mathrm{out}} \tag{A-1}$$

The concept of "stored" energy $(\mathrm{E}_{\mathrm{stored}})$ naturally lends itself to the characteristic expression *internal energy* (U). In order to calculate this new quantity, however, some knowledge of the forms of energy that may enter and/or leave the system is then required (where *system* refers to some part of the physical world, separated by a conceptual boundary).

Here I take some liberties on the historical development, and simply state that heat and work have been identified as forms of energy. [30] Where *heat* can be considered transient-energy resulting from temperature differences and *work* can be considered a characteristic-form of energy (typically associated with expenditure). These two energy terms may be used to rewrite the 1st Law in its *traditional form*, a closed system which neglects mass transfer across the system boundaries:

$$\underbrace{d(nu) = dU = \delta Q + \delta W}_{Traditional\ form} \tag{A-2}$$

However this equation cannot be regarded as giving an explicit definition of internal energy, in fact no such definition is known to exist. The postulated existence of internal energy as a property of the system's state (a *state-property*) has proven time and time again to be *consistent* with the 1st Law of Thermodynamics; therefore experience proves its existence:

> One such historical test was the application of the 1st Law to nuclear reactions. For a while it was thought that the 1st Law had a "mass defect" (Müller, 2007), but Einstein was able to establish a relationship between mass and energy $(E = mc^2)$ which further bolstered the 1st

[30] For the interested reader Ingo Müller has written a good book (Müller, 2007) on the historical development of thermodynamics; although some have criticised his depiction, it nonetheless acts as a good springboard for further indulgence.

Law as a universal-truth. This minor digression makes an important point: an essential part of utilizing the thermodynamic framework, in a consistent manner, lies in the ability to *strictly define* the system being considered.

In accordance, considering a closed system going through a quasi-static change of state (series of very small equilibrium steps where all energy is recovered—considered completely *reversible*), where only expansion or compression of the system and heat transfer can take place, enables the following definitions to be made:

$$\begin{aligned} \delta W_{rev} &= -Pd(nv) \\ &= -PdV \end{aligned} \tag{A-3}$$

$$\begin{aligned} \delta Q_{rev} &= Td(ns) \\ &= TdS \end{aligned} \tag{A-4}$$

The total system volume ($V = n \cdot v$) and total system entropy ($S = n \cdot s$) are considered *extensive* state-properties of the system (i.e. dependent on the mass and state of the system, just like internal energy), and can be used to facilitate the calculation of the change in internal energy by different processes using appropriate substitutions:

$$dU = TdS - PdV \tag{A-5}$$

Since the internal energy is now in a form that *only* depends on the state of the system (i.e. not on the process or path that produces the state) the relationship is also suitable to describe irreversible systems (i.e. physical reality).

A.2.2. Second Law of Thermodynamics

As with the conservation of energy, further historical observations have led to an additional universal-truth; specifically, that energy cannot be transformed or moved without wasting some in the process. This is in reference to the extensive state-property called entropy, a convenience-variable that was introduced by Clausius to represent the quantity $\delta Q/T$; conceptually entropy represents the *wasted effort* (or *lost* energy) involved whenever energy is moved and/or transformed. This is summed up nicely by the following citation (Müller, 2007):

> *Clausius summarized his work in the triumphant slogan*
>
> > *Die Energie der Welt ist konstant.*
> >
> > *Die Entropie der Welt strebt einem Maximum zu.*
>
> *Die Welt (the universe) was chosen in this statement as being the ultimate thermodynamic system, which presumably is not subject to heating and working, so that $dU = 0$ holds, as well as $dS > 0$.*

This is known as the *Second Law of Thermodynamics*, and is commonly written symbolically using the definition of entropy as

$$dS \geq \frac{\delta Q}{T} \geq 0 \tag{A-6}$$

where the equal sign signifies the limiting value of zero (reversibility). This expression is often combined with the 1st law to obtain the *practical form,*

$$\underbrace{dU \leq TdS - PdV}_{Practical\ form} \tag{A-7}$$

The 2nd Law can conveniently be considered as a *constraining relationship* of the 1st Law, which places restrictions on what can and cannot be accomplished in physical reality—nature *naturally* tends towards increasing disorder (entropy).

A.2.3. Third Law of Thermodynamics

The third and last historical observation, like the others, has also proven true 100 of the time; simply stated, that it is impossible to remove all of the heat from an object. This constitutes as the *Third Law of Thermodynamics*, and naturally lends itself to the definition of the lowest point on the *thermodynamic temperature scale* (absolute zero, 0 Kelvin).

The statement implies that it is impossible to reach absolute zero, where all of the *heat* (energy) of a system would be removed (creating a perfect crystal). If thought of in terms of the 2nd Law, it is impossible to have a system with zero entropy; in physical reality this minimum is unrealistic and has never been realized—a universal-truth.[31]

A.2.4. Expanding Results to Open Systems

In the previous subchapters the *traditional* and *practical forms* of the 1st Law were derived on the basis of a *closed system* (no mass transfer across system boundaries); however a form that is *open* to the environment (everything outside the system's conceptual boundary) is required for many practical situations (multiple phases, where each phase is considered a system). For a closed system internal energy was found to be a function of the extensive properties entropy and volume, and can therefore be represented by the total derivative of the continuous-function. The total internal energy of the system, therefore, can be written as the following:

$$nu\ (\text{or}\ U) = f(ns, nv) = f(S, V) \tag{A-8}$$

$$\underbrace{dU = \underbrace{\left[\frac{\partial U}{\partial S}\right]_V}_{T} dS + \underbrace{\left[\frac{\partial U}{\partial V}\right]_S}_{-P} dV}_{Traditional\ form} \tag{A-9}$$

[31] The current world record for the lowest temperature observed stands at 50 pK (NASA, 2003). This is further astounding if you consider that the cosmic (or background) radiation that fills the observable part of the universe is equivalent to ~3 K from a blackbody (Müller, 2007).

Comparing the total derivative with the traditional form of the 1st Law allows the *intensive* state-properties (independent of system mass—temperature and pressure) to be readily identified with their partial derivative equivalents. From this mathematical perspective (entirely consistent with observations), the internal energy may also be extended to open systems via the *conservation of mass* principle:

$$Conservation\ of\ Mass \Longrightarrow n = n_1 + n_2 + \cdots + n_{Comp} \tag{A-10}$$

$$U = f\left(S, V, n_1, n_2, \cdots, n_{Comp}\right) \tag{A-11}$$

$$\underbrace{dU \leq \underbrace{\left[\frac{\partial U}{\partial S}\right]_{V,n}}_{T} dS + \underbrace{\left[\frac{\partial U}{\partial V}\right]_{S,n}}_{-P} dV + \sum_{i=1}^{Comp} \underbrace{\left[\frac{\partial U}{\partial n_i}\right]_{V,S,n_{j\neq i}}}_{\mu_i} dn_i}_{Functional\ form} \tag{A-12}$$

where the *chemical potential* is defined for convenience as the following:

$$\mu_i = \left[\frac{\partial U}{\partial n_i}\right]_{V,S,n_{j\neq i}} \tag{A-13}$$

Like the temperature and pressure of the system, the chemical potential is independent of the quantity contained within the system (an *intensive* state property).

A.3. Auxiliary Energy Functions

Since no entropy meter is known to exist, researchers have been guided to represent the fundamental law by alternative functions that are more readily determined by practitioners (auxiliary properties). Given the functional dependence of internal energy on the intensive $[T, P, \mu_i]$ and extensive $[nv, ns, n]$ state quantities of a system, new properties may be defined by considering various linear changes of these interrelated-variables on internal energy. Legendre transformations facilitate this process (Alberty, 1994; Alberty, 2001), and can be used to obtain the equivalent potentials of Enthalpy (H), Helmholtz energy (A), and Gibbs energy (G).

A.3.1. Enthalpy (Energy)

$$nh\ (\text{or } H) \equiv (nu) + P(nv) \equiv U + PV \tag{A-14}$$

$$dH = dU + PdV + VdP \tag{A-15}$$

$$H = f\left(S, P, n_1, n_2, \cdots, n_{Comp}\right) \tag{A-16}$$

$$\overbrace{dH \leq \underbrace{\left[\frac{\partial H}{\partial S}\right]_{P,n}}_{T} dS + \underbrace{\left[\frac{\partial H}{\partial P}\right]_{S,n}}_{V} dP + \sum_{i=1}^{Comp} \underbrace{\left[\frac{\partial H}{\partial n_i}\right]_{S,P,n_{j\neq i}}}_{\mu_i} dn_i}^{Functional\ form} \tag{A-17}$$

A.3.2. Helmholtz Energy

$$na\ (\text{or } A) \equiv (nu) - T = U - TS \tag{A-18}$$

$$dA = dU - TdS - SdT \tag{A-19}$$

$$A = f\left(T, V, n_1, n_2, \cdots, n_{Comp}\right) \tag{A-20}$$

$$\overbrace{dA \leq \underbrace{\left[\frac{\partial A}{\partial T}\right]_{V,n}}_{-S} dT + \underbrace{\left[\frac{\partial A}{\partial V}\right]_{T,n}}_{-P} dV + \sum_{i=1}^{Comp} \underbrace{\left[\frac{\partial A}{\partial n_i}\right]_{T,V,n_{j\neq i}}}_{\mu_i} dn_i}^{Functional\ form} \tag{A-21}$$

A.3.3. Gibbs Energy

$$ng\ (or\ G) \equiv \overbrace{\overbrace{(nu) + P(nv) - T(ns)}^{\substack{(nh)-T(ns)\\ P(nv)+(na)}}}^{\substack{H-TS\\ PV+A}} \equiv \overbrace{U + PV - TS} \tag{A-22}$$

$$dG = \overbrace{dU + PdV + VdP - TdS - SdT}^{\substack{=dH-TdS-SdT \\ =PdV+VdP+dA}} \tag{A-23}$$

$$G = f\left(T, P, n_1, n_2, \cdots, n_{Comp}\right) \tag{A-24}$$

$$\overbrace{dG \leq \underbrace{\left[\frac{\partial G}{\partial T}\right]_{P,n}}_{-S} dT + \underbrace{\left[\frac{\partial G}{\partial P}\right]_{T,n}}_{V} dP + \sum_{i=1}^{Comp} \underbrace{\left[\frac{\partial G}{\partial n_i}\right]_{T,P,n_{j\neq i}}}_{\mu_i} dn_i}^{Functional\ form} \tag{A-25}$$

A.4. Applied Framework

Given the basis upon which the fundamental equations were founded, we have come to believe that fluid properties of homogenous fluids at equilibrium are functions of temperature, pressure, and composition only (van Ness, et al., 1981). These observations were formalized by Willard Gibbs; for his numerous contributions to the field, it was in his honour that the most readily applied auxiliary function was named. Building atop the fundamental foundations, Gibbs proved that uniformity of temperature, pressure, and composition between the various phases is a necessary criterion to establish an "equilibrium state:"

$$\begin{gathered} dT = 0\ \mathrm{K} \\ dP = 0\ \mathrm{kPa} \\ \sum_{i=1}^{Comp} \mu_i dn_i = 0 \end{gathered} \tag{A-26}$$

Furthermore in order for this condition to be valid over multiple phases, an additional and necessary criterion must be established. Given the framework that has already been constructed, the following must also be true for all components:

$$\sum_{p=1}^{Phase} \mu_i^p dn_i^p = 0 \tag{A-27}$$

In context of the conservation of mass principle, this explicitly requires that the chemical potentials of each component across all phases *must be equal*.

A.4.1. Fugacity as a Solution Property

Given that temperature and pressure are easily measured, a way to determine the chemical potentials is needed before the framework can be put to practical use. As is often the case with abstract concepts, it is often easiest to generalize from simplified ideal behaviour.

Lewis was the first to consider the chemical potential for a pure ideal gas, and then generalized the results to all systems (Prausnitz, et al., 1986). Using the Gibbs energy function as a starting point,

and applying the relationship to one mole of a single-phase pure fluid at isothermal conditions, he obtained

$$dG_i = V_i dP \tag{A-28}$$

Since an ideal gas represents the simplest *known* condition/relationship, the component volume was replaced with the ideal gas equation:

$$dG_i = \frac{RT}{P} dP = RTd(ln\, P) \tag{A-29}$$

The resulting expression quantifies the relationship between the Gibbs energy and pressure for an ideal gas at constant temperature. To generalize his result Lewis introduced a new function *fugacity* to stand for the *true* (observable) system pressure, compensated for by molecular interactions. This is written as,

$$dG_i = RT \overbrace{d(ln\, f)}^{\substack{Ideal\ gas \\ correction}} \tag{A-30}$$

where the equation is then integrated from a *known* standard state (designated by a superscript 0) to obtain the following relationship:

$$G - G^0 = RTln\frac{f}{f^0} \tag{A-31}$$

In order for the fugacity definition to be universally valid, however, the relationship must reduce to the ideal gas value at the pressure limit (the basis of the derivation). Thus, the following criterion is a *necessary* component of the fugacity definition:

$$\lim_{P \to 0} \left(\frac{f}{P}\right) = 1 \tag{A-32}$$

A.4.2. An Additional Criterion for Phase Equilibrium

As mentioned earlier, the equality of the chemical potential of a component in all phases is a criterion for phase equilibrium. Given the abstract nature of chemical potential a new property was defined for convenience – fugacity. Using the fundamental framework, the fugacity will be shown to be a suitable alternative to chemical potential in describing the state of equilibrium. For each component (i) in solution, the fugacity (conveniently thought of as a *utility-function*) can be rewritten as

$$d\mu_i \equiv d\bar{G}_i = RTd\ln \hat{f}_i \tag{A-33}$$

$$\therefore \mu_i = \bar{G}_i = G_i^0 + RT\ln\frac{\hat{f}_i}{f_i^0} \tag{A-34}$$

$$\lim_{P\to 0}\left(\frac{\hat{f}_i}{x_i P}\right) = 1 \tag{A-35}$$

where the circumflex (^) distinguishes the component-fugacity from the solution property (f). For each component in each phase (p); integration at constant temperature yields

$$\mu_i^p(Final) = \mu_i^p(Initial) + RTd\ln\frac{\hat{f}_i^p(Final)}{\hat{f}_i^p(Initial)} \tag{A-36}$$

Since the integrand is typically evaluated from a known standard state, the *same* initial state can be selected for each component in each phase of the system (it is completely arbitrary). Given the equality of chemical potentials at equilibrium, it can be easily shown that the fugacities in each phase must also have the same value. For a hypothetical system consisting of phases α through π it can be easily shown that

$$\hat{f}_i^{\alpha}(Final) = \hat{f}_i^{\beta}(Final) = \cdots = \hat{f}_i^{\pi}(Final) \tag{A-37}$$

This constitutes a major justification for the introduction of the fugacity as a thermodynamic variable (van Ness, et al., 1981).

A.4.2.1. Ideal Mixture

Given the usefulness of fugacity in representing the chemical potential, we can properly define an *ideal mixture* by integrating the utility-function from the *pure* state to the actual state of the *mixture*:

$$\mu_i - \mu_i^0 = RT\ln\frac{\hat{f}_i^{is}}{f_i} = RT\ln\frac{x_i f_i}{f_i} = RT\ln x_i \tag{A-38}$$

Keeping in mind that the chemical potential is an intensive property that, like the Gibbs energy, depends on temperature, pressure, and composition, an *ideal mixture* can be formally defined as

$$\therefore \mu_i(P,T,x) \equiv \mu_i^0(P,T) + RT\ln x_i \tag{A-39}$$

This definition will prove to be useful in developing the following chapter.

A.4.3. Excess Properties & Activity Coefficients

Since many of the fundamental properties we wish to use are in the form of derivatives, it is often helpful to adopt a standard datum from which to calculate the change. For this purpose it is common practice to relate properties to their *excess* values – property deviations from their ideal-solution values (i.e. from a known condition to an actual condition). This concept can be generalized as

$$M^E = M - M^{is} \tag{A-40}$$

where M represents any *real/actual* property value, M^{is} the ideal solution value, and M^E the excess quantity of that property value; since this definition is only shifting the original value, all of the preceding energy relationships (including partial derivatives) can be directly written in terms of these excess values. By applying this definition the chemical potential may be written as,

$$\mu_i^E = \mu - \mu^{is} = \underbrace{[\mu - \mu_i]}_{RT\ln\frac{f}{f_i}} - RT\ln x_i \tag{A-41}$$

Given that this relationship has proven quite useful in practice, it is common to introduce a convenience variable known as the *activity coefficient:*

$$\gamma_i \equiv \frac{\hat{f}_i}{x f_i} \tag{A-42}$$

$$\therefore \mu^E = RT\ln\gamma_i \equiv \left[\frac{\partial(G^E/RT)}{\partial n_i}\right]_{T,P,n_{j\neq i}} \tag{A-43}$$

This means that for a real mixture, the chemical potential can be represented by an augmented ideal mixture value:

$$\mu_i(P,T,x) = \mu_i^0(P,T) + RT\ln x_i + \mu^E \tag{A-44}$$

$$\mu_i(P,T,x) = \mu_i^0(P,T) + RT\ln x_i + \underbrace{RT\ln\gamma_i\,(T,P,x)}_{\substack{Excess\ contribution \\ to\ the\ ideal\ solution \\ value}} \tag{A-45}$$

A.4.4. Partial Molar Properties

Given the functional dependence of ng (or G) that has been established, the mathematical definition of exactness can be used to obtain

$$dG = n\left[\frac{\partial g}{\partial T}\right]_{P,n} dT + n\left[\frac{\partial g}{\partial P}\right]_{T,n} dP + \sum_{i=1}^{Comp}\left[\frac{\partial G}{\partial n_i}\right]_{T,P,n_{j\neq i}} dn_i \tag{A-46}$$

Here the chemical potential can formally be defined as (for convenience),

$$\mu_i \equiv \left[\frac{\partial G}{\partial n_i}\right]_{T,P,n_{j\neq i}} \equiv \left[\frac{\partial A}{\partial n_i}\right]_{T,nV,n_{j\neq i}} \equiv \left[\frac{\partial H}{\partial n_i}\right]_{nS,P,n_{j\neq i}} \equiv \left[\frac{\partial U}{\partial n_i}\right]_{nV,nS,n_{j\neq i}} \tag{A-47}$$

Some insight into the nature of the chemical potential can be gained by application of Euler's theorem on homogeneous functions, in this case, of degree zero:

$$G = \sum_{i=1}^{Comp} x_i\mu_i \tag{A-48}$$

This explicitly states that the chemical potential must be a function of temperature, pressure, and composition (as is the Gibbs energy); furthermore, the chemical potentials must also be intensive properties of the system.

It should now be apparent that this quantity is important, but its current form is not entirely useful; as stated elsewhere (Prausnitz, et al., 1986), much of the present work in phase-equilibrium thermodynamics is to relate the *abstract* nature of the chemical potential to physically measurable quantities such as temperature, pressure, and composition. This need becomes especially apparent after integrating the differential forms of H, A, and G (see section A.3):

$$H = TS + \sum_{i=1}^{Comp} n_i \mu_i \tag{A-49}$$

$$A = -PV + \sum_{i=1}^{Comp} n_i \mu_i \tag{A-50}$$

$$G = \sum_{i=1}^{Comp} n_i \mu_i \tag{A-51}$$

So the Gibbs energy is the only auxiliary property that can be *entirely* related through the component contributions within the system—useful indeed.

A.4.4.1. Gibbs-Duhem Relation

In the previous subchapter, the astute observer would have noticed *two* different relationships describing the Gibbs energy, one describing a *change* (Equation (2-28)) and the other an *equilibrium-state* (Equation (2-30)). Moreover each of these relationships was obtained by different mathematical operations, but are they both thermodynamically consistent within the framework that has been built?

In order for both expressions to be correct, they must prove equivalent. If we consider a homogeneous equilibrium state, then any differential change resulting from changes in T, P, n_i must be given by the total differential of G (energy and matter is *conserved*):

$$dG = d\left(\sum_{i=1}^{Comp} x_i \mu_i\right) = \sum_{i=1}^{Comp} x_i d\mu_i + \sum_{i=1}^{Comp} \mu_i dx_i \tag{A-52}$$

For consistency, this expression *must be* e*quivalent* to the exact differential describing the interrelationships of G, T, P, and composition:

$$dG = \left[\frac{\partial G}{\partial T}\right]_{P,x} dT + \left[\frac{\partial G}{\partial P}\right]_{T,x} dP + \sum_{i=1}^{Comp} \underbrace{\left[\frac{\partial G}{\partial n_i}\right]_{T,P,n_{j\neq i}}}_{\mu_i} dx_i \tag{A-53}$$

Accordingly, the following identity is required in order to avoid any contradictions to the thermodynamic framework (built upon observations that have proven universal-truths)—resulting from equating Equation (2-34) and Equation (2-35):

$$\left[\frac{\partial G}{\partial T}\right]_{P,x} dT + \left[\frac{\partial G}{\partial P}\right]_{T,x} dP - \sum_{i=1}^{Comp} x_i d\mu_i = 0 \qquad \text{(A-54)}$$

This identity is commonly known as the *Gibbs-Duhem equation* (also called the zero-function), and represents a condition that must be obeyed (if you will, a grammatical-law of the language of thermodynamics). Therefore, if a system at constant temperature and pressure is considered, we once again obtain a relationship explicitly stating the concentration dependence of the chemical potential (clearly important). Moreover, it places a restriction on the simultaneous behaviour of T, P, and μ_i for a single phase ($\text{number of components} + 1$ *degree of freedom*).

A.4.5. Mathematical Relations of Thermodynamic Properties

The laws of thermodynamics form the foundation for the development of a vast network of interrelated equations (and properties). The process is purely mathematical, and takes advantage of the fact that the fundamental functions for energy (U, H, A and G) are continuous, as they are themselves functions of state variables (i.e. temperature, pressure and composition only). This fact was used previously, for instance, to develop alternative (but equivalent) energy functions in place of U (and the thermodynamic properties of V and S)—see Appendix A.3. starting on Page 145. This network of equations, therefore, are internally consistent with each other, and can be used to derive still more thermodynamic properties that also must be consistent within this same framework. Only a few of these can be directly measured, however, like P, V or ρ and T along with m and V (i.e. composition), while other thermodynamic properties can only be calculated using derived relationships based on one of the fundamental energy functions.

Equations of state explicate in Helmholtz, like the PC-SAFT equation that is used in this project, can then be used to calculate all thermodynamic properties. A complete listing of the relationships needed to calculate most (if not all) of the required thermodynamic properties from Helmholtz can be found (in detail) in the work of Span (Span, 2000). A full listing of the relationships are not needed for the present discussion, however, and **Figure A- 1** below is used instead, which schematically depicts the functional relationship between a select number of properties and the reduced residual Helmholtz energy state function F. Thermodynamic properties like the isobaric and isochoric heat capacities are contained within rectangular blocks, while arrows (originating from the blocks of properties) indicate their relationship to the partial derivative(s) of F. The calculation of the heat of vaporisation, for example, requires both F and it's temperature-derivative. Other properties can be similarly read. It is also important to note that similar (and equivalent) diagrams for these same properties can be made in terms of the other fundamental functions of energy U, H and G.

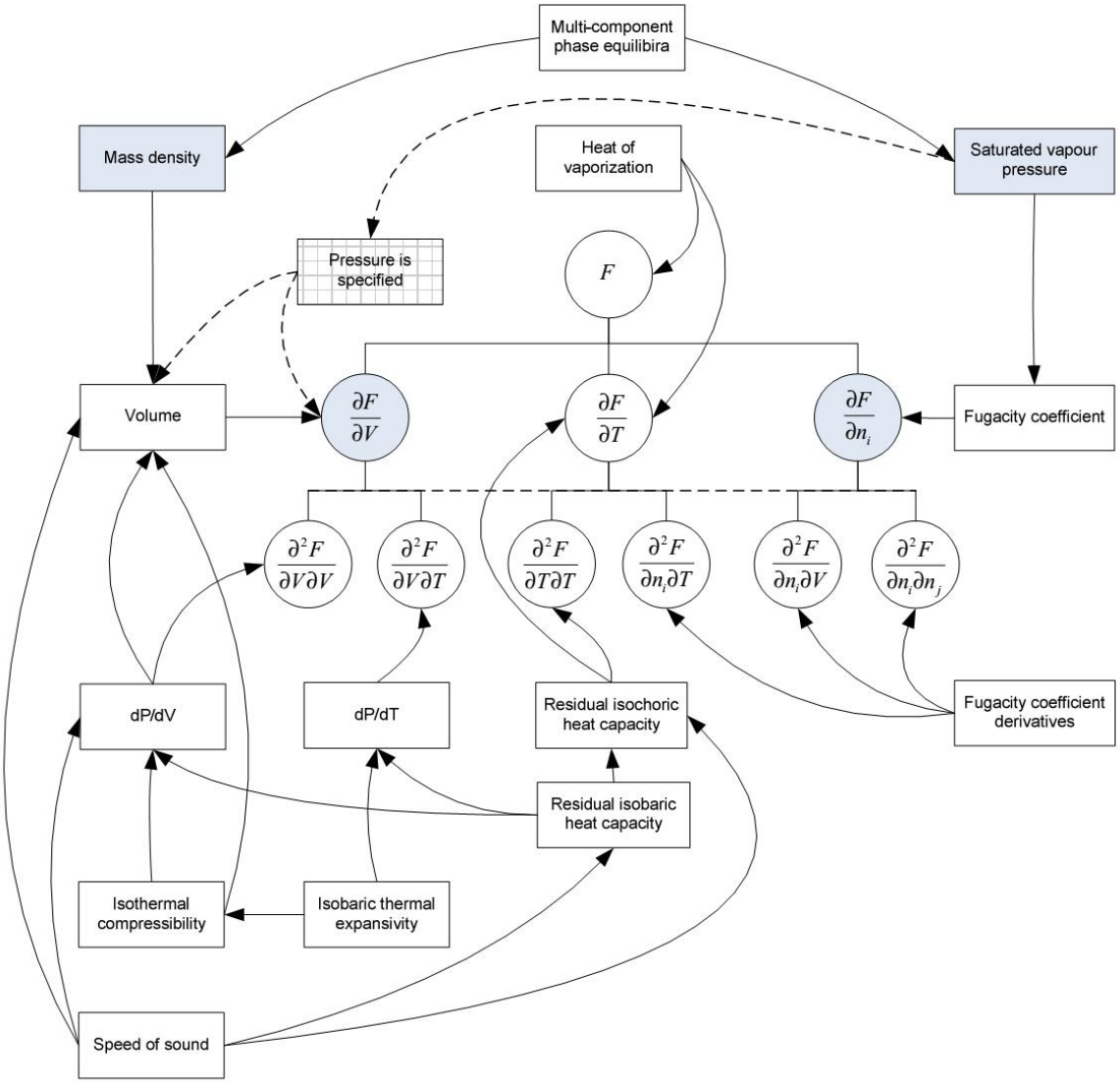

Figure A- 1: Schematic diagram illustrating the relationship between the partial derivatives of the reduced residual Helmholtz energy state function (F) and thermodynamic properties (de Villiers, 2011).

Appendix B

The Evolution of the Ideal Gas Equation of State[32]

Ancient Greek philosophers pondered whether matter could be divided into smaller and smaller pieces, or if there was a point, at which you could not divide matter any further. In this regards there were two trains of thought. Democritus (460 BC–370 BC) believed that matter was composed of individual (discrete) particles he called "atomos" (the ultimate particle), which he considered the most basic building block of all matter. About 100 years after Democritus, however, a contrary philosophy arose in which Aristotle (384 BC–322 BC) proposed the continuum theory of matter, which held that matter could in fact be divided into smaller and smaller pieces without end. At the time, however, there was no evidence to support either philosophy (or speculation), but for whatever the Aristotle's continuum theory of matter came to dominate and prevailed all the way until the 17th century (Ceyer, 2005).

As time went on suitable experimental evidence, i.e. controlled observations, began to show that matter was actually behaving much more as having some discrete nature to it, however, and not in itself as a continuum. These controlled observations (or experiments) in large part began with Antoine Lavoisier (1743–1794) who used the "dephologisticated air" discovered by Joseph Priestly (1733–1804) to study the rusting of metal. The careful measurements carried out by him and his wife then showed that this special air (what Lavoisier later named as elemental oxygen) was "adding to" the metal, and that this chemical reaction of oxidation could be written down as an algebraic equation. This eventually led Lavoisier to propose the law of conservations of mass, and the idea of elements (such as those forming the periodic table) that somehow combine to form new compounds (or molecules) such as Fe_2O_3 in the case of rust. Matter, therefore, is behaving as having some discrete nature to it $(1 + 1 = 2)$.

In lines with the discrete nature of matter, John Dalton developed his Atomic Theory (1803–1808)— (Giunta, 2010). He realised that he could begin to understand observations such as Lavoisier's if he went back to Democritus's idea of the *atomos* (individual discrete particles of matter), where he proposed that

- Each element is composed of atoms,
- That the atoms of any given element are exactly the same,
- That compounds form when atoms of more than one element combine, and
- That these atoms are neither created nor destroyed (i.e. the ultimate particle).

Of course much like the philosophers Democritus and Aristotle, Dalton was just making sense of observations at this point, which he could do so in terms of his atomic framework. As a result, for a period of time, the atom was believed to be the most basic constituent of matter, the so-called

[32] Unless otherwise referenced, the specific dates used in conjunction with events, people, etc. were obtained from Wikipedia online (Wikipedia), which the author considers a suitable resource for obtaining such information in the level of detail required for storytelling purposes (such is the case here).

"elementary particle". By the 1800's, it was believed that the theoretical structure of the universe was completely understood (Ceyer, 2005), from Newtonian mechanics on a planetary scale to the statistical mechanics of atoms within the framework of Dalton's Atomic Theory. To dispel these erroneous notions, further observations and experimental evidence were required. It was around these times that the idea for an equation of state of gases was established.

B.1. Historical Context

Multiple, independent, observations made during the 1800's led to the independent development of certain gas laws, equations which describe the relationships between the pressure, volume and temperature of simple gases[33]. Robert Boyle developed the first of these laws in 1662, who observed that the quantity $(P \cdot V)$ is constant for any gas as long as the temperature is also held constant (Barnett, 1941),

$$P * V = constant$$
$$\Rightarrow P_1 V_1 = P_2 V_2 \tag{B-1}$$

If, for example, the volume of a container with a fixed number of atoms (or mass) inside is reduced, then more of these same atoms (in terms of Dalton's atomic theory) will hit the walls of the container i.e. the pressure will increase. Next came the separate observations of Guillaume Amontons (1699), Jacques Charles (1787) and Joseph Louis Gay-Lussac in 1802 who quantified the effect of temperature on the pressure and volume of a gas (Walas, 1985):[34]

$$\overbrace{\left[\frac{P}{T} = constant\right]_{mass,V} \Rightarrow \frac{P_1}{T_1} = \frac{P_2}{T_2}}^{Amontons\ formulation} \tag{B-2}$$

Or alternatively,

$$\underbrace{\left[\frac{V}{T} = constant\right]_{mass,P} \Rightarrow \frac{V_1}{T_1} = \frac{V_2}{T_2}}_{\text{Charles and Gay-Lussac formulation (commonly refered to as Charles's law)}}$$

Then in 1834 Emile Clapeyron (Ramjugernath, 2000) combined these ideal gas laws (or observations) into the first formulation of the ideal gas equation of state, which can be derived from the kinetic theory of gase particles in the form

$$PV = NkT \tag{B-3}$$

where the actual number of particles N (atoms or molecules) is taken into account, and each of these particles is said to have an average energy k (called the Boltzmann constant). This represents a radicle

[33] A *simple gas* is, in general, used implies either a noble gases like Argon, or some simple diatomic gas molecule such as hydrogen.

[34] Where Amontons measure the change in temperature in terms of a proportional change in pressure (at constant $mass$ and V, hence the subscripts), and Charles and Gay-Lussac both measured the change in temperature in terms of a proportional change in volume (read in a likewise fashion, at constant $mass$ and P).

departure from Dalton's atomic theory (Brush, 1974; Brush, 2003), which is compatible with the idea that heat is a fluid (the dominant theory of his time called *caloric*, or calorique as originally introduced). In terms of the calorique theory, the gas pressure increases with temperature because the gas acquires more of the self-repelling calorique fluid (i.e. temperature itself could then be defined as the density of calorique for instance). This means that gas pressure is due to short-range repulsive forces between atoms in an atmosphere of self-repelling calorique particles—the temperature increases when a gas is compressed because calorique is concentrated in a smaller volume. Moreover, Dalton's believed that atoms of different elements should have different sizes (in explanation of Charles's law), which means that an equal number would occupy different volumes (consistent within the framework of Dalton's atomic theory).

Observations made by Gay-Lussac, however, were in direct contradiction to Dalton's ideas. What Gay-Lussac discovered is that in gaseous reactions the volumes of the reactants and products are related to each other by rational numbers (the volume of each gas is proportional to the number of particles it contains)—the law of combining volumes. Thus if 1-liter of hydrogen is combined with 1-liter of oxygen to form 2-liters of water, then 2-particles of hydrogen would combine with 1-particle of oxygen to form 2-particles of water. This implies that the volume of each gas is proportional to the number of particles/atoms it contains, and that a particle of oxygen can split into two parts, or that elemental gases may be composed of two or more atoms of the same kind! According to Dalton, the volume of a gas cannot be proportional to the number of atoms/particles (as Dalton has defined them) since they have different sizes for different elements; worse, the idea of a molecule composed of two oxygen atoms violates the notion that atoms of the same kind repel each other (which he used to explain pressure).

Finally it took the work of Lorenzo Ramano Amedeo Carlo Avogadro, who studied how the amount of gas affects the volume of the gas in 1811 (Hinshelwood, et al., 1956)—he was the first to fully articulate and explore the consequences of Charles's law and to put the atomic theory into its modern form. He showed that equal volumes of gases (at the same temperature and pressure) always have equal numbers of molecules—the concept of a mole was born (which is just a number[35], where $1\ mole \approx 6.022 \times 10^{23}\ atoms$). This means that in terms of the kinetic theory, the numbers of particles are not atoms (as in Dalton's theory) but molecules (modern theory), which may contain one or more atoms of the same or different kinds (Brush, 2003):

> *"Avogadro's hypothesis is favourable to the kinetic theory of gases insofar as it implies that the volume occupied by a certain number of molecules is independent of their size and shape, which suggests they are not ordinarily in contact. But it was not until 1859 that Maxwell showed that the hypothesis could be derived from the kinetic theory…"*

Therefore, using Avogadro's law, the ideal gas equation of state can be written in these terms:

$$PV = nRT \tag{B-4}$$

[35] Avogadro himself did not give any estimate of this number, but only postulated that it should have the same value for all gases.

where n is the amount of substance in moles of a gas, and R is just some constant resulting from the combination of the laws (commonly referred to as the ideal gas, or universal, constant, equal to the product of Boltzmann's constant and Avogadro's constant). Although no gas is truly ideal, many gasses (such as those [simple gases] studied in the derivation of the ideal gas laws) follow this equation very closely at sufficiently low pressures.

Incidentally, it follows that an ideal gas according to the kinetic theory has the following properties:

- Gas molecules have insignificant volume of their own, and are conceptually thus able to move freely through empty space (a vacuum).
- Molecules have no attractive forces between each other or with their container, and so they move in perfectly straight lines—individual molecules are blind and they interact with no one, not even each other.
- Collisions are completely elastic and, thus, do not use up energy; instead, they resist compression (repel) and expand to fill any available space.

Therefore, the kinetic theory of gases accounts for the pressure by counting the number of individual impacts and the average kinetic energy involved with each and nothing else.

For low to moderate pressures, simple gases such as oxygen, nitrogen and argon etc. can be represented quite well using ideal gas equation of state. This same equation, however, was known only to provide an approximation of the real behaviour of gases, even these simple gases could transform into a liquid under the right conditions. Therefore, for instance, there has to be at least some attractive forces involved which hold these molecules together in the liquid phase, and it then follows that the volumes of these molecules is not insignificant.

Appendix C

Intermolecular Forces

The ideal gas equation marks the beginning of the development for equations of state (see **Appendix B**) but it cannot in itself be considered a quantitatively accurate model. At best, it can only provide an approximation of the real behaviour for simple gases. After all, molecules of real fluids do not possess the properties of an ideal gas:

(1) Molecules of a real gas can have significant volumes of their own.
(2) Molecules do push and pull on each other.
(3) Molecules do not necessarily move in straight lines.
(4) Molecular collisions are not completely elastic.

When you move on the molecular level, for instance, whether it is in a gas or a liquid state, a molecule will experience a drag force i.e. resistance to movement in its surroundings. This concept is experienced everyday on the macroscopic level, and depends on the shape and size of the object (or molecule), the medium in which it is moving through, and the relative speed and direction in which it is moving. At high pressures and/or low temperatures, for example, gases have smaller volumes so that the gas molecules are packed closer together so that they interact with each other and their surroundings more than when they are far apart. It is no longer true, in such a case, to say that the molecules have no effective forces of attraction between each other or with their container. Since the total volume is smaller, the amount of space taken up by the gas molecules becomes more important, i.e. the volume of the gas molecules and their repulsive forces can no longer be ignored. Under any conditions that allow “forces” between molecules to occur (such as in the liquefaction of gases), the molecules involved will no longer behave as an ideal gas.

Nowadays, of course, we know that the atom is not the most basic building block of matter. That an atom is, in fact, made up of even smaller particles: a nucleus composed of both positively-charged protons and neutral particles called neutrons, which in turn are surrounded by negatively-charged electrons etc. This consequently brought about a new way of thinking, because you cannot use Newtonian mechanics (classical physics) to explain how these same subatomic particles remain together forming atoms, or even pairs of atoms, i.e. molecules and even individual atoms are charged particles capable of pushing and pulling on each other. Even if a given molecule is electrically neutral, it does not mean that its surrounding medium cannot influence its charge like character (or behaviour). Much like a magnet can be used to magnetize a paperclip, forces of attraction and repulsion are inherently involved in e.g. the condensation of gases (forces of attraction) and the resistance of the liquefied gas to further compression (forces of repulsion).

Of course, our current understanding is that electrons do not travel in a fixed orbit. They are probabilistic. This means that at any given moment in time these electrons could be anywhere around the nucleus. In fact, the probability that these electrons are evenly spaced around an atom is very low. This characteristic behaviour, for instance, is responsible for atoms or ions binding together in compounds (or molecules) by sharing electrons with each other by forming metallic, ionic and covalent bonds. There are, of course, many more types of intermolecular forces that can operate between

molecules, where most "bonding" interactions involve mixtures of various types (Prausnitz, et al., 1986):

(1) Electrostatic forces between charged particles (ions) and between permanent dipoles, quadrupoles, and higher multipoles.
(2) Induction forces between a permanent dipole (or quadrupole) and an induced dipole.
(3) Forces of attraction (dispersion forces) and repulsion between nonpolar molecules.
(4) Specific (chemical) forces leading to association and complex formation, i.e., to the formation of loose chemical bonds; hydrogen bonds are perhaps the best example.

For discussion purposes, however, the focus for the remainder of this appendix has been limited to London forces, dipole-dipole and hydrogen bonding interactions, since they are the types indirectly or directly accounted for by the PC-SAFT equation of state used in this project. These three types are commonly referred to as van der Waals forces, which is a classification used to represent all intermolecular forces that cannot be called either a covalent bond or ionic bond. Each of these intermolecular forces are briefly discussed in turn below.

C.1. London Dispersion (Induced Dipole) Forces

Noble gases are essentially happy; they have a full outer shell of electrons. They should just float around, but the fact that they have a liquid state means that there must be "some" attractive force acting between these atoms (all atoms), these molecules (all molecules). The fact that electrons are not in a fixed orbit explains this weak attraction; a molecule can temporarily have a slight charge in one direction or another at any time i.e. at any moment an electron's location is probabilistic. If there is always going to be some type of distribution, then it stands to reason that there is always going to be at least some charge, however weak, that can instantaneously polarise even molecules without permanent dipoles. This small charge is called a London dispersion (or induced dipole) force, and is the weakest of the so-called van der Waals forces. These London dispersion forces are so weak, for instance, that it takes very little energy to overcome them e.g. which is why gases exist. At low enough temperatures these forces become strong enough to cause gas molecules to condense to form liquids, or to solidify to form solids. They are, however, most likely to behave like an ideal gas around standard temperatures and pressures, given the very small attractions between like nonpolar molecules (Nannoolal, 2004):

> *"As London forces diminish very quickly with growing distance, one can distinguish roughly between molecules 'in contact' and 'not in contact'. The energy difference between these two states is the London interaction for one molecular contact. Application of the Boltzmann distribution law shows, that a significant portion of the molecules in a liquid can be assumed to be in mutual contact. This is the reason why models based on the number of intermolecular contacts perform analogous to those which calculate the total energy by special integration of the intermolecular potential times radial distribution function."*

The magnitude of this type of interaction, and of the van der Waals type forces in general, then depends on the energy required to displace the electrons of a molecule (the *first ionization potential*) and the likelihood that the molecule will form a dipole (the *polarisability*). The ionisation potential generally decreases with molecular size and degree of unsaturation, while the polarisability is

proportional to the size of the 'electron cloud' for a molecule, which is directly proportional to a molecule's volume (Nannoolal, 2004). Furthermore, since all molecules possess nonzero ionization potentials and polarisability, then all molecular pairs experience these very weak dispersive interactions (Smith, et al., 2001).

C.2. Permanent Dipole Forces

Now consider a molecule that is maybe a little more polar than the noble gases, like hydrochloric acid (HCl) for instance. In this case the chlorine atom is electronegative, and shares an electron with an atom of hydrogen. The bond between these two atoms, therefore, causes the electrons to favour a certain orientation that makes the chlorine side more negative and the hydrogen side more positive at any point in time. This is called a *permanent dipole*, because this charge distribution is always present e.g. unlike the induced molecular dipoles of the preceding section that fluctuate rapidly. If you have two HCl molecules in close proximity, for example, then you will have what is known as a dipole-dipole interaction, which is sometimes referred to as a dipole-dipole bond to sound more "permanent" e.g. like the intramolecular attractions responsible covalent bonds (the sharing of electrons) between atoms. Because of this, on average, dipoles of molecules in a liquid tend to orient themselves to form attractive interactions with their neighbours depending on the thermal motion (or temperature) of the system. This implies, for instance, that dipole interactions may not always be additive, although it is likely a reasonable assumption to make in most cases.

If there was a mixture of nonpolar and polar molecules, for example, the stronger permanent dipoles of the polar molecules would dominate the intermolecular forces of the mixture at most conditions. In this case, the magnitude of the dispersive interactions between these molecules would be marginal in comparison. In fact, the permanent dipoles would repel the electrons of the nonpolar molecules, and would actually "induce" a dipole moment similar to the temporary dipole moments resulting from dispersive interactions, but understandably much stronger. In addition to dipole moments (induced or permanent), it is also possible for molecules to have multipoles e.g. quadrupoles and higher moments. Carbon dioxide, for example, has a quadrupole moment having four electric charges at four separate points in the molecule, but their effects are typically small in most cases and are often ignored in favour of simplicity.

C.3. Hydrogen Bonding

If small *and* extremely electronegative atoms like nitrogen, oxygen, or fluorine are involved with hydrogen, then this represents the special case of hydrogen bonding. In the case of hydrogen fluoride (HF), for instance, the high electronegativity of the fluorine atom effectively draws the lone electron of hydrogen to itself. Since hydrogen only has a lone electron, this means that its positively charged nucleus is practically "unshielded" to one side. This gives the hydrogen atom a relatively high positive charge, which is powerfully attracted to the highly negative charge concentrated around the small fluorine atom of a neighbouring HF molecule. Although hydrogen bonding is a type of dipole-dipole interaction, some hydrogen bonds more resemble ion-dipole attractions in magnitude (which is why they are, in themselves, given distinction). The strong attraction forces involved in these bonds increase the heat of vaporization; the extra energy required to break these bonds is the main reason why molecules with hydrogen bonds have much higher boiling points.

Appendix D

The Phase Behaviour of Real Substances

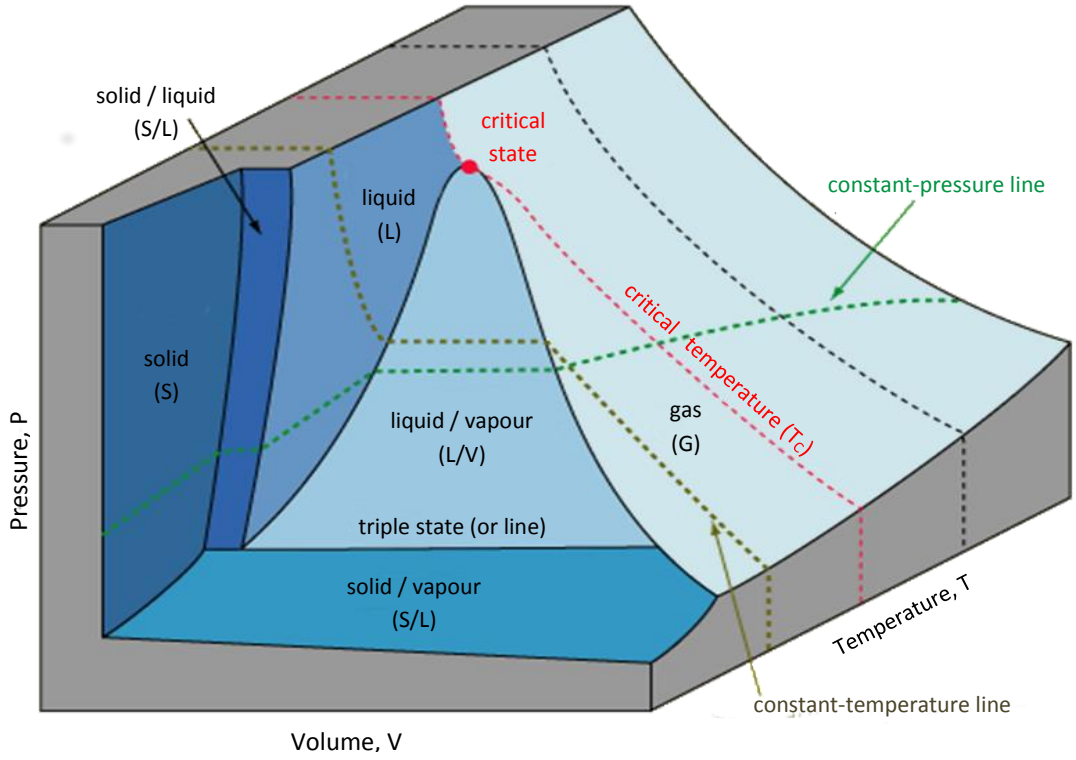

Figure D-1: PVT surface in three dimensions for a fluid that expands on melting (Nave).

Through experimentation (observations) it is quite well known that substances can exist in three phases, and which phase a substance takes then depends on the intermolecular forces occurring between the molecules of that substance (or mixture) and the state (or conditions) in which the molecules are in. Furthermore, *all* substances have the "opportunity" to exist in anyone of these phases; therefore, *all* substances will experience a phase transition when moving from one phase into the next. A substance does not cease to exist in one phase and then pop into existence in another—mass *is* a continuum, mass *is* conserved.

Therefore, if enough measurements are performed on a pure substance in various equilibrium states, then a PVT surface in three dimensions could be obtained. **Figure D-1** above is one such diagram (for an arbitrary pure-substance). Portions of the surface labelled solid, liquid and gas then correspond to states of a *single-phase* at equilibrium. Portions of the surface labelled with a pair of names then relate the coexistence of *two* phases in equilibrium. It then follows that the solid lines separating the various regions form the boundaries of the parts of the surface representing individual phases. The triple state marks the intersections of the three two-phase regions; this is called the *triple line*, along which solid, liquid, and gas phases exist in three-phase equilibrium. Above this line, the area under the bell-shaped curve then delineates the region of vapour-liquid-equilibrium (VLE), which then terminates at the so-called *critical point*.

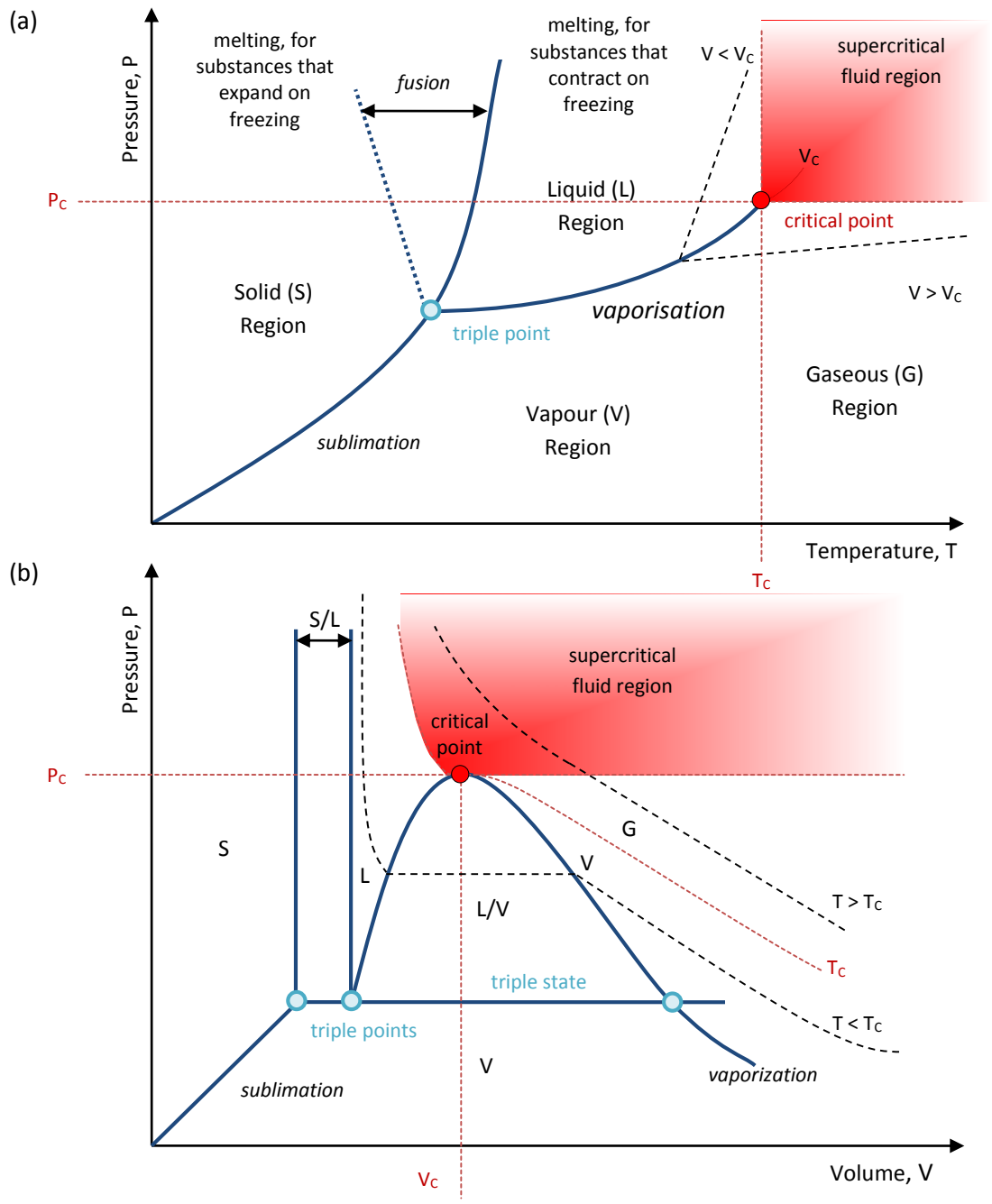

Figure D-2: PT-diagram shown in part (a) of the figure, and PV-diagram shown as part (b).

Projections in two-dimensions can then be obtained of the PVT surface onto two planes. **Figure D-2** shows constructions yielding the PT-diagram (a) and the PV-diagram (b) of a pure substance—comparison between **Figure D-1** and **Figure D-2** shows that these diagrams are not drawn to scale. With reference to **Figure D-1** and **Figure D-2**, the two-phase regions are projected as lines on the PT-diagram of **Figure D-2** (a); this is a consequence of the relationships that exist between pressure, temperature and volume for phases in equilibrium. It then follows that the regions solid/liquid (S/L), solid/vapour (S/V), and liquid/vapour (L/V) on the surface of **Figure D-1** then correspond to the three saturation curves on **Figure D-2**, labelled on **Figure D-2** (a) as the fusion curve, the sublimation curve, and vaporisation curves. The limits of the vaporization curve are then defined by the triple line and the Liquid/Gas critical point projected on the P-T diagram. Although the

vaporisation curve ends at the critical point, the fusion curve continues upward indefinitely, or until it intercepts another Solid/Liquid saturation curve.

Because of the abrupt termination of the vaporisation curve at the critical point, there is some arbitrariness in the assignment of names to the nonsolid equilibrium phases of a substance; the labels on **Figure D-2** serve as well as any for discussion purposes. Thus, a *vapour* is a gas phase that can be condensed both by an isothermal increase of pressure and by an isobaric decrease of temperature. The term *fluid* designates any nonsolid phase; in particular, it can be used as a label for the region for which both $T > T_C$ and $P > P_C$, where the terms *liquid* and *gas* seem inappropriate (i.e. the *supercritical fluid* region).

The dashed lines on **Figure D-2** (a) are isochores, lines of constant volume. Isochores intersecting the vaporization curve from above $(V < V_C)$ are for the liquid phase, and those from below $(V > V_C)$ for the vapour phase. The dashed line labelled V_C is the critical isochore; it is collinear with the vaporization curve at the critical point. The isochores are drawn as straight lines on **Figure D-2** (a); however they actually should show some small curvature which is not shown.

It then follows that the two-phase regions of the PVT surface from **Figure D-1** project as areas on the PV-diagram. On **Figure D-2** (b) the area corresponding to Vapour/Liquid (V/L) equilibrium is separated from regions of single-phase equilibrium by a dome-shaped curve. The left segment of this curve $(V < V_C)$ represents states of saturated liquid and the right segment $(V > V_C)$ represents states of saturated vapour. The two segments join smoothly at the critical point, and thus at the critical state the liquid and vapour phases in equilibrium become identical.

On the PV-diagram of **Figure D-2** (b), isotherms are shown by dashed lines. For very high temperatures, these curves approach the shape of rectangular hyperbolas, given by the ideal-gas equation (see Equation (B-4)). As temperature decreases, deviations from the ideal-gas equation become more prominent, until the critical temperature is reached. The critical isotherm, labelled T_C, exhibits a singular behaviour; it has a horizontal inflection at the critical point, implying that the 1st and 2nd derivatives of the critical isotherm are both zero at this point.

Subcritical isotherms $(T < T_C)$ consist of three branches. The left branch corresponds to states of subcooled liquid; because liquids are relatively incompressible, this branch is steep. The right branch represents states of superheated vapour. Connecting these two branches is the third section of the isotherm, a horizontal line representing states of vapour/liquid equilibrium (VLE). The intersections of the horizontal segment with the liquid and vapour branches of the isotherm define the states of saturated liquid and saturated vapour. The pressure corresponding to this horizontal section is the saturation pressure at VLE, or P_i^{sat}. It is a single point on the vaporisation curve of **Figure D-2** (a).

Appendix E

Computer Program Outline

Computational tools such as process simulation software, data bank programs, etc. play an important role in chemical engineering. Although the number of software packages (and smaller software tools) available to the practicing engineer are ever growing, it is often the case that the solution to a given problem requires multiple resources. Some of these software "tools", however, require intimate knowledge to use effectively. For unique and rare problems requiring multiple resources, for instance, it is often sufficient to pull in specialists (with different backgrounds) for a once-off solution to the problem, but for routine problems it is often more desirable to simplify the solution for general use, i.e. specialists are a limited and expensive source of tacit knowledge. Likewise, in research especially, functionality is often required that cannot be found in available tools. This often means designing a new "tool" to solve a specific and reoccurring problem by linking multiple existing tools together to obtain a workable solution.

The code (program) developed for this project, for instance, is a patch-work of existing functionality from other resources: Aspen Plus, Dortmund Databank (DDB), Microsoft Office Applications, etc. A general schematic of how these different applications and resources are linked together using MS-Excel-VBA is provided in **Figure E-1** below (on the next page). Experimental data from the Dortmund Data Bank (DDB), for instance, can be imported into the VBA project, stored in an external MS-Access database file, and uploaded into an Aspen Plus simulation file for e.g. evaluation purposes. The routines developed to link these programs have been integrated into the Thermodynamic Research Utilities for Excel (TRUx) utility that the author has been developing. It currently consists of roughly 50,000+ non-blank lines of code (1,000+ pages) containing about 1.5+ million non-blank characters (or 300,000+ words). Although particulars of the program are not further discussed here, the author plans to eventually publish additional details (e.g. source code or completed project files) online at www.chejunkie.com (the author's personal website).

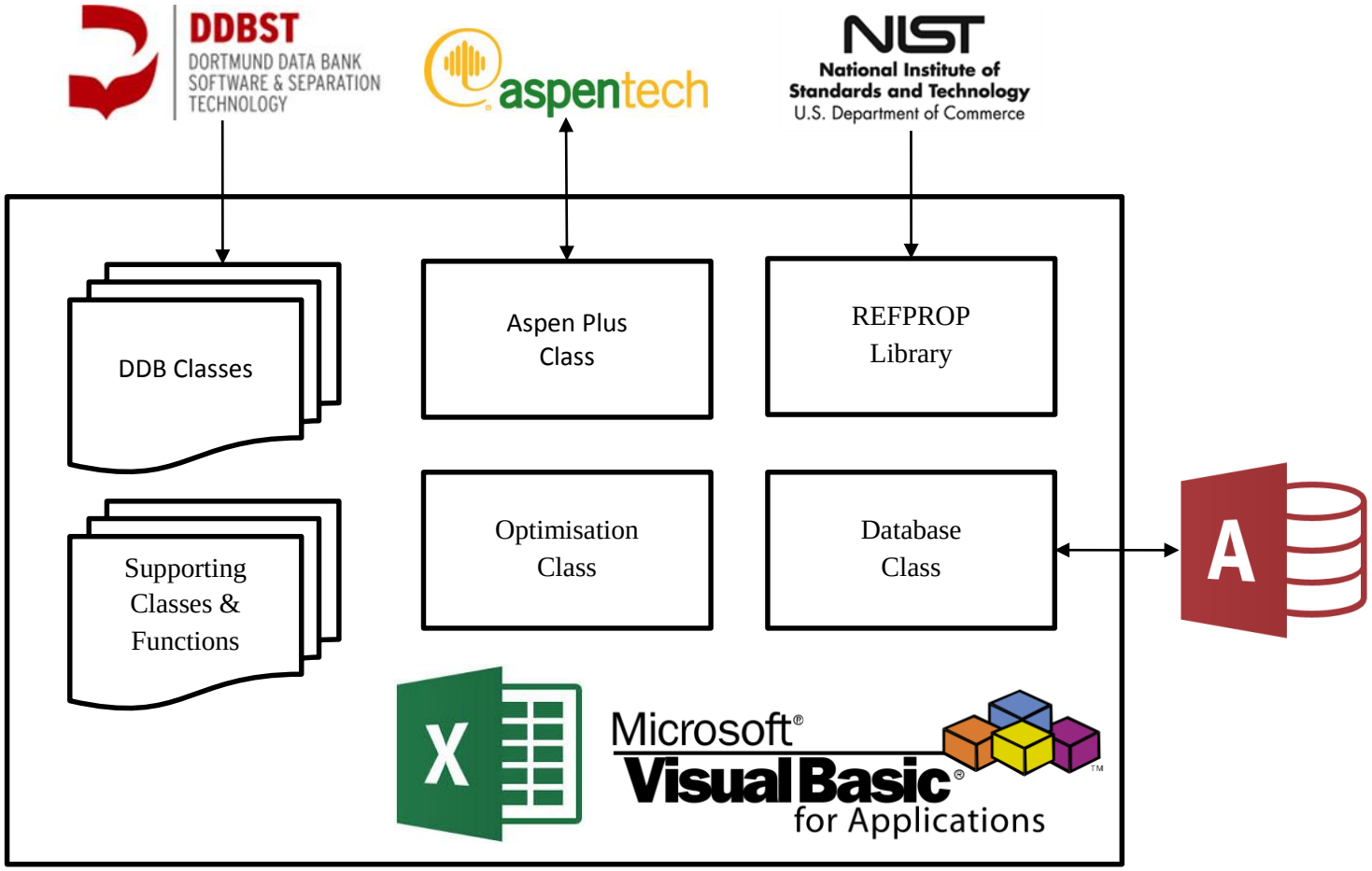

Figure E-1: Diagram outlining the Thermodynamic Research Utilities for Excel (TRUx) utility.

Appendix F

Fitting Results

F.1. PC-SAFT Parameters

DDB	Aspen Alias	Name	O.F.	PC-SAFT Parameters			T_b	ρ_b	$\Delta h_{v,b}$
				m	σ [Å]	ε/K [K]	[K]	[kg/m^3]	[J/mol]
1056	N2	Nitrogen [R-728]	7.2E-08	0.3920	5.3455	114.03	77.355	806.08	5579.6
1057	CO	Carbon monoxide	7.3E-08	0.3684	5.5348	116.56	81.63817	793.22	6013.4
2021	F2	Fluorine [R-784]	0	0.3706	4.9571	127.34	85.03679	1501.80	6625.1
1058	AR	Argon [R-740]	0	0.4491	4.7250	141.26	87.30214	1395.40	6437.0
1051	CH4	Methane [R-50]	0	1.0039	3.6984	149.70	111.6672	422.35	8195.1
1060	KR	Krypton [R-784]	6.4E-08	0.9673	3.6476	166.78	119.7349	2416.67	8971.1
1423	NF3	Nitrogen trifluoride	0	1.7302	3.2302	141.98	144.1381	1537.49	11554.1
1014	CF4	Tetrafluoromethane [R-14]	0	2.2472	3.1048	120.48	145.1048	1603.21	11831.1
1062	XE	Xenon	0	1.0017	3.9181	227.46	165.0513	2941.93	12548.9
1053	C2H4	Ethylene [R-1150]	1.0E-07	1.5440	3.4481	180.36	169.3786	567.65	13532.8
1054	C2H6	Ethane [R-170]	0	1.5644	3.5612	194.45	184.5686	543.84	14716.0
1061	N2O	Dinitrogen monoxide	0	2.0807	2.7948	171.49	184.6839	1230.45	16473.4
1073	CHF3	Fluoroform [R-23]	0	2.3673	2.9401	160.28	191.1321	1445.64	16758.1
446	CCLF3	Chlorotrifluoromethane [R-13]	0	2.1138	3.4232	165.82	191.6736	1521.42	15601.6
1050	CO2	Carbon dioxide [R-744]	0	1.6305	3.0360	210.85	194.6855	1253.49	16852.7
1440	CH3F	Methyl fluoride [R-41]	0	1.6096	3.1459	210.64	194.8363	880.34	16602.7
1220	C2F6	Hexafluoroethane [R-116]	3.6E-07	2.8043	3.3183	140.70	195.0584	1604.92	16143.4
1294	SF6	Sulfur hexafluoride	0	2.0572	3.5820	184.02	209.7417	1910.55	16945.1

DDB	Aspen Alias	Name	O.F.	PC-SAFT Parameters			T_b	ρ_b	$\Delta h_{v,b}$
				m	σ [Å]	ε/K [K]	[K]	[kg/m^3]	[J/mol]
1065	H2S	Hydrogen sulfide	0	1.6432	3.0527	230.98	212.8549	949.22	18622.5
1158	CH2F2	Difluoromethane [R-32]	2.6E-07	2.1474	2.9355	201.86	221.4986	1212.93	19865.0
1363	COS	Carbonyl sulfide	0	1.5854	3.4663	239.70	222.9886	1174.29	18557.6
1224	C2HF5	Pentafluoroethane [R-125]	0	3.0853	3.1308	157.48	225.0614	1513.60	19695.4
1055	C3H6-2	Propylene [R-1270]	0	1.8853	3.5820	212.15	225.5307	610.07	18470.4
1072	C2H3F3	1,1,1-Trifluoroethane [R-143a]	0	2.3209	3.3690	187.33	225.9094	1166.39	19045.5
237	C3H8	Propane [R-290]	0	1.9224	3.6683	213.24	231.0362	580.89	18767.2
244	CHCLF2	Chlorodifluoromethane [R-22]	0	2.3461	3.1899	195.07	232.3395	1409.18	20211.3
550	C2CLF5	Chloroperfluoroethane [R-115]	0	2.7284	3.5251	171.88	233.9318	1546.63	19365.4
1348	C3F8	Perfluoropropane [R-218]	0	3.2696	3.4653	155.16	236.3611	1611.57	19774.9
210	H3N	Ammonia [R-717]	0	2.1075	2.4862	234.06	239.8236	681.98	23321.9
1693	C3H6-1	Cyclopropane	0	2.6815	3.0230	188.95	241.67	698.42	21727.8
245	CCL2F2	Dichlorodifluoromethane [R-12]	0	2.1470	3.6053	210.18	243.3977	1487.01	20092.2
2393	C2H2F4	1,1,1,2-Tetrafluoroethane [R-134a]	0	3.0550	3.0801	176.49	247.0762	1376.67	22137.5
1942	C3H4-2	Propyne	0	1.7883	3.4521	247.66	248.0149	695.25	21003.8
580	C2H6O-1	Dimethyl ether [RE-170]	0	2.0576	3.3706	226.20	248.3395	735.21	21263.4
911	C2H4F2	1,1-Difluoroethane [R-152a]	0	2.4046	3.2285	206.35	249.1279	1011.16	21790.9
2904	CF3I	Iodotrifluoromethane	0	1.9986	3.7838	225.42	251.2905	2248.88	20368.7
3959	C3HF7	1,1,1,2,3,3,3-Heptafluoropropane [R-227ea]	2.2E-07	3.5615	3.3019	163.38	256.8091	1544.34	22403.9
957	C2HCLF4	1-Chloro-1,2,2,2-tetrafluoroethane [R-124]	0	2.9484	3.3520	187.24	261.1869	1473.50	22630.9
316	C4H10-2	2-Methylpropane [R-600a]	0	2.1693	3.8140	221.75	261.401	593.83	21218.4
1300	O2S	Sulfur dioxide [R-764]	0	2.5945	2.7669	217.62	263.1322	1461.14	24924.8
1418	C2H3CLF2	1-Chloro-1,1-difluoroethane [R-142b]	0	2.4268	3.4925	213.37	264.0267	1192.64	22435.3
457	C4H8-5	Isobutylene	0	2.1628	3.7130	228.67	266.1458	626.50	21972.2
368	C4H8-1	1-Butene	0	2.1473	3.7244	230.26	266.844	625.64	22007.0
247	C4F8-D2	Perfluorocyclobutane [RC-318]	2.5E-07	3.8260	3.3393	162.61	267.1753	1615.16	23355.4
2938	C4F10	Perfluorobutane	0	3.8956	3.5205	160.80	271.0605	1591.33	23073.9
8773	C3H2F6-D1	1,1,1,3,3,3-Hexafluoropropane [R-236fa]	0	3.7616	3.1932	169.62	271.7097	1444.73	24387.3
41	C4H10-1	n-Butane [R-600]	0	2.2176	3.7713	229.65	272.6599	601.27	22417.7

DDB	Aspen Alias	Name	O.F.	PC-SAFT Parameters			T_b	ρ_b	$\Delta h_{v,b}$
				m	σ [Å]	ε/K [K]	[K]	[kg/m^3]	[J/mol]
450	C4H8-3	trans-2-Butene	0	2.1649	3.7134	236.01	274.0299	626.46	22733.2
551	C2CL2F4-2	1,2-Dichlorotetrafluoroethane [R-114]	0	2.8156	3.6298	200.78	276.7415	1518.09	23234.9
460	C4H8-2	cis-2-Butene	0	2.2476	3.6390	234.07	276.8735	640.08	23237.7
9650	C3H2F6	1,1,1,2,3,3-Hexafluoropropane [R-236ea]	2.1E-07	3.6363	3.2087	178.36	279.347	1482.62	25111.6
552	CHCL2F	Dichlorofluoromethane [R-21]	0	2.3716	3.3712	235.69	282.0119	1405.48	24643.1
468	C5H12-3	2,2-Dimethylpropane	0	2.3449	3.9604	226.30	282.655	601.18	22775.9
12112	C3H3F5-D1	1,1,1,3,3-Pentafluoropropane [R-245fa]	0	3.6728	3.1551	184.38	288.2893	1364.91	26283.4
1194	CCL3F	Trichlorofluoromethane [R-11]	0	2.2219	3.7258	252.96	296.8581	1479.33	24912.4
11005	C3H3F5-D2	1,1,2,2,3-Pentafluoropropane [R-245ca]	0	3.3806	3.2391	200.22	298.2815	1385.97	26940.7
3051	C2HCL2F3-D1	1,1-Dichloro-2,2,2-trifluoroethane [R-123]	0	2.8788	3.5267	218.98	300.973	1456.64	26027.1
94	C5H12-2	2-Methylbutane	0	2.4438	3.8833	237.32	300.9763	612.09	24768.1
218	C5F12	Perfluoropentane [R-4-1-12]	0	4.6314	3.5064	163.95	302.9041	1597.21	26448.8
2485	C2H3CL2F	1,1-Dichloro-1-fluoroethane [R-141b]	0	2.4505	3.6339	245.66	305.1954	1220.04	26045.2
134	C5H12-1	Pentane [R-601]	0	2.5798	3.8140	237.01	309.2136	609.72	25798.7
12111	C4H5F5	1,1,1,3,3-Pentafluorobutane [HFC-365mfc]	1.8E-07	3.5927	3.4027	200.40	313.3431	1223.95	27866.1
220	C2CL3F3	1,1,2-Trichloro-1,2,2-trifluoroethane [R-113]	0	2.7575	3.7827	236.55	320.7352	1508.19	27041.8
4	C3H6O-1	Acetone	0	2.3397	3.4578	279.95	329.2249	748.96	29123.9
111	C6H14-2	2-Methylpentane	0	2.8177	3.9010	240.98	333.3621	615.09	27840.1
110	CH4O	Methanol	0	3.5756	2.4504	238.57	337.6323	748.36	35286.6
89	C6H14-1	Hexane	0	2.9253	3.8537	242.61	341.8645	613.02	28863.0
11	C2H6O-2	Ethanol	0	5.8303	2.3072	188.53	351.3866	736.45	39157.6
31	C6H6	Benzene	0	2.4480	3.6452	288.56	353.2341	813.56	30826.4
50	C6H12-1	Cyclohexane	0	2.4529	3.8787	283.25	353.8858	719.53	29960.6
91	C7H16-1	Heptane	0	3.2881	3.8752	245.95	371.5333	614.23	31752.8
174	H2O	Water [R-718]	0	2.4463	2.1591	353.68	373.1243	958.37	40651.3
887	D2O	Deuterium oxide <Heavy water>	0	2.6760	2.0923	336.39	374.5397	1062.22	41464.5
161	C7H8	Toluene	0	2.6132	3.8086	298.33	383.7457	779.16	33235.4
128	C8H18-1	Octane	2.2E-07	3.6835	3.8817	247.25	398.7737	612.22	34520.7

DDB	Aspen Alias	Name	O.F.	PC-SAFT Parameters			T_b	ρ_b	$\Delta h_{v,b}$
				m	σ [Å]	ε/K [K]	[K]	[kg/m^3]	[J/mol]
398	C9H20-1	Nonane	0	4.0181	3.9087	250.07	423.913	608.96	37010.0

Table F-1: The results of fitting PC-SAFT parameters to REFPROP predictions using Aspen Plus.

F.2. Potential Blends to Replace R-22

Blend Components	O.F.	Compositions		T_b	ρ_b	$\Delta h_{v,b}$
		Moles	Mass	[K]	[kg/m^3]	[J/mol]
R-22	----	----	----	232.34	1409.18	20211.3
R-152a/-125	0.0146	(27.0/73.0)	[16.9/83.1]	229.04	1404.67	20680.0
RE-170/-125	0.0206	(18.1/81.9)	[7.8/92.2]	227.59	1405.06	20280.0
R-125/{Propyne}	0.0207	(81.4/18.6)	[92.9/7.1]	227.58	1405.22	20220.0
R-125/{Cyclopropane}	0.0237	(82.7/17.3)	[93.2/6.8]	226.87	1405.80	20120.0
R-125/-134a	0.0257	(34.3/65.7)	[38.0/62.0]	236.58	1434.60	21810.0
R-290/-125	0.0273	(12.1/87.9)	[4.8/95.2]	226.01	1407.18	19630.0
R-143a/-125	0.0294	(32.8/67.2)	[25.4/74.6]	225.51	1408.37	19470.0
R-1270/-125	0.0298	(13.4/86.6)	[5.1/94.9]	225.41	1408.47	19580.0
R-125/{COS}	0.0370	(57.2/42.8)	[72.7/27.3]	223.75	1412.15	19240.0
R-32/-134a	0.0385	(28.2/71.8)	[16.7/83.3]	236.39	1360.96	22020.0
R-32/-125	0.0465	(52.1/47.9)	[32.1/67.9]	221.57	1414.30	19570.0
{COS}/R-134a	0.0521	(23.9/76.1)	[15.6/84.4]	239.67	1350.77	21750.0
R-143a/-134a	0.0615	(14.3/85.7)	[12.1/87.9]	242.96	1351.30	21940.0
R-143a/{COS}	0.1713	(21.7/78.3)	[28.0/72.0]	223.16	1174.31	18620.0
{Cyclopropane}/{Propyne}	0.5060	(98.9/1.1)	[98.9/1.1]	241.75	698.46	21726.4
R-143a/-125/-134a	0.0015	(16.6/39.9/43.4)	[13.1/45.1/41.7]	232.34	1409.18	21160.0
R-290/-125/-134a	0.0015	(6.3/51.7/42.1)	[2.6/57.6/39.8]	232.33	1409.21	21180.0
R-125/{COS}/-134a	0.0016	(32.0/20.3/47.7)	[38.7/12.3/49.0]	232.34	1409.18	21220.0

Blend Components	O.F.	Compositions		T_b	ρ_b	$\Delta h_{v,b}$
		Moles	Mass	[K]	[kg/m^3]	[J/mol]
R-22	----	----	----	232.34	1409.18	20211.3
R-1270/-125/-134a	0.0016	(6.7/49.2/44.1)	[2.6/55.2/42.2]	232.34	1409.18	21220.0
R-125/{Propyne}/-134a	0.0016	(53.7/10.7/35.6)	[61.4/4.1/34.5]	232.34	1409.18	21250.0
RE-170/-125/-134a	0.0016	(10.4/54.1/35.6)	[4.5/61.2/34.2]	232.34	1409.18	21270.0
R-125/{Cyclopropane}/-134a	0.0016	(51.9/9.4/38.7)	[58.9/3.7/37.3]	232.34	1409.18	21290.0
R-152a/-125/-134a	0.0016	(17.6/54.3/28.1)	[11.0/61.8/27.2]	232.34	1409.18	21290.0
R-32/-125/-134a	0.0019	(21.1/24.3/54.6)	[11.5/30.4/58.1]	232.34	1409.18	21640.0
R-152a/-125/{Propyne}	0.0150	(25.4/73.5/1.1)	[15.9/83.7/0.4]	228.95	1404.63	20650.0
RE-170/-152a/-125	0.0150	(1.1/25.4/73.5)	[0.5/15.9/83.6]	228.95	1404.56	20660.0
R-152a/-125/{Cyclopropane}	0.0152	(25.3/73.6/1.1)	[15.8/83.7/0.4]	228.90	1404.76	20650.0
R-152a/-125/{COS}	0.0152	(26.4/72.4/1.2)	[16.6/82.7/0.7]	228.90	1404.42	20650.0
R-290/-152a/-125	0.0159	(1.2/24.5/74.3)	[0.5/15.3/84.2]	228.75	1404.13	20590.0
RE-170/-125/{Propyne}	0.0206	(16.9/81.9/1.2)	[7.3/92.3/0.4]	227.59	1405.15	20280.0
RE-170/-125/{Cyclopropane}	0.0208	(17.0/82.0/1.0)	[7.3/92.3/0.4]	227.55	1405.14	20280.0
R-125/{Cyclopropane}/{Propyne}	0.0209	(81.5/1.1/17.5)	[92.9/0.4/6.7]	227.53	1405.20	20220.0
R-290/E-170/-125	0.0212	(1.0/16.6/82.4)	[0.4/7.1/92.4]	227.46	1405.09	20230.0
R-143a/-125/{Propyne}	0.0212	(2.0/80.5/17.5)	[1.6/91.7/6.7]	227.45	1405.35	20180.0
R-290/-125/{Propyne}	0.0212	(1.0/81.9/17.1)	[0.4/93.1/6.5]	227.45	1405.19	20170.0
RE-170/-32/-125	0.0214	(17.7/1.2/81.1)	[7.7/0.6/91.7]	227.42	1405.15	20270.0
RE-170/-125/{COS}	0.0214	(17.2/80.7/2.1)	[7.5/91.3/1.2]	227.40	1405.21	20240.0
R-125/{COS}/{Propyne}	0.0215	(80.2/2.1/17.8)	[92.0/1.2/6.8]	227.39	1405.36	20180.0
R-125/{COS}/{Cyclopropane}	0.0240	(82.1/1.0/16.8)	[92.7/0.6/6.7]	226.79	1406.03	20100.0
R-143a/-125/{Cyclopropane}	0.0240	(2.1/81.7/16.2)	[1.7/92.0/6.4]	226.79	1405.81	20080.0
R-32/-125/{Cyclopropane}	0.0242	(1.0/82.1/16.9)	[0.5/92.8/6.7]	226.73	1406.05	20110.0
R-290/-1270/-125	0.0275	(11.2/1.0/87.8)	[4.5/0.4/95.1]	225.97	1406.86	19620.0
R-290/-125/{COS}	0.0276	(11.7/86.8/1.6)	[4.7/94.5/0.8]	225.92	1407.11	19660.0

Blend Components	O.F.	Compositions		T_b	ρ_b	$\Delta h_{v,b}$
		Moles	Mass	[K]	[kg/m^3]	[J/mol]
R-22	----	----	----	232.34	1409.18	20211.3
R-290/-32/-125	0.0278	(11.8/1.2/87.0)	[4.7/0.6/94.7]	225.87	1407.42	19630.0
R-1270/-143a/-125	0.0294	(1.2/29.9/68.9)	[0.5/23.2/76.3]	225.51	1408.28	19470.0
R-143a/-125/{COS}	0.0296	(32.0/66.9/1.1)	[24.9/74.5/0.6]	225.46	1408.31	19500.0
R-143a/-32/-125	0.0300	(31.9/1.5/66.6)	[24.9/0.7/74.3]	225.37	1408.51	19470.0
R-1270/-125/{COS}	0.0301	(12.9/85.6/1.5)	[5.0/94.2/0.8]	225.35	1408.62	19570.0
R-1270/-32/-125	0.0304	(13.0/1.5/85.5)	[5.0/0.7/94.3]	225.27	1408.73	19580.0
R-1270/-143a/-125/-134a	0.0015	(1.2/13.6/41.6/43.6)	[0.5/10.8/47.0/41.8]	232.34	1409.18	21170.0
R-143a/-125/{Cyclopropane}/-134a	0.0015	(14.5/41.5/1.2/42.8)	[11.5/46.9/0.5/41.1]	232.34	1409.18	21180.0
R-290/-125/{Propyne}/-134a	0.0015	(5.5/51.9/1.2/41.4)	[2.3/58.0/0.5/39.3]	232.34	1409.18	21190.0
R-152a/-143a/-125/-134a	0.0015	(4.0/12.9/43.2/40.0)	[2.5/10.2/48.9/38.5]	232.34	1409.18	21190.0
R-143a/-125/{COS}/-134a	0.0015	(8.5/35.9/10.0/45.6)	[7.0/41.9/5.8/45.3]	232.33	1409.16	21190.0
R-290/-1270/-125/-134a	0.0015	(4.5/1.9/51.0/42.6)	[1.8/0.7/57.0/40.5]	232.33	1409.17	21190.0
R-290/E-170/-125/-134a	0.0016	(5.5/1.3/52.0/41.3)	[2.2/0.6/58.0/39.2]	232.34	1409.18	21200.0
R-290/-125/{COS}/-134a	0.0016	(1.6/36.9/15.1/46.3)	[0.7/43.7/9.0/46.6]	232.33	1409.14	21210.0
R-1270/-125/{COS}/-134a	0.0016	(2.1/37.3/13.9/46.7)	[0.9/44.0/8.2/46.9]	232.34	1409.17	21220.0
R-125/{COS}/{Propyne}/-134a	0.0016	(34.8/17.6/1.4/46.1)	[41.8/10.6/0.6/47.0]	232.34	1409.17	21220.0
R-1270/-125/{Propyne}/-134a	0.0016	(4.5/50.7/3.5/41.3)	[1.8/57.2/1.3/39.7]	232.34	1409.18	21230.0
R-290/-125/{Cyclopropane}/-134a	0.0016	(3.4/51.8/4.3/40.5)	[1.4/58.2/1.7/38.7]	232.34	1409.18	21230.0
R-152a/-125/{COS}/-134a	0.0016	(3.7/36.6/16.1/43.6)	[2.4/43.7/9.6/44.2]	232.32	1409.19	21230.0
RE-170/-125/{Propyne}/-134a	0.0016	(5.5/53.9/5.0/35.6)	[2.4/61.3/1.9/34.4]	232.34	1409.18	21260.0
RE-170/-1270/-125/-134a	0.0016	(8.4/1.2/53.2/37.2)	[3.7/0.5/60.1/35.7]	232.34	1409.18	21260.0
R-125/{Cyclopropane}/{Propyne}/-134a	0.0016	(53.2/3.2/7.1/36.5)	[60.6/1.3/2.7/35.4]	232.32	1409.20	21260.0
R-290/-152a/-125/-134a	0.0016	(1.1/14.5/53.8/30.6)	[0.5/9.0/61.0/29.5]	232.34	1409.18	21270.0
R-1270/-125/{Cyclopropane}/-134a	0.0016	(1.3/51.5/7.6/39.6)	[0.5/58.4/3.0/38.1]	232.31	1409.20	21270.0
RE-170/-152a/-125/-134a	0.0016	(4.9/9.4/54.2/31.6)	[2.1/5.8/61.5/30.5]	232.34	1409.18	21280.0

Blend Components	O.F.	Compositions		T_b	ρ_b	$\Delta h_{v,b}$
		Moles	Mass	[K]	[kg/m^3]	[J/mol]
R-22	----	----	----	232.34	1409.18	20211.3
R-152a/-1270/-125/-134a	0.0016	(14.4/1.2/53.3/31.1)	[9.0/0.5/60.6/30.0]	232.34	1409.18	21280.0
R-152a/-125/{Propyne}/-134a	0.0016	(10.8/54.1/4.1/31.0)	[6.8/61.6/1.6/30.0]	232.34	1409.18	21280.0
RE-170/-125/{Cyclopropane}/-134a	0.0016	(6.3/53.2/3.7/36.8)	[2.7/60.3/1.5/35.5]	232.34	1409.18	21280.0
R-152a/-125/{Cyclopropane}/-134a	0.0016	(13.4/53.7/2.2/30.6)	[8.4/61.1/0.9/29.6]	232.34	1409.19	21290.0
R-1270/-32/-125/-134a	0.0017	(5.0/5.3/42.5/47.2)	[2.0/2.7/49.0/46.3]	232.34	1409.17	21340.0
R-32/-125/{COS}/-134a	0.0017	(10.5/28.2/10.4/50.9)	[5.6/34.7/6.4/53.3]	232.34	1409.18	21420.0
R-32/-125/{Propyne}/-134a	0.0018	(14.2/33.5/3.5/48.9)	[7.5/40.7/1.4/50.5]	232.34	1409.18	21530.0
R-152a/-32/-125/-134a	0.0018	(6.5/13.3/34.9/45.4)	[4.3/7.0/42.2/46.6]	232.34	1409.18	21530.0
R-290/-32/-125/-134a	0.0018	(1.5/16.0/30.5/52.0)	[0.7/8.4/37.1/53.8]	232.34	1409.18	21550.0
RE-170/-32/-125/-134a	0.0018	(3.0/14.8/32.6/49.5)	[1.4/7.8/39.6/51.1]	232.34	1409.18	21550.0
R-32/-125/{Cyclopropane}/-134a	0.0018	(16.4/30.1/2.1/51.5)	[8.7/36.8/0.9/53.6]	232.34	1409.18	21580.0
R-143a/-32/-125/-134a	0.0019	(1.1/19.7/25.2/53.9)	[1.0/10.6/31.4/57.0]	232.34	1409.18	21610.0
R-152a/-125/{COS}/{Cyclopropane}	0.0157	(25.0/72.9/1.0/1.0)	[15.7/83.3/0.6/0.4]	228.81	1403.83	20630.0
RE-170/-152a/-143a/-125	0.0158	(1.5/23.6/1.5/73.4)	[0.6/14.8/1.2/83.4]	228.76	1404.61	20600.0
RE-170/-152a/-125/{COS}	0.0158	(1.4/24.1/73.1/1.4)	[0.6/15.1/83.5/0.8]	228.75	1404.72	20610.0
R-290/-152a/-143a/-125	0.0163	(1.1/23.7/1.1/74.0)	[0.5/14.8/0.9/83.9]	228.64	1404.43	20560.0
RE-170/-125/{Cyclopropane}/{Propyne}	0.0209	(8.9/81.7/1.3/8.1)	[3.8/92.6/0.5/3.1]	227.53	1405.08	20250.0
RE-170/-143a/-125/{Propyne}	0.0209	(8.0/1.0/81.2/9.8)	[3.5/0.8/92.0/3.7]	227.52	1405.20	20230.0
RE-170/-125/{COS}/{Propyne}	0.0211	(1.6/80.8/1.0/16.6)	[0.7/92.4/0.6/6.3]	227.49	1405.17	20200.0
R-290/E-170/-125/{Propyne}	0.0214	(1.3/14.2/82.5/2.0)	[0.5/6.1/92.6/0.7]	227.42	1405.19	20210.0
RE-170/-143a/-125/{COS}	0.0215	(16.8/1.4/80.5/1.4)	[7.3/1.1/90.9/0.8]	227.39	1405.04	20220.0
R-143a/-125/{COS}/{Propyne}	0.0215	(1.3/80.0/1.3/17.3)	[1.1/91.6/0.8/6.6]	227.37	1405.34	20160.0
R-290/-143a/-125/{Propyne}	0.0216	(1.1/1.1/81.5/16.4)	[0.5/0.9/92.5/6.2]	227.37	1405.25	20150.0
R-290/E-170/-125/{Cyclopropane}	0.0216	(1.3/14.7/82.6/1.3)	[0.5/6.3/92.6/0.5]	227.36	1405.30	20210.0
R-290/-125/{Cyclopropane}/{Propyne}	0.0216	(1.3/82.2/1.3/15.2)	[0.6/93.2/0.5/5.7]	227.35	1405.39	20150.0

Blend Components	O.F.	Compositions		T_b	ρ_b	$\Delta h_{v,b}$
		Moles	Mass	[K]	[kg/m^3]	[J/mol]
R-22	----	----	----	232.34	1409.18	20211.3
RE-170/-1270/-125/{Cyclopropane}	0.0218	(14.9/1.3/82.4/1.3)	[6.4/0.5/92.5/0.5]	227.32	1405.29	20210.0
RE-170/-1270/-143a/-125	0.0220	(15.4/1.4/1.4/81.8)	[6.6/0.6/1.1/91.7]	227.27	1405.37	20180.0
R-1270/-125/{Cyclopropane}/{Propyne}	0.0221	(1.7/82.1/1.7/14.6)	[0.7/93.2/0.7/5.5]	227.24	1405.43	20140.0
R-143a/-32/-125/{Propyne}	0.0226	(2.2/2.2/78.9/16.7)	[1.8/1.1/90.7/6.4]	227.13	1405.53	20160.0
RE-170/-143a/-32/-125	0.0228	(15.9/2.5/2.5/79.1)	[6.9/2.0/1.2/89.8]	227.08	1405.54	20200.0
R-1270/-125/{COS}/{Propyne}	0.0228	(2.0/80.9/2.0/15.1)	[0.8/92.3/1.2/5.7]	227.07	1405.58	20090.0
R-290/-143a/-125/{Cyclopropane}	0.0242	(1.2/1.2/82.7/14.9)	[0.5/1.0/92.7/5.8]	226.74	1405.91	20050.0
R-290/-1270/-125/{Cyclopropane}	0.0245	(1.1/1.1/83.5/14.3)	[0.4/0.4/93.5/5.6]	226.68	1405.91	20040.0
R-143a/-125/{COS}/{Cyclopropane}	0.0246	(2.1/80.4/2.1/15.3)	[1.7/91.0/1.2/6.1]	226.63	1406.37	20040.0
R-143a/-32/-125/{Cyclopropane}	0.0250	(1.8/1.8/80.7/15.6)	[1.5/0.9/91.4/6.2]	226.55	1406.74	20070.0
R-1270/-143a/-125/{Cyclopropane}	0.0255	(3.0/3.0/82.2/11.8)	[1.2/2.3/91.8/4.6]	226.43	1406.49	19950.0
R-290/-1270/-143a/-125	0.0276	(10.2/1.5/1.6/86.7)	[4.1/0.6/1.2/94.2]	225.92	1407.08	19610.0
R-290/-1270/-125/{COS}	0.0278	(10.7/1.2/86.9/1.2)	[4.3/0.5/94.6/0.7]	225.88	1407.01	19650.0
R-143a/-32/-125/{COS}	0.0301	(31.2/1.1/66.5/1.2)	[24.4/0.5/74.3/0.7]	225.35	1408.66	19510.0
RE-170/-32/{COS}/-134a	0.0431	(1.0/25.9/1.0/72.1)	[0.5/15.3/0.7/83.5]	236.92	1355.26	22020.0
R-32/{COS}/{Cyclopropane}/-134a	0.0432	(26.2/1.0/1.0/71.8)	[15.5/0.7/0.5/83.3]	236.76	1354.66	22010.0
RE-170/-152a/-143a/-32	0.1530	(1.0/1.0/1.6/96.4)	[0.9/1.3/2.5/95.3]	221.83	1203.17	19920.0
RE-170/-152a/-32/{Propyne}	0.1569	(1.0/1.0/96.9/1.0)	[0.9/1.3/97.0/0.8]	221.99	1197.11	19990.0
R-152a/-32/{Cyclopropane}/{Propyne}	0.1573	(1.0/96.9/1.0/1.0)	[1.3/97.1/0.8/0.8]	221.96	1196.66	19980.0
RE-170/-152a/{COS}/{Propyne}	0.1797	(1.0/1.0/96.9/1.1)	[0.8/1.1/97.4/0.7]	223.48	1161.75	18700.0
RE-170/-152a/-143a/{Propyne}	0.1801	(1.0/1.0/97.0/1.0)	[0.6/0.8/98.2/0.5]	226.32	1158.02	19160.0
RE-170/-143a/{Cyclopropane}/{Propyne}	0.1820	(1.0/96.9/1.0/1.0)	[0.6/98.4/0.5/0.5]	226.29	1155.31	19150.0

Table F-2: Blend compositions for potential R-22 replacements, fitted to the pure component properties of R-22 calculated using REFPROP.

F.3. Blend Compositions Fitted to Process

Blend Components	O.F.	Compositions		COP	CPLMX	M_W
		Moles	Mass	----	[J/mol-K]	[g/mol]
R-22	----	----	----	4.48	103.7	86.5
{COS}/R-134a	0.0437	(62.6/37.4)	[49.6/50.4]	4.73	108.0	75.8
R-1270/{Cyclopropane}	0.0792	(56.1/43.9)	[56.1/43.9]	4.11	115.5	42.1
R-1270/{Propyne}	0.0817	(65.6/34.4)	[66.7/33.3]	3.96	112.4	41.4
R-32/-134a	0.0920	(52.2/47.8)	[35.7/64.3]	4.62	120.9	75.9
R-290/{COS}	0.0983	(43.9/56.1)	[36.5/63.5]	4.25	104.1	53.1
RE-170/-1270	0.1036	(33.7/66.3)	[35.7/64.3]	3.84	116.6	43.4
R-152a/-1270	0.1141	(32.0/68.0)	[42.4/57.6]	3.82	119.4	49.7
R-143a/{Cyclopropane}	0.1243	(32.6/67.4)	[49.1/50.9]	4.11	122.2	55.7
R-125/{Cyclopropane}	0.1385	(19.7/80.3)	[41.2/58.8]	4.23	124.9	57.4
R-152a/-32	0.1409	(52.0/48.0)	[57.9/42.1]	5.50	104.3	59.3
R-143a/{Propyne}	0.1440	(48.5/51.5)	[66.4/33.6]	3.76	120.6	61.4
R-290/-32	0.1478	(56.1/43.9)	[52.0/48.0]	4.02	113.2	47.6
R-152a/{COS}	0.1515	(41.5/58.5)	[43.8/56.2]	5.45	96.5	62.6
R-1270/{COS}	0.1519	(47.6/52.4)	[38.9/61.1]	4.46	101.2	51.5
RE-170/-32	0.1570	(51.7/48.3)	[48.7/51.3]	5.58	99.8	48.9
R-290/{Cyclopropane}	0.1604	(47.4/52.6)	[48.6/51.4]	3.83	119.5	43.0
RE-170/{COS}	0.1627	(41.5/58.5)	[35.3/64.7]	5.50	93.2	54.3
R-125/{Propyne}	0.1785	(34.9/65.1)	[61.6/38.4]	3.74	125.8	67.9
R-143a/{COS}	0.1807	(24.4/75.6)	[31.1/68.9]	4.75	98.4	65.9
R-1270/-134a	0.1904	(76.9/23.1)	[57.9/42.1]	3.43	129.5	55.9
{COS}/{Propyne}	0.1977	(61.9/38.1)	[70.9/29.1]	5.81	88.0	52.5
R-125/{COS}	0.1999	(13.9/86.1)	[24.4/75.6]	4.98	96.6	68.4
R-32/{Propyne}	0.2017	(48.7/51.3)	[55.2/44.8]	5.91	94.0	45.9
R-1270/-32	0.2039	(69.3/30.7)	[64.6/35.4]	4.03	112.6	45.1
{Cyclopropane}/R-134a	0.2166	(93.7/6.3)	[86.0/14.0]	4.69	113.5	45.9

Blend Components	O.F.	Compositions		COP	CPLMX	M_W
		Moles	Mass	----	[J/mol-K]	[g/mol]
R-22	----	----	----	4.48	103.7	86.5
R-143a/-32	0.3185	(32.9/67.1)	[44.2/55.8]	4.51	111.3	62.6
R-143a/-134a	0.3205	(48.7/51.3)	[43.9/56.1]	2.95	152.9	93.3
R-32/-125	0.3705	(93.8/6.2)	[86.8/13.2]	5.55	99.0	56.2
R-1270/{COS}/{Propyne}	0.0127	(48.1/25.0/27.0)	[43.9/32.6/23.5]	4.44	104.2	46.0
R-290/E-170/{COS}	0.0131	(34.9/19.0/46.1)	[29.7/16.9/53.4]	4.43	103.9	51.8
R-290/{COS}/{Cyclopropane}	0.0132	(34.9/40.9/24.1)	[30.7/49.0/20.3]	4.47	105.3	50.1
R-290/-152a/{COS}	0.0136	(34.2/18.7/47.1)	[27.1/22.1/50.8]	4.46	104.9	55.7
R-290/-32/{Propyne}	0.0140	(37.7/37.6/24.7)	[36.1/42.4/21.5]	4.51	106.2	46.1
R-290/{COS}/{Propyne}	0.0144	(37.5/44.0/18.5)	[32.8/52.5/14.7]	4.41	103.0	50.4
R-1270/-32/{Propyne}	0.0145	(48.2/21.3/30.5)	[46.5/25.4/28.0]	4.49	106.1	43.6
RE-170/-1270/{COS}	0.0145	(27.0/42.9/30.1)	[25.6/37.2/37.3]	4.47	105.3	48.6
R-143a/{COS}/{Propyne}	0.0165	(31.1/36.8/32.2)	[42.8/36.2/21.1]	4.51	106.3	61.1
R-152a/-1270/{COS}	0.0192	(26.2/41.4/32.4)	[32.0/32.1/35.9]	4.51	106.6	54.2
R-1270/{COS}/{Cyclopropane}	0.0208	(41.7/23.8/34.5)	[37.9/30.8/31.4]	4.53	107.1	46.4
RE-170/-143a/{COS}	0.0212	(31.5/26.9/41.6)	[23.4/36.4/40.2]	4.54	107.2	62.1
RE-170/-1270/-32	0.0229	(31.7/42.3/26.0)	[31.8/38.8/29.5]	4.53	107.9	45.9
R-290/{COS}/-134a	0.0250	(15.8/57.6/26.5)	[10.2/50.4/39.4]	4.53	108.0	68.7
R-125/{COS}/{Propyne}	0.0281	(21.7/41.7/36.6)	[39.6/38.1/22.3]	4.60	108.3	65.8
R-152a/-143a/{COS}	0.0287	(30.8/25.3/44.0)	[29.9/31.2/38.9]	4.58	108.5	68.0
R-1270/{COS}/-134a	0.0306	(13.2/55.2/31.6)	[7.9/46.8/45.4]	4.58	109.0	70.9
R-290/-32/{Cyclopropane}	0.0312	(33.4/32.1/34.5)	[32.0/36.4/31.6]	4.57	109.7	45.9
R-143a/-32/{Propyne}	0.0319	(31.5/29.6/38.9)	[46.1/26.8/27.1]	4.60	109.6	57.5
R-1270/-32/{Cyclopropane}	0.0325	(40.5/18.5/41.0)	[38.8/21.9/39.3]	4.57	109.9	43.9
R-143a/{COS}/{Cyclopropane}	0.0326	(24.6/33.9/41.5)	[35.4/34.8/29.9]	4.62	109.1	58.5
R-143a/{COS}/-134a	0.0341	(6.2/60.1/33.7)	[6.9/47.7/45.4]	4.62	109.4	75.7
R-125/{COS}/-134a	0.0365	(3.4/61.8/34.9)	[5.3/48.4/46.4]	4.65	109.6	76.7
R-32/{COS}/-134a	0.0433	(5.3/56.8/37.9)	[3.7/45.2/51.2]	4.73	108.9	75.5

Blend Components	O.F.	Compositions		COP	CPLMX	M_W
		Moles	Mass	----	[J/mol-K]	[g/mol]
R-22	----	----	----	4.48	103.7	86.5
R-32/-125/{Propyne}	0.0499	(32.0/22.2/45.8)	[27.0/43.2/29.8]	4.71	112.4	61.6
R-143a/-32/{Cyclopropane}	0.0535	(22.2/24.1/53.8)	[34.7/23.3/42.1]	4.70	113.5	53.8
R-32/{Propyne}/-134a	0.0690	(49.5/12.5/38.0)	[37.0/7.2/55.8]	4.85	114.9	69.5
R-1270/{Cyclopropane}/{Propyne}	0.0787	(59.1/31.2/9.7)	[59.4/31.4/9.3]	4.08	114.5	41.9
R-290/-32/{COS}/{Propyne}	0.0099	(37.5/20.5/20.5/21.5)	[34.3/22.2/25.6/17.9]	4.46	104.5	48.1
R-290/-143a/{COS}/{Propyne}	0.0116	(21.1/13.6/40.9/24.3)	[16.9/20.8/44.6/17.7]	4.45	104.4	55.1
R-290/-125/{COS}/{Propyne}	0.0117	(27.5/5.9/43.5/23.1)	[22.3/12.9/47.9/16.9]	4.45	104.4	54.6
R-290/E-170/-32/{COS}	0.0118	(34.6/20.6/10.3/34.6)	[30.0/18.7/10.5/40.8]	4.46	104.7	50.8
R-290/{COS}/{Cyclopropane}/{Propyne}	0.0120	(36.1/42.1/14.1/7.7)	[31.7/50.4/11.8/6.1]	4.45	104.3	50.2
R-290/{COS}/{Propyne}/-134a	0.0122	(31.9/47.3/13.8/7.0)	[25.5/51.5/10.0/12.9]	4.44	104.3	55.1
R-290/E-170/{COS}/{Cyclopropane}	0.0124	(35.0/10.1/43.6/11.3)	[30.2/9.1/51.3/9.3]	4.45	104.5	51.0
R-1270/-143a/{COS}/{Propyne}	0.0125	(39.3/5.7/27.2/27.9)	[33.9/9.8/33.4/22.9]	4.45	104.6	48.8
R-1270/-125/{COS}/{Propyne}	0.0126	(44.8/1.5/26.1/27.6)	[39.8/3.8/33.1/23.3]	4.45	104.5	47.4
R-290/E-170/-143a/{COS}	0.0126	(29.0/21.1/4.6/45.4)	[23.9/18.1/7.2/50.9]	4.45	104.4	53.6
R-1270/{COS}/{Cyclopropane}/{Propyne}	0.0126	(47.8/24.8/1.9/25.5)	[43.7/32.4/1.7/22.2]	4.45	104.4	46.0
R-290/E-170/-125/{COS}	0.0126	(31.2/20.6/2.0/46.2)	[25.8/17.8/4.5/51.9]	4.45	104.4	53.4
R-290/-1270/{COS}/{Propyne}	0.0127	(2.6/44.7/26.3/26.4)	[2.5/40.6/34.1/22.8]	4.44	104.1	46.3
R-290/E-170/{COS}/-134a	0.0127	(32.6/16.8/47.4/3.2)	[26.7/14.4/52.9/6.1]	4.44	104.4	53.9
R-290/-152a/{COS}/{Propyne}	0.0129	(35.6/10.9/45.8/7.7)	[29.4/13.4/51.4/5.8]	4.44	104.1	53.5
R-290/E-170/-1270/{COS}	0.0129	(27.7/20.6/8.9/42.8)	[23.9/18.6/7.3/50.3]	4.44	104.1	51.2
R-290/E-170/-152a/{COS}	0.0130	(34.7/13.9/5.0/46.4)	[28.9/12.1/6.3/52.7]	4.44	104.1	52.9
R-125/{COS}/{Cyclopropane}/{Propyne}	0.0287	(21.5/41.5/1.5/35.6)	[39.3/38.0/0.9/21.7]	4.61	108.3	65.6

Table F- 3: Blend compositions for potential R-22 replacements, fitted to an existing process using R-22 using Aspen Plus.